STRENGTH OF HORIZONTAL SHEAR REINFORCEMENT WITH LIMITED

DEVELOPMENT

by

REGINA NYAMBURA WAWERU

Presented to the Faculty of the Graduate School of

The University of Texas at Arlington in Partial Fulfillment

of the Requirements

for the Degree of

DOCTOR OF PHILOSOPHY

THE UNIVERSITY OF TEXAS AT ARLINGTON

MAY 2015

Acknowledgements

Abstract

STRENGTH OF HORIZONTAL SHEAR REINFORCEMENT WITH LIMITED

DEVELOPMENT

REGINA NYAMBURA WAWERU, PhD

The University of Texas at Arlington, 2015

Supervising Professor: Shih-Ho Chao

In order for the composite action between the precast beam and the cast-in-place deck to be effective, sufficient horizontal (interface) shear strength needs to be provided at the interface of the two concrete elements to prevent slip. Horizontal shear strength is provided by three main components: the protrusions on the crack faces (cohesion/aggregate interlock), friction between the faces resulting from the normal compressive stress, and the dowel action of the reinforcing bars. AASHTO LRFD equation assumes that all reinforcement crossing the interface would be fully developed on both sides of the interface at ultimate shear strength.

This study examines if adequate horizontal shear capacity is provided by a very short embedded length (approximately 2-in.) commonly used in composite slab and box bridge beams in Texas. A number of component test that included push-off test and bar pullout tests were conducted to evaluate each component of horizontal shear. Seven full-scale composite prestressed bridge beams were tested to evaluate the contribution of dowel action of the reinforcement on horizontal shear capacity. These beams included two beams designed according to the current TxDOT specifications and two beams designed without any horizontal shear reinforcement. The interface area was reduced in the last three full-scale beams so as to force a horizontal shear failure and hence obtain the horizontal shear strength in those specimens.

Results revealed that although the component tests show that the interface reinforcement with 2-in. embedded length could not be fully developed, the full-scale tests (with reduced interface area) indicate that the actual boundary conditions in the composite beams could provide abundant confinement to develop the reinforcement. Experimental results show that current AASHTO provisions for horizontal shear in composite concrete beams could over-estimate the horizontal shear contribution from dowel action of the reinforcement and do not represent the true behavior of the horizontal shear resistance mechanism.

Table of Contents

List of Illustrations

List of Tables

Chapter 1

INTRODUCTION

1.1 Background

Composite construction is an economical way of increasing the stiffness and strength, or reducing the member depth in order to resist the applied loads. The success of composite action depends on the shear resistance at the interface between the precast element and the cast-in-place (CIP) element to allow full transfer of interface stresses. The problem of shear transfer in composite beams has been thoroughly researched (Hanson, 1960; Saemann and Washa, 1964; Birkeland and Birkeland, 1966; Badoux and Hulsbos, 1967; Mattock and Hawkins, 1972; Mattock et al., 1976; Tassios and Vintzeleou, 1987; Walraven et al., 1987; Bass et al., 1989; Loov and Patnaik, 1994; Ali and White, 1999; Hwang et al., 2000; Mattock, 2001). If no shear resistance exists and a load is applied to the composite beam, the slab would slide with respect to the beam and the system would act as if two separate elements were used (Figure 1-1 (b)). However, if sufficient shear resistance is provided, the slip between the two elements can be prevented and composite action can be counted on (Figure 1-1 (c)). Thus a good connection between the two components of the composite system is essential.

This can be achieved by artificially roughening the interface, providing a bonding agent, and/or using shear connectors or ties, mostly in the form of extended stirrups or hooks. Reinforcement is generally placed at right angles to the shear plane so as to provide a clamping force between the two potential sliding surfaces.

The bars have to be adequately anchored to ensure yielding before debonding/pullout. The clamping action of the reinforcement only comes into play once the crack between the surfaces slightly opens.

1
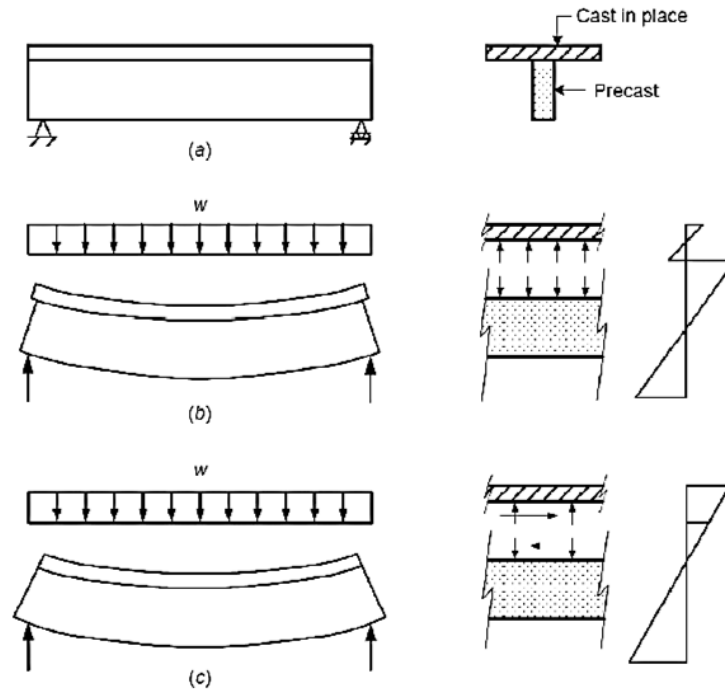
Figure 1-1 (a) Typical precast beam and CIP slab (b) Non-composite action. (c)

Composite action (Naaman, 2012)

The horizontal shear stress at the interface between the precast beam and the CIP slab is generated by the loads acting on the composite section only. The horizontal shear stress due to bending is equal in magnitude to the vertical shear stress and can be derived either based on the classical strength of materials approach or by considering the shear force at strength limit state as given by AASHTO Section C5.8.4.2 (AASHTO, 2014).

Horizontal shear is resisted by a combination of;

1. Resistance of the protrusions on the crack faces to shearing (i.e. cohesion and/or aggregate interlock) also referred to as "cohesion factor" by AASHTO

2. Friction between the crack faces

3. Dowel action of the reinforcement

The AASHTO nominal shear resistance of the interface plane is given by:

$$V_{ni} = cA_{cv} + \mu(A_{vf}f_y + P_c) \qquad\qquad [1\text{-}1]$$

Where,

cA_{cv} = cohesion and/or aggregate interlock (1)

μP_c = friction between the crack faces (2)

$\mu A_{vf}f_y$ = dowel action of the reinforcement (3)

The shear friction concept is used in today's design specifications for horizontal shear transfer, which describes the behavior of a cracked material or an interface between two elements. When the two sides of a cracked specimen try to shear past each other, friction resists their motion (Figure 1-2). The crack also opens up thus separating the materials. This dilatation is resisted by the clamping force provided by steel reinforcement which bridges the interface. The area of steel (A_{vf}) is assumed to be loaded to its yield strength (f_y) thus causing a net compressive force to act normal to the interface. The friction force along the interface is the product of the friction coefficient (μ) and the normal force $(A_{vf}f_y)$.
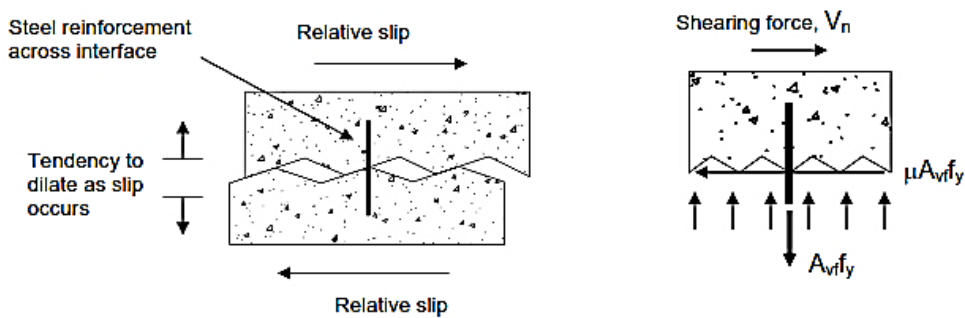
Figure 1-2 Shear friction concept (Scholz, 2004)

3

1.2 Objectives

Horizontal cracks between the precast beams and the CIP decks have been noticed in several old TxDOT bridges. Figure 1-3 below shows horizontal cracks on the Riverside Drive Underpass at I-35 in Austin. These cracks could result from shrinkage or excessive shear forces. Shrinkage of the deck can induce significant stresses along the interface between the precast beam and the CIP deck leading to cracking or slip if shear resistance at the interface is insufficient. More details regarding the cracks observed are discussed in Section 3.2.

Figure 1-3 Interface cracks on Riverside Dr. Underpass at I-35

As shown in the AASHTO equation (Eq. 1-1), the three major contributions to the horizontal shear resistance are (1) cohesion and/or aggregate interlock, (2) friction between the crack faces, and (3) dowel action of the reinforcement. The objective of this research was therefore two-fold:

Determine the influence of horizontal shear reinforcement on interface shear despite limited development:

TxDOT specifies a 5-in. thick composite concrete deck to be used on prestressed slab beams and box beams. AASHTO LRFD Bridge Design Specifications (2014) section

4

5.8.4.1 requires that all reinforcement crossing the interface should be fully developed on both sides of the interface by embedment, hooks, or other methods to develop the design yield stress. AASHTO Section 5.11.2.4 provides guidelines for determining the development length needed for standard hooks in tension. The equation provided results in an embedded length of 6.7-in. not possible in a 5-in. CIP slab. However, horizontal shear reinforcement do not qualify to be considered as "standard hooks" according to AASHTO and there is no equation suitable for typical horizontal shear reinforcement. Since the shear friction action of the interface shear reinforcement relies on yielding of the bars (Item 3 of Eq. 1-1), a short embedded length inside the composite slab can fail by premature pullout due to localized concrete fracture prior to yielding, thus providing insufficient clamping force. The embedded length of interface shear reinforcement is only 2-in. in the current TxDOT prestressed slab beams and box beams (Figure 1-5).

Typical 4B20 Section (Previous Design Practice)
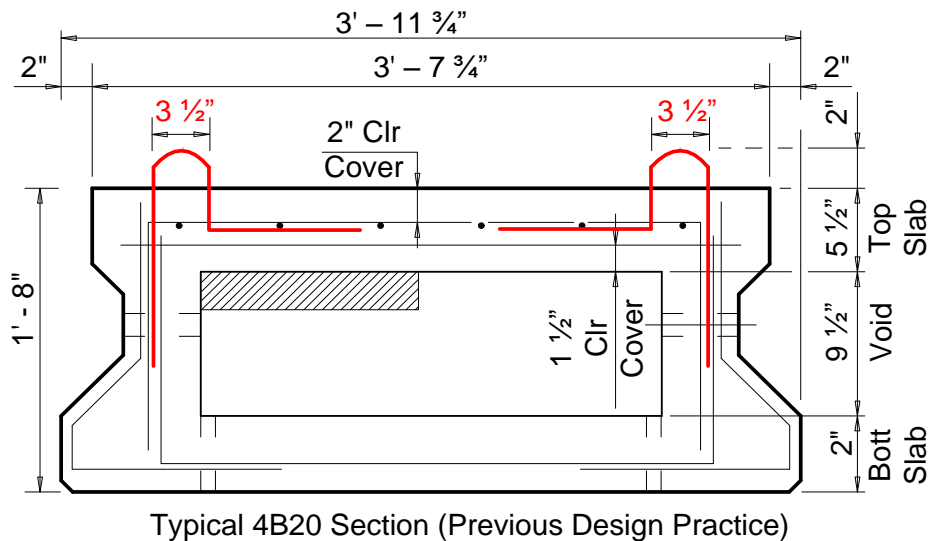
Figure 1-4 Figure 1 4 Standard TxDOT box and slab beam details (before 2012)
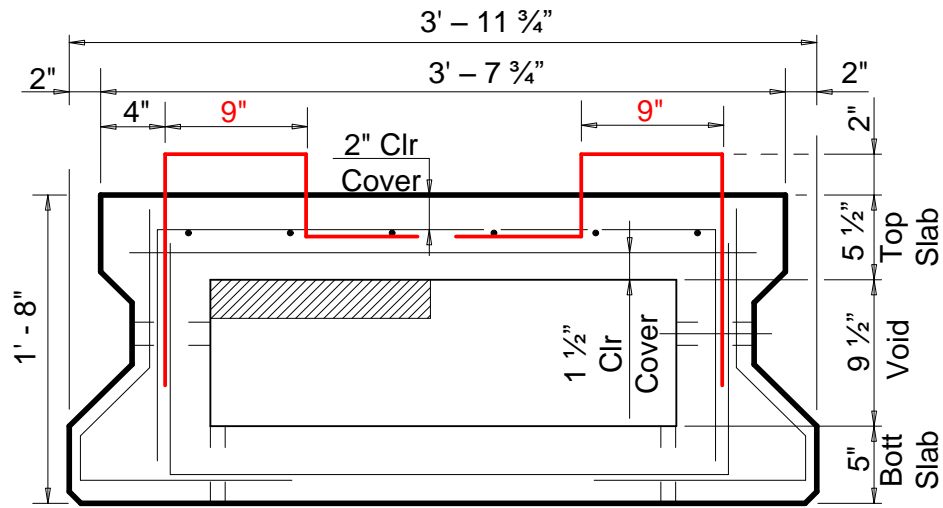
Typical 4B20 Section (Current Design Practice since 2012)

(a)
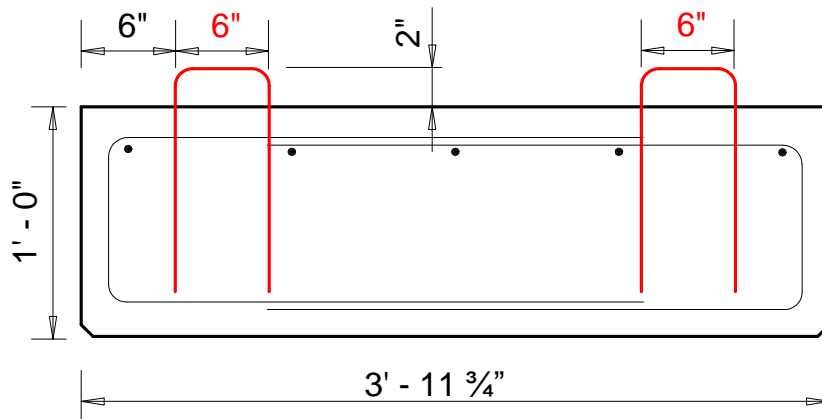
Typical 4SB12 Section

(b)

Figure 1-5 Standard TxDOT box and slab beam current details

Determine the influence of different surface profiles on interface shear strength:

AASHTO Section 5.8.4.3 (AASHTO, 2014) specifies c = 0.28 ksi and μ = 1.0 for a surface roughened to an amplitude of 0.25-in. This indicates that both the cohesion

factor c and friction factor μ are affected by the surface roughness. Current TxDOT standards state that "Finished, unformed surfaces must not have distortions greater than 0.25-in." (TxDOT, 2004). A number of the precast plants in Texas typically give a wood float finish on box and slab beams. This is done by sliding a wooden float across the top of the wet concrete resulting in a coarse finish. This is why it is very important to investigate the effects of a wood float surface finish on the shear transfer across an interface. An effective means to improve the horizontal shear resistance is to specify a rougher finish (i.e. amplitude of roughness greater than 0.25-in.) on top of the beam to improve horizontal shear capacity. An experimental study carried out by Saemann and Washa (1964) has shown that the horizontal shear strength is increased by increasing the surface roughness. Also, TxDOT is moving towards using the ICRI (International Concrete Repair Institute) guidelines for concrete surface preparation as a measure of surface roughness. The ICRI guidelines offer nine distinct surface configurations from smooth to very rough (Figure 1-6). These configurations are identified as concrete surface profiles (CSP) ranging from CSP 1 which is nearly flat to CSP 9 which is very rough. The Precast Panel-Fabrication Standard recommends that the top of the panel should be finished to a roughness between a CSP 6 and a CSP 9. Therefore by investigating these different surface configurations, we can recommend the roughness that will lead to an improvement in the horizontal shear resistance of composite TxDOT beams.
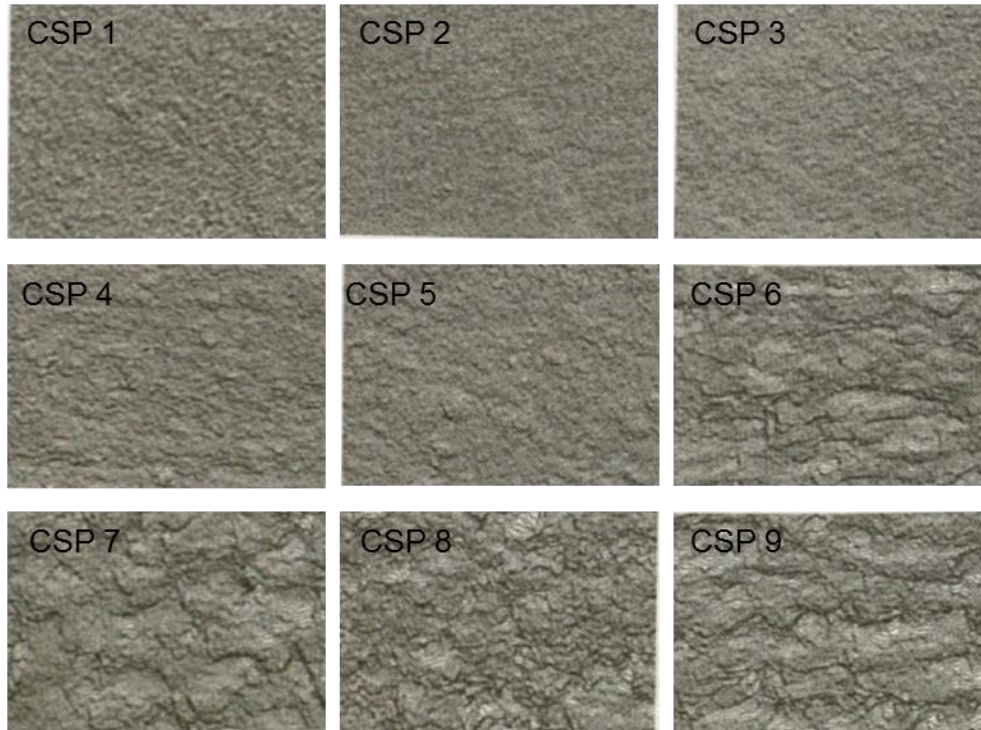
Figure 1-6 ICRI concrete surface profiles (CSP)

The experimental program consists primarily of push-off specimens, pullout specimens and full-scale composite beam tests. The following parameters were investigated in the experimental program.

1. Interface surface roughness (Palacios, 2015)

2. Friction factor μ (Palacios, 2015)

3. Embedment length of horizontal shear reinforcement

4. Width of horizontal shear reinforcement

5. Bend curvature of the horizontal shear reinforcement: A 180° and 90° degree bend were investigated.

The objective of this project is to determine if adequate horizontal shear capacity is provided by the 5-in. concrete deck on slab and box beams, despite lack of reinforcement development. Secondly, this project strives to determine the effect of

8

surface finish on the horizontal shear capacity and determine a surface configuration that will lead to an improvement in the horizontal shear resistance. This dissertation covers the first objective (the influence of the horizontal shear reinforcement on horizontal shear resistance) whereas the second objective (effect of interface surface roughness on horizontal shear resistance) is covered in Palacios (2015).

1.3 Organization of this Dissertation

This dissertation is organized into six chapters. Details of each chapter are described as follows.

Chapter 2- Literature Review

A general review of previous studies related to horizontal shear in composite concrete beams and design equations based on shear friction and push-off tests is presented. All previous work done on all parameters of horizontal shear for instance dowel action, cohesion and friction factor are also outlined.

Chapter 3- Field Study and Other DOT Practices

Details the field work study undertaken to observe bridges suspected of displaying horizontal shear cracks as well local precast plants that fabricate box and slab beams. A review of the DOT practices of all 50 states concerning the detailing of slab and box beams is also presented in this chapter.

Chapter 4-Experimental Program

Details the overall experimental program including the test matrix, test procedures, and the design and layout of test samples are outlined. Material properties of the matrices, reinforcements and prestressing strands are also elaborated. Specimen preparation and casting procedures are presented as well as test set-up, instrumentation and testing procedures.

Chapter 5- Test Results and Analysis

This chapter discusses the results achieved from the push-off, pullout and full-scale specimens. It details the shear strength, pullout strength, the development of horizontal shear reinforcement and slip characteristics realized from the specimens. A finite element analysis conducted on a composite beam is also outlined.

Chapter 6-Summary and Conclusions

The summary of the overall research study is presented in this chapter. Main conclusions are outlined based on experimental and analytical results. Recommendations for future research and revisions for AASHTO specifications are also provided.

```
┌─────────────────────────┐
│   Experimental Program  │
└─────────────────────────┘
```

Push-off Test

Task 2
Evaluate Horizontal Shear Component: cA_cv
(cohesion and/or aggregate interlock)

Task 3
Evaluate Horizontal Shear Component: μP_c
(friction between the crack faces)

Task 4
Evaluate Horizontal Shear Component: μA_vf f_y
(dowel action of the reinforcement)

Task 5
Bar Pullout Test

Task 6
Full-Scale Composite Beam Test:
current practice

Task 7
Full-Scale Composite Beam Test:
further investigation

Task 8
Final Report (Research Findings and Design
Recommendations)

Figure 1-7 Flowchart of experimental program

Chapter 2

LITERATURE REVIEW

2.1 Introduction

Interface (or Horizontal) Shear

The horizontal shear stress at the interface between the precast beam and the CIP slab is generated by the loads acting on the composite section only. The horizontal shear stress due to bending is equal in magnitude to the vertical shear stress (Figure 2-1) and can be derived either based on the classical strength of materials approach or an alternative considering the shear force at strength limit state as given by AASHTO Section C5.8.4.2 (AASHTO, 2014).
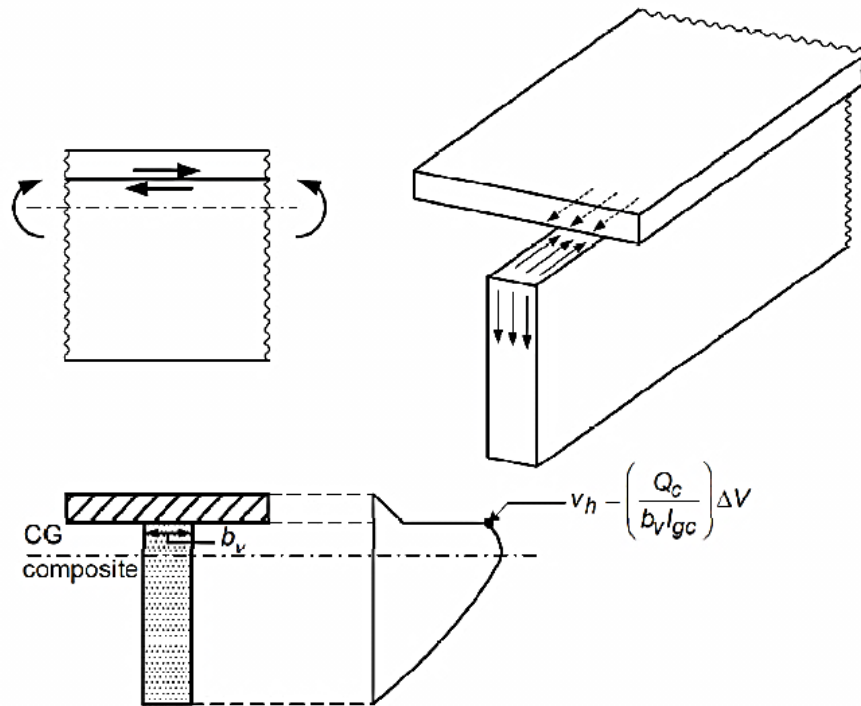
Figure 2-1 Interface horizontal shear stress (Naaman, 2012)

Horizontal Shear Resistance of the Interface Plane

The horizontal shear is resisted by a combination of:

(1) Resistance of the protrusions on the crack faces to shearing (i.e. cohesion and/or aggregate interlock). For simplicity, AASHTO uses the term "cohesion factor" to capture the effects of this contribution listed,

(2) Friction between the crack faces, and

(3) Dowel action of the reinforcement.

Mast (1968), Hanson (1960), and Kaar et al. (1960) first introduced the shear friction equation (Eq. 2-1). This was the basis of the shear-friction design procedure found in Section 11.6.4 of ACI 318-11.

$$v_{nh} = \rho_v f_y \mu \qquad\qquad [2-1]$$

v_{nh} = nominal horizontal shear stress

μ = friction coefficient between the two surfaces

A number of assumptions and limitations were used in formulating the shear friction equation as listed below (Kamel, 1996):

- Interface must be clean and free of laitance.

- Well confinement of the concrete.

- Reinforcement crossing the interface must be well anchored.

- A certain level of relative slip at the interface is permitted.

- Bond and cohesion do not develop shear resistance, only friction does.

- Bar size is limited to ¾-in. and yield strength of 60 ksi for the steel crossing the interface.

- Shear resistance is based on the ultimate load after cracking and is not valid when fatigue or slip is critical.

- The equation is only valid for normal weight concrete.

- The coefficient of friction does not depend on the concrete strength.

- The coefficient of friction is apparent and applicable to low stress levels only

- Clamping stress is limited to $0.15f_c'$.

Following research by Hanson (1960) and Kaar et al. (1960), the American Concrete Institute (ACI) Code in its 1963 provisions introduced the design provisions for steel crossing the interface between CIP slabs and precast beams. Push-off tests were found to be a relatively simple and inexpensive way of determining the horizontal shear strength compared to conducting full-scale tests on composite beams. The concept of "shear friction" was modified in the ACI Code (1970) based on push-off tests by Kriz et al. (1965), Birkeland and Birkeland (1966), Mast (1968), and Hofbeck et al. (1969). The Prestressed Concrete Institute (PCI) Design Handbook uses a procedure for calculating the shear strength based on the research conducted by Shaik (1978) as outlined in Section 2.5. Shaik's (1978) and Birkeland's (1966) equations provides a close representation of the test data but does not include the effect of concrete strength.

Diagonal principal stresses will be generated when shear is transferred along an un-cracked shear plane. This leads to short cracks less than or equal to 45° forming across the shear plane (Figure 2-2). Shear will be transferred by a truss mechanism if horizontal shear reinforcement is present.

Reinforcement and external compression provides the clamping force N. Failure occurs when the transverse steel yields permitting the concrete struts to rotate and the cracks to propagate at a flat angle that is almost parallel with the shear plane.

14
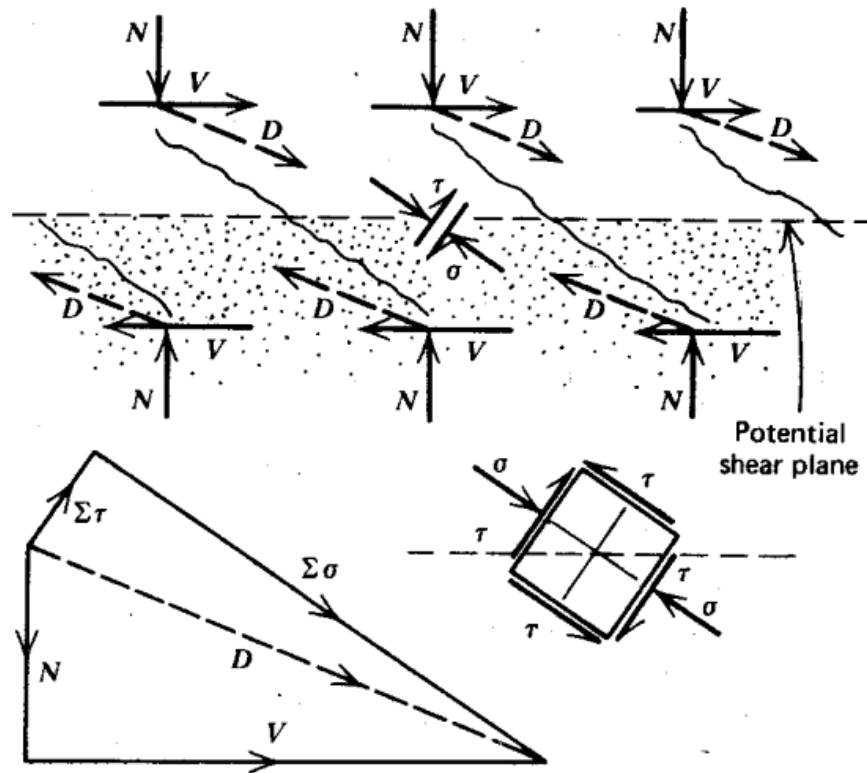
Figure 2-2 Interface shear mechanism along an un-cracked plane (Park and Paulay, 1975)

When the interface is already cracked, the mechanism of aggregate interlock is engaged. The larger the crack width, the larger the shear displacement and the smaller the ultimate strength attained. The addition of reinforcement across the shear plane can help with controlling the opening of the crack. These reinforcements will also be subjected to shear displacement hence increasing shear strength due to dowel action. Park and Paulay (1975) have identified three mechanisms of dowel action (Figure 2-3):

- The flexure of the reinforcing bar

- The shear strength across the bar

- Kinking of the bar

FLEXURE
$$V_d = \frac{2M}{\ell} = \frac{4d_b}{3\pi} \frac{A_s f_y}{\ell}$$

SHEAR
$$V_d = \frac{A_s f_y}{\sqrt{3}}$$

KINKING
$$V_d = A_s f_y \cos\alpha$$
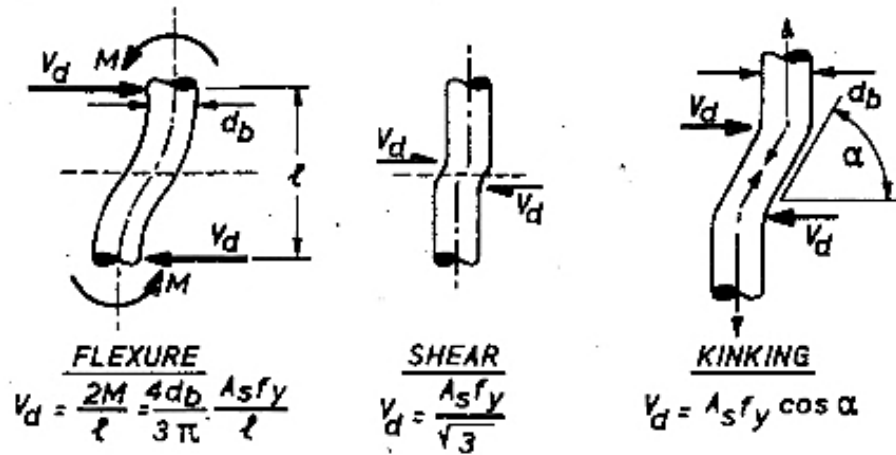
Figure 2-3 Dowel action along an interface (Park and Paulay, 1975)

Note that the yielding strength of the bar cannot be fully utilized for dowel action if the same bar is to provide clamping force for a bar in flexure or shear. Research conducted by Philips (1974) indicated that especially for small bars, the major source of dowel action is by kinking. Park and Paulay (1975) stated that dowel action is not a major component of shear-resisting mechanism when the crack at the interface is at acceptable limits. This is because considerably larger aggregate interlock shear stress would be developed.

2.2 Push-off Tests

The push-off test has been used to verify the concept of shear friction in laboratory experiments. Two L-shaped specimens are used to form the push-off specimen. One L-shaped concrete specimen is precast with or without steel reinforcing extending from the lower leg. The second L-shaped specimen is cast on top of the precast specimen to simulate a cast-in-place slab and the combined unit is loaded in direct shear along the interface. A typical push-off specimen is shown in Figure 2-4.

16
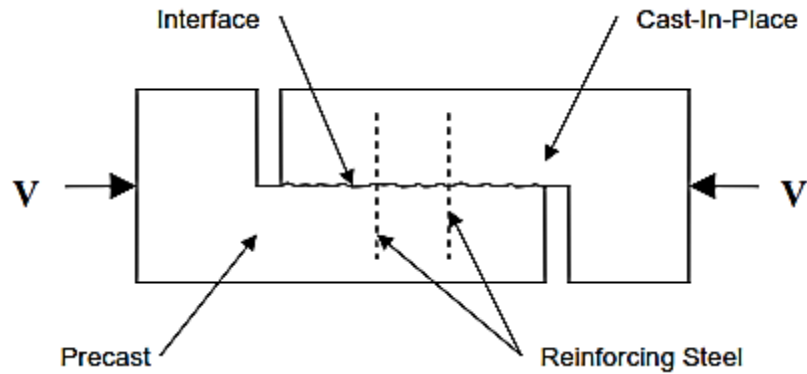
Figure 2-4 Typical push-off specimen (Sholz, 2004)

The push-off test has been used extensively by Birkeland (1966), Mast (1968), and Mattock (1969, 1972, and 1976) to quantify horizontal shear capacity between a precast and CIP concrete interface. To investigate shear transfer between a steel girder and precast concrete slab that were joined with steel studs and a mortar, the test was modified by Shim et al. (2000, 2001) by combining thin precast decks (250 mm) with steel beams using non-shrink grout in shear pockets (Figure 2-5).
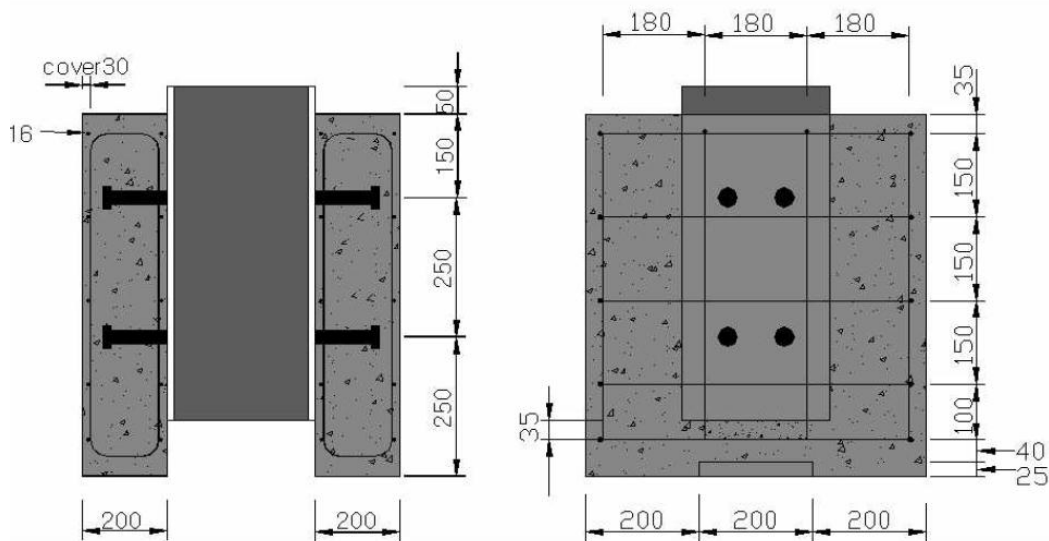
Figure 2-5 Typical push-off specimen for CIP slab (Shim et al., 2000)

The following is a summary on the different research carried out on interface shear using push-off specimens.

Menkulasi and Roberts-Wollmann (2002, 2003) modified the push-off test to represent a precast deck panel system with a haunch space between two precast L-shaped specimens and a shear pocket block-out in the deck side specimen (Figure 2-6). They performed three series of twelve push-off tests with three varying parameters: the haunch height, the mortar type, and shear connectors. For push-off specimens without shear connectors, a maximum shear stress of 125 psi was realized.

They compared their tests results to the ACI 318-11 (ACI, 2011), AASHTO Specification for Highway Bridges (2012) and AASHTO LRFD Bridge Design Specifications (2012) design equations for horizontal shear strength and found that the AASHTO LRFD method best predicted the precast deck panel system's behavior. The researchers then developed equations for predicting the horizontal shear strength based on their data.

For un-cracked interfaces the nominal horizontal shear resistance in terms of stress is:

$$v_{nh} = 0.16 + 0.51(A_{vh} \times f_y + P_{n)}/(b_v s) \quad \text{(best fit equation) (ksi)} \qquad \text{[2-2]}$$

For cracked interfaces the nominal horizontal shear resistance in terms of stress is:

$$v_{nh} = 0.02 + 0.86(A_{vh} \times f_y + P_{n)}/(b_v s) \quad \text{(best fit equation)   (ksi)} \qquad \text{[2-3]}$$

where:

v_{nh} = the nominal horizontal shear resistance in terms of stress (ksi.)

A_{vh} = area of reinforcement that crosses the interface (in.)

f_y = yield stress of the reinforcement (ksi.)

b_v = width of the interface (in.)

s = length of the interface (in.)
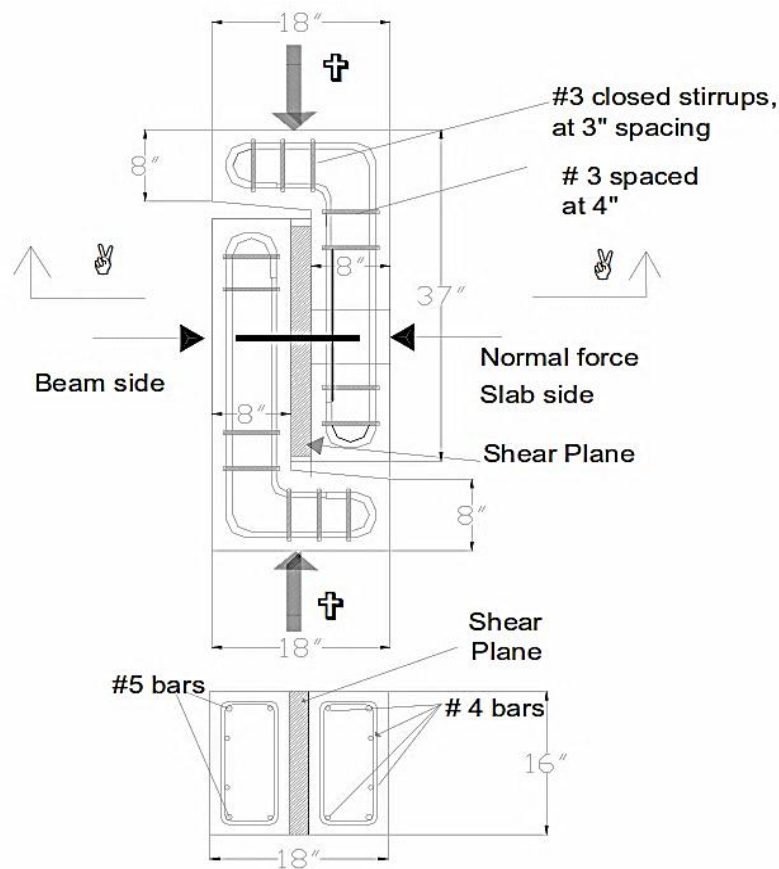
Figure 2-6 Typical push-off test specimen (Menkulasi and Wollmann, 2003)

Scholz (2004) investigated the mortar or grout system used to connect the precast panels to the bridge girders by filling the space in the horizontal shear pockets and the haunches. Several important mortar characteristics were identified and investigated in order to create a specification that indicates required performance criteria for mortars. He conducted push-off tests on six specimens with three different mortar types and a rake surface finish was provided with amplitude of ¼-in. Each test consisted of two L-shaped concrete blocks, one representing the girder and one representing the

deck panel slab. The shear pocket and haunch were filled with the mortar. The specimen was then loaded directly along the center line of the haunch to failure (Figure 2-7). A small normal force (2.5 kips) was also provided to simulate the clamping stress resulting from the tributary weight of a deck panel per girder spacing as well as other dead loads.

He concluded that sandblasting is unnecessary because it did not significantly increase the bonding capabilities of a concrete surface which had already been raked to amplitude of ¼-in.. He recommended a ¼-in. amplitude on the top flange of conventional girders.
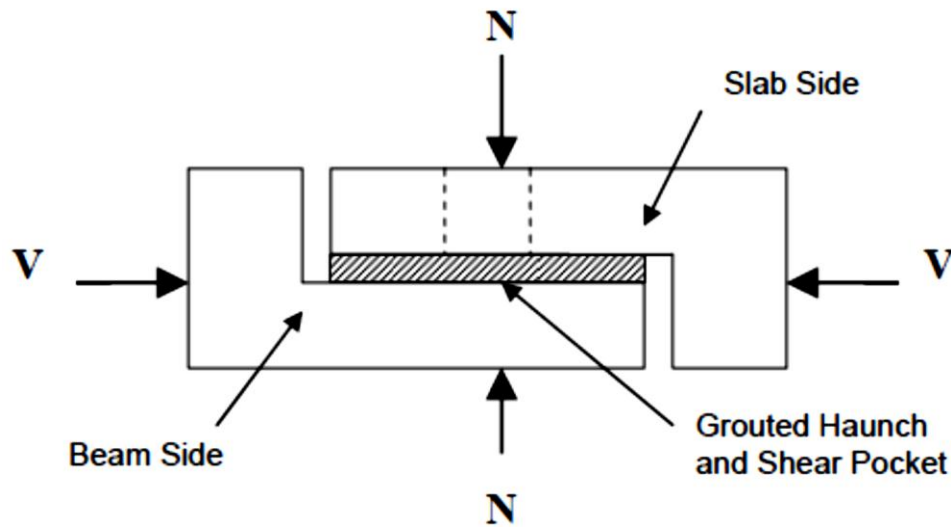
Figure 2-7 Typical push-off specimen (Scholz, 2004)

Trejo and Kim (2010) used the push-off test to assess the performance of different shear connector designs. Figure 2-8 shows a schematic of the push-off sample tested in the laboratory.

The 1.25-in. and 0.75-in. diameter all-thread rods were used as shear connectors, as recommended by TxDOT personnel.
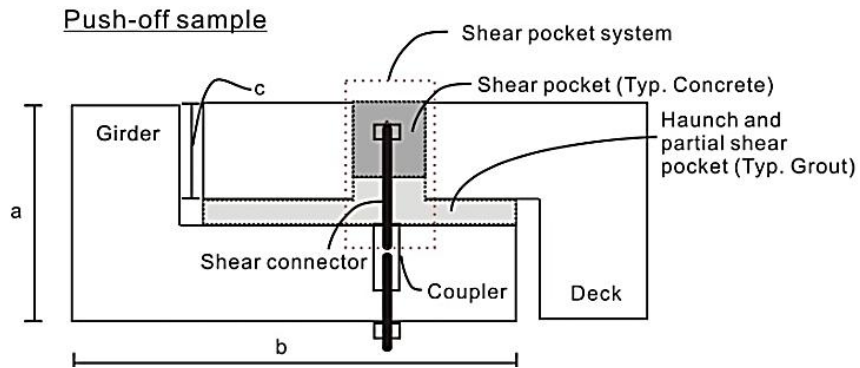
Figure 2-8 Push-off specimen with shear pocket (Trejo and Kim, 2010)

The researchers identified five stages of shear transfer and failure mechanisms (Figure 2-9):

- Initial adhesion loss (Stage 1),

- Shear key action (Stage 2),

- Shear key action failure at peak load (Stage 3),

- Dowel action of the shear connectors at sustained load (Stage 4), and

- Final failure of the system (Stage 5).
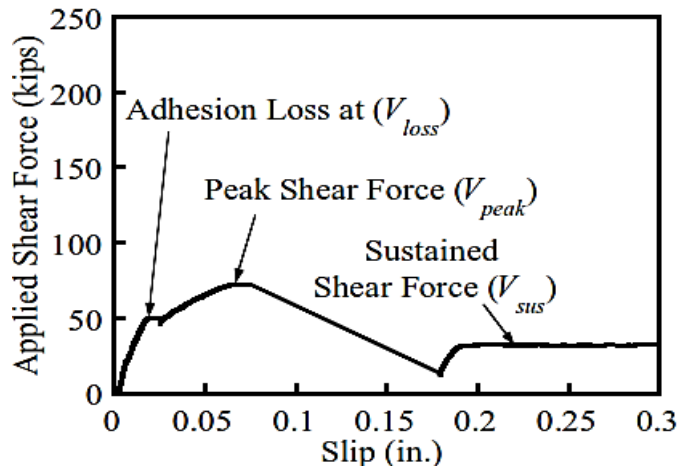
Figure 2-9 Typical failure mode (Trejo and Kim, 2010)

From the results gathered, the researchers proposed a new design equation to estimate the shear capacity of the girder-haunch-deck systems.

$$min \begin{cases} V_{peak} = c' \cdot n \cdot A'_{cv} + \mu_p \cdot (\Sigma A_s \cdot f_y) \cdot n \\ V_{sus} = \mu_r (A_s f_y + P_n) \cdot n \end{cases} \qquad \text{[2-4]}$$

V_{loss} = shear force at the adhesion loss,

V_{peak} = peak shear force,

V_{sus} = sustained or post-peak force,

c = the adhesion stress on the interface between girder and deck,

A_{cv} = effective interface area of concrete engaged in shear transfer (haunch and deck contact area),

c' = interlock of the crack surface in the shear pocket system,

A' = effective interface area of the concrete engaged in shear transfer (referred to as the cracked area in the shear pocket system),

A_{sc} = cross-sectional area of shear connectors,

f_y = yield strength of the shear connector,

μ_p = coefficient of friction at peak shear force for surfaces roughened to an amplitude of approximately 0.20-in. to 0.25-in.,

μ_r = coefficient of friction at sustained force (herein 80% of V_{sus}) for surfaces roughened to an amplitude of approximately 0.20-in. to 0.25-in., and

P_n = permanent normal force to the shear plane.

n = number of pockets per overhang panel.

The results from the test revealed that the roughened surface on the girder provides a stronger adhesion between the haunch material and the adjacent girder surface in the push-off specimens. However, dowel action of the shear connectors was seen as likely the main source of the interface shear capacity after shear key failure.

National Cooperative Highway Research Program (NCHRP) (2008) investigated the shear capacity of headed-studs as shear connectors between concrete panels and structural steel girders. The researchers conducted push-off tests on the systems with four and eight headed-studs (each 1.25-in. in diameter). Cross ties and steel tube systems were used to confine the grout in the shear pocket that surrounds the shear connectors so as to improve the interface shear capacity. The results from the test indicated that push-off tests are sufficient to reflect the performance of full-size specimens. They also found that the HSS (hollow structural section) steel tubes could effectively confine the grout that surrounds the shear studs in the shear pockets. However, test results showed high peak loads with relatively low ductility. They proposed design recommendations to achieve the peak shear resistance of the system based on this study.

Hanson (1960) studied the composite action between concrete girders with CIP concrete slabs. He cast and tested sixty-two push-off specimens and ten composite T-beams to investigate the horizontal shear transfer strength. The push-off specimens contained horizontal shear reinforcement embedded 4-in. into the CIP slab (Figure 2-10). The horizontal shear reinforcement was positioned in most cases at the center of the shear length (which varied from 6-in., 12-in. or 24-in.) but in some specimens two or three horizontal shear reinforcements were placed evenly along the shear length.

Several finishes were applied at the interface;

- Smooth: surface trowelled to a relatively smooth condition.
- Rough: surface roughened by scraping with the edge of a metal sheet (3/8-in. amplitude).
- Bond: concrete cast directly on to a dry girder surface.

- Un-bonded: surface painted with a silicone compound to prevent the new concrete from bonding with the precast concrete.

- Smooth aggregate bare: aggregates protruding on the surface.

- Rough aggregate bare: no paste on projecting aggregates.

- Shear keys: 5-in. square in the direction of the shear force and 2.5-in. deep into the girder concrete.
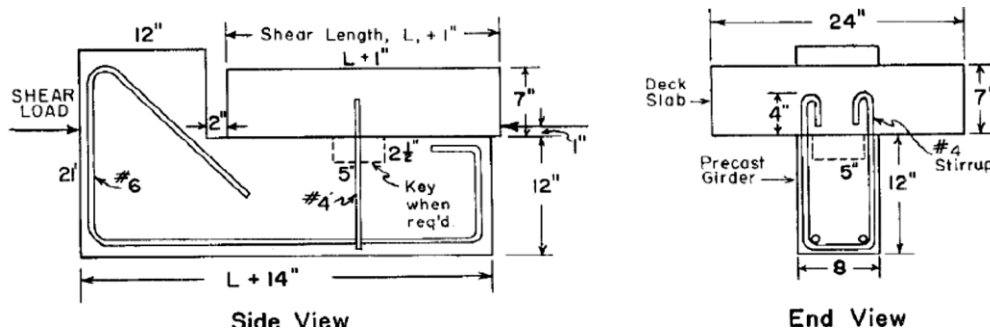
Figure 2-10 Typical push-off specimen (Hanson, 1960)

Test results indicated that the shear keys led to a slight change in the shear-slip curves. The contact area was found to act as a unit and failed without the effects of the key being realized. This indicated that the bond had to be broken before the shear key acts. Although concrete strength was not the main focus in this research, tests revealed that shear stress appeared to be approximately proportional to the concrete strength of the CIP slab.

Birkeland and Birkeland (1966) postulated that a crack that forms in a monolithic concrete block along the failure plane will lead to slippage along the shear plane when an external shear load V is applied. The slippage is resisted by the friction μP resulting from the clamping force P. They also showed that the tension T due to reinforcement across the interface produced the equivalent of the external clamping force P (Figure 2-11).
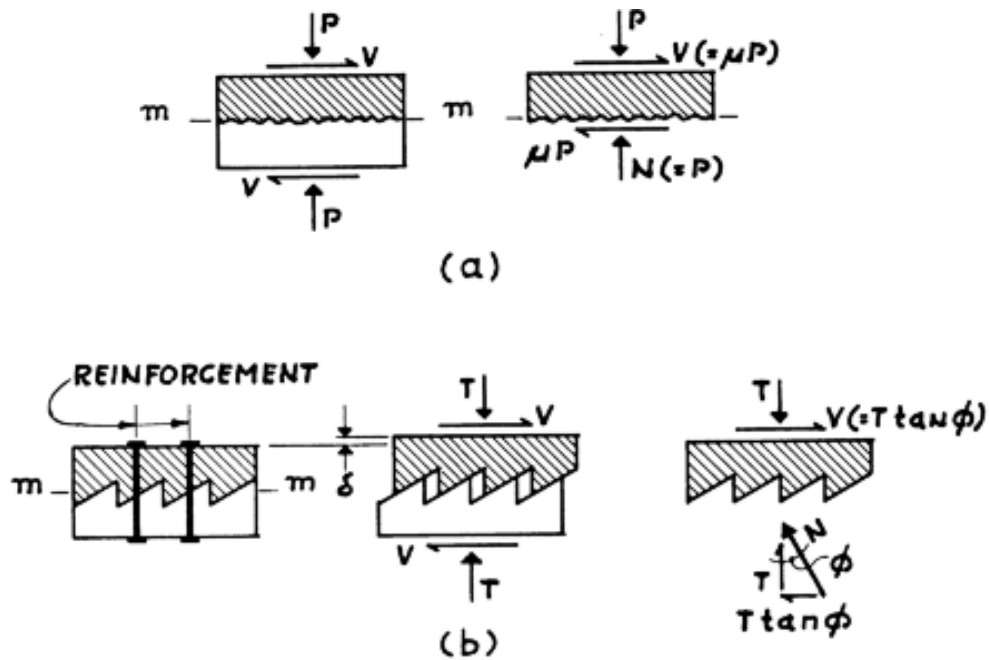
Figure 2-11 Shear friction hypothesis (Birkeland and Birkeland, 1966)

They then introduced a parabolic function for the horizontal shear strength at the interface as shown below:

$$v_{nh} = 33.5\sqrt{r_v f_y} \qquad \text{(psi)} \qquad\qquad [2\text{-}5]$$

They supported their hypothesis by the use of Hanson's (1960) push-off test to represent rough-bonded and rough-unbounded specimens, Anderson's (1960) push-off specimens to simulate building connections, and Mast's (1968) specimens to prove the design of horizontal shear connection between the precast longitudinal strips of a barrel shell roof. The strength data was then plotted to compare their hypothesis to the test data from these researchers. They then concluded that the shear friction hypothesis is an extremely useful tool which is simple and easy to apply and suggested that a test program be conducted to specifically verify the hypothesis.

Hofbeck et al. (1969) investigated the horizontal shear transfer across a plane for cracked and pre-cracked interfaces. The clamping stress, concrete strength, and

reinforcement yield strength were investigated by testing thirty-eight push-off specimens. The researchers concluded that a pre-existing crack along the shear plane reduced the ultimate shear transfer and increased the horizontal slip. A 250 psi reduction in the shear strength was expected for a 4000 psi normal weight concrete with clamping stresses between 200 psi and 1000 psi. The reduction was higher for lower values of clamping stress. For clamping stresses above 1000 psi, there is a very slow rate of increase in the interface shear strength of initially un-cracked specimens with an increase in clamping stress, while the strength of the initially cracked specimens continued to increase at the same rate as for lower clamping stresses. Consequently, the horizontal shear strength for cracked and un-cracked interface was approximately equal for a clamping stress of 1,340 psi as shown in Figure 2-12.
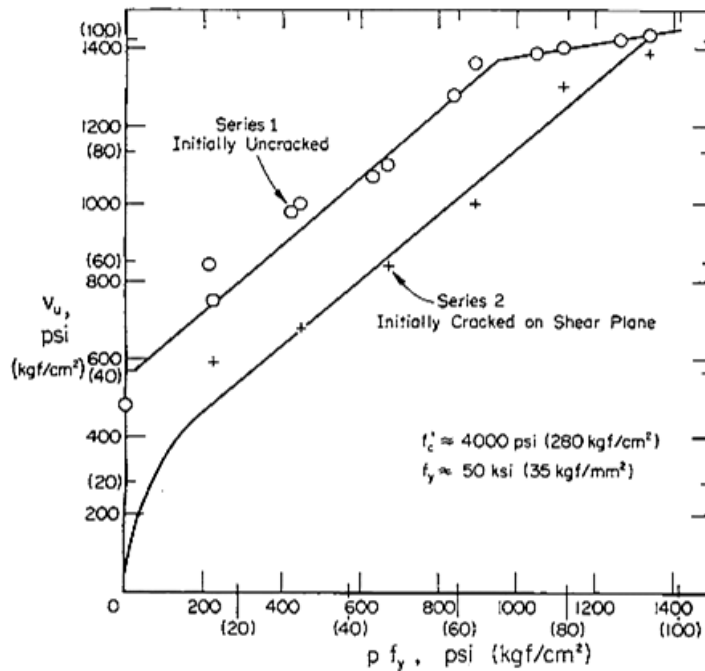
Figure 2-12 Push-off test results (Hofbeck et al., 1969)

Hofbeck et al. (1969) also noted that the shear strength of initially cracked specimens is not directly proportional to the amount of reinforcement. Specimens with a

26

pre-existing interface crack were found not to be affected by the concrete strength for values of clamping stress of up to 600 psi. Changes in strength, size and spacing of grade 60 reinforcement did not affect the horizontal shear strength for the same clamping stresses. They also concluded that dowel action does not contribute significantly to the shear transfer strength of initially un-cracked specimens but has a significant effect in initially cracked specimens. Hence the shear friction theory was found adequate in estimating the shear strength for the case of initially cracked specimens with a friction coefficient of $\mu = 1.4$ but conservative in the case of an un-cracked interface.

Kamel (1996) carried out push-off tests to evaluate the performance of several different types of shear connection schemes under ultimate horizontal shear stress and fatigue. A series of tests were carried out on specimens having a double shear interface and a single shear interface. Among the steel shear connectors applied were headed and headless high-strength bars and reinforcement stirrups whereas the type of interface included debonded shear keys, bonded roughened interfaces, unbonded roughened interfaces, smooth interfaces (both debonded and bonded). The roughened interface was applied to the top surface of the precast concrete section using a stiff bristled brush. The brush was moved in a circular motion to produce a ¼-in. amplitude on the surface. Specimens containing a roughened interface were used to evaluate the ability to remove the top concrete deck from the bottom girder using a 60 pound jack hammer.

Results from his fatigue tests showed that the specimens behaved in a similar manner under ultimate strength as an identical specimen that was not subjected to fatigue after the test was completed. He thus concluded that fatigue will have no effect on the service or ultimate capacity of these types of connections. The author concluded that the steel connectors do not necessarily contribute to the shear resistance in bonded systems until the bond is broken. He also suggested that a spacing greater than 24-in.

currently specified by AASHTO Standard Specifications (2014) can be applied for design for sections with bonded interfaces. The author observed that the shear stress for debonded smooth interface was generally constant for all levels of clamping stress whereas the shear stress for debonded shear keys was seen to increase with increase in clamping stress. The author observed that all three components of the horizontal resistance contributed to the resistance in his fatigue tests.

Mattock and Hawkins (1972) conducted investigations to show how concrete strength, shear plane characteristics, reinforcement and direct stress (stresses acting parallel or transverse to the shear plane) affect the interface shear strength of reinforced concrete. Pull-off and modified push-off specimens were used to study the influence of direct stresses acting parallel and transverse to the shear plane respectively.
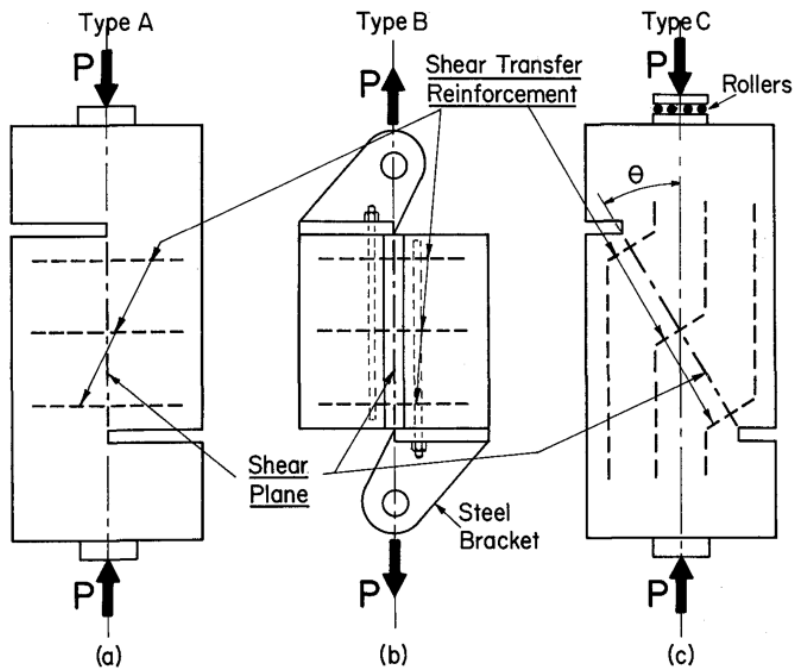
Figure 2-13 (a) push-off; (b) pull-off; and (c) modified push-off specimens

(Mattock, 1969)

The length and width of the shear planes were 10×5-in., 12×4.75-in. and 12×6-in. in the push-off, pull-off and modified push-off specimens, respectively. The specimens were monotonically loaded to failure and slip measured along the shear plane as well as lateral separation at the shear plane.

Mattock also tested pre-cracked shear transfer specimens to account for the possibility of a crack existing along the shear plane. The results showed that the slip in a pre-cracked specimen was greater in all stages of loading than for an un-cracked specimen. Furthermore, the ultimate shear strength is reduced if the specimen is also under-reinforced. This decrease was seen to happen more in the push-off specimens than in the pull-off specimens. They also found out that for values of ρf_y below 600 psi, the concrete strength does not appear to affect the shear strength. On the other hand, for higher values of ρf_y, the shear strength is lower for the lower strength concrete.

They then conducted an analytical study to determine the influence that direct stress parallel to the shear plane has on the shear strength. They concluded that the shear strength of initially cracked concrete with moderate amount of reinforcement is primarily developed by frictional resistance to sliding between the faces of the crack and by dowel action of the reinforcement crossing the crack.

Mattock et al. (1976) investigated the shear transfer strength of lightweight aggregate concrete. They tested both initially un-cracked specimens and specimens cracked in the shear plane. Ten series of push-off specimens with a shear plane area of 50 in^2 were tested. For the initially un-cracked specimens, neither slip along the shear plane nor separation across the shear plane occurred until the formation of diagonal tension cracks in the region of the shear plane. Slip occurred along the pre-crack in the shear plane from the commencement of the loading and at a progressively increasing rate. They concluded that the shear strength of lightweight concrete is less than that of

sand and gravel concrete (normal weight concrete) having the same compressive strength.

Mattock, Johal, and Chow (1975) conducted tests on six series of specimens, four corbel type push-off specimens and two standard push-off specimens, in order to view the influence of moment or tension acting on the shear plane has on shear transfer as well as to validate the assumptions made in Section 11.5 of ACI 318-71. The researchers discovered that there is no interaction between moment and shear transfer, meaning that an additional applied moment will not reduce the shear transfer across a crack. Furthermore, the assumptions made in section 11.5 of ACI 318-71 that reinforcement needed to carry both shear and tension across a crack can simply be added were validated by the test results. The results also found that it is more appropriate to add the normal stress parameter to the reinforcement parameter when calculating shear transfer strength. They then concluded that the design equation provided by ACI 318-71 were conservative for small values of ρf_y and unnecessarily limited the ultimate shear transfer stress to 800 psi. They instead suggested the equations proposed by Birkeland (1968) where, $v_u = 33.5\sqrt{\rho_v f_y}$, and Mattock (1974) where, $v_u = 400 + 0.8\rho f_y$ but not less than $0.3f_c'$, were both equally acceptable and more economical for design use.

Walraven, Frenay and Pruijssers (1987) conducted a statistical analysis to propose new shear friction equations for determining the shear capacity of the cracked interface of reinforced concrete members. They based their research on existing test data collected from eighty-eight push-off test results by Hofbeck (1969), Frenay (1985), Walraven (1981) and Pruijssers (1989). They proposed that the influence of concrete strength is a basic parameter to consider in calculating the horizontal shear strength.

From their analysis they concluded that the traditional shear friction equation without cohesion term is conservative especially in the region of low reinforcement ratios or high concrete strengths. Also that great accuracy can be achieved by considering the concrete strength as a basic parameter. They formulated an equation that is accurate over a wide range of parameters.

$$1000 < \rho_v f_y < 1500 \, psi$$

$$2500 < f_c' < 9000 \, psi \qquad\qquad\qquad [2\text{-}6]$$

The above equation is valid in conditions whereby the aggregate is sufficiently strong to resist breaking by cracking due to horizontal shear.

Khan and Mitchell (2002) carried out an experimental study on fifty push-off specimens with cracked, pre-cracked, and cold-joint interfaces to determine if the current ACI codes were applicable for high strength concrete. They designed the specimens to be identical to those used by Hofbeck (1969), Mattock (1976), and Anderson (1960) for comparison purposes. The cold-joint specimens were not floated or intentionally roughened but left as cast. Results showed that the un-cracked and cold-joint specimens developed diagonal cracks between 15° and 45° to the shear plane at loads between 50% and 75% of the peak ultimate capacity. On the other hand, in the pre-cracked specimens, slip between the two faces began immediately upon load application. Cracking away from the shear plane was not observed until significant yielding of the reinforcement had occurred. They concluded that the ACI 318-99 shear friction provisions give a conservative estimate for the interface shear strength for high-strength concrete.

Paulay, Park, and Phillips (1974) investigated the contribution of dowel action, surface preparation, and reinforcement content towards the shear strength of construction joints subjected to monotonic and cyclic loading. They tested thirty-six push-off specimens having varying surface preparation and three different amounts of

31

reinforcement across the joints. To eliminate shear transfer in some of the specimens, bond was minimized by spraying varnish on some rough surfaces or applying melted wax on some smooth surfaces. The purpose of these specimens was to determine the load-slip relationship for dowel action. The researchers concluded that for design purposes, the contribution of the dowel action of the reinforcement should be ignored. Although significant dowel forces can be generated, excessive slips are expected along the joint.

Kent et al. (2012) carried out an in-depth review of previous work on interface shear as well as complementing it with an experimental study. The researchers set out to prove that the interface shear equations in ACI 318-08 are more conservative than those of AASHTO (2007). They also argued that that the inclusion of the cA_{cv} term in AASHTO (2007) increases the shear-friction capacity to unwarranted levels and does not help to calibrate the equation with existing experimental data as asserted in the commentary of the AASHTO (2007) provisions. They tested eight typical push-off specimens (Figure 2-14) having steel ties across the interface that simulated interface reinforcement. No. 3 and No. 4 bars were tested having two steel grades, ASTM A1035/A1035M high-strength (f_y = 100 ksi) steel and ASTM A615/A615M (f_y = 60 ksi) steel.

It was observed that the use of ASTM A1035/A1035M high-strength steel instead of ASTM A615/A615M steel at the interface did not increase the shear friction capacity of the specimens significantly. This is because the ultimate shear capacity was controlled by concrete behavior and was reached well before steel yielding occurred. They therefore suggested that the clamping force is a function of the steel modulus rather than the yield strength.
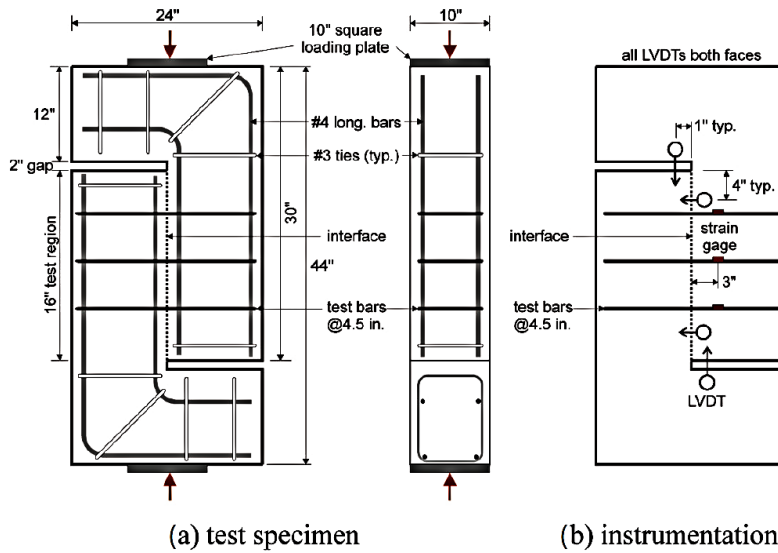
Figure 2-14 Typical push-off specimen (Kent et al., 2012)

The researchers concluded that while the reinforcing ratio affects the shear-friction capacity, the steel grade does not. He also concluded, similar to Park and Paulay (1974), that due to the complex nature of the shear friction mechanism, it is not possible to explicitly separate all parameters contributing to shear-friction behavior or establish explicit predictive behavior. They concluded that the AASHTO (2007) relationship for shear friction capacity does not capture the mechanism of shear friction and incorrectly implies that the interface reinforcement yields as the ultimate capacity is reached.

Mones and Brena (2013) investigated the influence of surface preparation techniques on interface shear strength between hollow core slabs and cast-in-place toppings. Both dry-mix and wet-mix hollow-core slabs were tested. The researchers tested twenty-four specimens having two different methods of hollow-core production. The tests were conducted on push-off specimens consisting of two blocks of concrete cast at different times. The interface was finished using different methods; machine-

33

finished surfaces, longitudinally raked surfaces, sandblasted surfaces, longitudinally or transversely broomed surfaces with grout added to some of those surfaces.
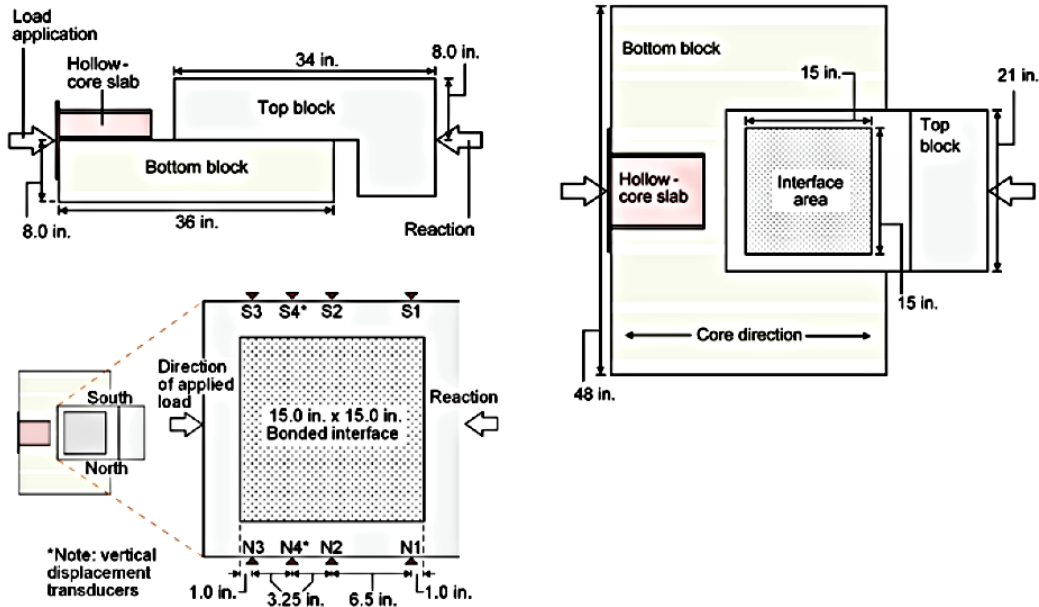
Figure 2-15 Typical push-off specimen and instrumentation (Mones and Brena, 2013)

They measured the surface roughness qualitatively using the sand patch test (ASTM E96). The test revealed that the surface of the wet-mix bottom blocks generally contained laitance compared to the dry-mix specimens. It typically gathered within valleys of the roughness undulations of wet-mix specimens especially on broomed surfaces. They concluded that laitance could be the cause for high variability observed in strength results of replicate wet-mix specimens. They also carried out a parametric study to estimate the maximum superimposed live load that different hollow-core slab cross-sections can support without reaching flexural, vertical shear or horizontal shear failure. They concluded that roughened interfaces developed higher strength and higher horizontal slip capacity compared to machine-finished interfaces. Roughening was more effective when it was perpendicular to the applied shear force. They also concluded that

dry-mix hollow-core slabs had higher interface shear strength than wet-mix. This was due to the presence of laitance in the wet-mix hollow-core slabs. Analysis of simply supported hollow-core slabs under distributed load showed that horizontal shear strength only governs when the web is thick and the slab is of a short span.

2.3 Pullout Tests

Rehm (1969) carried out pullout tests to demonstrate that a bend with less than 180° turn does not necessarily provide anchorage superior to a straight bar of the same length. The bend introduces stress concentrations, consequently large local deformations in the concrete, which in turn lead to increased slip at the loaded end of an embedded bent bar, For the same embedded length of bar, the bar with smaller curvature gives smaller slip. Figure 2-16 (a), in which bars with different bend angles but identical embedded lengths are compared, illustrates this observation. Another important factor affecting bar slip is the direction of casting. The difference in performance between various bend angles become significant when the bar is pulled in the direction of concrete casting (Figure 2-16 (a)), which is the case for the CIP composite slabs. This is due to the fact that the bond between the anchored bars and the concrete is affected by water and mortar migration toward the inward side of the bars, which in turn leads to a weakened zone upon bearing.

(a)   (b)
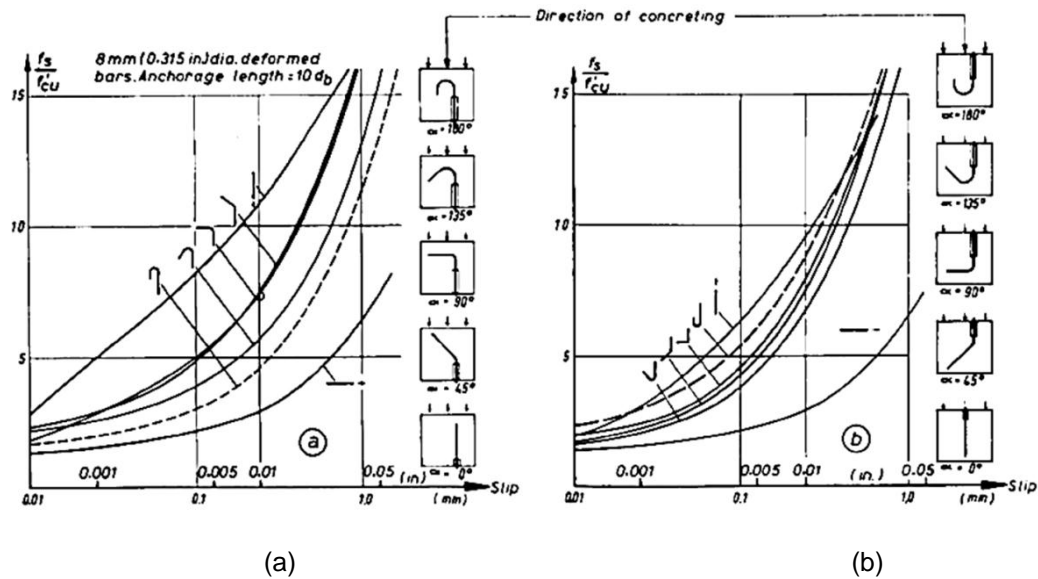
Figure 2-16 Performance of anchorages of deformed bars with various degrees of bends:

(a) Top-cast bars (similar to that used to cast the CIP deck); (b) Bottom-cast bars (Rehm,

1969)

Marques and Jirsa (1975) carried out experimental study regarding the pullout behavior of hooked bars. The stresses and slip measured at points along the hook of a bar in tests of 90° and 180° hooks (No. 7 bars) are plotted in Figure 2-17. The axial stresses in the bar decreased due to the bond on the lead-in length and the bond and friction on the inside of the bar. The magnitude and direction of slip at A, B, and C are shown by the arrows. It is interesting to observe that, for the 180° hook, the slip measured at A was 1.75 times that measured at A in the 90° hook. When it is realized that a bend introduces stress concentrations, consequently large local deformations in the concrete, which in turn lead to increased slip at the loaded end of an embedded bent bar, it is not surprising that for the same embedded length of bar, the bar with a smaller curvature gives better performance (Rehm, 1969).

36

(b) Stresses and slip—90° standard hook.

(c) Stresses and slip—180° standard hook
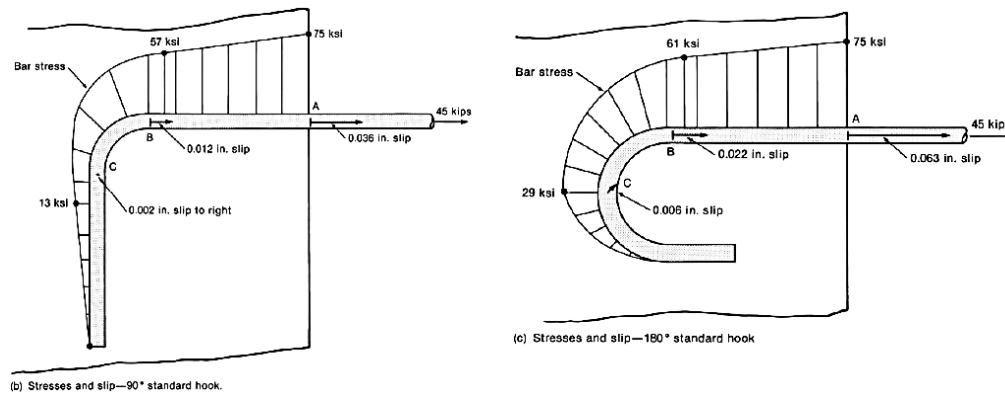
Figure 2-17 Stress and slip on hooked bars (Marques and Jirsa, 1975)

Mattock (1987) reported tests of hook and loop stirrup anchorages in thin toppings cast against precast members (Figure 2-18). Variables included stirrups size, topping thickness, topping concrete strength, rough or smooth interface, and tensile strain normal to the anchorage.

It is shown that No. 3, No. 4, and No. 5 bar stirrups can be anchored in 3-in., 3.5-in., and 4-in. thick, normal weight concrete toppings, respectively. For design purposes, he suggested that either standard 90° hooks or closed loop anchorages of overall width w (see Figure 2-18), at least 9-in. This is 2.6 and 1.5 times the widths of the interface reinforcement used in the TxDOT box (before 2012) and slab beams, respectively. The embedded length of the No. 4 reinforcement in a 3.5-in. thick topping in his study was 2.75-in., which is close to the one used in current TxDOT practice (2-in.). However, Mattock's set-up is not representative of what occurs in real bridges. It provides concrete confinement due to the compressive force applied by the hydraulic ram which delays the concrete from cracking (Figure 2-19).
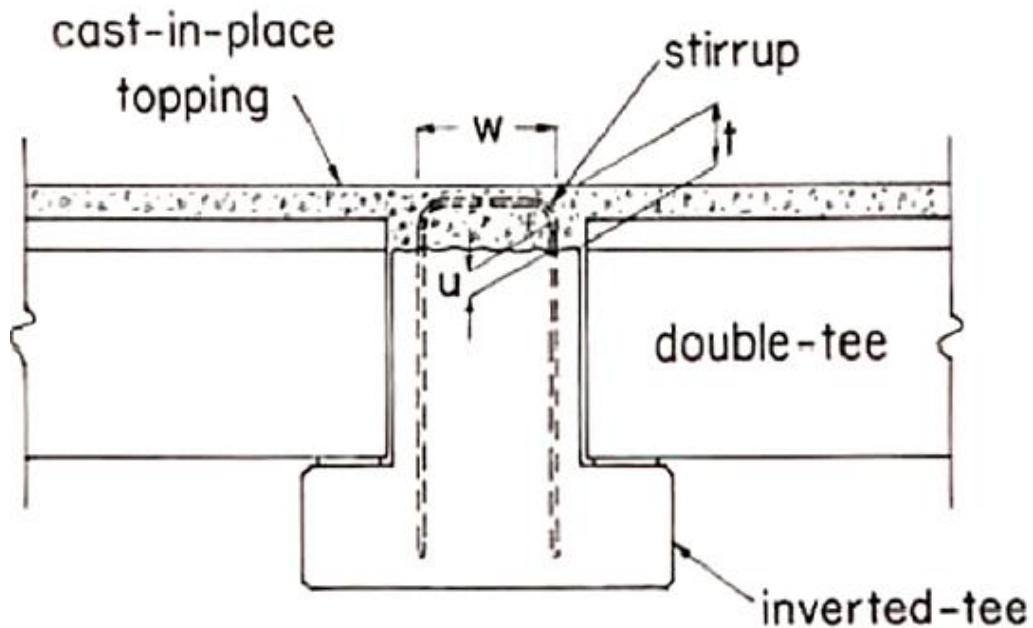
Figure 2-18 Typical test specimen (Mattock, 1987)

This may have resulted in a higher pullout capacity and possibly yielding of the reinforcement before bond failure, giving un-conservative results for design. In light of this, the bar pullout test set-up used in this TxDOT research was designed to provide the least confinement to the concrete and hence lead to more realistic results. The bar pullout test set-up is described in Chapter 4.
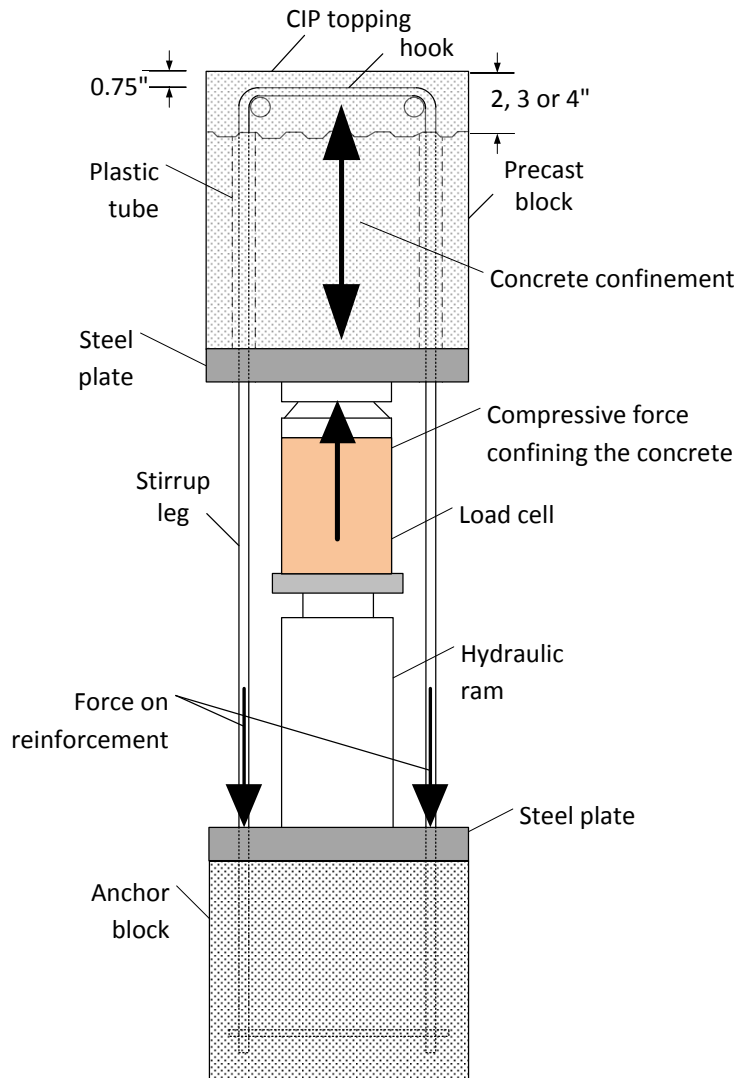
Figure 2-19 Test set-up used by Mattock (1987)

2.4 Full-scale Beam Tests

Hanson (1960) studied the composite action between concrete beam girders with CIP concrete slabs. He cast and tested sixty-two push-off specimens and ten composite T-beams to investigate the horizontal shear transfer strength. The beams were designed to reach high horizontal shear at the interface at a load well below flexural failure. The

beams were tested in two series: in series-I beams were loaded at two points, and in series-II beams were loaded at three points.
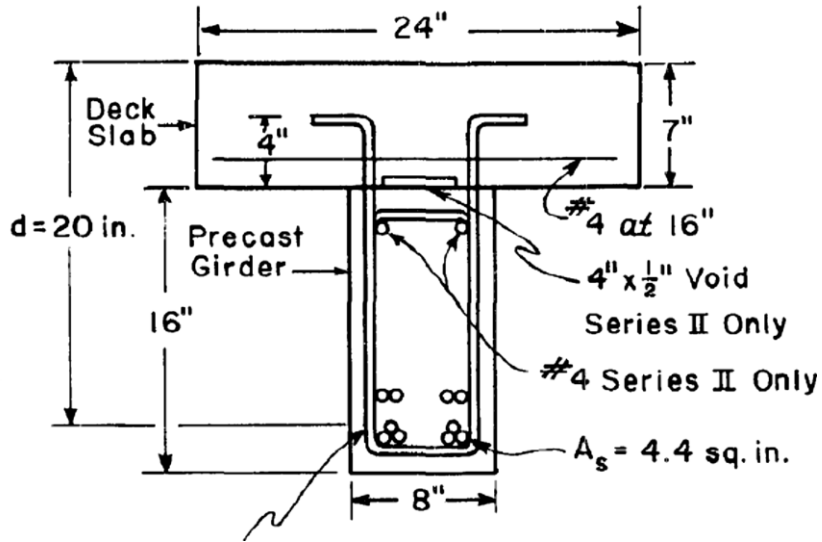
Figure 2-20 Cross section of beams (Hanson, 1960)
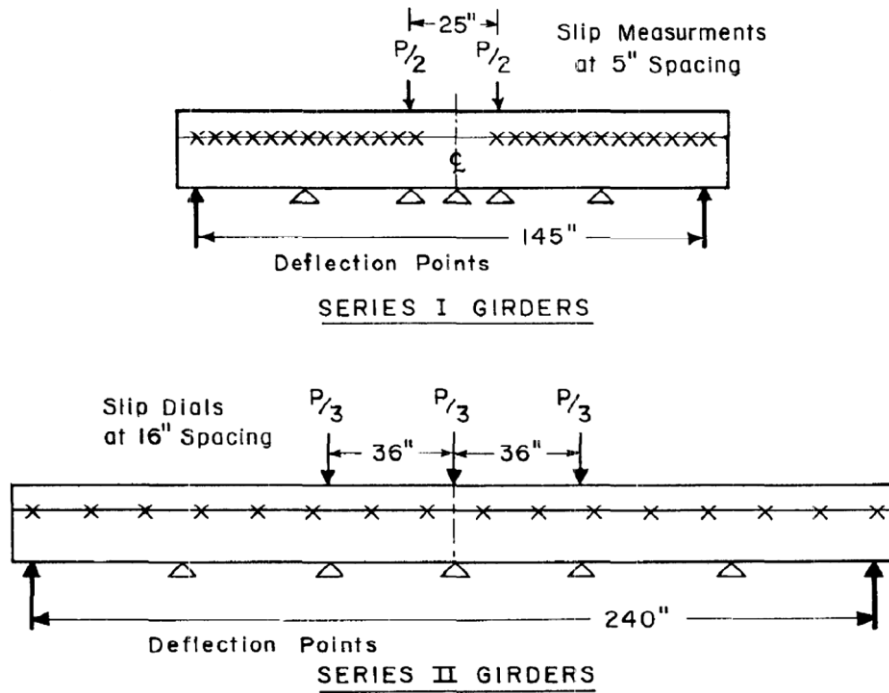
Figure 2-21 Test set-up for series I and II (Hanson, 1960)

From the results of the beam test, Hanson concluded that composite action was lost at the critical slip value of 0.005-in. He suggested that a maximum shearing stress for composite action to be 500 psi for a roughened bonded interface for concrete strength between 3000 psi and 5000 psi. If additional steel reinforcement crossing the interface is to be provided in excess of the required amount, an additional horizontal shear capacity of 175 psi may be added for each percent of stirrup reinforcement.

Loov and Patnaik (1994) conducted an extensive study on the horizontal shear strength of composite concrete beams with roughened interface for a wide range of steel ratios. Sixteen composite beams with different geometries (Figure 2-23) were tested. The major variables in their study were the clamping stress and the concrete strengths. The clamping stress was varied by adjusting the amount of steel crossing the interface and the width of the precast concrete girder. The interface was left as-cast with some aggregate protruding. The beams were simply supported and loaded with a point load at the center span. The beams were designed to be strong in vertical shear and flexure so that the first mode of failure is horizontal shear. Their test showed that slip was insignificant up to a horizontal shear stress of 220 to 290 psi. It increased with stress up to a slip ranging from 0.01-in. to 0.03-in. They also observed that there was little difference between the shear stress at a slip of 0.2-in. and the shear stress at peak load.

Their results showed that stirrups were not stressed until a horizontal shear stress of about 220-290 psi (Figure 2-24) and did not yield at a slip of 0.005-in. as was proposed by Hanson (1960) but instead began to yield at a slip of 0.02-in. He concluded that elastic analysis using cracked transformed section properties is a valid assumption and a simple method for estimating the horizontal shear stresses in composite concrete beams at failure.

(a) Test Beam with Full Length Flanges

(b) Test Beam with Short Flanges

All Dimensions are in mm
(1mm = 0.0394")
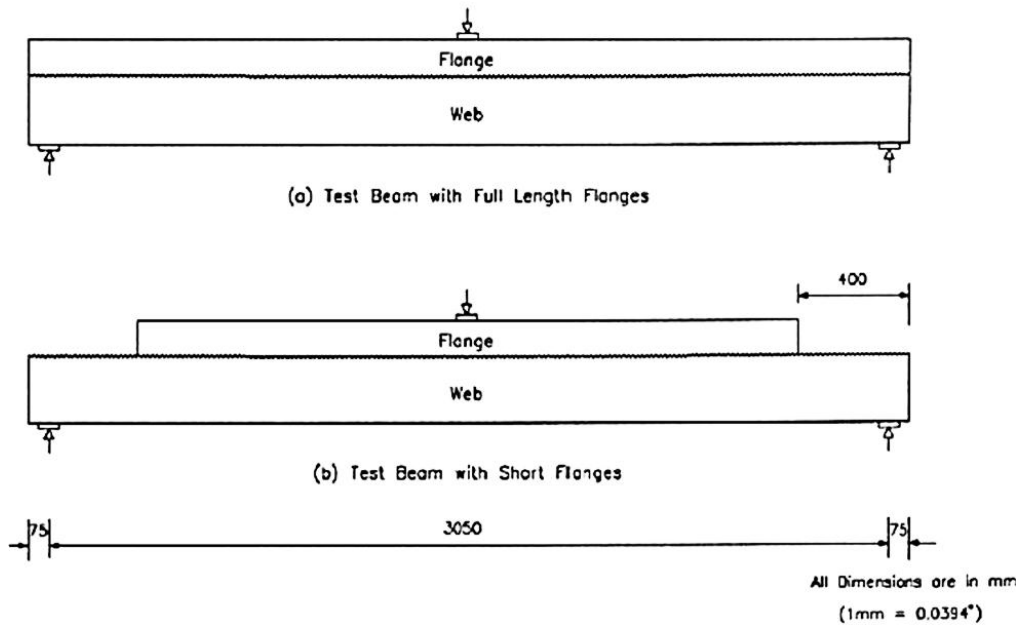
Figure 2-22 Typical test beams (Loov and Patnaik, 1994)

(a) Beam Section with Thin Web   (b) Beam Section with Uniform Web Width
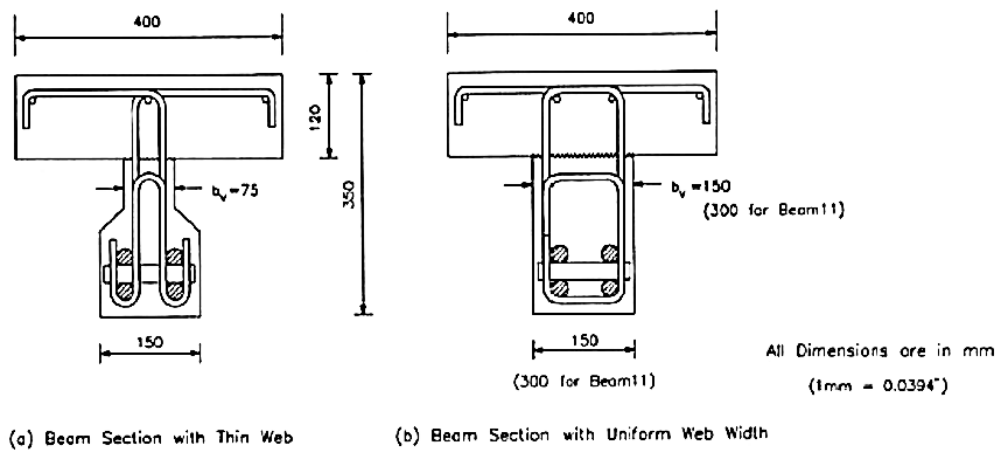
Figure 2-23 Typical cross-section of test beams (Loov and Patnaik, 1994)
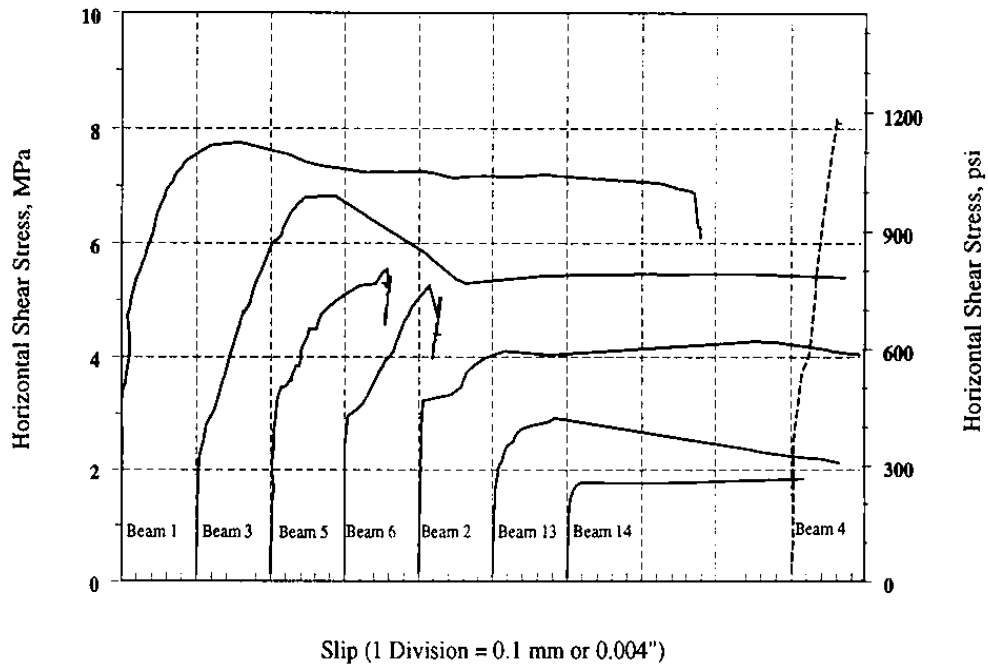
Figure 2-24 Test results for beams 1 through 6 and beams 13 and 14 (Loov and Patnaik, 1994)

Seible and Latham (1990) conducted preliminary studies on the horizontal shear transfer behavior of overlaid reinforced concrete bridge decks combined with experimental results of the effects of interface preparations and dowels on horizontal load transfer. Shear block tests, full-scale transverse bridge deck slab panel tests and a full-scale prototype bridge deck test were conducted. They investigated six different surface preparations. These included:

- Monolithic: specimen cast monolithically.

- Lubricated: a rough construction joint was sprayed with a bond breaking agent to eliminate chemical bond between the old and new concrete.

- Surface rough: wood float finish and light sandblasted interlayer surface.

- Scarified: grooves greater than 1/8-in. deep cut into the old concrete with a jack hammer.

- Lubricated and dowels.

- Surface rough and dowels.

- Scarified and dowels.

Results from the shear block and slab panel test showed that the vertical construction joint performance is evidently influenced by the surface preparation. Also that the dowel-reinforced specimens were controlled by dowel yield at a level of ρ_d =0.28% dowel reinforcement. The lubricated specimens exhibited very early delamination of the interlayer and independent flexural cracks developed in the old and new concrete slabs. The surface rough specimens had the initiation of flexural crack propagation into the overlay with only temporary arrests and slight horizontal deviations. Failure occurred by delamination well above the flexural yield limits. Differences in behavior between surface rough and scarified specimens were only noticed at ultimate failure. They also came to the conclusion that the 0.07% dowel reinforcement did not influence the crack pattern development and was not sufficient to control the ultimate delamination crack. They stated that interface dowels are only beneficial in confining the crack after the fact. The following conclusions were made by the researchers:

- A delamination of a rough and clean interface is not likely to occur under service and overloads.

- Reinforcement dowels in horizontal construction joints for full depth structural concrete overlays are not effective as long as a rough and clean interface is provided.

- The minimum interface reinforcement of 0.08% by AASHTO (1983) proved inefficient once delamination occurred. The dowel reinforcement ratio of

0.28% provided in the shear blocks was clearly sufficient to control interlayer slip behavior.

Tan et al. (1999) conducted tests on four composite beams loaded in indirect two-point load to ascertain their horizontal shear strength. Two shapes of ties were used; open and closed ties (Figure 2-25).
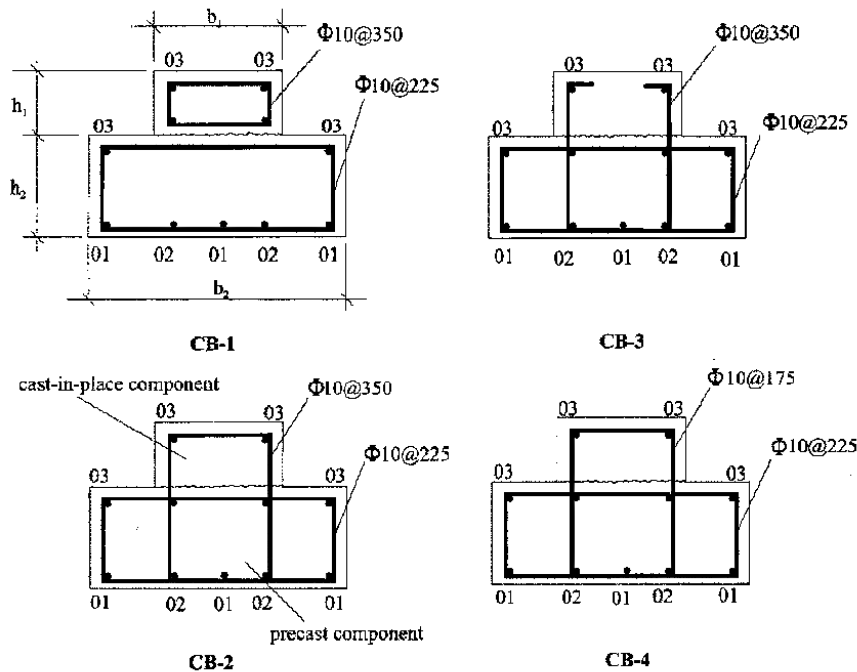
Figure 2-25 Test specimens (Tan et al., 1999)

The beams were tested monotonically to failure. The researchers concluded that the shapes of ties across the interface may not significantly influence the horizontal shear strength as long as adequate anchorage of ties is provided. They also concluded that indirect loading has an adverse effect on the horizontal shear strength.

Kovach and Naito (2008) investigated the shear friction of girder-deck systems having no shear connectors. Their research aimed to determining if there was a possibility of increasing the allowable horizontal shear capacity between a precast beam

and CIP slab without the use of horizontal shear reinforcements. The interface width on some beams (Figure 2-26(a)) was reduced by cutting 1.5-in. of concrete from each side with a concrete saw in order to ensure horizontal shear failure. A five-point loading configuration was employed to examine the service state of horizontal shear stresses whereas a two-point loading configuration was used to examine the failure state of the horizontal shear stresses.
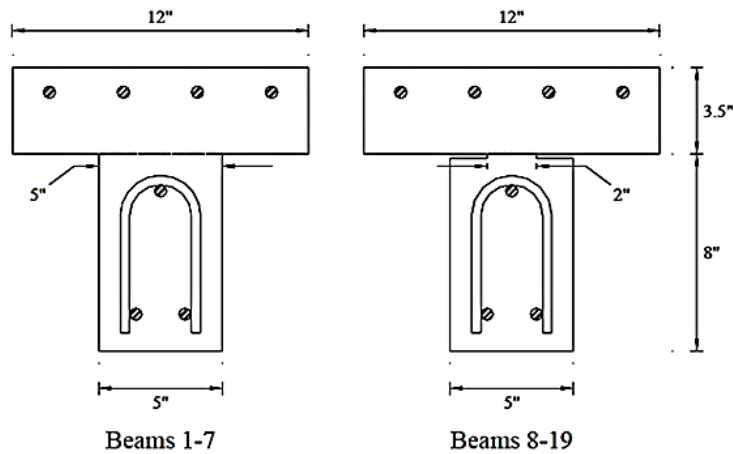
(a) Cross-section
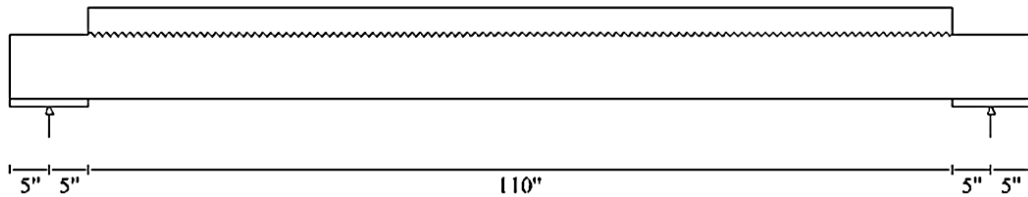
(b) Elevation

Figure 2-26 Typical test beams (Kovach and Naito, 2008)

Their findings suggested that the cohesion and adhesion between the girder and deck could provide sufficient shear resistance. In addition, they concluded that the interface roughness had a pronounced effect on the composite shear action and a

sufficient level of roughness could help obtain a high level of horizontal shear capacity. The surface condition, cohesion, and adhesion therefore should be considered for the design and practice.

2.5 Design and Code Equations

Mast Equation:

Mast was the first researcher to propose the following linear shear friction equation. It was later modified by Birkeland and Anderson (1960):

$$v_n = \rho_v f_y \mu$$ [2-7]

Loov and Patnaik (1994) however concluded from their research that this equation is very conservative for low clamping stresses and unsafe for sections with high clamping stresses.

Saemann and Washa Equation:

Saemann and Washa (1964) came up with Eq. 2-8 for determining the horizontal shear strength of a composite section from tests performed on full-size beams. The effects of surface conditions were not included in the equation since it was discovered that the contributions from surface conditions were diminished as the amount of reinforcement crossing the interfaces increased.

$$Y = \frac{2700}{X+5} + 300P\left(\frac{33-X}{X^2+6X+5}\right) psi$$ [2-8]

Where;

Y = ultimate shear strength

P = percent of steel crossing interface

X = effective depth of the section

First part of the equation represents the shear strength when no reinforcing steel is crossing the interface whereas the second part represents the strength due to clamping force when reinforcing steel is used.

Birkeland Equation:

Birkeland and Birkeland (1966) were the first to propose a parabolic equation for the horizontal shear strength (Equation 2-9):

$$v_n = 33.5\sqrt{\rho_v f_y} \ psi \tag{2-9}$$

This equation only included the clamping stress multiplied by a factor and did not account for the concrete strength or varying surface treatments.

Walraven Equations:

In his numerous tests on push-off specimens, he developed the following equations which consider the concrete compressive strength:

$$v_n = C_3\left(0.0007\rho_v f_y\right)^{C_4} psi \tag{2-10}$$

Where,

$$C_3 = 16.8(f_c')^{0.406} \tag{2-11}$$

$$C_4 = 0.0371(f_c')^{0.303}$$

Mattock Equations:

Mattock (1969) proposed an equation for horizontal shear strength which has been provided in the commentary of Section 11.6.3 of ACI 318-11 as shown below:

$$v_n = 0.8 \times A_{vf} f_y + A_c k_1 \tag{2-12}$$

Mattock further modified and simplified Walraven's equation by eliminating the c factors:

$$v_n = 400 + 0.8\rho_v f_y \ psi \tag{2-13}$$

From his research on lightweight concrete summarized above, Mattock et al. (1976) concluded that shear strength of lightweight concrete is less than that of normal weight concrete.

Loov Equation:

Loov (1978) was among the first researchers to incorporate the influence of concrete strength directly into the horizontal shear equation (Equation 2-14).

$$v_n = k\sqrt{\rho_v f_y f_c'}$$ [2-14]

k = 0.5 for initially un-cracked surface

Hsu et al. (1987) proposed a k = 0.66 on a similar equation for both cracked and un-cracked interfaces.

Shaikh Equation:

Shaikh (1978) developed Equation 2-15 for horizontal shear strength which was adapted by PCI Design Handbook (1992) as the basis for their design equations.

$$v_n = \emptyset \rho_v f_y \mu_e$$ [2-15]

Where;

$\emptyset = 0.85$ for shear

$$\mu_e = \frac{1000\lambda^2}{v_n}$$

λ = 1.0 for normal weight concrete

λ = 0.85 for sand-lightweight concrete

λ = 0.75 for all lightweight concrete

The PCI Design Handbook (1992) uses a simplified form of the equation as shown below:

$$v_n = \lambda\sqrt{1000\emptyset\rho_v f_y} \leq 0.25 f_c' \lambda^2 \; and \; 1000\lambda^2 \; psi$$ [2-16]

Loov and Patnaik Equation:

As mentioned above, Loov and Patnaik (1994) combined the equation by Loov (1978) with the horizontal strength of composite beam without shear connectors. The equation is applicable for both high and low clamping stresses:

$$v_n = k\lambda \sqrt{(15 + \rho_v f_y) f_c'}$$ [2-17]

$k = 0.6$

λ = same as used by PCI

In 2001, Patnaik proposed a linear variation on his previous shear equations:

$$v_n = 87 + \rho_v f_y \leq 0.2 f_c' \ and \ 800 \ psi$$

$$v_n = 0 \quad for \ \rho_v f_y \leq 50 \ psi$$ [2-18]

2014 AASHTO LRFD Bridge Design Specifications for Horizontal Shear

The specifications propose that the interface shear transfer should be considered across a plane at:

- An existing or potential crack,

- An interface between two concretes cast at different times,

- An interface between dissimilar materials, or

- The interface between different elements of the cross-section.

The nominal shear resistance of the interface plane is represented as a linear equation as shown:

$$V_{ni} = cA_{cv} + \mu(A_{vf} f_y + P_c)$$ [2-19]

The nominal shear resistance should however not be greater than the lesser of:

$$V_{ni} \leq K_1 f_c' A_{cv} , \ or$$

$$V_{ni} \leq K_2 A_{cv}$$

where:

c = cohesion factor

μ = friction factor

A_{cv} = interface area (in^2)

A_{vf} = area of shear reinforcement crossing the shear plane within area A_{cv} (in^2)

The AASHTO provisions give the following recommendations for cohesion and friction factors.

For normal weight concrete placed against a clean concrete surface, free of laitance and intentionally roughened 0.25-in.

c = 0.24 ksi

μ = 1.0

For concrete placed against clean, hardened concrete not intentionally roughened but free of laitance and clean

c = 0.075 ksi

μ = 0.6

For a CIP concrete slab on clean concrete girder surfaces, free of laitance and intentionally roughened 0.25-in.

c = 0.28 ksi

μ = 1.0

ACI 318-14

ACI 318-14 (ACI, 2014) Section 16.4 recommends the equations for horizontal shear design. ACI outlines that the design of horizontal shear is based on the following equation.

$V_u \leq \emptyset V_{nh}$ (ACI equation 16.4.3.1) [2-20]

Where:

V_u = factored shear strength

V_{nh} = nominal horizontal shear resistance

$\emptyset$ = strength reduction factor (0.75)

The horizontal shear resistance is determined as follows:

If $V_u \leq \emptyset 500 b_v d$ then,

For contact surfaces that are clean, free of laitance and intentionally roughened,

$$V_{nh} \leq 80 b_v d \qquad\qquad\qquad\qquad\qquad\qquad [2\text{-}21]$$

For contact surfaces that are clean, free of laitance, but not intentionally roughened, having minimum tie reinforcement,

$$V_{nh} \leq 80 b_v d \qquad\qquad\qquad\qquad\qquad\qquad [2\text{-}22]$$

For contact surfaces that are clean, free of laitance, having minimum tie reinforcement and intentionally roughened to a full amplitude of approximately ¼-in.,

$$V_{nh} = \left(260 + 0.6\rho_v f_y\right)\lambda b_v d \leq 500 b_v d \qquad\qquad [2\text{-}23]$$

If $V_u > \emptyset 500 b_v d$ then,

$$V_{nh} = A_{vf} f_y \mu \leq \min(0.2 f_c' A_c \; or \; 800 A_c) \qquad\qquad [2\text{-}24]$$

Where,

b_v = width of the interface (in.)

d = distance from the extreme compression fiber to centroid of tension reinforcement for the entire composite section (in.)

A_{vf} = area of shear reinforcement crossing the interface (in^2)

f_y = yield stress of the shear reinforcement (psi)

μ = coefficient of friction which depends on surface

= 1.0 λ for concrete placed against hardened concrete with intentionally roughened surface.

= 1.4λ for concrete cast monolithically.

= 0.6λ for concrete placed against hardened concrete with surface not intentionally roughened.

= 0.7 λ for concrete anchored to as-rolled structural steel by headed studs or by reinforcing bars.

λ = 1.0 for normal weight concrete

λ = 0.85 for sand-lightweight concrete

λ = 0.75 for all lightweight concrete

A_c = area of concrete engaged in shear transfer (in^2)

$$\rho_v = \frac{A_v}{b_v s}$$

Chapter 3

SITE VISITS AND REVIEW OF OTHER DOT PRACTICES

3.1 Introduction

As a part of the research project, site visits were conducted on bridges in Austin as well as Fort Worth to observe horizontal shear cracks. In addition, visits were made to two precast plants in Texas to observe their beam fabrication and surface finishing process at the interface. A survey was also conducted to have a better understanding of the horizontal shear reinforcement details for box and slab beams of all 50 DOTs in the United States.

3.2 Bridge Site Visits

Riverside Bridge (Austin)

A visit was made to the Riverside Bridge (Intersection of I-35 and Riverside Rd.) to observe the horizontal shear cracks. The location of the bridge and design drawings can be seen in Figure 3-1. Observation of the bridge revealed extensive horizontal cracks at the end spans and the middle span of the bridge. Crack widths as wide as 10 mm were measured. It is important to note however that this bridge uses an asphaltic concrete overlay of 2-in. as opposed to a CIP slab.

Although this bridge did not have a cast-in-place slab, its deterioration and condition prompted TxDOT to question if details for horizontal shear resistance in box and slab beams are adequate to prevent horizontal shear failure. TxDOT slab and box beams are more susceptible to this due to the thin CIP slab provided compared to I-beams which have a CIP slab of 8-in.

(a)
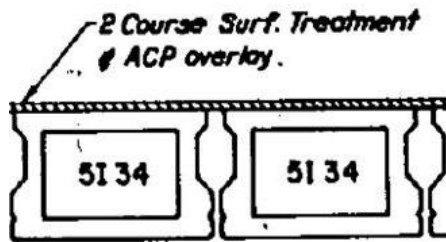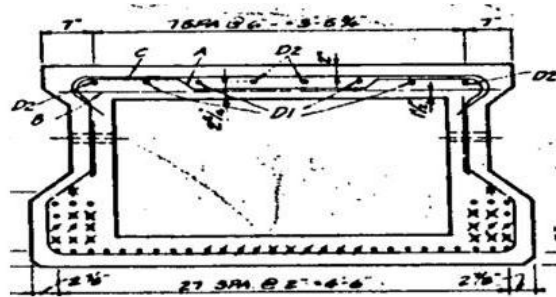
(b)

Figure 3-1 Riverside bridge (a) location and (b) design drawings

There was therefore no horizontal shear reinforcement at the interface. The only composite section on the beam was observed to be between the precast beam and the sidewalk. The interface at this section was also observed to be very smooth (Figure 3-2).
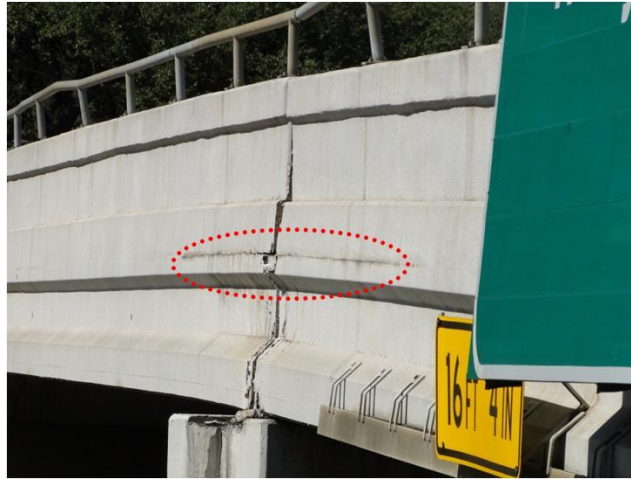
(a) Horizontal cracking at the ends of box beams
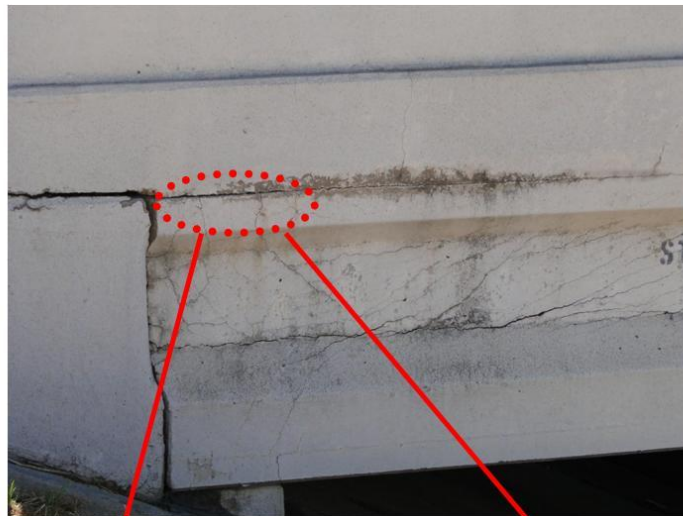
(b) Crack width

Figure 3-2 Horizontal shear cracks at the interface of beam and sidewalk

Ft. Worth Bridge Site Visits

Two bridge sites were visited in Ft. Worth to observe the possible occurrence of interface shear cracks. The first bridge was an older bridge located near the intersection of E Long Avenue and Beach St (Figure 3-3). This bridge was constructed with concrete box beams and a 2-in. asphalt overlay on the surface. These types of bridges use shear keys to connect the girder and the deck and do not use any type of steel reinforcing along the interface.

Figure 3-3 Location of Long Ave. Bridge

It was observed on arrival that this bridge did not have any interface shear damage; however other forms of damage were seen. A number of shear cracks and crushing was observed at the ends of the girders. Figure 3-4 shows an example of some of the observed shear cracks. Horizontal shear cracks were present on the girders but did not extend into the deck interface.
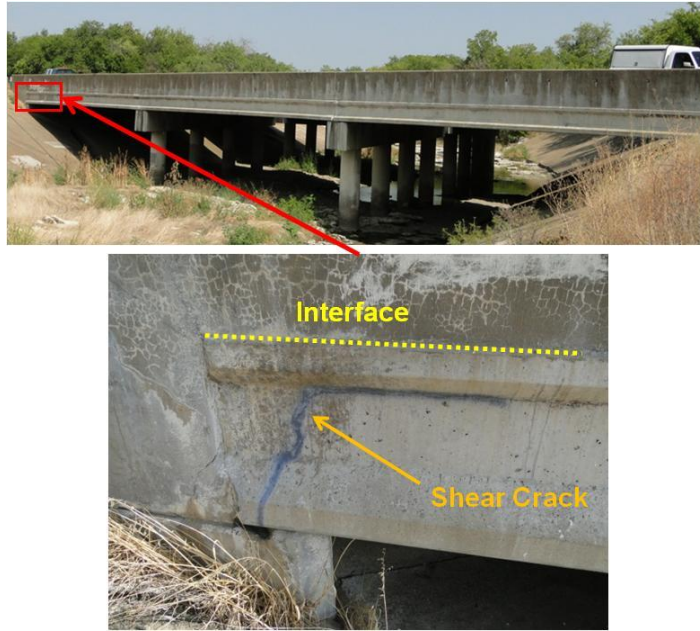
Figure 3-4 Shear cracks observed at the South-West end of the Long Ave. Bridge

The second bridge that was visited was located at Cattlebaron Drive at Silver Creek (Figure 3-5). The bridge is a slab beam bridge with a CIP reinforced concrete deck similar to the bridges that we are currently investigating. Since the bridge was newly constructed, there was no visible damage to study.

Figure 3-5 Location of Cattlebaron Dr. Bridge

3.3 Plant Visits

A number of companies within Texas are approved to fabricate TxDOT precast prestressed members. This companies need to go through rigorous tests by TxDOT to ascertain that their concrete meets the standards set out in TxDOT specifications. Figure 3-6 shows the table provided by TxDOT under materials producers list that shows the companies that are TxDOT approved to fabricate prestressed, precast concrete members. This project visited Texas Concrete Partners, L.P., Bexar Concrete works Ltd., and Atesvi US to observe their fabrication practices. The full-scale specimens were finally fabricated at Flexicore of Texas, Inc. in Houston.

Major Prestressed Member Fabrication Plants (Multi-Project)		
Producer Code	**Fabricator**	**Location**
98296	Atesvi US	Irving, TX
99725	Bexar Concrete Works I, Ltd.	San Antonio, TX
99693	Flexicore of Texas, Inc.	Houston, TX
99716	Heldenfels Enterprises, Inc.	San Marcos, TX
99701	Texas Concrete Partners, L.P., Victoria Division (formerly Texas Concrete Company)	Victoria, TX
99723	Texas Concrete Partners, L.P., Waco Division (formerly Texas Prestressed Concrete, Inc.)	Waco, TX
99437	Valley Prestressed Products, Inc.	Eagle Lake, TX

Figure 3-6 Excerpt from TxDOT material producers list (2015)

Texas Concrete Partners, L.P. (formerly Texas Prestressed Concrete Inc.)

A visit to the Texas Prestressed Concrete Plant in Elm Mott was conducted to get an idea on the process involved in manufacturing a slab beam. River gravel (¾-in.) was used as the coarse aggregates while river sand was used as the fine aggregates. Horizontal shear reinforcement (Grade 60, No. 4 bar) is spaced at 12-in. and has an embedment length of 2-in. as per TxDOT specifications (Figure 3-7 and Figure 3-8).

Figure 3-7 Spacing of horizontal shear reinforcement

Figure 3-8 Horizontal shear reinforcement details

The slab beams are typically finished by a wood float finish (Figure 3-9). On comparing the surface finish with the CSP surface profiles, while it was not easy to determine which surface profile matched the surface roughness, it was observed that the surface roughness for the conventional concrete slab beam was between a CSP 6 and a CSP 7 (Figure 3-11) while an SCC slab had a surface roughness of CSP 4 (Figure 3-10).

Figure 3-9 Application of wood float finish

Figure 3-10 SCC concrete surface compared to CSP 4

| (a) | (b) |

Figure 3-11 Wood float concrete surface compared to (a) CSP 6 and (b) CSP 7

Texas Prestressed Concrete typically does not fabricate box beams due to their complicated construction and cost. The plant mentioned that they would be willing to change their process of roughening the surface if a faster method (say broom or rake finish) was specified.

Bexar Concrete Works LTD

Unlike Texas Prestressed Concrete, Bexar uses ¾-in. limestone aggregates for the coarse aggregate and manufactured sand as the fine aggregates. They fabricate both box (Figure 3-12) and slab beams.

Figure 3-12 Finished box beam

The horizontal shear reinforcement of the box beam is spaced at approximately 12-in. spacing and 8-in. at the ends. The horizontal shear reinforcement is 2-in. high with a width of 3.5-in. and placed at a distance of 6-in. from the edge of the box beam (Figure 3-13).

(a)

(b)

Figure 3-13 Horizontal shear reinforcement details (a) spacing between reinforcement and (b) spacing from edge of beam to reinforcement

A wood float finish is provided on the surfaces of all TxDOT box and slab beams. The wood float finish creates a surface roughness between CSP 7 and CSP 9 as shown in Figure 3-14.

(a)

(b)

Figure 3-14 Box beam surface roughness compared to CSPs

Bexar provides a broom finish on precast panels (Figure 3-15), suggesting that other methods of surface preparation may be applied to box and slab beams if necessary.

Figure 3-15 Surface finish on precast panel

Atesvi US

Specializes in precast concrete I-girders and concrete panels (Figure 3-16).

Figure 3-16 I-girder fabricated by Atesvi US

Ready-mix concrete from a TxDOT approved supplier was used in fabricating the beams (Figure 3-17). A wood float finish was observed to be provided (Figure 3-18) at the surface of I-girders.

Figure 3-17 Casting of I-girders

Figure 3-18 Wood float finish provided

Atesvi provides a surface roughness of between CSP 6 to CSP 9 on precast panels according to the Precast Panel-Fabrication Standard.
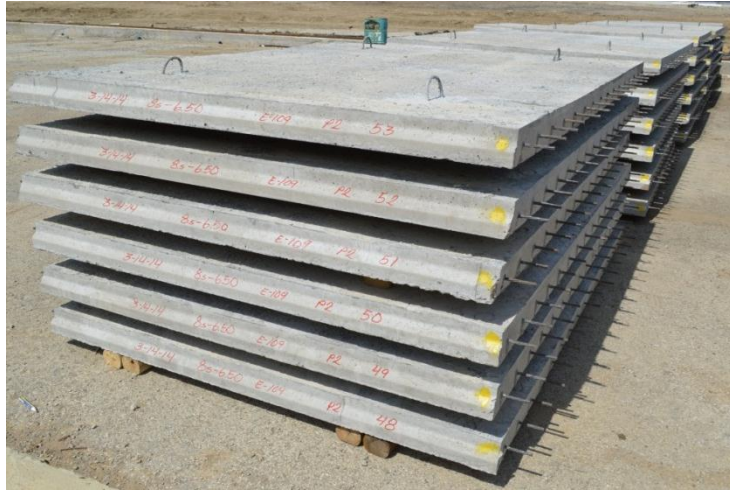
Figure 3-19 Concrete panels fabricated by Atesvi US

Figure 3-20 Surface roughness on precast panels

3.4 Study of Other DOTs' Practices

According to a survey of state highway agencies conducted by the AASHTO Highway Subcommittee on Bridges and Structures, at least 78% of the states have fully

implemented the AASHTO LRFD Bridge Design Specifications. This research therefore involved gathering of information on the current practice used for box and slab beams of the 50 states in the U.S. The study set out to determine other DOTs' practices especially the geometry, width, and embedded depth of horizontal shear reinforcements in box and slab beams with a CIP slab. Information was gathered by visiting state DOT websites to view standard drawings. Incase no drawings existed on their website, follow-up phone calls and emails were used to get the relevant information. Figure 3-21 below summarizes the usage of box and slab beams in USA.

Figure 3-21 Use of box and slab beams in USA

In cases whereby the states replied that they "rarely or typically" do not use box or slab beams, we decided to include them in states that use box or slab beams. This

includes Wyoming DOT which has only one box beam, Iowa DOT who replied that they typically do not use precast prestressed box beams or slab beams due to their poor performance and New Mexico and Louisiana DOT replied that they rarely use box or slab beams hence have no standard plans available. The survey revealed that at least 70% of the state DOTs use either box or slab beams on their bridges.

Width of horizontal shear reinforcement

In this survey, the width of the horizontal shear reinforcement was investigated for both the slab and box beam. Although some states had this information specified in their standard drawings, some states did not because they use an asphaltic concrete overlay as the wearing surface. Although Illinois DOT provides a 5-in. concrete wearing surface on deck beams, it is non-composite and just serves as a plate to help reduce reflective shear key cracking and improve rideability hence no interface shear reinforcement is provided. Connecticut DOT previously used a water proof membrane on top of the precast beams with a minimal of 3.5-in. bituminous overlay. However, 20 years later, they began to experience some pre-mature failures due to the failure of the waterproof membrane. They have more recently started using cast-in-place slab but have no standard details available yet. Idaho DOT does not provide details and drawings for the box beams. On further inquiry I was informed that the girder stirrups are designed to project into the concrete decks although no details are provided. The width of the horizontal shear reinforcement was seen to span the full width of the beam for Maryland and Michigan DOT. Widths of 6-in. and 9-in. were found to be the most common as shown in Figure 3-22.
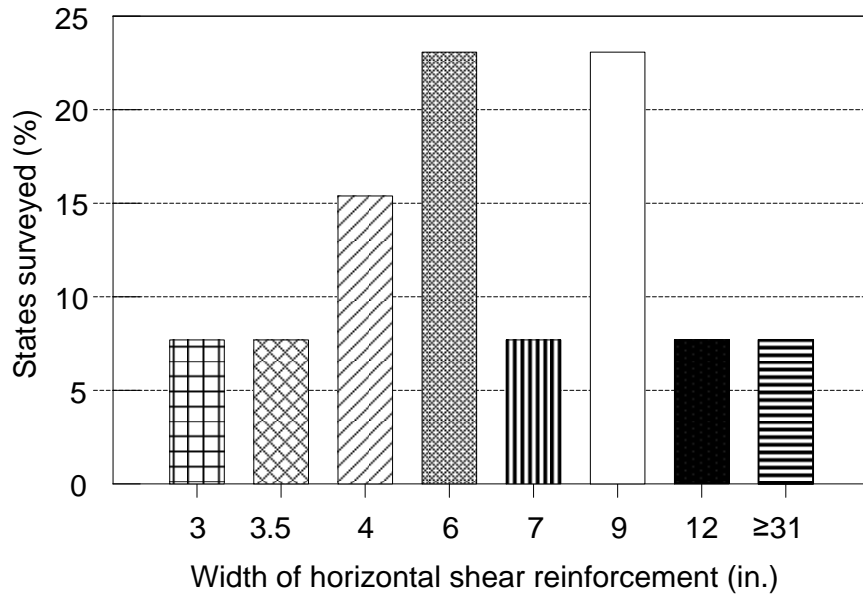
Figure 3-22 Width of horizontal shear reinforcement

Embedded length of horizontal shear reinforcement

The embedded length of the horizontal shear reinforcement varied between 2-in. and 6-in. depending on the thickness of the CIP slab used in the respective state. As noted earlier, some states do not use either box or slab beam, while some states provide a thin asphaltic concrete as the wearing surface and hence do not provide horizontal shear reinforcement. An embedment length of about 2-in. to 2.5-in. was observed in nearly 70% of the states having box and slab beams (Figure 3-23). West Virginia and Minnesota DOT were seen to provide embedded lengths of 5-in. and 6-in. respectively.
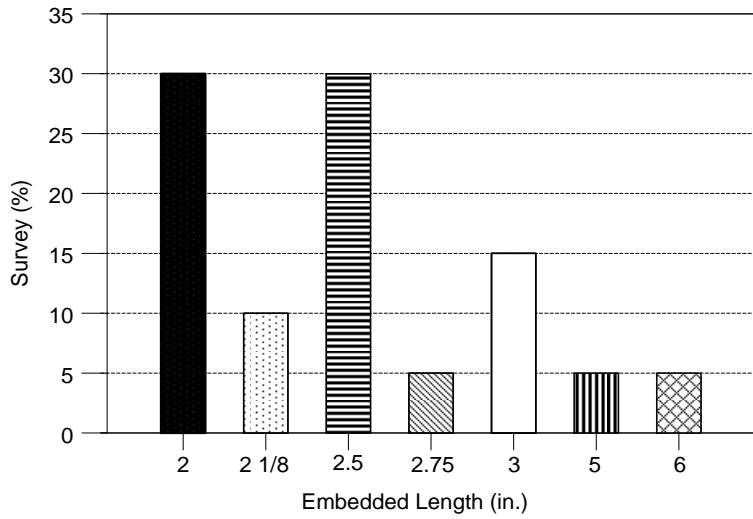
Figure 3-23 Embedded length

It was observed that there are essentially six types of horizontal shear reinforcement (Figure 3-25 and Table 3-1) being used in different states. Type 6 beams correspond to a case in which the horizontal shear reinforcement is placed perpendicular to the cross sections observed in Maine, Massachusetts and Rhode Island DOT.
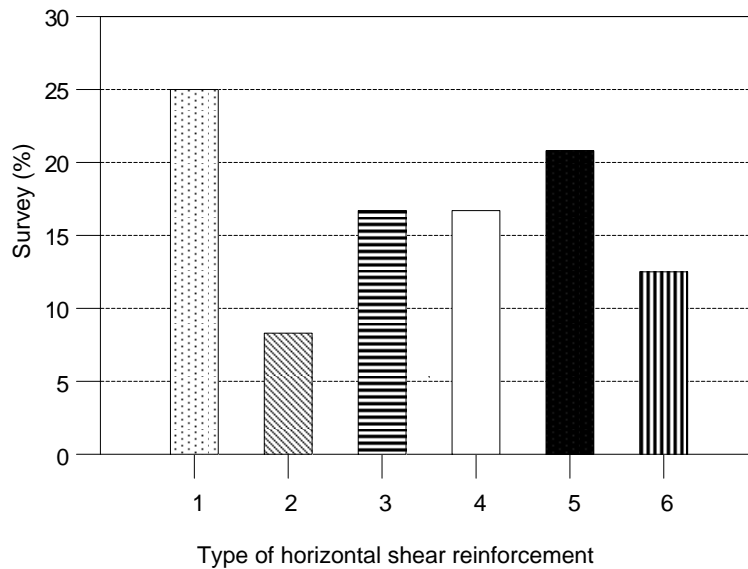
Figure 3-24 Type of horizontal shear reinforcement
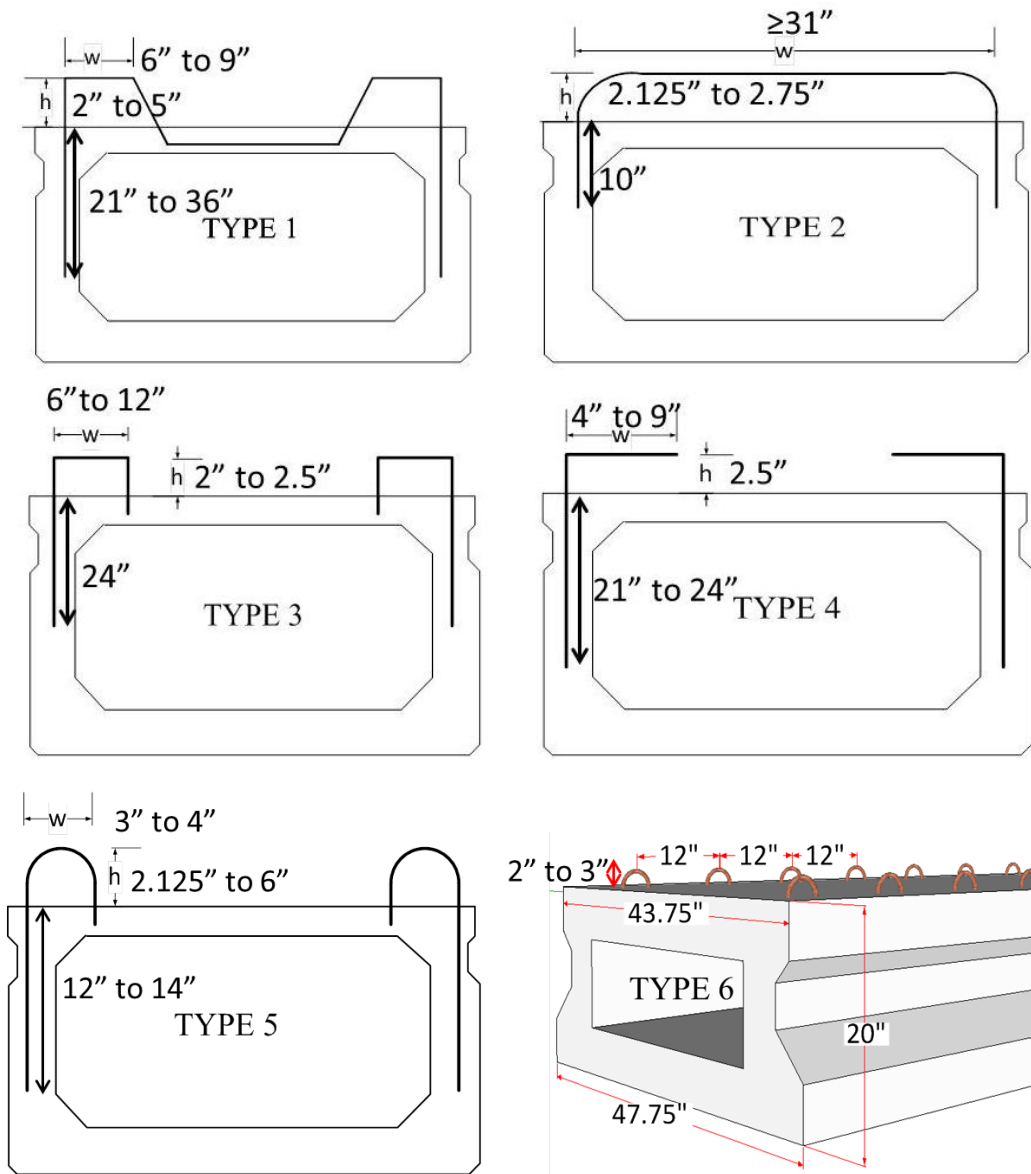
Figure 3-25 Types of Standard box beams for DOTs in the US

Table 3-1 State DOT configuration for horizontal shear reinforcement

Type of horizontal shear reinforcement	State DOT
1	Ohio, North Dakota, West Virginia, Texas, Delaware, Illinois
2	Maryland, Michigan
3	Colorado, Missouri, Texas, Florida
4	Missouri, Alabama, Washington, Tennessee
5	Indiana, Kentucky, Minnesota, Pennsylvania, Texas*
6	Maine, Massachusetts, Rhode Island

* TxDOT standard prior to 2012.

It is clear from this study that the width of horizontal shear reinforcement used in other states is generally the same as that used in the current TxDOT practice. Also of interest is the effectiveness of using the reinforcement perpendicular to the cross-section (Type 6). Therefore the testing matrix adopted in Task 5 of this research (Bar pullout test) is justified as it will enable us to determine the effectiveness of different widths and curvatures of the reinforcement. Although wood float finish is the most popular finish being used, other kind of finishing (broom finish, rake finish) should also be considered for their effectiveness. The full report on the study can be found in Appendix A.

Chapter 4

EXPERIMENTAL PROGRAM

4.1 Introduction

This section presents the experimental work carried out in this research. The research is divided into seven tasks as shown in the flowchart on (Figure 1-7). The detailed design of each task's specimens is presented. The characteristics of the materials used for each specimen as well as the casting procedures are then presented. The test procedure adopted for each task is also outlined.

4.2 Horizontal Shear Test Specimens and Experimental Design

4.2.1 TASK 4- Evaluate Horizontal Shear Component: $\mu A_{vf}f_y$ (dowel action of the reinforcement)

Eighteen push-off specimens were tested to investigate the contribution of dowel action towards the horizontal shear strength of composite beams. The horizontal push-off test was utilized with no additional dead load (P_c) applied to the specimens. No. 4 interface reinforcement bars were used having various widths and embedment length (see Table 4-1). The widths selected were based on the study of other DOT practices as discussed in Chapter 3 as well as TxDOT current and previous practices. It was noted from studies conducted on other department of transportation practices that some states (Maine DOT and Massachusetts DOT) place the interface shear reinforcement in the longitudinal direction (Figure 4-1). Specimens having the interface shear reinforcement in the longitudinal direction will also be tested to ascertain if there are any advantages in using this configuration. Two embedded lengths were considered; a 2-in. embedded length was used to match what is currently used in TxDOT and in most other DOTs as discussed in Chapter 3 and a 4-in. embedded length was also considered to determine

its influence on the development of the bar. A wood float finish as specified by TxDOT was provided to all the specimens at the interface for consistency.
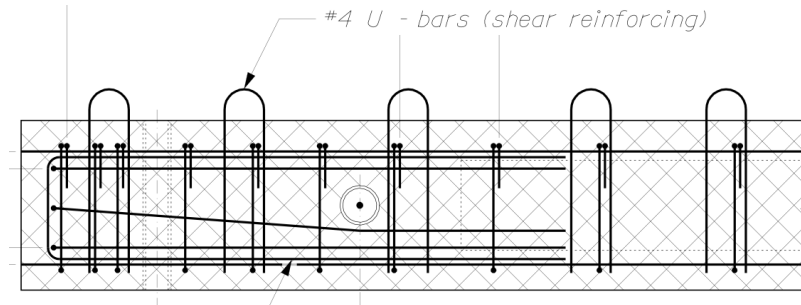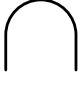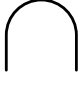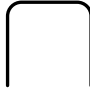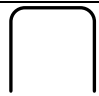
Figure 4-1 Horizontal reinforcement oriented in the longitudinal direction (Maine DOT)

Table 4-1 Testing Matrix for Task 4

Bent-bar Specification	Quantity
3.5-in. width (180° curvature)*	3
3.5-in. width (180° curvature, longitudinally placed)	3
6-in. width (90° curvature) £	3
6-in. width (90° curvature, 4-in. embedment)	3
9-in. width (90° curvature) §	3
9-in. width (90° curvature, 4-in. embedment)	3
Total Note: *TxDOT practice before 2012 for box beams; £ Details as shown in TxDOT standard drawings for slab beams; §Current TxDOT practice for box beams; Width measured from center-to-center; No. 4 bar used in all configurations.	**18**

Specimen geometry

Each test specimen measured 30×14×10-in., this size provided a shear interface area of 252 in^2 (18×14-in.). In this type of specimen, the bottom half of the specimen represents the precast part whereas the top half represents the CIP slab. Minimum longitudinal and transverse reinforcement was also provided to prevent premature flexural failure. Longitudinal bars were placed at both the top and bottom of the specimen spaced at 3-in. on center. No. 5 bars were provided for the bottom longitudinal reinforcement whereas No. 4 bars were used for the top longitudinal reinforcement. This was necessary to prevent flexural cracking induced by load eccentricity from occurring before failure by interface shear was reached. No. 3 bar lateral reinforcement was also provided at 5-in. spacing. The reinforcement layout chosen was similar to the one used by Mattock (1972). It should be noted that this reinforcement layout provides a higher reinforcement ratio (almost three times) as compared to that used in actual girder/deck (Figure 4-2). The typical specimen used is shown in Figure 4-3.

Figure 4-2 TxDOT box beam reinforcement layout

(a) Elevation

(b) Cross-section

Figure 4-3 Reinforcement layout

4.2.2 TASK 5- Evaluate the Bend Curvatures of Interface Shear Reinforcement

Twenty-four pullout specimens were cast to evaluate the effect of bend curvature on the horizontal shear reinforcement. The pullout specimens simulate horizontal shear reinforcement that is embedded in the CIP slab. The AASHTO nominal shear resistance equation assumes that the bar yields before pullout hence this test will verify if the bar yielding would occur by using different bar configurations.

Eight different bar geometric configurations were used to evaluate the effects of bond length and bend angle on the pullout strength of horizontal shear reinforcement. Bars with widths of 3.5-in., 6-in., 9-in. and 12-in. were cast as shown in Table 4-2.
Bars with 3.5-in. width had a bend angle of 90° and 180° bend curvature while the rest had 90° curvatures. Lapped bars were used for the 6-in., 9-in., and 12-in. bar widths to observe if this arrangement had any effect on the pullout characteristics.
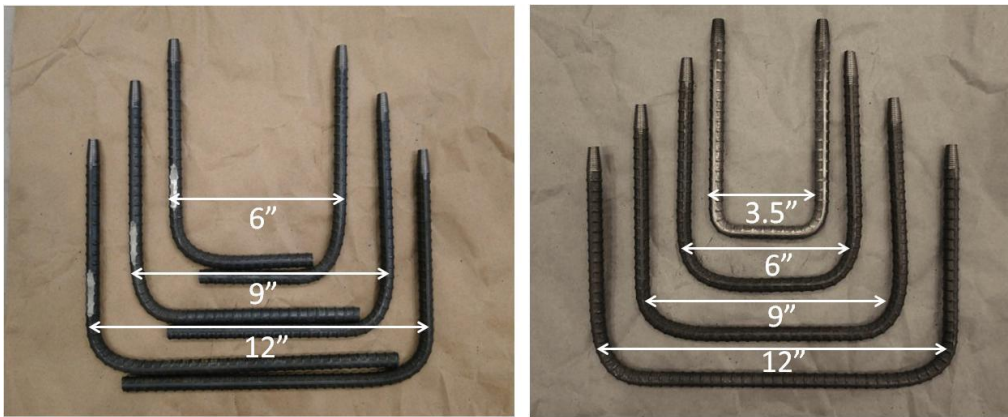
Figure 4-4 Reinforcement configuration for bar pullout specimen

According to TxDOT standard drawings (Figure 4-6), the transverse reinforcement is spaced at 6-in. maximum whereas the longitudinal reinforcement is spaced at 12-in. maximum.

Hence transverse reinforcement in all the specimens were provided at 6-in. and longitudinal reinforcement at 12-in. spacing with a 2.5-in. clear cover as specified in the standards.

Table 4-2 Bar Specification

Bent-bar Specification	Quantity
3.5-in. width (180° curvature) *	3
6-in. width (90° curvature) £	3
3.5-in. width and 90° curvature (90° curvature)	3
9-in. width (90° curvature) §	3
12-in. width (90° curvature)	3
6-in. width and 90° curvature long tail (tail length to be determined)	3
9-in. width and 90° curvature long tail (tail length to be determined)	3
12-in. width and 90° curvature long tail (tail length to be determined)	3
Total Note: *TxDOT practice before 2012 for box beams; £ Details as shown in TxDOT standard drawings for slab beams; §Current TxDOT practice for box beams; Width measured from center-to-center; No. 4 bar used in all configurations.	**24**

The TxDOT standard drawings also show that the horizontal shear reinforcement is located at 6-in. from the end. This dimension was maintained for all of the four different bar widths, therefore the total length of each specimen was the bar width plus 6-in. on both sides, to represent the shortest dimension in the standard drawings that will result in less confinement of the horizontal shear reinforcement by the surrounding concrete.

The dimensions for the four specimens are as shown in Figure 4-7. No. 4 bars were used for the longitudinal reinforcement whereas No. 5 bars were used for the transverse reinforcement as specified by TxDOT.
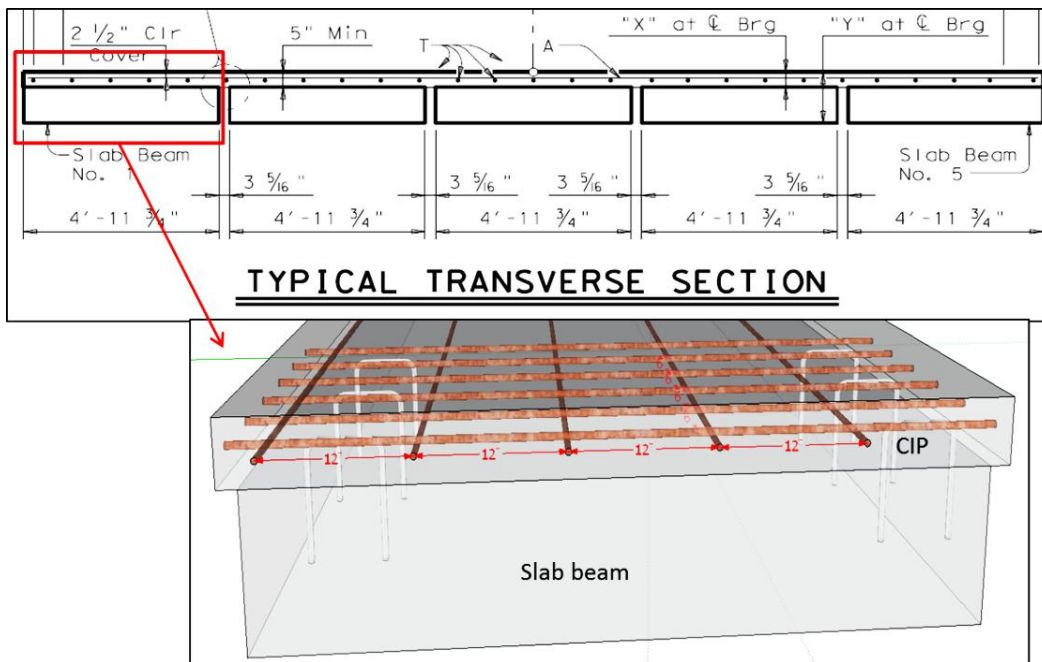
Figure 4-5 Typical transverse section of composite slab beam
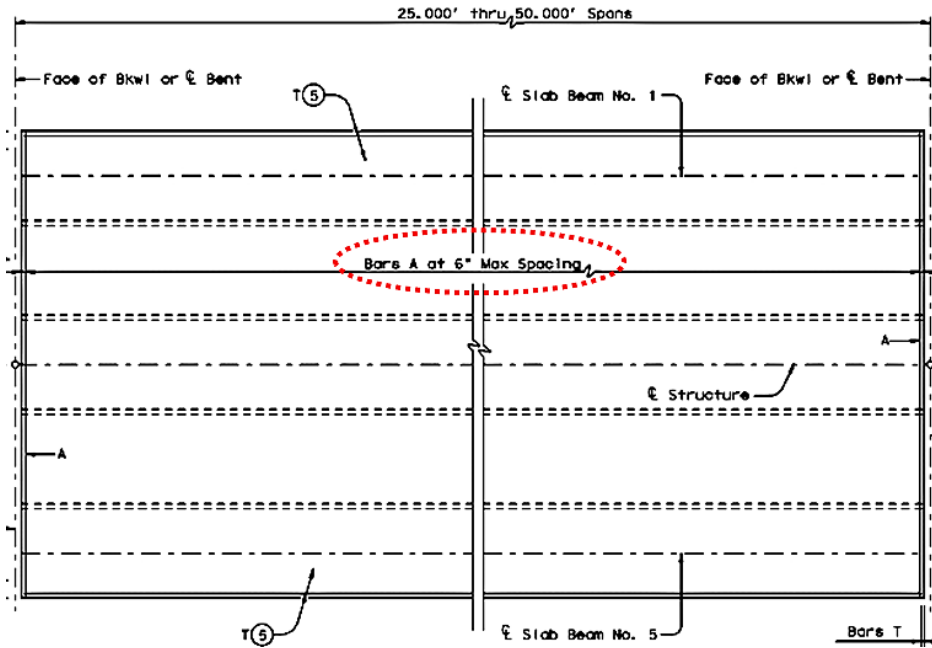
(a) Plan view
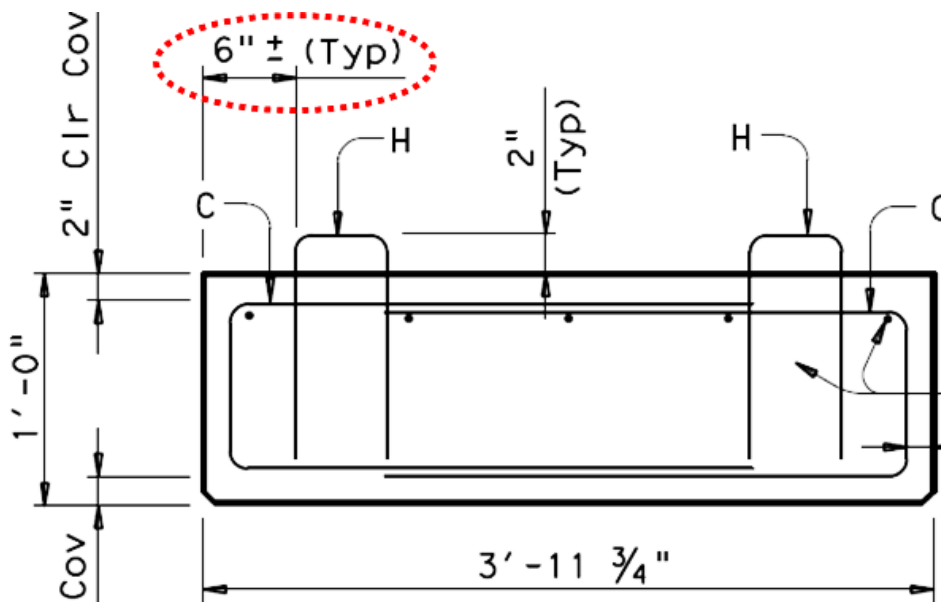
(b) Section

Figure 4-6 Slab beam reinforcement layout

80
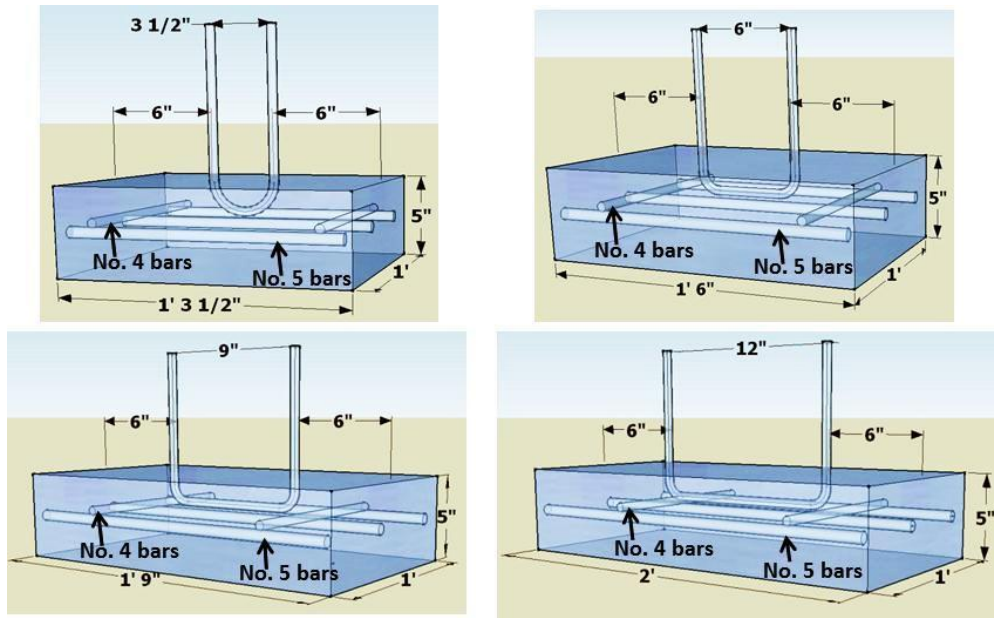
Figure 4-7 Pullout specimen configuration

Terminators (Figure 4-8) were used at the end of the bar through a threaded end to fasten it to the top part of the test set-up. The combination of the tapered threaded end and the terminator does not reduce the tensile strength at the ends, thus ensuring that the bar would yield (if it happens) at the interface. The bars and terminators were obtained from Electric Railway Improvement Company (ERICO) and later bent to the required widths by a local fabricator. Slotted holes were provided at the bottom part of the test set-up to accommodate the different configuration of specimens.

Figure 4-8 Bar terminators

4.2.3 TASK 6- Composite Box and Slab Beams (Current TxDOT Details)

The objective of this task was to determine if adequate horizontal shear capacity is provided by the 5-in. concrete deck in current TxDOT slab and box beams, despite lack of reinforcement development. This means that horizontal shear failure will not happen before a drop in strength occurs due to flexural failure.

PGSuper Beam Analysis and Design

PGSuper Bridge Engineering Software was used to design the box and the slab beams for Task 6. A 30 ft. long composite beam was selected for both the slab and box beams due to the lifting capacity of the crane in UT Arlington CELB. The beam selected was one that did not exceed the crane capacity of 15 tons.
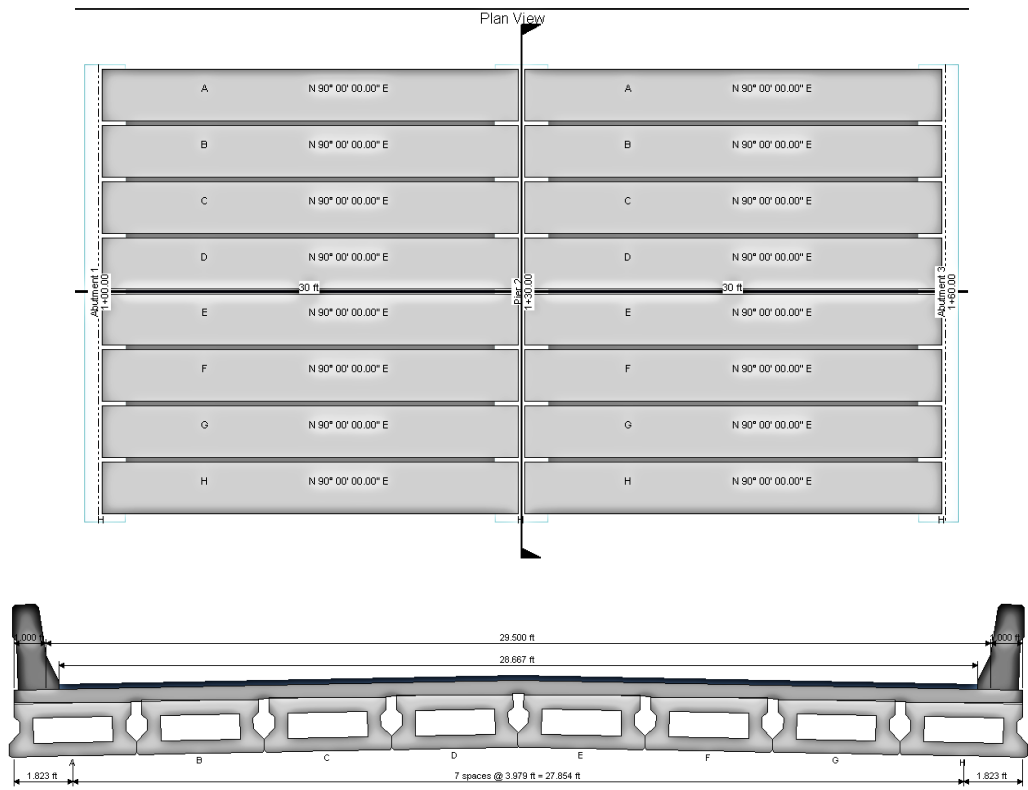
Figure 4-9 PGSuper model

The PGSuper analysis determined that the 4B20 box beam and 4SB12 slab beam, having a length of 30 ft., were the optimum choice of beams to be used for this task. The design of the beams was performed according to the current TxDOT standards using the PSBSD and BBSDS standard design as guidelines (see Appendix B). To increase the shear demand and simulate the most critical condition, four additional prestressing strands were added to the beam. The analysis determined that a flexural failure will occur before shear or horizontal shear failure occurs.

Specimen Configuration

Two types of full-scale composite beams: TxDOT box beam (4B20) and TxDOT slab beam (4SB12) (see Table 4-3) were tested. The precast beams with a 5-in. composite deck were constructed and instrumented at Flexicore in Houston and then delivered to UT Arlington CELB for testing.

Table 4-3 Testing Matrix for Task 6

Full-Scale Beam Test	Number of Tests
30-ft Composite Box Beam, 4B20 (current TxDOT details)	2
30-ft Composite Slab Beam, 4SB12 (current TxDOT details)	2

The slab beams measured 360×47.75×12-in. (length×width×height) whereas the box beams measured 360×47.75×20-in. One of the box beams (4B20#1) and slab beams (4SB12#1) was designed using the current reinforcement detail according to TxDOT specifications to represent a typical beam used in practice (Figure 4-10 and Figure 4-11). Given the difficulty in placing strain gauges on the prestressing strands, it was decided that two No. 3 bars will be placed along the strand with strain gauges mounted on them.

From ACI 318-11 Sec. 12.2.2 (Equation 2-1), an adequate developmental length was determined to avoid bar pullout before yielding. Strain gauges were mounted on the horizontal shear reinforcement to provide useful information to check the calculations. Shop drawings are provided in Appendix C.

Typical 4SB12 Section
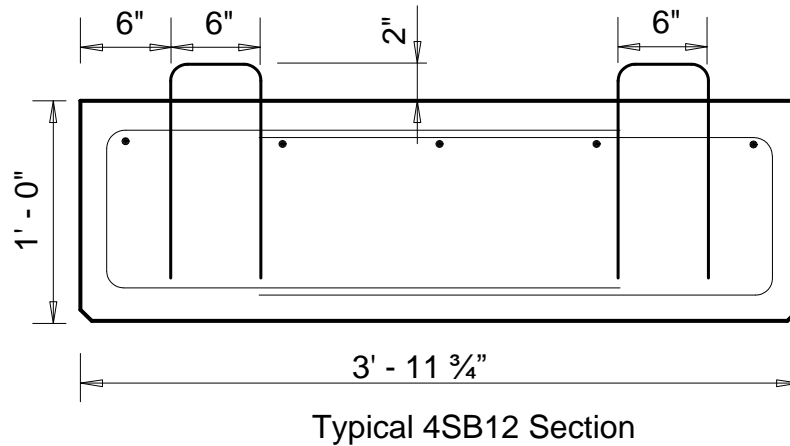
Figure 4-10 Typical slab beam section

Typical 4B20 Section (Current Design Practice since 2012)
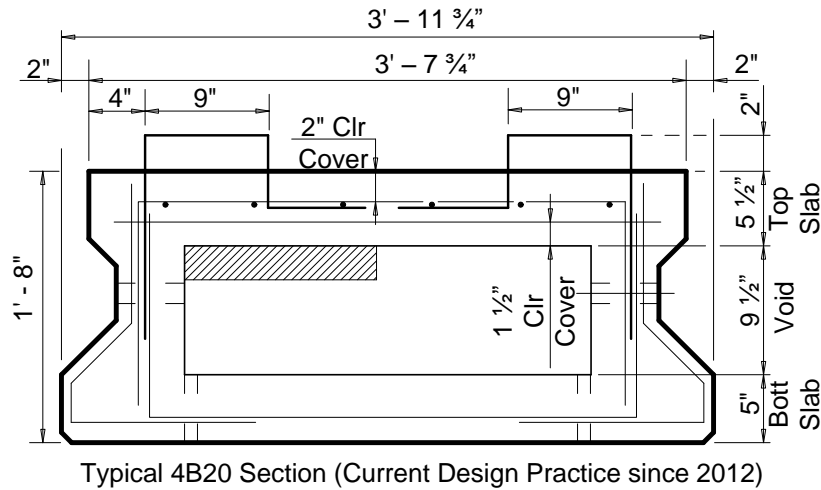
Figure 4-11 Typical box beam section

Moment Capacity

The results from PGSuper analysis show that the moment capacity of each beam is more than two times the moment demand. Using the simple calculation shown in

Figure 4-12 the expected failure load was calculated to be 81 kips and 160 kips for typical TxDOT slab beams and box beam respectively.
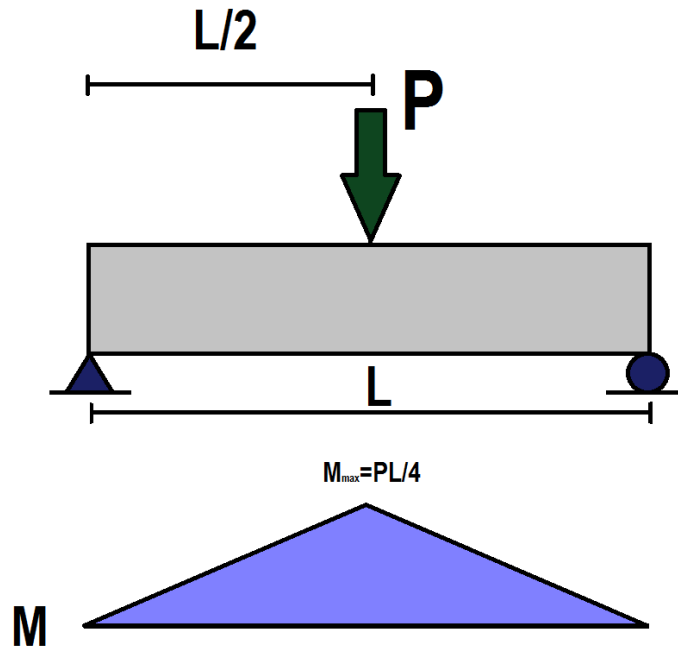
Figure 4-12 Moment Diagram of Simply Supported Beam with Point Load at Mid-span

Horizontal Shear Strength

PGSuper analysis also reveals that the design horizontal interface shear strength is at least four times that of the interface shear demand. The load needed to fail the beam by horizontal shear is significantly higher than that needed to cause a flexural failure. It was therefore unlikely that a horizontal shear failure will occur before flexural failure. Table 4-4 summarizes the maximum moment, shear and horizontal shear results from the PGSuper design for the two current TxDOT standard beams. The peak load shows the expected load needed to fail the beam in flexure whereas the full analysis report on moment, shear and horizontal shear is provided in Appendix D.

Table 4-4 Maximum Moment, Shear, and Horizontal Shear from PGSuper Design

Beam Type	No. of Strands	M_u* (kip-ft)	ΦM_n (kip-ft)	V_u (kip)	ΦV_n (kip)	V_{ui} (kip/ft)	V_{ni} (kip/ft)	Peak Load (kips)
4SB12	14	427.63	593.14	57.48	337.59	50.50	173.29	82
4B20	16	452.83	1161.13	88.05	304.15	40.12	175.58	161

* Based on HL-93 loading

A comparison was made between the beam with the maximum horizontal shear demand and the beam proposed for this design to determine the difference in the shear demand between the two. From the analysis, it was found that a 65 ft. box beam 5B20 and a 50 ft. slab beam 5SB15 provided the maximum possible horizontal shear demand. This has been tabulated in Table 4-5.

Table 4-5 Shear Stress Demand Comparison

Beam Type	Span Length (ft)	Shear Stress Demand (kip/ft^2)
4B20	30	10.99
5B20	65	15.48
4SB12	30	12.70
5SB15	50	14.66

The same detailing was maintained for the second box (4B20-modified) and slab beam (4SB12-modified) with the addition of flexural reinforcement in an attempt to force a horizontal shear failure and evaluate the horizontal shear strength of the beam as a whole. A total of fifteen No. 8 bars were added as flexural reinforcement in the box beam while twelve No. 8 bars were added in the slab beams. These beams were designed to result in a shear demand higher than that in the strongest TxDOT box beams and slab

beams typically used in practice. The flexural reinforcements were placed in the most convenient spacing in order to avoid congestion with the strands and facilitate concrete placement (Figure 4-13 and Figure 4-14). The beams were designed to ensure tension-controlled behavior and no premature shear failure even with the additional longitudinal reinforcement. Results from push-off and pullout tests had shown that horizontal shear reinforcement provide a minor contribution to the interface shear strength, hence they were completely eliminated in these two beams. Strain gauges were mounted on the flexural reinforcements to measure strain on the bars during the test.

Since PGSuper does not consider the additional mild steel reinforcement in calculating the moment, hand calculations were performed to determine the moment capacity of the beams.
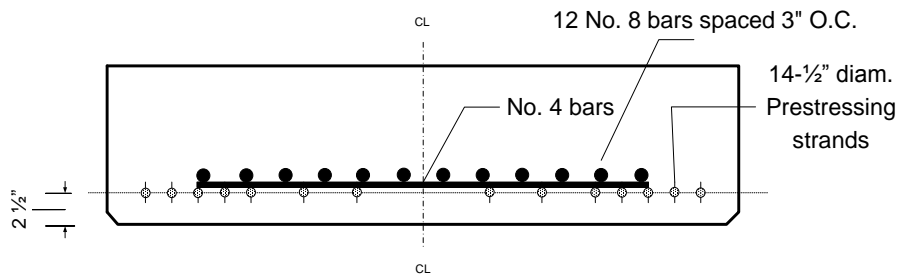
Figure 4-13 Slab beam without shear reinforcement
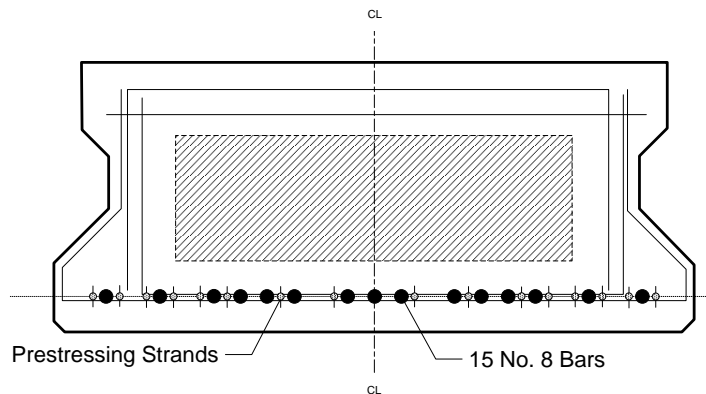
Figure 4-14 Box beam without shear reinforcement

Table 4-6 summarizes the moment capacity as well as the peak load required to fail the specimen by flexure. The full analysis report of the moment, shear and horizontal shear of the beams using PGSuper is provided in Appendix D.

Table 4-6 Moment capacity and peak load of over-reinforced beams

Beam Type	No. of Strands	No. of bars	$M_u{}^*$ (kip-ft)	ΦM_n (kip-ft)	ΦV_n (kip)	V_{ui} (kip/ft)	V_{ni} (kip/ft)	Peak Load (kips)
4SB12	14	12	427.63	1163.43	337.59	50.50	173.29	160
4B20	16	15	452.83	2126.15	304.15	40.12	175.58	310

Since Flexicore of Texas provides a rake finish on all slab and box beams, a rake finish was provided on all the specimens.

4.2.4 TASK 7- Full-scale Tests on Composite Box and Slab Beams (Additional Investigation)

Based on component testing from Task 2 through Task 5, it was discovered that a change in bar configuration with a 2-in. embedment will have little effect on the shear strength of the beams. Task 6 proved that horizontal shear failure will not occur for TxDOT beams with a rake finish even without shear reinforcement. Therefore the proposed detail for Task 7 was to ensure horizontal shear failure by reducing the interface area, to get a better idea of the actual values of the horizontal shear strength (stress unit). It is expected that a reduction in shear reinforcement combined with wood float finish would significantly facilitate the fabrication of composite slab and box beams.

TxDOT is pushing towards the use of self-consolidating concrete (SCC) on precast beams although it has not been widely accepted by fabricators. However, on our visit to Texas Prestressed Concrete plant (Chapter 3), we observed that they do use SCC in their slab beams. It was observed that a wood float finish on SCC slab beams resulted

in a much smoother interface (Figure 4-15). There is currently no known research that investigates the horizontal shear resistance of beams constructed with SCC. Therefore, testing SCC beams would provide valuable information to determine the effect of a much smoother interface on the horizontal shear resistance. It should also be noted that although AASHTO recommends a cohesion factor of 0.28 ksi for a surface roughened to an amplitude of 0.25-in., it does not address the fact that a smoother interface may result from the use of SCC. Consequently, there is no cohesion and friction factor suggested in the case where SCC is used.

Figure 4-15 Surface finish on SCC slab beams comparable to CSP 4

In this task two slabs and one box beams will be tested (Table 4-7) as explained below.

Table 4-7 Testing Matrix for Task 7

Full-Scale Beam Test	Number of Tests
30-ft Composite Box Beam, 4B20 (Reduced Area-Wood Float)	2
30-ft Composite Slab Beam, 4SB12 (Reduced Area-Wood Float)	1
30-ft Composite Slab Beam, 4SB12 (Reduced Area-Wood Float, SCC)	1

Two slab beams were cast using Self-Consolidating Concrete (SCC) in one of the beams and conventional concrete in the other. Horizontal shear reinforcement was provided in these beams and the interface area reduced to force a horizontal shear failure in order to evaluate the contribution of the horizontal shear reinforcement. Additional mild steel flexural reinforcement was added to increase the shear demand with the addition of twelve No.8 tension reinforcements (Figure 4-16). Since PGSuper does not consider flexural reinforcement in calculating the moment, hand calculations were performed to determine the moment capacity of the beams. A wood float finish was provided at the interface. A 5-in. thick CIP slab was later cast on the precast beams to form a composite beam section. Table 4-8 summarizes the maximum moment, shear, and horizontal shear results from the PGSuper design. The peak load shows the expected load needed to fail the beam in flexure. This peak load has been calculated based on a point load application at mid-span.

Table 4-8 Slab Beam Design

Beam Type	No. of Strands	No. of bars	M_u^* (kip-ft)	ΦM_n (kip-ft)	ΦV_n (kip)	V_{ui} (kip/ft)	V_{ni} (kip/ft)	Peak load for horizontal shear
4SB12	12	12	428	1163	338	51	72	674

(a)

(b)
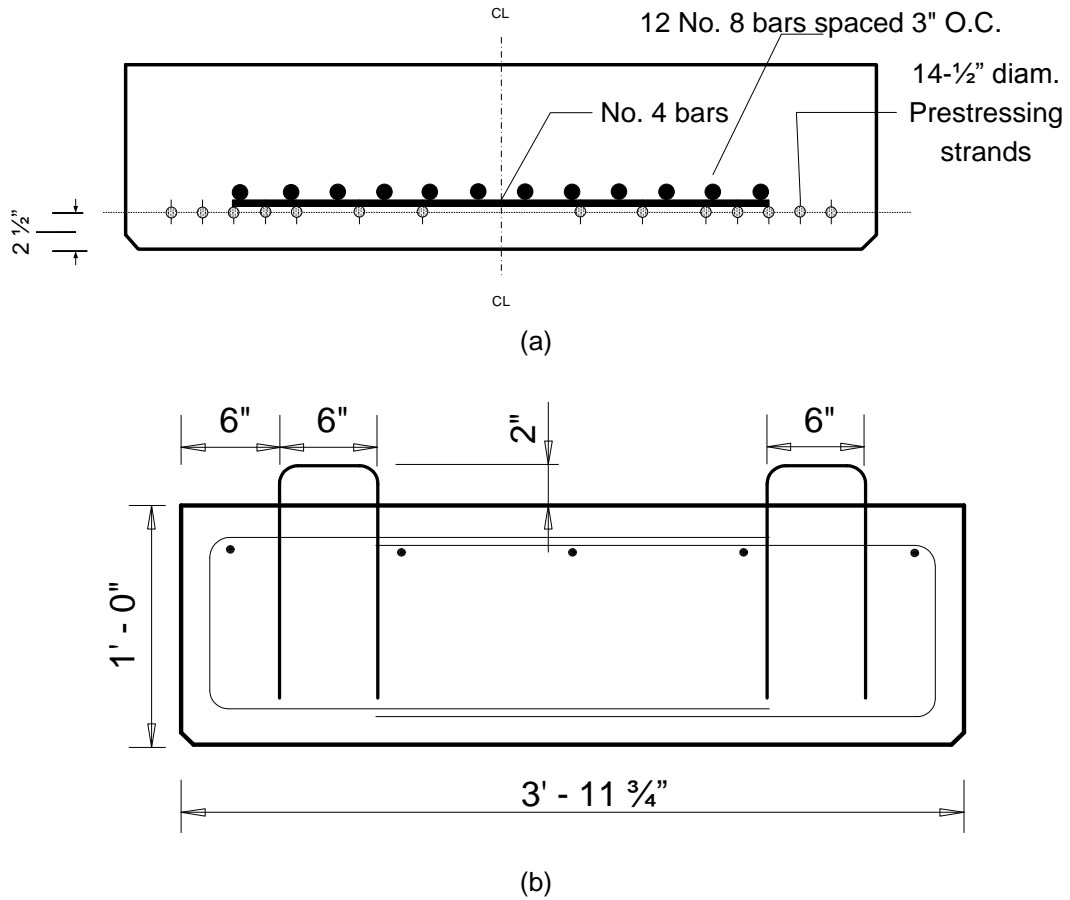
Figure 4-16 4SB12 section with (a) tension reinforcements and (b) horizontal shear

reinforcements

The size of interface area needed to ensure a horizontal shear failure was calculated based on both the elastic method (VQ/Ib_v) and the simplified elastic method (V/b_vd). Three different contact widths (10-in., 12-in. and 14-in.) were used for the calculations and the resulting horizontal shear stress compared to the demand horizontal shear stress (Table 4-9). A reduction of the contact area to 12-in. width was found to be sufficient to lead to horizontal shear failure. Therefore the contact area was reduced from a 47.75-in. width to a 12-in. width.

Table 4-9 Horizontal Shear Stress Calculations

Shear Force (kip)	Horizontal Shear Stress (ksi) (Demand=0.30ksi)					
	14		12		10	
	VQ/Ib_v	V/b_vd	VQ/Ib_v	V/b_vd	VQ/Ib_v	V/b_vd
80	0.41	0.39	0.49	0.46	0.59	0.55
60 (0.75V_u)	0.31	0.30	0.37	0.34	0.44	0.41
40 (0.5V_u)	0.21	0.20	0.24	0.23	0.29	0.28

Block-outs are provided on box beams to act as longitudinal joints/connection between adjacent beams. An example of a block-out can be seen in Figure 4-17. To investigate the effect that the block-out on box beams has on horizontal shear resistance, a box beam was cast with the CIP slab extending onto the block-out on one side (Figure 4-18).

(a) Actual box beam
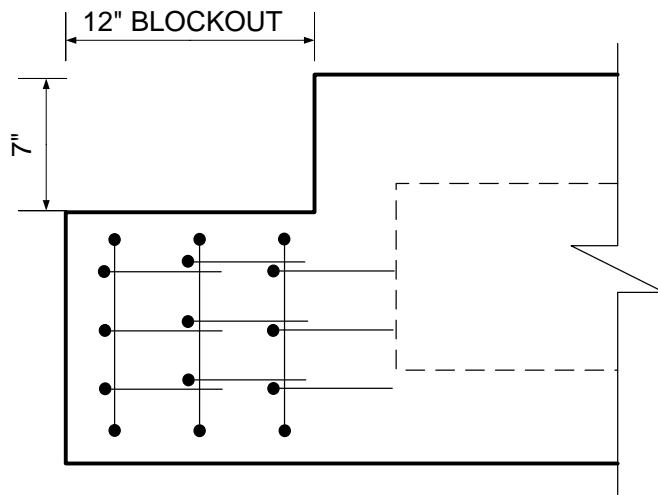
(b) Blockout reinforcement

Figure 4-17 Blockout on box beam

The load was applied at 7 ft. from the support on one end as shown in Figure 4-19 to increase the shear demand. The beam was then be flipped and the load applied 7 ft. from the other end of the beam on which the CIP slab does not extended into the block-out.
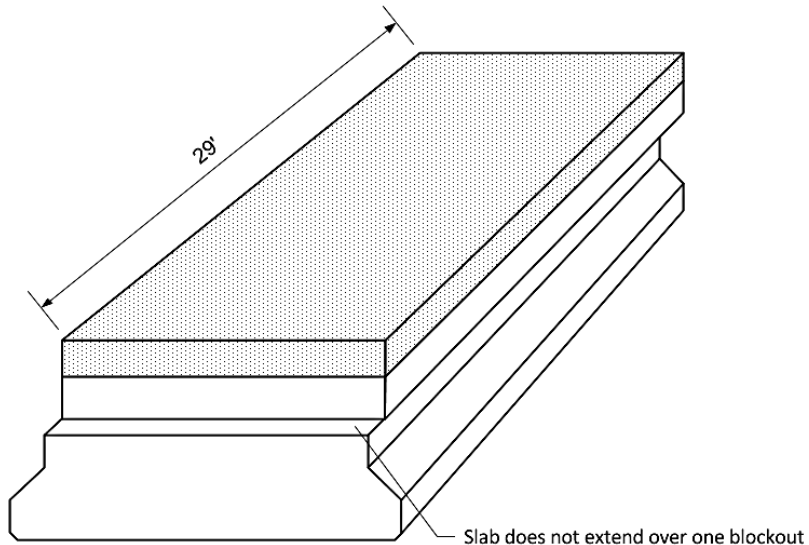
Figure 4-18 CIP slab on box beam
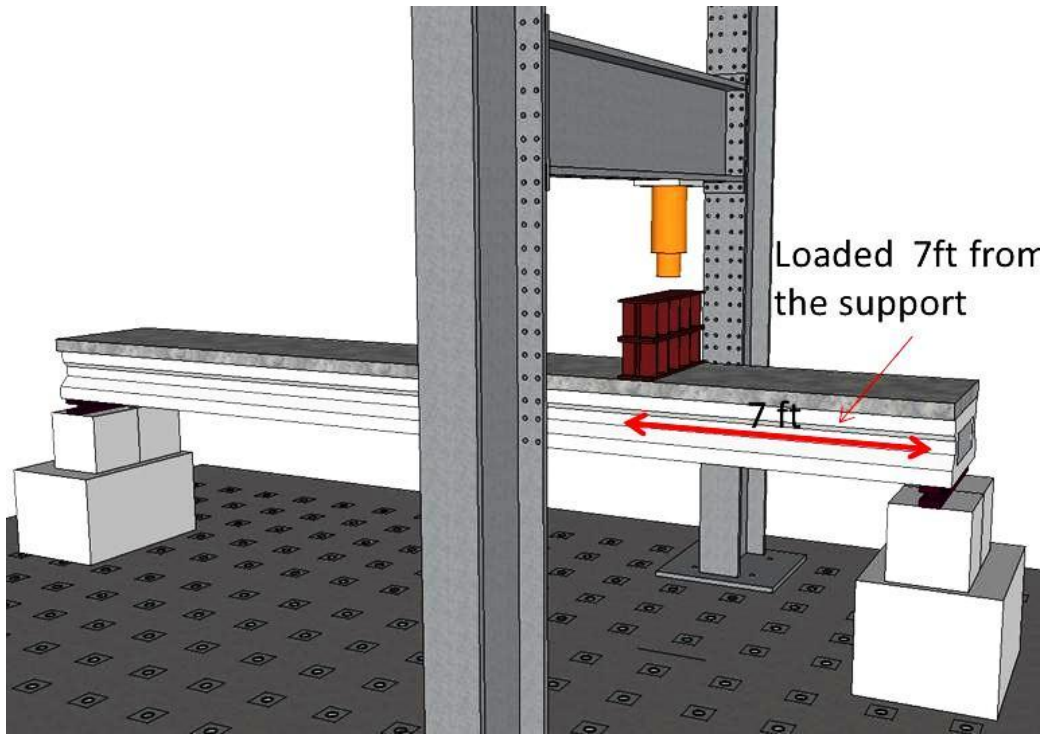
Figure 4-19 Box beam test set-up

To ensure failure by horizontal shear, the interface area was reduced to 14-in. Four No.8 longitudinal mild steel reinforcements were added to increase the shear strength. A cross-sectional view of the 4B20 beam can be seen in Figure 4-20.

Horizontal shear reinforcement was provided at a spacing of 24-in., the maximum spacing allowed by AASHTO. A wood float finish was provided at the interface.

4 No. 8 Bars
spaced at 3" O.C

Prestressing Strands

No. 4 bar

CL

(a)

3' − 11 ¾"

2"

3' − 7 ¾"

2"

4"

9"

9"

2"

2" Clr
Cover

5 ½" Top Slab

1' - 8"

1 ½" Clr Cover

9 ½" Void

5" Bott Slab
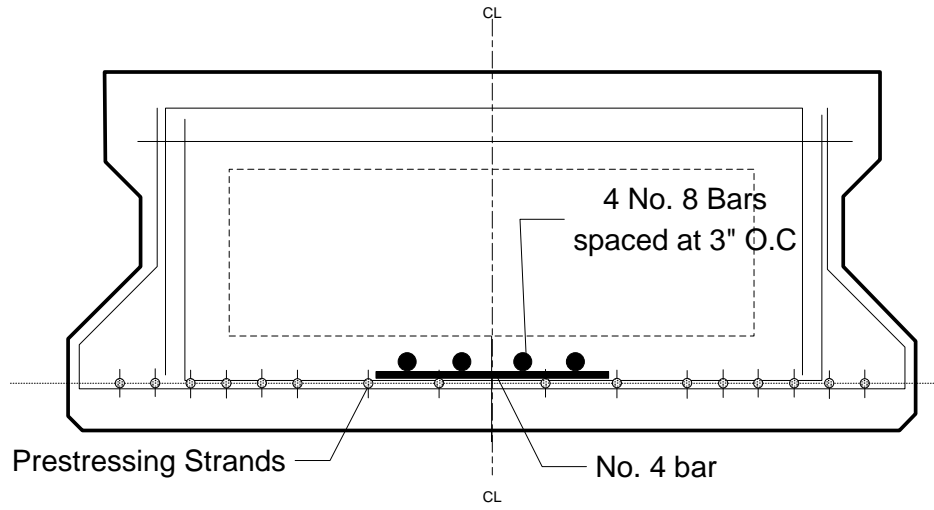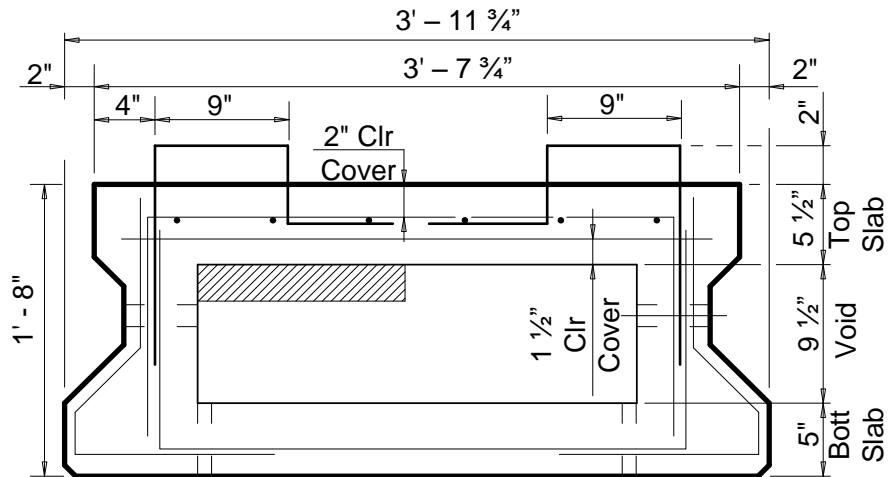
(b)

Figure 4-20 4B20 section with (a) tension reinforcements and (b) horizontal shear

reinforcements

95

Table 4-10 Box beam design

Beam Type	No. of Strands	M_u (kip-ft)	ΦM_n (kip-ft)	V_u (kip)	ΦV_n (kip)	V_{ui} (kip/ft)	V_{ni} (kip/ft)	Peak load for horizontal shear (kip)
4B20-7ft-4#8	16	1035.32	1398.15	149.55	238.41	68.14	71.13	150

The size of interface area needed to ensure a horizontal shear failure was calculated based on both the classical elastic method (VQ/Ib_v) and the simplified elastic method suggested by AASHTO LRFD 2014 5.8.4.2 (V/b_vd). Three different contact widths (10-in., 12-in., and 14-in.) were used for the calculations and the resulting horizontal shear stress compared to the demand horizontal shear stress (Table 4-11). A reduction of the contact area to 14-in. width was found to be sufficient to lead to horizontal shear failure. Therefore the contact area was reduced from a 43.75-in. width to a 14-in. width.

Table 4-11 Horizontal Shear Stress Calculations

Shear Force (kip)	Horizontal Shear Stress (ksi) (Demand=0.36ksi)					
	14		12		10	
	VQ/Ib_v	V/b_vd	VQ/Ib_v	V/b_vd	VQ/Ib_v	V/b_vd
200	0.54	0.63	0.63	0.74	0.76	0.89
150($0.75V_u$)	0.41	0.48	0.47	0.56	0.57	0.67
100($0.5V_u$)	0.27	0.32	0.32	0.37	0.38	0.44

4.3 Materials and Casting Procedures

4.3.1 Materials

This section presents characteristics of the materials used for the small scale and full-scale specimens.

<u>*Concrete*</u>

Ready-mix concrete from a local plant was procured for casting the push-off and pullout specimens. Since TxDOT precast box and slab beams are fabricated by concrete Class H and the CIP slab by concrete Class S, a ready-mix company that is TxDOT approved to supply those two classes of concrete was chosen. TxDOT Class H concrete is usually proportioned for a minimum initial compressive strength of $f'_{ci} = 4.0$ ksi and $f'_c = 5.0$ ksi and a maximum of $f'_{ci} = 6.0$ ksi and $f'_c = 8.5$ ksi whereas Class S is proportioned for a minimum compressive strength of $f'_c = 5.0$ ksi. The material specifications as provided in the TxDOT Standard Specifications are shown in Table 4-12.

Table 4-12 TxDOT material specification

Class of concrete	Design strength, Min 28-day f'_c (psi)	Maximum W/C ratio	Coarse aggregate grades
H	5000	0.45	3-6
S	4000	0.45	2-5

The mix proportion used by the ready-mix company is shown in Table 4-13.

.

Table 4-13 Concrete mix proportions

Properties	Class H	Class S
Type III cement	611 lb	423 lb
Fly ash	-	141 lb
Lime	1840 lb	1840 lb
Coarse aggregates (3/4")	1331 lb	1255 lb
Fine aggregates	Not specified	50%
Retarder	9.02 oz	11.3 oz
Water-cement ratio	0.45	0.45

*Quantities per cubic yard of concrete.

Reinforcement

Grade 60 reinforcement meeting ASTM *A615 "Standard Specification for Deformed and Plain Carbon-Steel Bars for Concrete Reinforcement"* (2014) was used on all specimens.

Prestressing strands

0.5-in. low-relaxation strands meeting "*Standard Specification for Steel Strand, Uncoated Seven-Wire for Prestressed Concrete" (2014)* were used having a specified tensile strength (f_{pu}) of 270 ksi.

4.3.2 Casting Procedure

4.3.2.1 Task 4

The reinforcement caging for the push-off specimen was constructed according to the layout provided in Section 4.2.1. The horizontal shear reinforcements were strain gauged on both sides of the interface to obtain strain information. The strain gauges were

located 0.5-in. away from the interface to ensure they were not damaged once a crack occurred. The horizontal shear reinforcement bars were then tied to the reinforcement caging at approximately center of the interface area (Figure 4-21).

Figure 4-21 Caging for precast part of specimen

The formwork was oiled to enable easy demoulding and the cages then placed in the formwork for casting. Figure 4-22 through Figure 4-24 shows the different configurations for the horizontal shear reinforcement.

Figure 4-22 3.5-in. wide horizontal shear reinforcement with 2-in. embedment (180° bend) placed in the (a) transverse and (b) longitudinal direction

Figure 4-23 6-in. wide horizontal shear reinforcement with 2-in. embedment (90°

bend)

Figure 4-24 (a) 6-in. and (b) 9-in. wide horizontal shear reinforcement with 4-in.

embedment (90° bend)

The concrete mix used was chosen according to TxDOT specifications (Section 4.3.1). Box and slab beams are typically cast with concrete class "H", while the CIP slab is commonly cast with concrete class "S". Therefore the precast section of the push-off specimens was cast and vibrated first (Figure 4-25) with concrete class "H", then the surfaces of all specimens were finished with a wood float as shown on Figure 4-26. The completed precast sections of the specimens can be seen in Figure 4-27. Cylinders were also cast to test the compressive strength of the mix after 28 days. One inch Styrofoam pieces were used to provide the notches for the specimens.

Figure 4-25 Casting of the precast section

Figure 4-26 Wood float finish on all specimens

The specimens were then covered by a plastic sheet for curing.

Figure 4-27 Completed precast section casting

The surfaces of the precast part were air blown to remove dust and dirt particles before casting of the CIP part. The reinforcement cage was then placed on top of the precast section within the formwork (Figure 4-28) and the concrete (Class "S") was cast (Figure 4-29). The completed specimens after casting are shown in Figure 4-30.

Figure 4-28 CIP caging and formwork

Figure 4-29 Casting of CIP part of specimens

Figure 4-30 Finished specimens

The specimens were then covered with a plastic sheet and cured for 28 days after which they were demoulded and prepared for testing. The concrete strength after 28 days was 5.5 ksi for the precast part and 3.9 ksi for the CIP part.

4.3.2.2 Task 5

As mentioned in Section 4.2.2, bar pullout specimens were cast to represent the horizontal shear reinforcement embedded within the CIP slab. As has been pointed out in Section 2.3 (Rehm, 1969), the direction of casting is an important factor that affects bar slip. Rehm observed that the difference in performance between various bend angles became significant when the bar is pulled in the direction of concrete casting (which is the case for the CIP composite slabs) due to the fact that the bond between the anchored bars and the concrete is affected by water and mortar migration toward the inward side of the bars. This leads to a weakened zone upon bearing. This phenomenon is also known as the top-bar effect. The pullout specimens were therefore cast in the manner in which they would have been cast in the field so as to factor in this effect.

Strain gauges were mounted on the bars within 1-in. from the embedded length above the concrete to measure the strains in the bar.

Figure 4-31 Mounted strain gauge

Figure 4-32 Strain gauge location

The caging for the transverse and longitudinal reinforcement was then constructed for all the specimens according to the proposed spacing.

Figure 4-33 Caging for pullout specimens

The bars and the caging were then placed inside the formwork for casting (Figure 4-34). Since there was a possibility of the horizontal shear reinforcement being pushed further in by the concrete pressure during casting, steel wires were used to hold it in place.
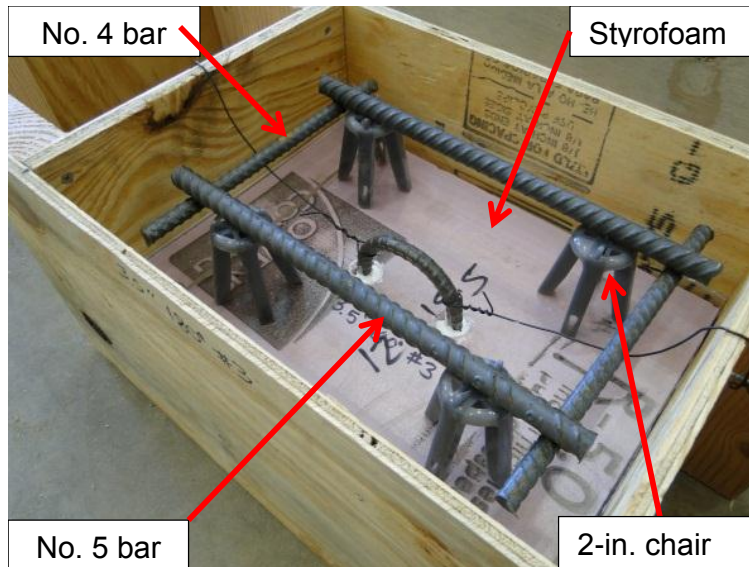
Figure 4-34 Bar pullout specimen preparation

The pullout specimens representing the CIP slab were cast with concrete Class "S"
typical of CIP slabs. The specimens were then covered with a plastic sheet and cured for
28 days after which they were demoulded and prepared for testing. The concrete
strength at the time of testing the specimens was 3.9 ksi. Figure 4-35 and Figure 4-36

Figure 4-36 Finished specimens

show the casting and the finished pullout specimens.

Figure 4-35 Specimen casting

Figure 4-36 Finished specimens

4.3.2.3 Task 6

<u>*Box Beam Specimens*</u>

The beams were prepared at Flexicore in Houston, Texas. The reinforcement layout is as shown inFigure 4-37. The prestressing bed was first cleaned and sprayed with water because of the high temperatures on the day of casting. The prestressing strands were then drawn and stressed at a jacking force of 31 kips per strand (Figure 4-38). The longitudinal reinforcement was then placed as well as the end mat

reinforcement. Bars C (Figure 90) were then positioned at a spacing of 6-in. whereas Bars U were placed at a spacing of 9-in. Strain gauges were installed on the longitudinal bars and the shear reinforcement to monitor the strains on the bars (Figure 4-39 to Figure 4-41). The horizontal shear reinforcement at both ends of the beam and the center were strain gauged on both sides of the interface to obtain strain information. Concrete cylinders were also cast to obtain the compressive strength of the mix after 28 days.
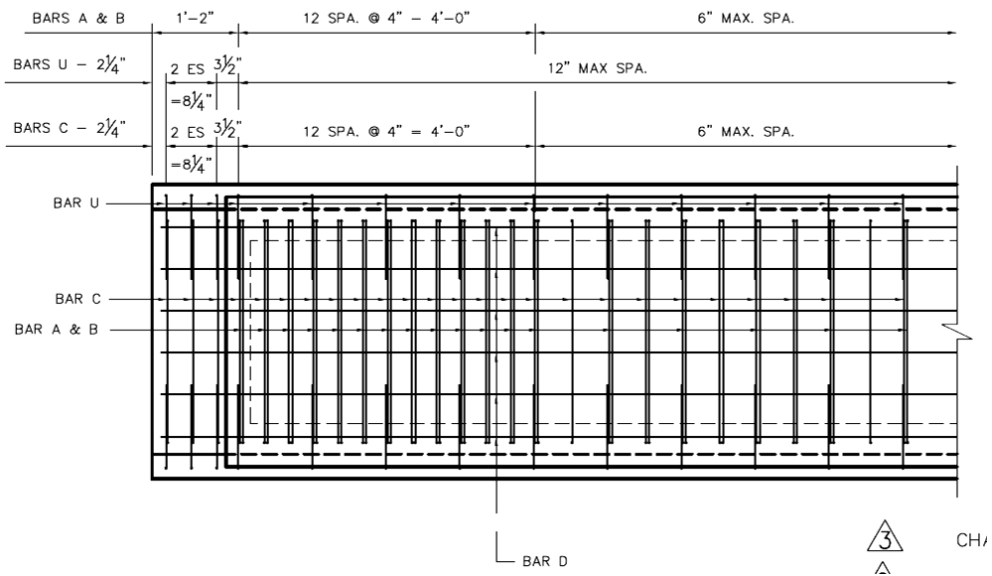
Figure 4-37 TxDOT box beam reinforcement layout

Figure 4-38 Prestressed strands

(a) Mounting of strain gauges

(b) Finished bars

Figure 4-39 Strain gauging of Bar U

Figure 4-40 Strain gauges on longitudinal reinforcement

Figure 4-41 Reinforcement layout

The concrete mix used was chosen according to TxDOT specifications. Box and slab beams are typically cast with concrete class "H", while the CIP slab is cast with concrete class "S" (see Section 4.3.1). The box beams were cast in two pours. After the bottom reinforcement was placed, the concrete was poured to a height of 5-in. after which Styrofoam was placed to create the hollow section of the box beam (Figure 4-42 and Figure 4-43).

Figure 4-42 Concrete poured to 5-in.

Figure 4-43 Placing of the Styrofoam

The reinforcement cage for the top portion of the box beam was then placed using a crane. Figure 4-44 shows the top reinforcement for the box beam with horizontal shear reinforcement. Figure 4-45 shows the top reinforcement for the box beam without

112

horizontal shear reinforcement. The concrete was then mixed at the plant and poured on top of the beams (Figure 4-46). As the concrete was poured the horizontal shear reinforcement was adjusted to its correct location and the surface was initially finished using a wood float.

Figure 4-44 Top reinforcement for box beam with horizontal shear reinforcement

Figure 4-45 Top reinforcement for box beam without horizontal shear

reinforcement

Figure 4-46 Casting of the top part of the box beam with horizontal shear reinforcement

Flexicore uses rake finish for all their box and slab beams therefore a rake finish was provided on all of our beam specimens. The rake was passed through the wet concrete surface transverse to the beam length as demonstrated in Figure 4-47.

Figure 4-47 Rake finish on box beams

The horizontal shear reinforcements were then lightly scrubbed by a steel wool to remove concrete from their surfaces. The completed box beam after concrete casting is shown in Figure 4-48.

The specimens were then covered to avoid moisture loss during curing. The prestressing strands were cut the next day and the beam specimens were demoulded for storage (Figure 4-49). The concrete strength after 28 days was 11 ksi for the precast box beams. The very high strength was attributed to the high temperature during the time period when the specimens were fabricated.

Figure 4-48 Finished box beam after casting

Figure 4-49 Finished box beam specimens

After the prestressing strands were stressed, the longitudinal bars were placed. The bars were supported on top of the strands by No. 4 bars placed transversely at intervals along the length of the slab beam (Figure 4-50). The shear reinforcements (Bar C) were then placed at 9-in. spacing from the center of the beams. Some of the stirrups were strain-gauged. Three of the longitudinal mild steel bars were strain-gauged as shown in Figure 4-51.
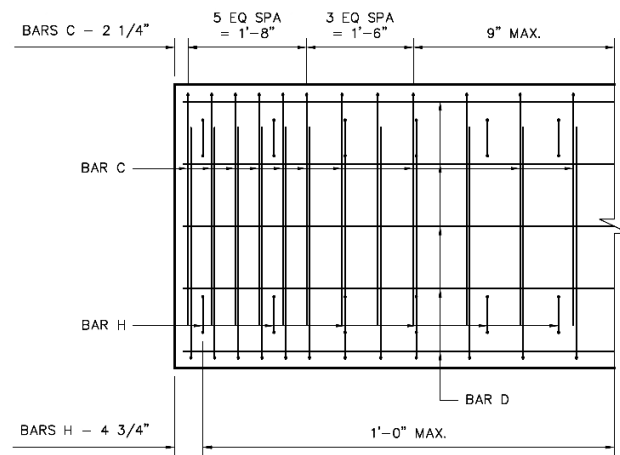
(a) Design layout

(b) Actual layout

Figure 4-50 TxDOT Slab Beam Reinforcement layout
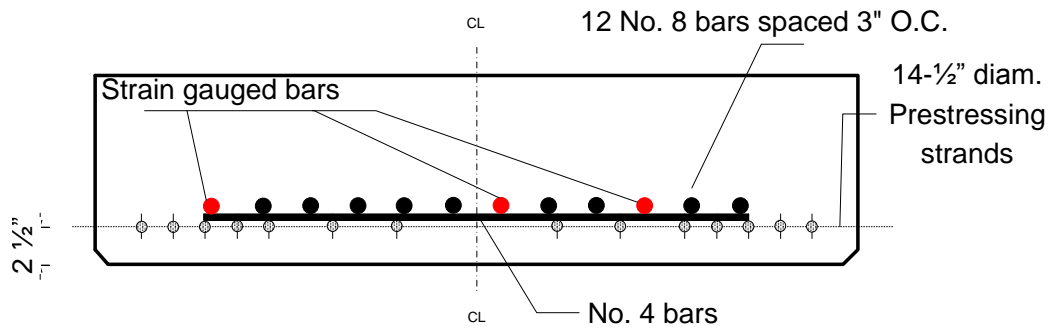
Figure 4-51 Slab beam section

Class "H" concrete was used for cast according to TxDOT specifications. The slab beams were cast in a single pour (Figure 4-52). A rake finish was applied on the wet concrete surface in the transverses direction (Figure 4-53) before the beams were covered for curing.

Figure 4-52 Slab beam casting

Figure 4-53 Rake finish

A longitudinal line was then made on the wet concrete at 6-in. from the edge to mark the position where the horizontal shear reinforcement would be placed. The horizontal shear reinforcement bars were then pushed into the wet concrete to a height of 2-in. from the concrete surface (Figure 4-54). The finished slab beams with and without horizontal shear reinforcements are shown in Figure 4-55 and Figure 4-56 respectively. The concrete strength after 28 days was 10 ksi for the precast slab beams.

Figure 4-54 Placing of horizontal shear reinforcement

Figure 4-55 Finished slab beam with horizontal shear reinforcement

Figure 4-56 Finished slab beam without horizontal shear reinforcement

CIP Slab

The CIP slab was cast on top of the precast beams after two weeks. The details

of the reinforcement for the CIP slab were consistent with that used on TxDOT bridges.

The CIP slab reinforcement details for the box beam are shown in Figure 4-57 to Figure

4-58. It should be noted that in order to study the effects of the block-out on the horizontal shear strength, the slab will not extend to one block-out (Figure 4-59).
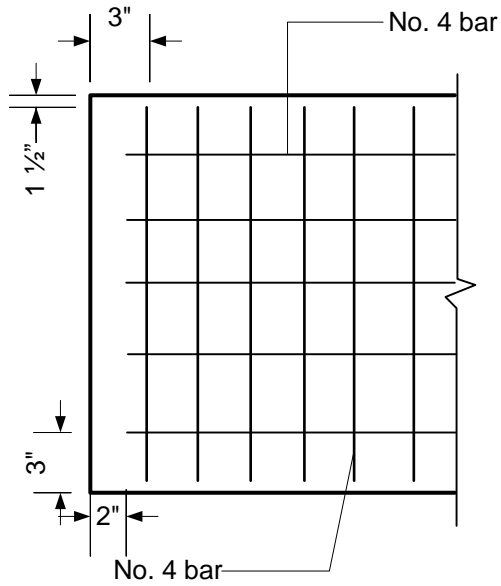
Figure 4-57 CIP slab reinforcement layout for box beam (Plan View)
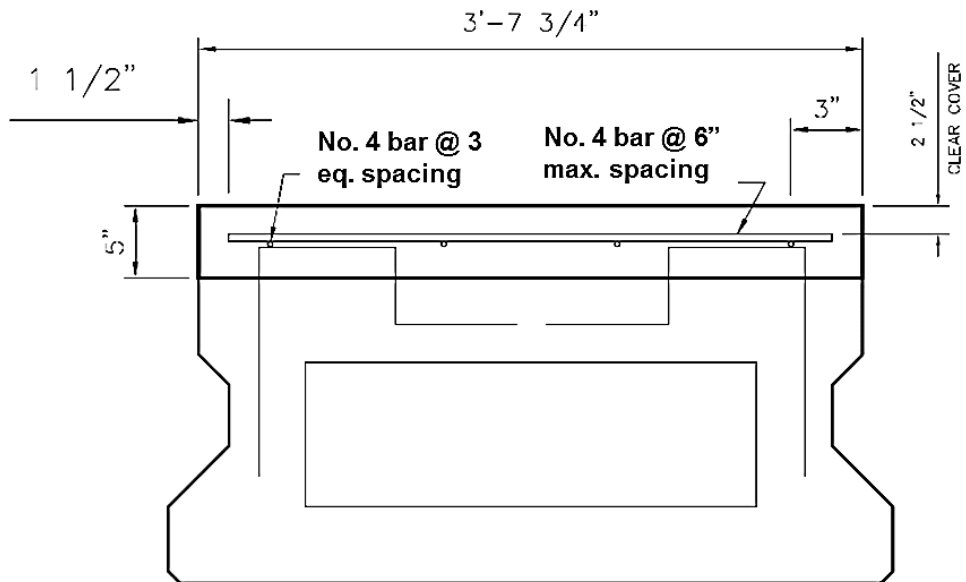
Figure 4-58 CIP slab detail for box beam
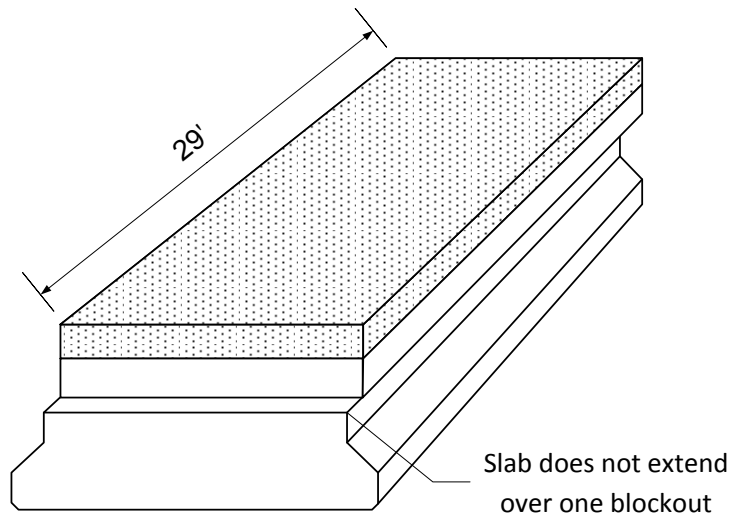
Figure 4-59 CIP slab in box beam does not extend to one block-out

The slab reinforcement details for the slab beam are shown in Figure 4-60 to Figure 4-61. The horizontal shear reinforcement was instrumented with strain gauges at mid-span and near the ends of the beams prior to casting.
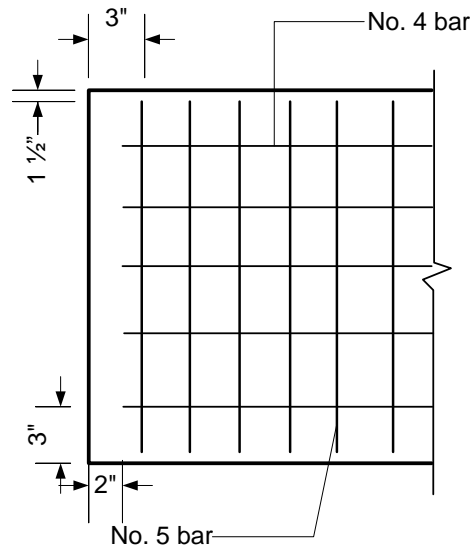
Figure 4-60 CIP slab reinforcement layout for slab beam (plan view)
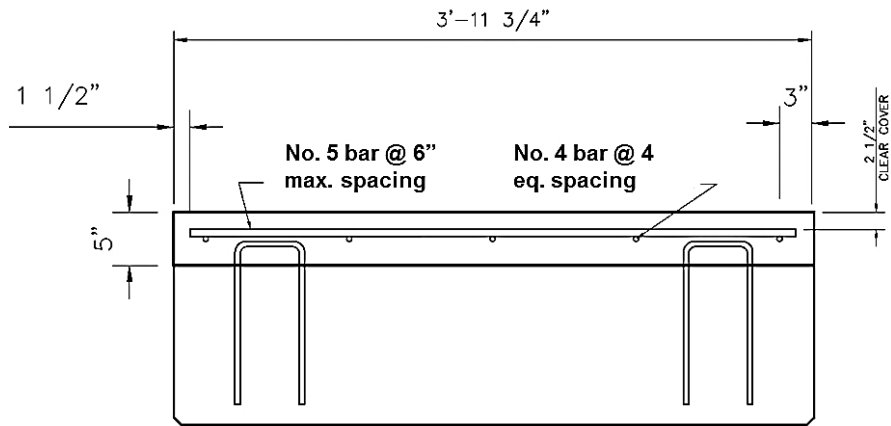
Figure 4-61 CIP slab detail for slab beam

The surfaces of the precast beams were cleaned to remove dust and dirt particles before casting. The reinforcement cage was then placed on the beams. The box and slab beam specimens with the added slab reinforcement prior to casting can be seen in Figure 4-62 to Figure 4-65. The CIP was cast with concrete Class "S" as shown in Figure 4-66. The slab surface was prepared using a wood float finish. The completed box beams after casting can be seen in Figure 4-67.

Figure 4-62 Box beam with CIP slab reinforcement and horizontal shear reinforcement

Figure 4-63 Slab beam with CIP slab reinforcement and horizontal shear reinforcement

Figure 4-64 Slab beam with CIP reinforcement but without shear reinforcement
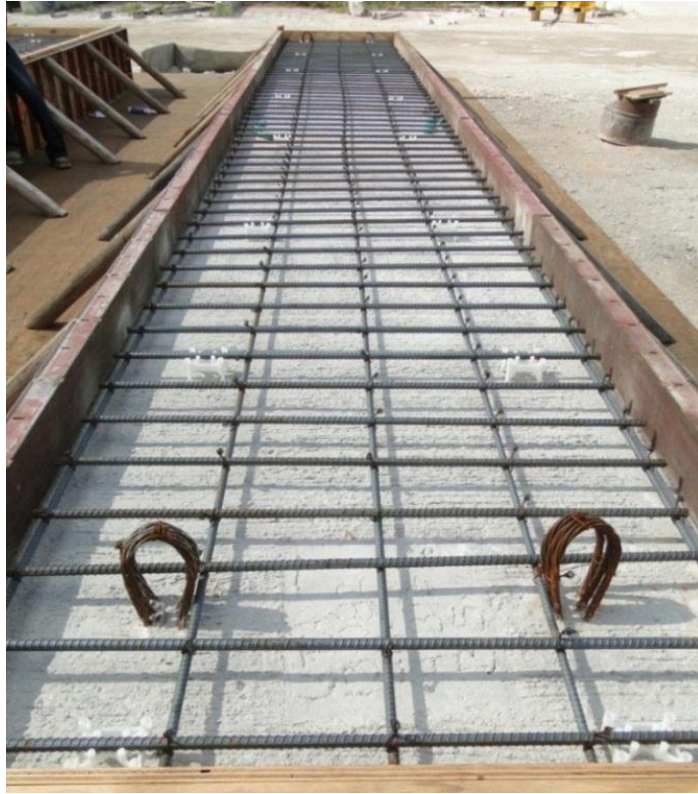
Figure 4-65 Box beam with CIP reinforcement but without shear reinforcement

Figure 4-66 Vibrating and wood float finishing

Figure 4-67 Finished box beam specimens

The specimens were then covered with a plastic sheet and cured, the next day they were demoulded and prepared for delivery to UTA. The concrete strength after 28 days was 11 ksi for the CIP slab. The beams were delivered to the UTA Civil Engineering Laboratory (Figure 4-68). North Texas Crane was hired to aid in unloading the beams from the delivery trucks (Figure 4-71).

Figure 4-68 Beams arrive at UTA Civil Engineering Laboratory

Figure 4-69 Unloading of slab beams

Figure 4-70 Unloading of box beams

Figure 4-71 Storing of the beams outside the lab

4.3.2.4 Task 7

<u>Box beam</u>

The same process as described in Task 6 was used in fabricating the precast beams in Task 7. Strain gauges were installed on the longitudinal bars and on shear reinforcements (Bars C) to monitor the strains on the bars (Figure 4-72 to Figure 4-73).

(a) Mounting strain gauges
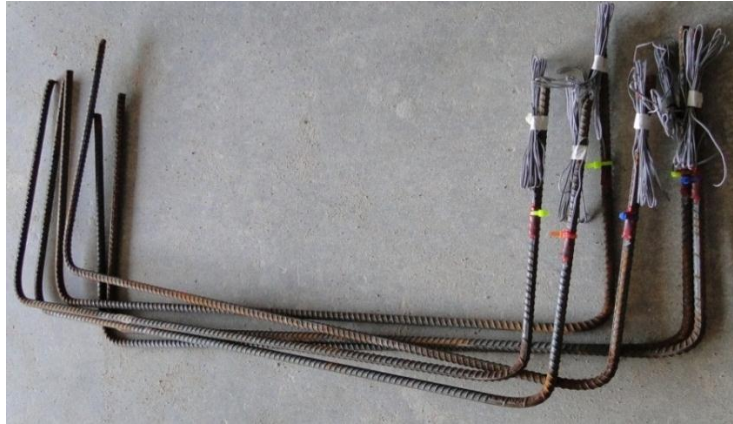
(b) Finished reinforcement

Figure 4-72 Strain gauging of shear reinforcement

Figure 4-73 Strain gauges on longitudinal reinforcement

The concrete mix used was chosen according to TxDOT specifications. Box and slab beams are typically cast with concrete class "H", while the CIP slab is commonly cast with concrete class "S" (Section 4.3.1). Unlike the box beam in Task 6, the horizontal shear reinforcements were spaced at a spacing of 24-in., which is the maximum allowed spacing for horizontal shear reinforcement by AASHTO (Figure 4-74). Figure 4-75 shows the casting of the top portion of the box beam after the placement of the Styrofoam and reinforcing cage. A wood float finish was then provided at the surface of all the beams (Figure 4-76).

Figure 4-74 Top reinforcement for box beam with shear reinforcement

Figure 4-75 Casting of the top part of the box beam

Figure 4-76 Wood float finish

The horizontal shear reinforcements were then lightly scrubbed by a steel wool to remove concrete from their surfaces. The box beam specimen was then covered to avoid moisture loss during curing. The prestressing strands were cut the next day and the specimen demoulded for storage. The completed box beam specimen can be seen in Figure 4-77, a closer look at the surface roughness provided by the wood float finish can be observed in Figure 4-78.

Figure 4-77 Finished box beam specimen

Figure 4-78 Surface finish on box beam

Slab beams

After prestressing the strands, the mild steel longitudinal bars were placed. The bars were supported on top of the strands by No. 4 bars placed transversely at intervals along the length of the slab beam (Figure 4-79). The shear reinforcements (Bar C) were then placed at 9-in. spacing from the center of the beams. Some of the shear reinforcements were strain-gauged (Figure 4-80). The longitudinal bars with strain gauges were placed at the furthest bar from the beam edge, and at the center of the beam (highlighted on Figure 4-79). The finished reinforcing cage for the slab beams is shown in Figure 130.
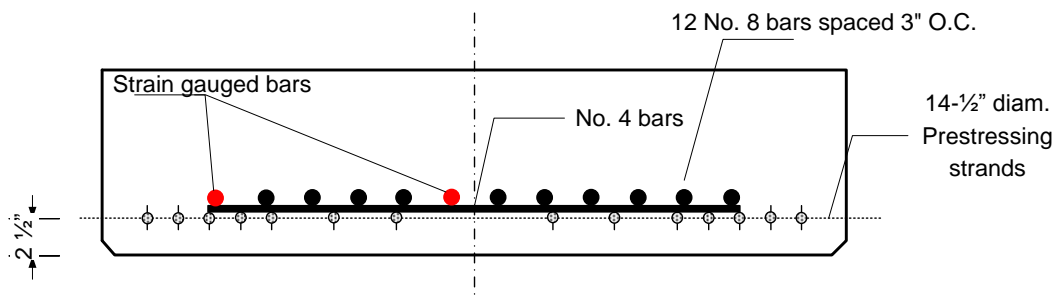
Figure 4-79 Slab beam section
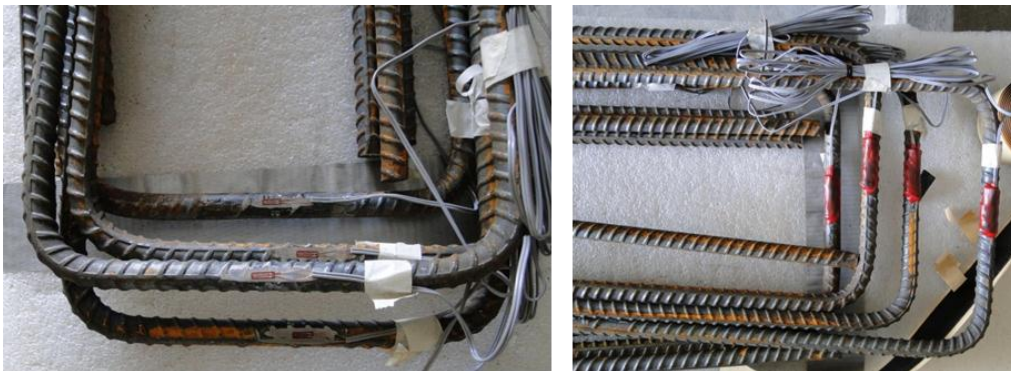
Figure 4-80 Strain gauges on the slab beam shear reinforcement

Figure 4-81 Finished slab beam reinforcement

The concrete mix used was chosen according to TxDOT specifications as mentioned earlier. One of the slab beams was cast with SCC (Figure 4-82) as typically used in their precast panels. Slab beams were cast in a single pour and a wood float finish rather than rake finish was provided to finish the surface (Figure 4-83).

Figure 4-82 SCC Slab beam casting

Figure 4-83 Wood float finish

A longitudinal line was then made on the wet concrete at 6-in. from the edge to mark the position of the horizontal shear reinforcement. The horizontal reinforcements were then pushed into the wet concrete to a height of 2-in. from the concrete surface (Figure 4-84).

Figure 4-84 Placing of horizontal shear reinforcement

The finished slab beam specimen after demoulding can be seen in Figure 4-85. It should be noted that there is a significant difference in surface roughness when comparing conventional concrete finished by a wood float (Figure 4-86) and SCC finished by a wood float (Figure 4-87). The self-consolidating characteristics of SCC allow for fewer exposed aggregate and a much smoother surface than that of conventional concrete. The 28-day compressive strength of the slab beams and box beam was determined to be 11 ksi.

Figure 4-85 Finished specimen

Figure 4-86 Surface finish on slab beam having conventional concrete

Figure 4-87 Surface finish on SCC slab beam

The reinforcement for the CIP slab was consistent with that used on actual bridges. Surfaces of the precast beam were cleaned to remove dust and dirt particles before casting. The reinforcement layout was similar to that used in Task 6 for both the slab beam and the box beam (Figure 4-88 and Figure 4-89) and the concrete (Class "S") was used for casting.
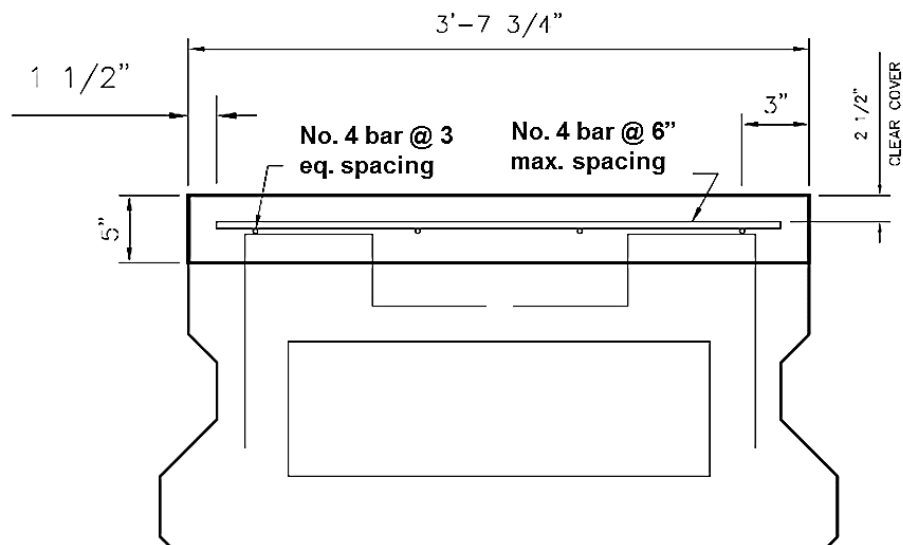
Figure 4-88 CIP slab detail for box beam
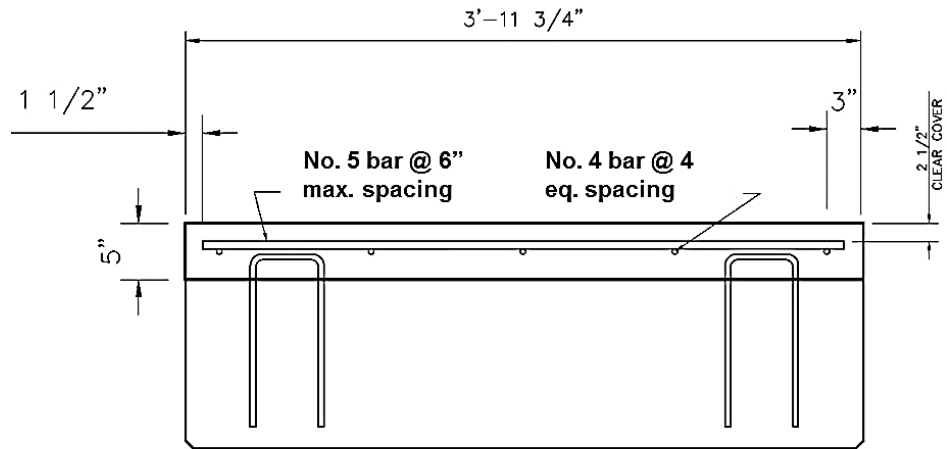
Figure 4-89 CIP slab detail for slab beam

Strain gauges were installed on the horizontal shear reinforcement prior casting of the CIP slab (Figure 4-90).

Figure 4-90 Strain gauges installation on horizontal shear reinforcements

To ensure failure by horizontal shear, it was determined to reduce the interface shear resistance by reducing the interface area. Three methods were suggested from previous research (Kono et al. (2003), Chung and Chung (1976) and Hanson (1960)) for reducing the interface are; using aluminum strips, using Styrofoam, or using polyethylene foam tape (Figure 4-91) at the interface to prevent contact between the precast beam

137

and the CIP slab. The most suitable method was one that provided the least resistance to sliding. Push-off specimens were therefore cast with the different methods to determine which method will be most suitable for the full-scale precast beams.
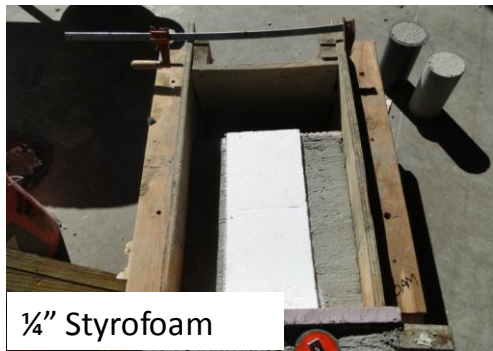
Figure 4-91 Push-off specimen with foam tape, aluminum strip and Styrofoam to reduce interface area

The foam tape was found to provide the least resistance to sliding compared to steel plate and Styrofoam (Figure 4-92). Foam tape was therefore chosen to reduce interface area on the full-scale specimens.
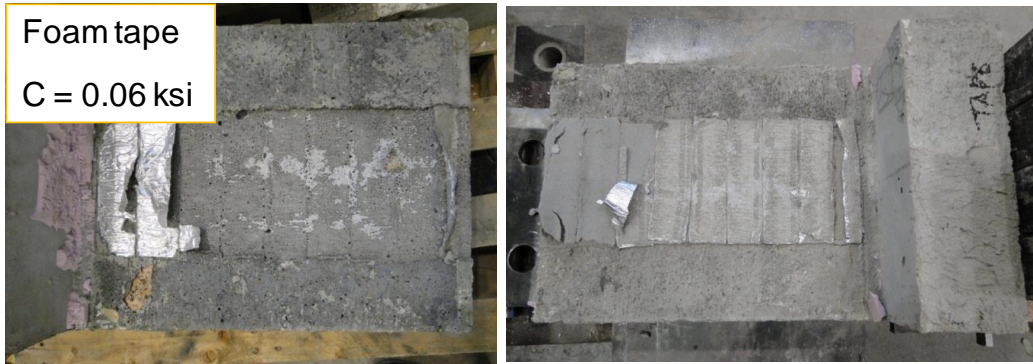
Foam tape
C = 0.06 ksi

Figure 4-92 Foam tape specimen at failure

The foam tape was then placed on the surface of the beams to reduce the interface area. The interface area of the slab beam was reduced from 47.75-in. to 12-in. (Figure 4-93), and the interface area for the box beam was reduced from 43.75-in. to 14-in. (Figure 4-94). The foam tape was placed in two layers to guarantee that no tear will occur during casting of the CIP slab.
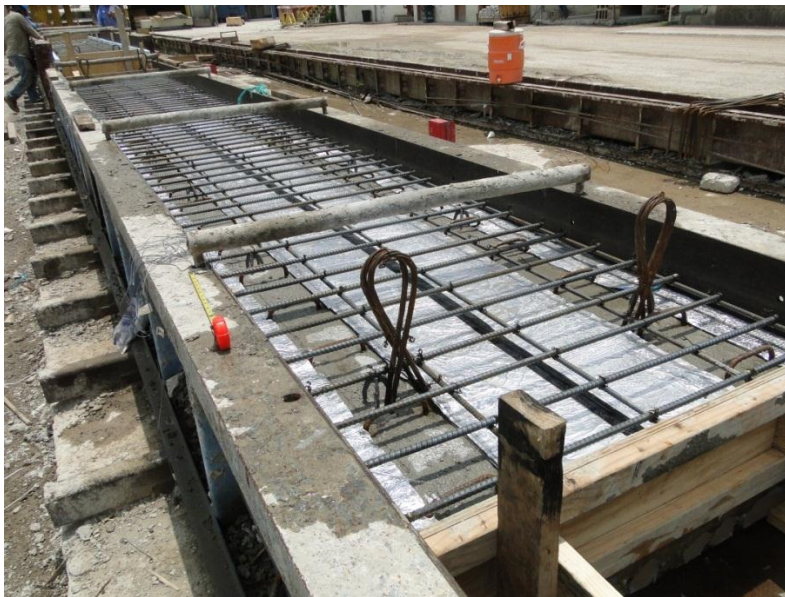
Figure 4-93 Foam tape on the slab beams

Figure 4-94 Foam tape on the box beam

The CIP slab was then cast as shown in Figure 4-96.

Figure 4-95 Casting of CIP slab

Figure 4-96 Finished CIP slab

The 28-day compressive strength of the CIP slab was determined to be 10ksi.

The beams were then delivered to the CELB (Figure 4-97).

Figure 4-97 Storing of the beams outside the lab

4.4 Testing Program and Procedure

4.4.1 Task 4 Test Set-up

The test set-up for the horizontal push-off test is shown in Figure 4-99. It consisted of a hydraulic cylinder that applies the horizontal force on the interface, a load cell to record the load being applied, and a W8×24 loading beam. A 14×1×0.5-in. steel strip was used to transfer the compression load to the specimen. The specimen was instrumented with two LVDTs placed on both the CIP and precast parts to measure the slip at the notch during testing. For specimens that had a 4-in. shear reinforcement embedded length, a vertical LVDT was placed to measure the crack opening at the interface.
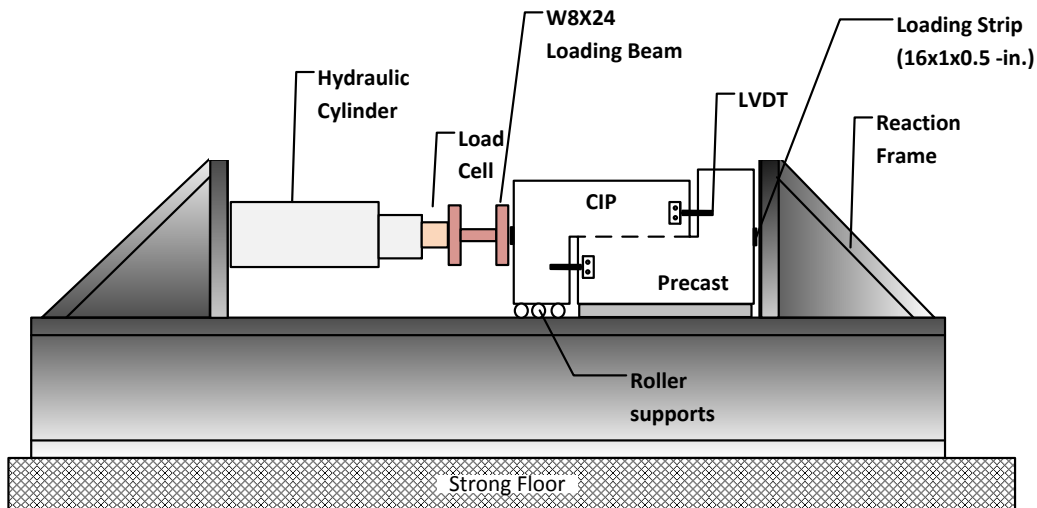
Figure 4-98 Schematic view of test set-up

To reduce any load eccentricities, the actual position of the loading beam and load cell were marked on the center of the specimen before testing. Load was applied at a rate of approximately 100 lb/sec, up to failure. Once interface failure occurred, the load

application was not stopped until the notch closed up. That is the load was applied up to a slip of 1-in.
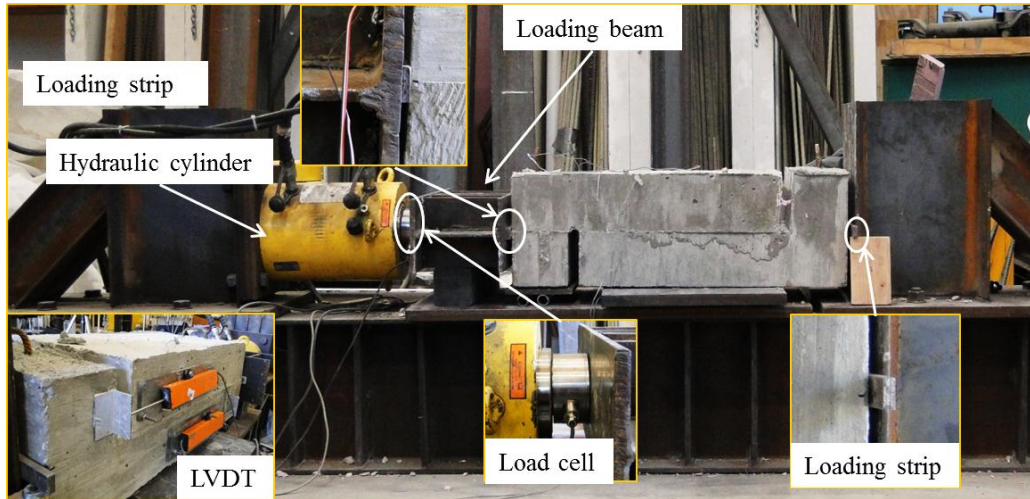
(a)

Figure 4-99 Task 4 (horizontal push-off test) (a) schematic view of the test set-up and (b) actual test set-up

4.4.2 Task 5 Test Set-up

The test set-up for the bar pullout test is as shown on Figure 4-100 through Figure 4-102. The force was applied by a 100-kip servo-controlled closed-loop MTS machine. The specimen was placed on top of the bottom plate and the two threaded bars are passed through the holes in the top plate which were pre-drilled for each respective bar width (refer to Table 4-2). The specimen was restrained by two restraining blocks on the bottom plate which had slotted holes to aid in adjusting the side plates to fit the specimens. The bars were fastened with a terminator onto the top block which was held in place as the MTS machine applies the tensile load. LVDTs were also provided to measure bar slip. Strain gauges were mounted on the bars to record strains.
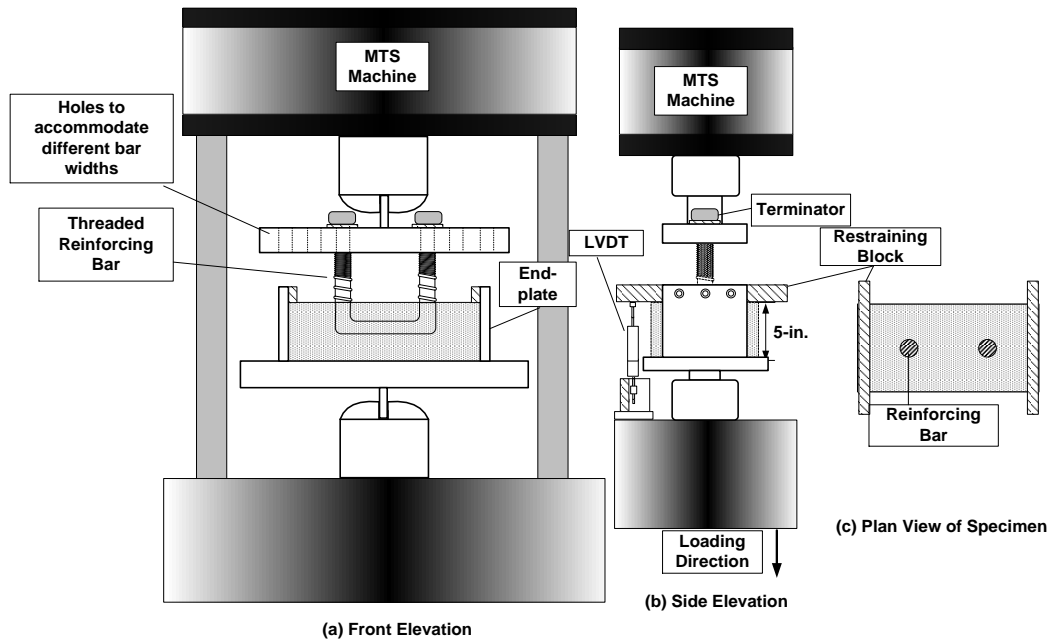
Figure 4-100 Schematic view of test set-up
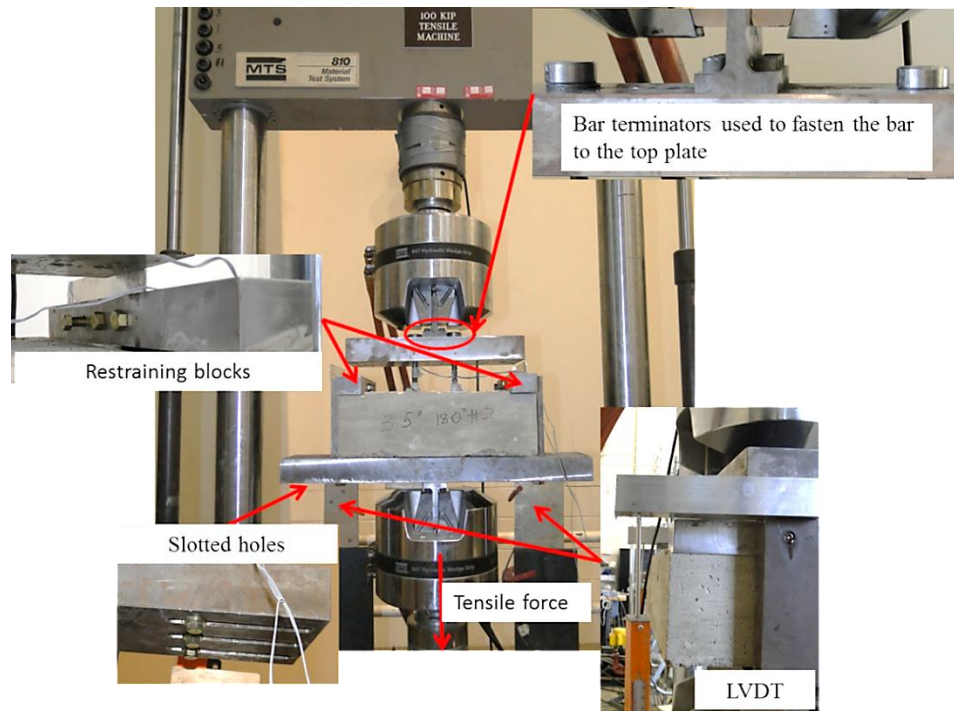
Figure 4-101 Actual test set-up

Figure 4-102 Test set-up showing terminator

This set-up, as was mentioned in Chapter 2 Section 2.3, minimizes confinement from the test set-up as compared to the set-up used by Mattock (1987) (Figure 2-19). A tensile force was applied at a rate of 0.01-in./min until the bar was pulled out and failure occurred.

4.4.3 Task 6 Test Set-up

Three-point loading was selected for this test because of the uniform shear force along the beam, which generates the maximum shear stress along the interface. The beam was monotonically loaded at the center. The test set-up for the full-scale beams (Figure 4-103) is composed of a reaction frame with a hydraulic cylinder attached to apply the load. Two W12x72 wide flange sections were used as the loading beam (stacked one on top of the other) so as to apply the load uniformly along the width of the beam. A load cell was placed between the hydraulic cylinder and the loading beam to accurately record the load being applied. The specimen was instrumented with three LVDT's placed at the interface to measure the relative slip between the precast and CIP

145

parts during testing. Two LVDTs were placed under the midpoint of the beam to measure the displacement during loading. To reduce any load eccentricities, the actual position of the loading beam and load cell were marked on the specimen before testing.

The load was then applied at the center of the beam at different loading intervals up to failure.
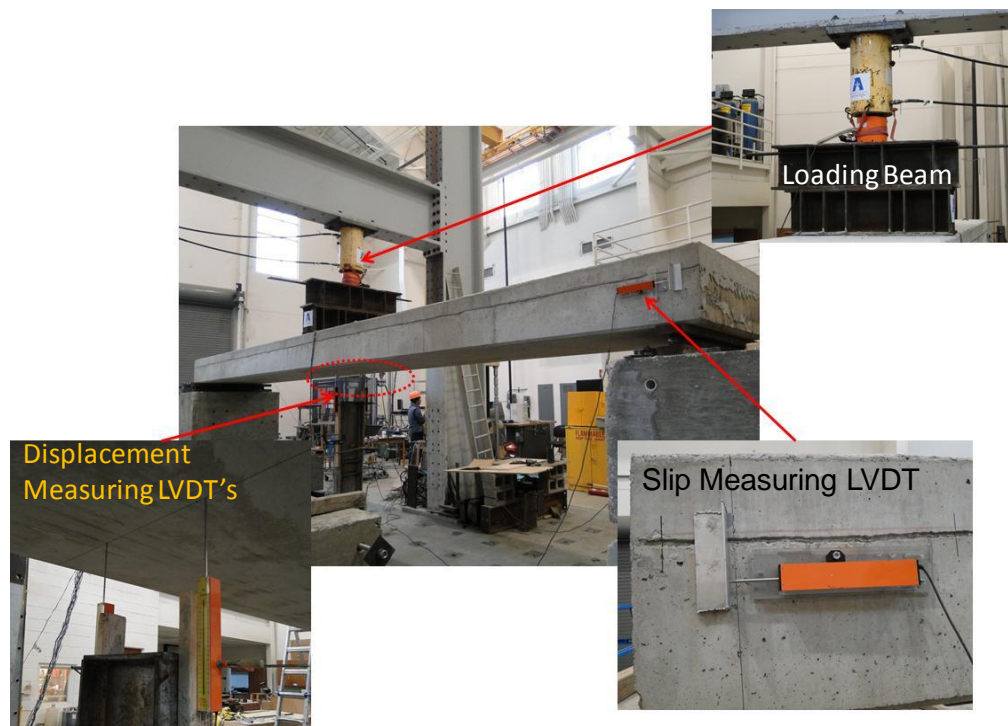
Figure 4-103 Test set-up: LVDT's and loading beams

4.4.4 Task 7 Test Set-up

The proposed test set-up for Task 7 was similar to that used in Task 6 with the exception of the position of the point load. To increase the shear demand on the beams in order to force horizontal shear failure, two approaches were used. The box beam was loaded 7 ft. from the support as explained in Chapter 4 Section 4.2 to increase the shear demand whereas the slab beams were loaded at the center in a similar way to Task 6 specimens (Figure 4-104).
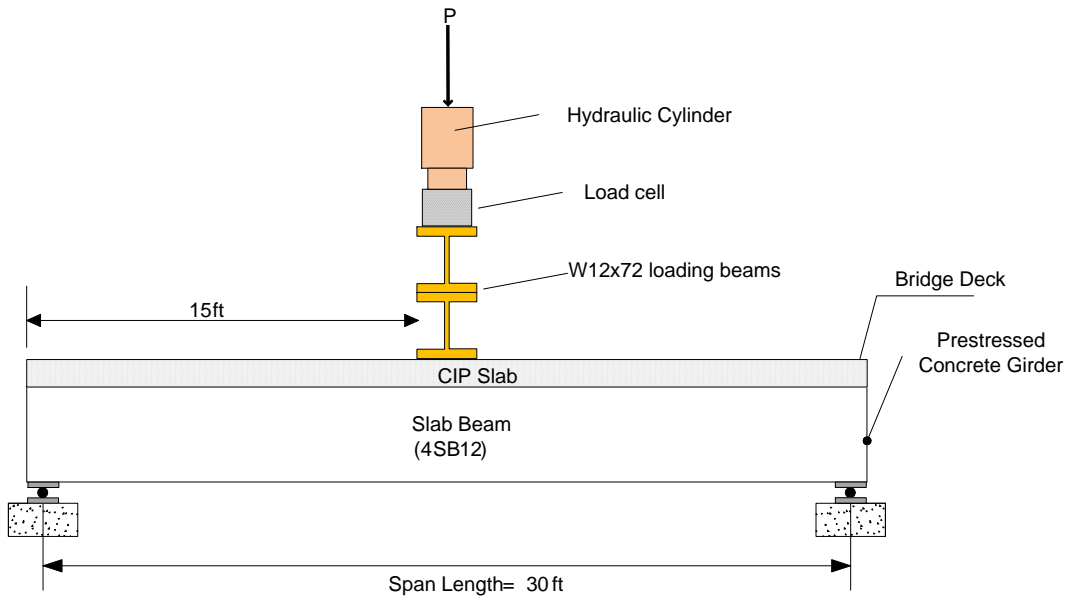
(a)
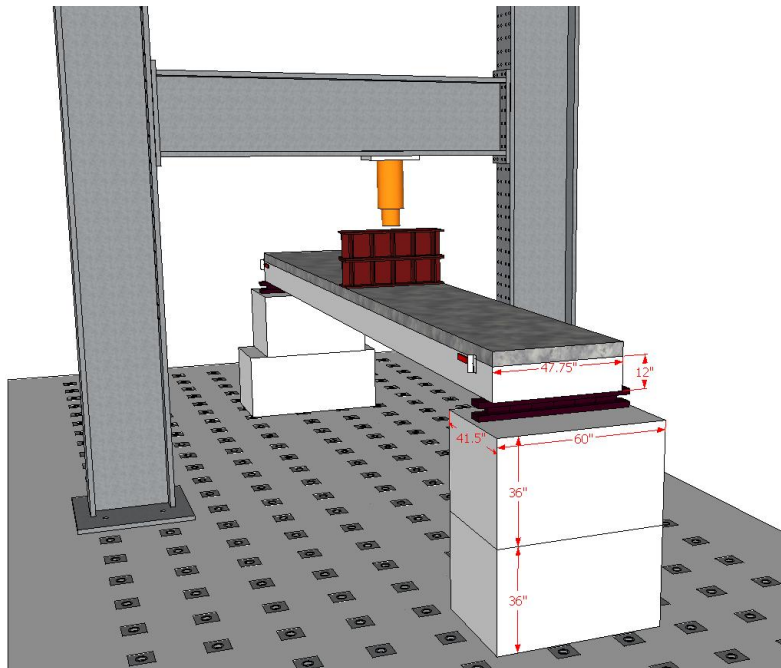
(b)

Figure 4-104 Schematic view of the slab beam test set-up

Once one side of the box beam having no blockout was tested (Figure 4-106(a)), the beam was flipped and the other side of the box beam (without CIP slab extending into the blockout) was tested at 7 ft. from the support (Figure 4-106(b)). The specimens were instrumented with two LVDTs placed on both the CIP and precast parts to measure the slip during testing. One LVDT was placed under the mid-span of the beams to measure the displacement during loading whereas one LVDT each was placed at the supports to check for any settlement occurring at the supports.
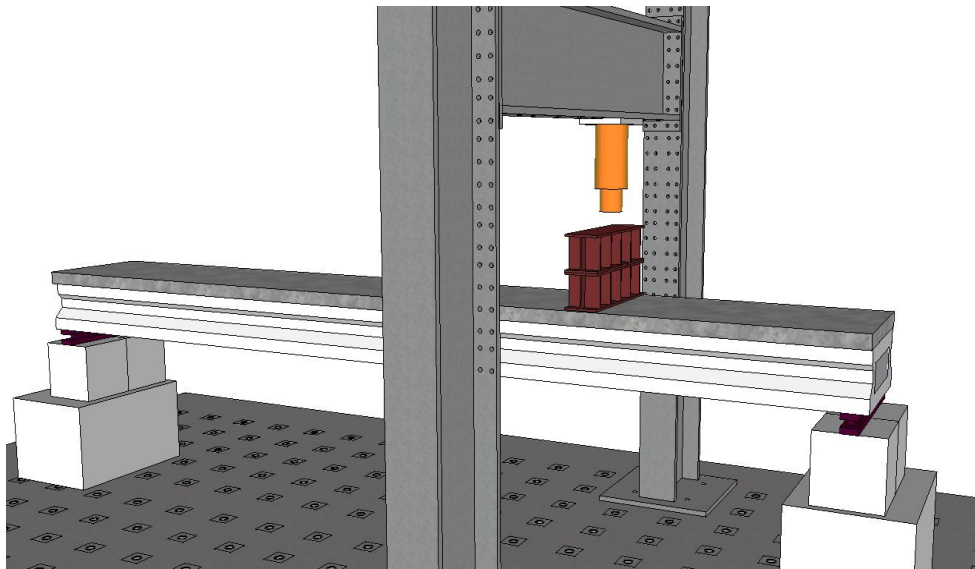
Figure 4-105 Schematic view of box beam set-up
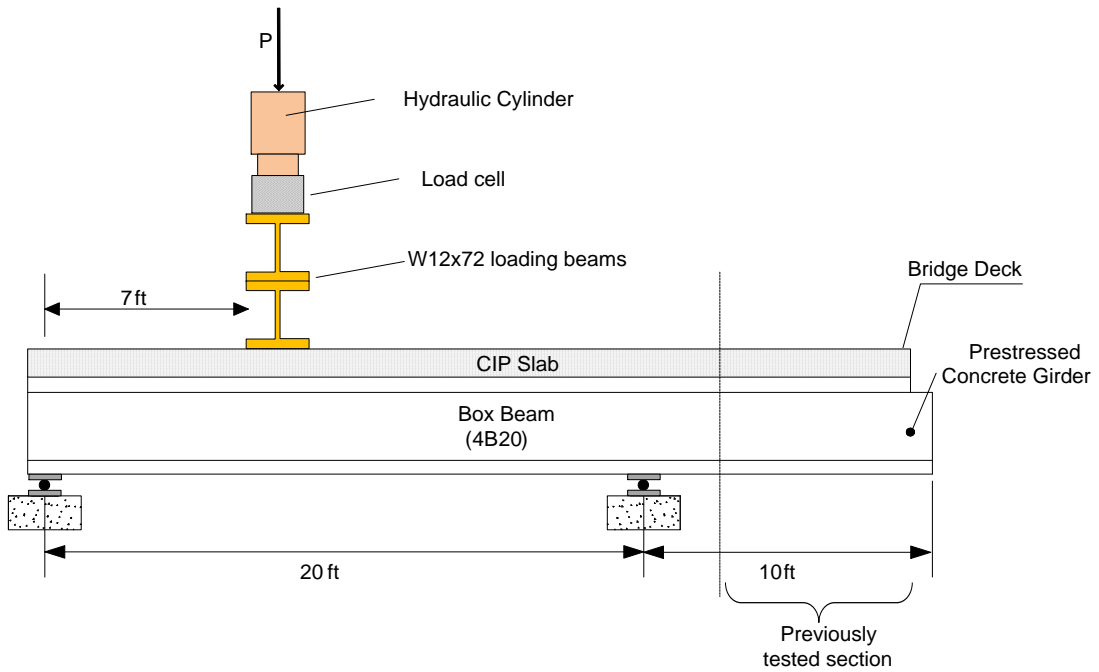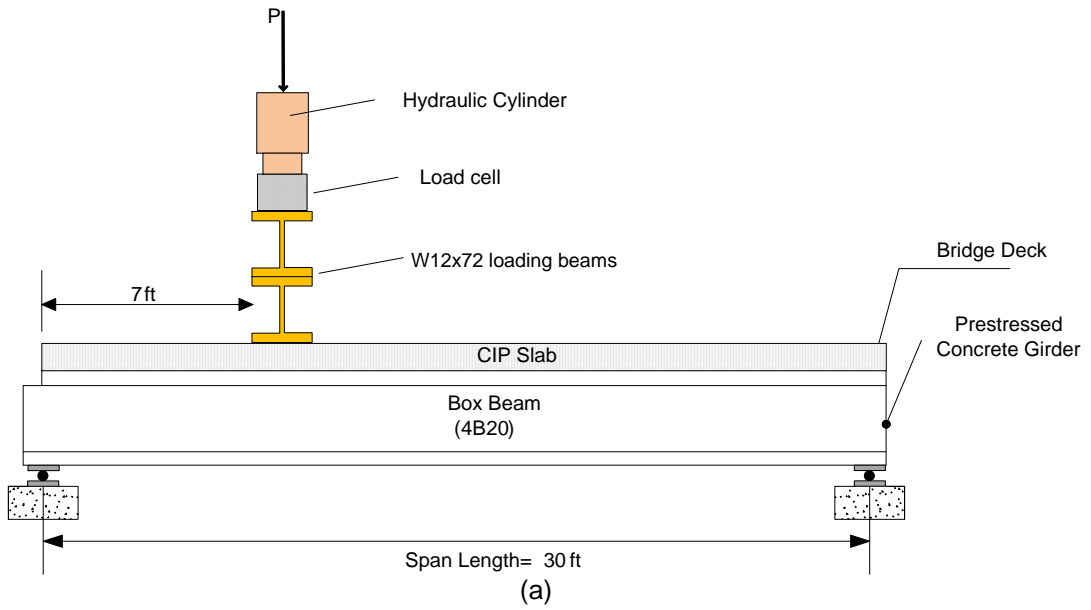
Figure 4-106 Schematic view of the box beam (a) without blockout and (b) with blockout

test set-up

Chapter 5

TEST RESULTS AND ANALYSIS

5.1 Task 4 Results

Figure 5-1 shows the typical failure mode observed for Task 4 specimens with a 2-in. embedment length. Individual specimen failure can be found in Appendix E. Results from specimens having horizontal shear reinforcement with a width of 3.5-in. placed in both the longitudinal and transverse location (used by Maine DOT, Rhode Island DOT and Massachusetts DOT), showed no significant change in the failure load. The bars did not yield and the main mechanism of failure was by bar pullout (Figure 5-2). These results are consistent with the results from bar pullout tests, which indicated that the short embedded length (2-in.) could not provide sufficient bond to allow bars to yield before pullout. A bar stress less than 24 ksi was recorded for these specimens.

Figure 5-1 Typical failure mode of push-off specimen failure with a 2-in. embedment; bar pulled out from the CIP slab

Figure 5-2 Task 4 (a) 3.5"-180° and (b) 3.5"L-180° failure plane showing bar pullout from

the CIP slab
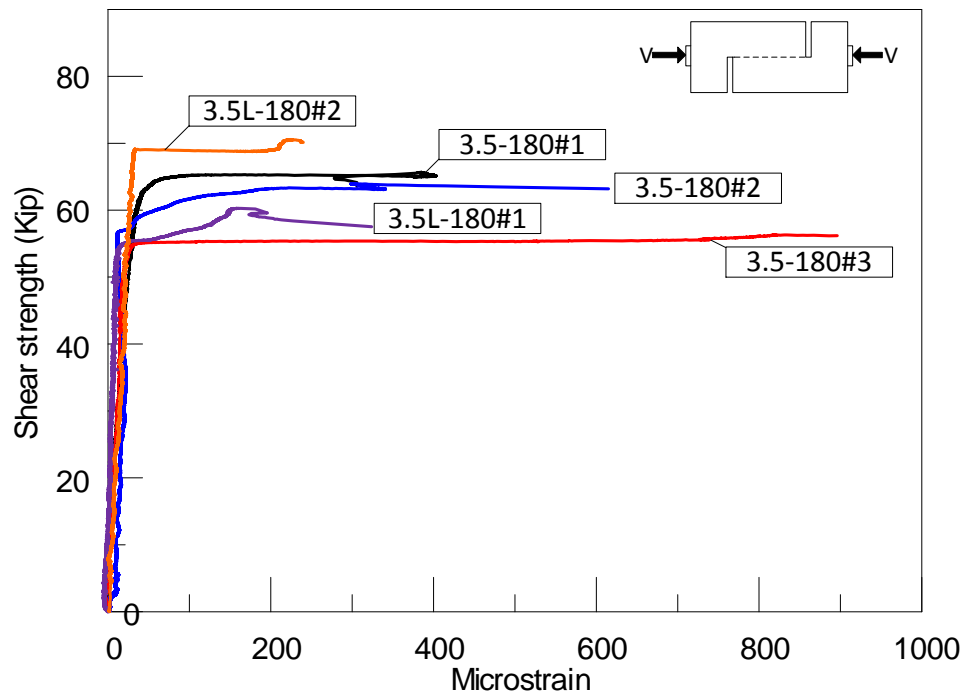
Figure 5-3 Shear strength vs strain plot of 3.5-in. push-off specimens

Specimens having a 6-in. width horizontal shear reinforcement with a 90° curvature (6"-

2"-90°), failed at the interface with the bar pulling out from the CIP part. An average peak

load of 63.5 kips with larger fractured volume of the concrete in the CIP part was

observed compared to the 3.5-in. horizontal shear reinforcement. The highest bar stress recorded was 18 ksi. On the other hand, specimens that had the 6-in. horizontal shear reinforcement embedded 4-in. into the CIP (6"- 4"-90°) showed higher peak loads. Bars in all the specimens in this case were very close to nominal yield strength at failure (Figure 5-4 and Figure 5-5) with yielding occurring at a slip of approximately 0.1-in. No pullout of the bar was observed (Figure 5-6) hence it was not possible to examine the failure plane after the test.
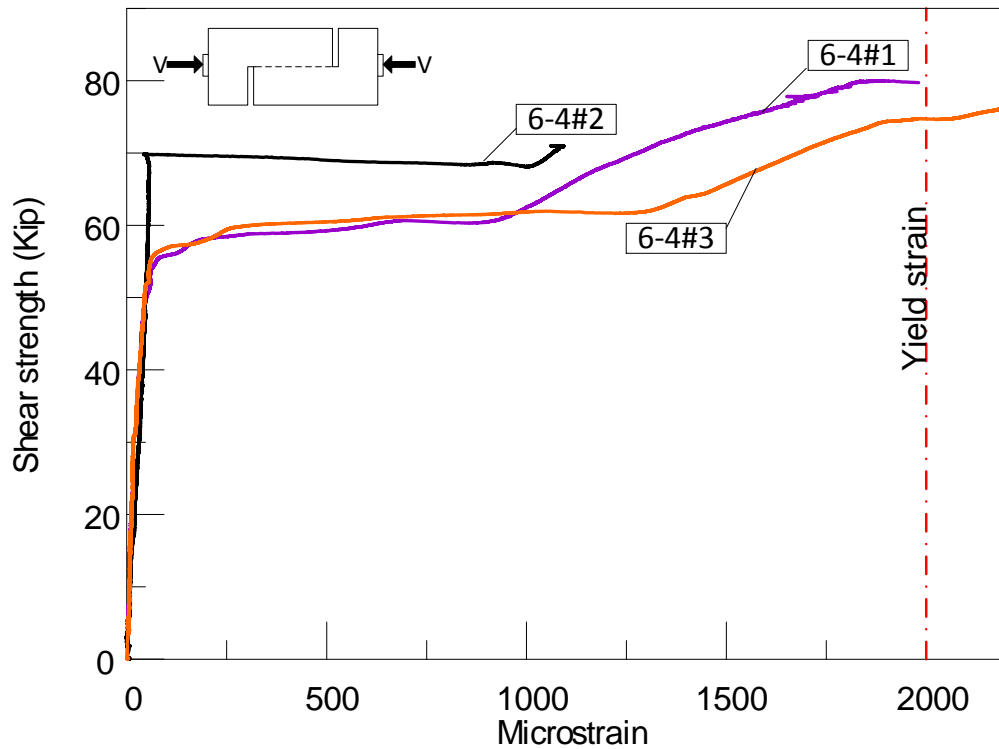
Figure 5-4 Shear strength vs strain plot of 6-in. width horizontal shear reinforcement with 4-in. embedded length push-off specimens
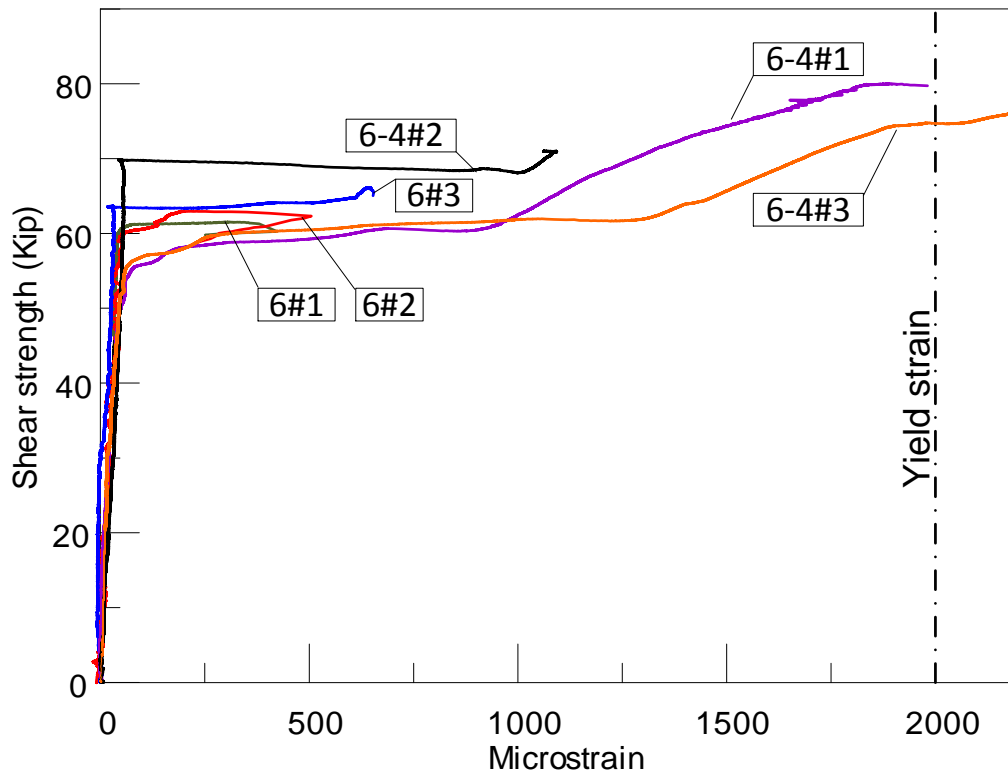
Figure 5-5 Shear strength vs strain plot of 6-in. width horizontal shear reinforcement with

2-in. and 4-in. embedded length push-off specimens

The specimens having a 9-in. width bar with a 90° curvature and a 2-in. embedment (9"- 2"-90°) showed an increase in the average peak load to 79.3 kips. The failure was by bar pullout with no yielding experienced in all the specimens and a maximum bar stress of 19 ksi recorded. Fracture of the concrete in the CIP part of the specimen was observed in most of the specimens. This is consistent with the large fracture volume noticed in the bar pullout test with the same configuration.

Figure 5-6 Typical failure mode of push-off specimen failure with a 4-in. embedment; no pullout of the bar was observed

For the specimens having a 4-in. embedded length (9"- 4"-90°), yielding of the bar occurred at a slip of less than 0.1-in. An average peak load of 76.4 kips was recorded for these specimens. Strain gauge information showed very small strains on the bars before the maximum horizontal shear strength was reached in the specimens having a 2-in. embedded length. This indicates that the dowel action of the bar had minor contribution to the shear strength. Although the 4-in. embedded length specimens registered higher strains on the horizontal shear reinforcement, the majority of specimens did not reach yielding at maximum peak load. The strains on the reinforcement markedly increased once a crack had occurred at the interface. This indicates that using the AASHTO (2014) equation could over-estimate the dowel action which assumes that the horizontal reinforcement can significantly contribute to the interface shear strength by yielding the reinforcement.
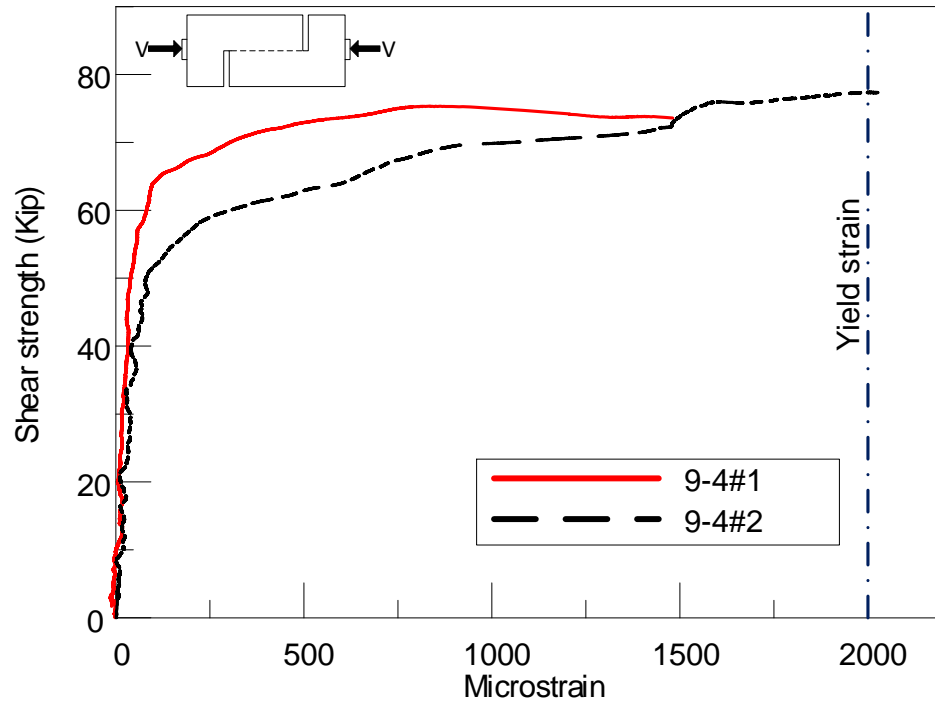
Figure 5-7 Shear strength vs strain plot of 9-in. width horizontal shear reinforcement with

4-in. embedded length push-off specimens

Previous tests had been conducted on push-off specimens without horizontal

shear reinforcement and having a wood float finish (Palacios, 2015). Comparing Task 2

results with a wood float finish to these, it was observed that there is a 50% increase in

horizontal shear strength regardless of the geometry and embedment length. It was

observed that although dowel action did not contribute to horizontal shear strength, the

presence of horizontal shear reinforcement provided an overall increase in horizontal

shear strength. The maximum horizontal shear strength recorded from these specimens

was lower than the horizontal shear strength predicted by AASHTO equation (Figure

5-8). The results of the push-off test are tabulated in Table 5-1.
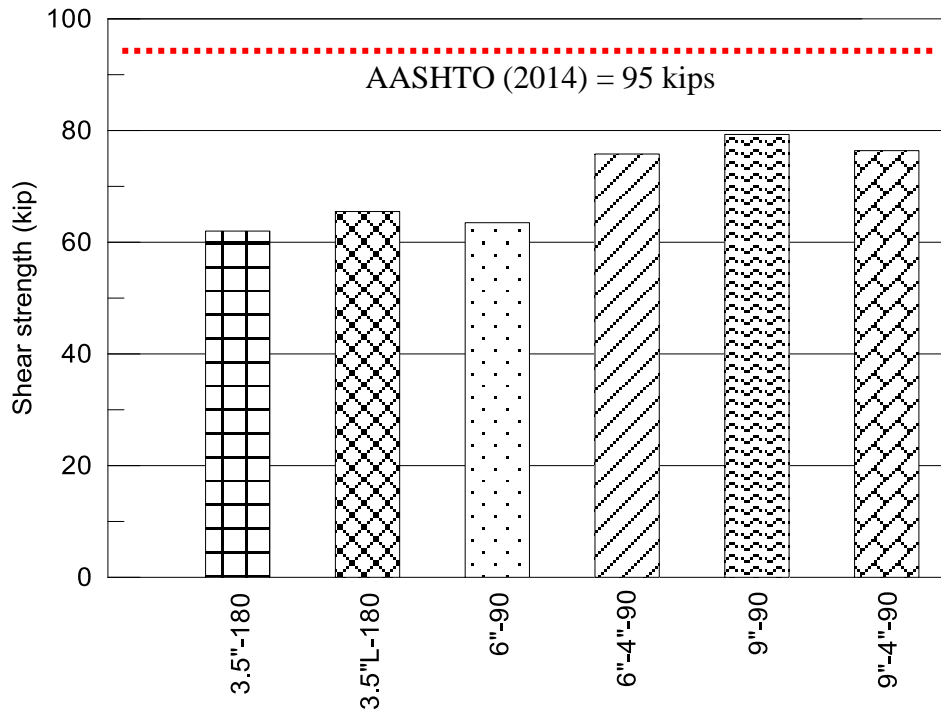
Figure 5-8 Horizontal shear strength comparison

Table 5-1 Task 4 Push-off Test Results

Specimen A - B - C	Failure Load (kip)	Average shear strength (kip)	Strain ε_{su} on bar at failure ($\mu\varepsilon$)	Stress σ_{su} on bar at failure (ksi)
3.5"- 2"-180°	65.7	62	143	4.1
	64		347	10
	56.3		826	24
3.5"L- 2"-180°	60.3	65.5	157	4.6
	‡		-	-
	70.6		323	9.4

Table 5-1 Continued

	61.5		294	8.5
6"- 2"-90°	63	63.5	230	6.7
	66.1		617	17.9
	80		1834	53.2
6"- 4"-90°	71	75.8	1084	31.4
	76.5		2271	65.9
	66.5		449	13.02
9"- 2"-90°	91.1	79.3	655	19
	80.2		574	16.6
	75.3		806	23.4
9"- 4"-90°	77.4	76.4	2030	59
	‡		-	-
*Specimen notation: (A) bar width, (B) Embedment length, (C) bend angle, L is reinforcement placed in the longitudinal direction. ‡Failure not at the interface (value neglected)				

5.2 Task 5 Results

All the test specimens exhibited similar modes of failure as seen in Figure 5-9 with specific failure attached in Appendix F. First cracking (hairline crack) of the concrete occurred on the front face (side facing the front of the MTS machine) and back face (side facing the back of the MTS machine) of the specimen radiating from the bar leading to a strength drop. As the load increased, cracks started forming around the bar. Once the cracks propagated around, the bar was gradually pulled out. The 12-in. specimens showed a more explosive failure after the concrete on the inside of the tail portion

cracked. Observation of the specimens after failure also implies that the bar tends to pull away from the concrete on the outside of the bend.
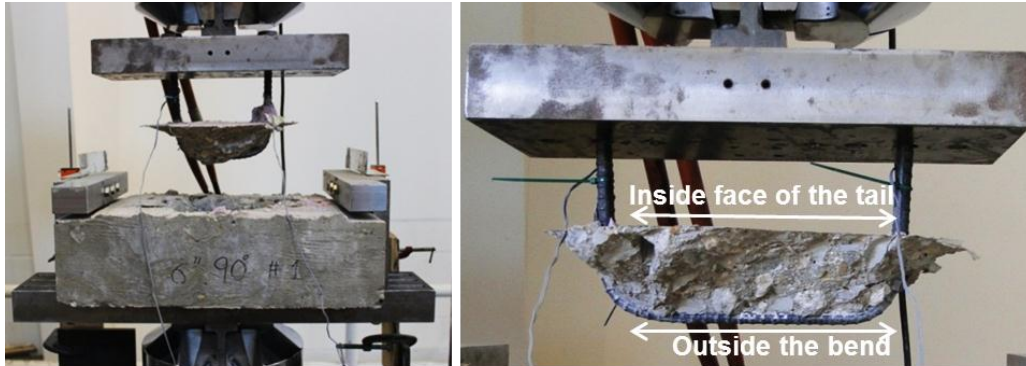
Figure 5-9 Pullout test modes of failure

The change in degree of bend for the specimens having 3.5-in. bar width did not show a significant increase in strength. It was also observed that 9-in. width horizontal shear reinforcement with a 90° bend (9-90) led to a marginal increase in the pullout strength compared to specimens having 3.5-in. width reinforcement and an 180° bend (3.5-180). This means that the latest modification in TxDOT details cannot improve the contribution to the horizontal shear resistance resulting from the horizontal shear reinforcement. However, the failure region did increase for a 90° bend compared to an 180° bend with deformation of the horizontal shear reinforcement (Figure 5-10). The specimens having lapped horizontal shear reinforcements (Figure 5-11) did not show any effect in the pullout strength or mode of failure.

Table 5-2 Task 5 Pullout Test Results

Specimen* A-B	Block size (in.)	Bend Angle (deg.)	Failure Load (kip)	Strain ε_{su} on bar (µε)	Stress σ_{su} on bar (ksi)
3.5-180	15.5 × 12 × 5	180	5.6	885	26
			6.3	522	15
			5.3	1011	29
3.5-90	15.5 × 12 × 5	90	5.3	1252	36
			6.2	927	27
			6.8	1055	31
6-90	18 × 12 × 5	90	6.3	1424	41
			4.6	1815	53
			5.5	978	28
6-90L	18 × 12 × 5	90	7.7	1387	40
			6.3	863	25
			5.0	1158	36

Table 5-3 Continued

			6.2	1241	36
9-90	21 × 12 × 5	90	6.5	1348	39
			6.0	785	23
			4.1	509	15
9-90L	21 × 12 × 5	90	6.1	875	25
			4.0	957	28
			5.7	1271	37
12-90	24 × 12 × 5	90	5.3	995	29
			8.1	1230	36
			6.9	1477	43
12-90L	24 × 12 × 5	90	6.9	910	26
			7.8	1637	47

*Specimen notation: (A) bar width, (B) bend angle, (L) spliced bars.

Figure 5-10 Fracture of concrete during pullout

(a)

(b)

Figure 5-11 6-in. 90° lap specimen at failure
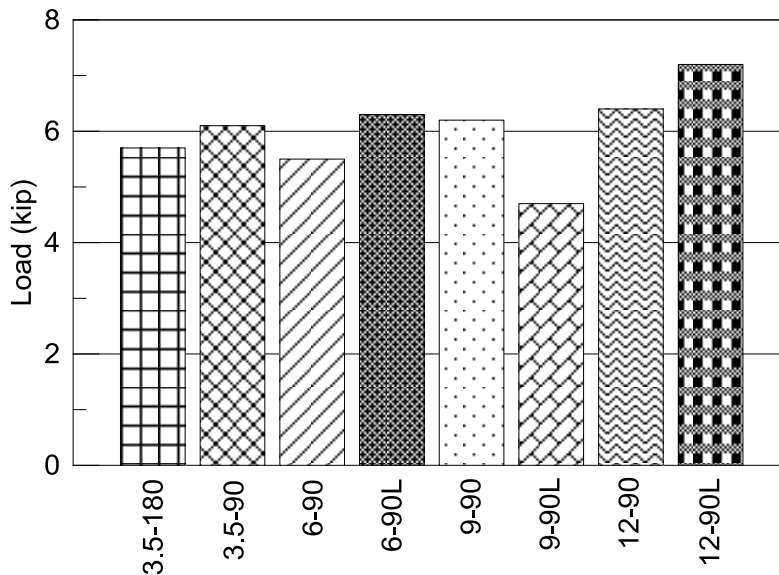
Figure 5-12 Bar pullout strength

5.3 Task 6 Results

5.3.1 4SB12#1 (slab beam)

The cracking moment was calculated to determine the load at which the first crack will occur. The load was first applied at 5 to 10 kip interval until the first flexural crack was observed at 55 kips, near the mid-span of the beam. With an applied load to 82 kips, the cracks continued to propagate and eventually reached the interface between the CIP slab and the precast beam. More flexural cracks continued to form on the beam further away from the midpoint corresponding to the increased deflection.

At 90 kips, the cracks propagated into the 5-in. CIP slab but not along the interface with a mid-span displacement of 2.5-in.. At a displacement of 3-in. and a load of 97 kips, the crack continued up towards the loading point. The compression zone (distance from the top of the beam to the crack) was measured to be 3.5-in. The crack width had widened to more than 3mm at that point.

162

The beam eventually failed in flexure at a peak load of 102 kips corresponding to a displacement of 7-in. Crushing of concrete occurred under the loading point (Figure 5-13) and the cracks significantly widened to more than 6 mm (Figure 5-14). No cracks at the interface were observed and no slips were recorded. No significant strain was measured from the strain gauge data of the horizontal shear reinforcement, thus indicating that there was very minor contribution from the horizontal shear reinforcement.

Figure 5-13 Crushing of concrete at loading point
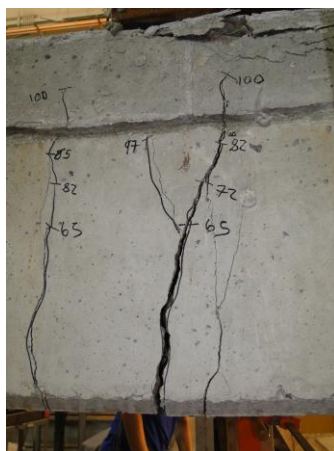
Figure 5-14 Crack widening at failure

5.3.2 4SB#2 (modified slab beam)

The beam was set up identically to specimen 4SB12#1 as shown in Figure 5-15. This beam as mentioned in Chapter 4 did not have any horizontal shear reinforcement. PGSuper analysis had determined that even without shear reinforcement, flexural failure would occur before horizontal shear failure (Appendix D). The beam was first loaded at intervals of 10 kips with inspection after each interval to determine the first crack.

(a)

(b)

Figure 5-15 Slab beam (4SB12#2) (a) elevation view and (b) top view of set-up

The first flexural crack was also observed at a load of 55 kips. The cracks had propagated into the CIP slab at a load of 180 kips. However, no cracks propagating along the interface were observed. The beam also failed by flexure at a load of 197 kips with crushing of the concrete at the loading point (Figure 5-16). The load then dropped to 177 kips after failure. The compression zone at failure was measured to be 4-in. (Figure 5-17).

Figure 5-16 Crushing of concrete at the top of the beam at failure
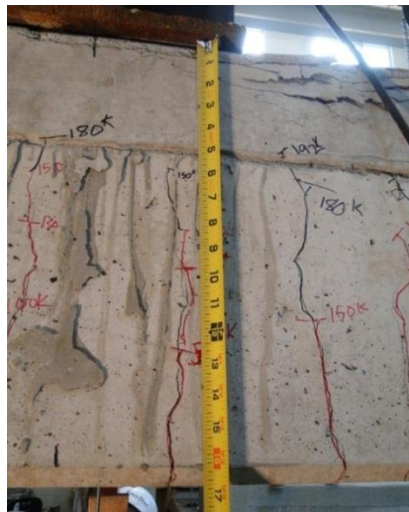
Figure 5-17 Compression zone

With continued load application, an explosive failure occurred with a decrease in load of more than 100 kips and the formation of a horizontal crack 2-in. below the interface (Figure 5-18 and Figure 5-19). The cracks widened to 5 mm and the concrete at the loading point was further crushed. The interface remained intact without any cracks forming across it. Although some hairline cracks propagated along the interface at failure (Figure 5-20) on the south-face side, it did not extend further and was not observed on the north-face side of the beam.

Figure 5-18 Failure at north-face side
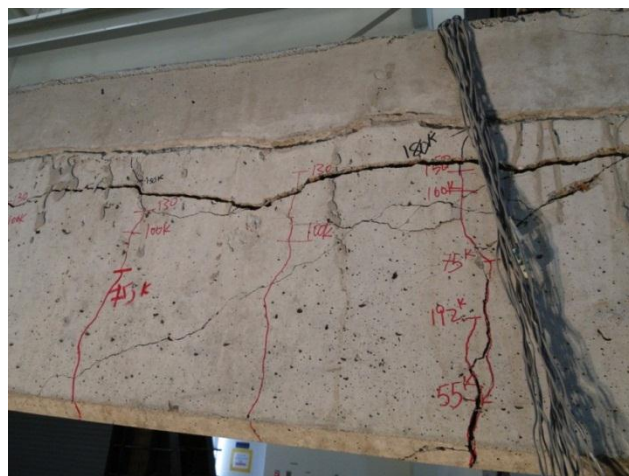
Figure 5-19 Horizontal crack at 74 kips after failure

166

Figure 5-20.Horizontal crack at the interface

5.3.3 4B20#1 (box beam)

The first box beam which represents that design typically used on TxDOT bridges was set up for testing (Figure 5-21 and Figure 5-22). The beam supports needed to be adjusted to accommodate the deeper section of 4B20 so that it may fit underneath the H-frame.

Figure 5-21 21 Box beam (4B20#1) elevation view of test set-up

Figure 5-22 Box beam (4B20#1) top view of test set-up

Because of the higher capacity of specimen 4B20#1, the load was first applied up to 50 kips and the beam was inspected for cracks. The beam was then loaded at intervals of 10 kips until the first crack was observed at 110 kips.

The first flexural crack in the box beam specimen was observed at 110 kips. At a load of 170 kips, flexural cracks had progressed reaching the interface of the CIP slab and the precast beam. Cracks of 1.0 mm in width were recorded with some spalling being observed. At 189 kips, the cracks progressed into the CIP slab (Figure 5-23) with crack widths as wide as 1.5 mm. It should be noted that the flexural cracks did not propagate along the interface but instead passed through the interface into the CIP slab.

(a)
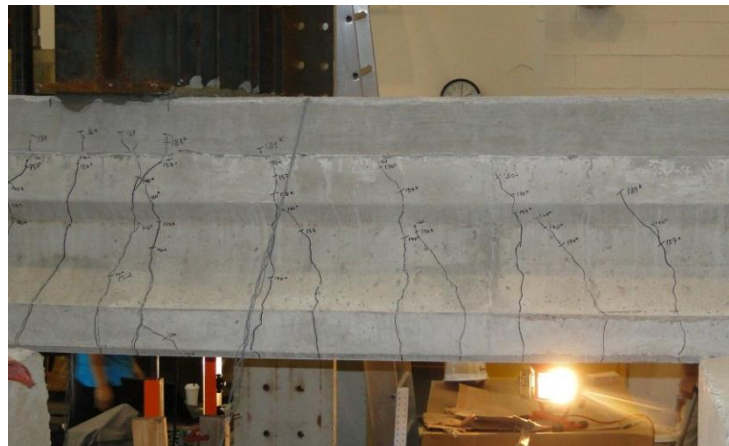
(b)

Figure 5-23 Flexural Cracks propagating into the CIP slab (a) east view and (b) west view

at 189 kips

The beam failed in flexure due to concrete crushing in the compression zone within the CIP slab (Figure 5-24 through Figure 5-26). No cracking was observed within the interface of the prestressed beam and the CIP slab. The compression zone was

measured to be about 2.5-in. and no cracking was observed within the interface of the prestressed beam and the CIP slab.
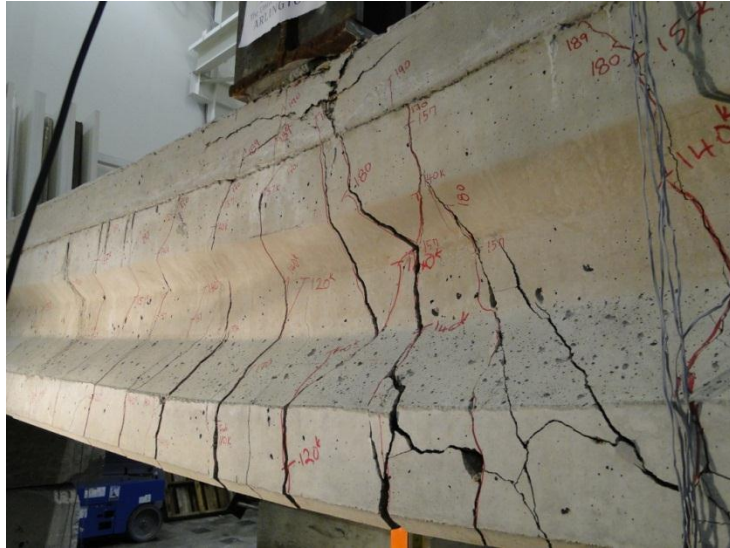
Figure 5-24 Specimen 4B20#1 at failure

Figure 5-25 Concrete crushing at failure

Figure 5-26 Crack width at failure

5.3.4 4B20#2 (modified box beam)

The second box beam was then set up for testing (Figure 5-27 and Figure 5-28).The setup was identical to the one previously used for specimen 4B20#1.

Figure 5-27 Overall test setup of specimen (top view)

Figure 5-28 Overall test setup of specimen (side elevation)

Similar results were observed for the box beam without horizontal shear reinforcement. The load was applied in constant intervals and the beam was periodically inspected for cracks until the first crack was observed. At 150 and 180 kips, cracks had progressed further up the beam with shear cracks being observed. At a load of 350 kips, the cracks had progressed up to the interface of the CIP and precast sections.

Initial crushing of the concrete under the loading point was observed at 400 kips. With increase in load, the concrete crushed and the cracking propagated into the interface leading to a sudden horizontal shear failure (Figure 5-30). However, the horizontal shear crack did not propagate the entire length of the beam. Therefore no slip was recorded by the LVDTs at the ends. Summary of all the test results is presented in Table 5-3

(a)

(b)

Figure 5-29 Cracks reaching the interface at 350 kips (South Side)

.

(a)

(b)

Figure 5-30 Flexural/ horizontal shear failure near mid-span
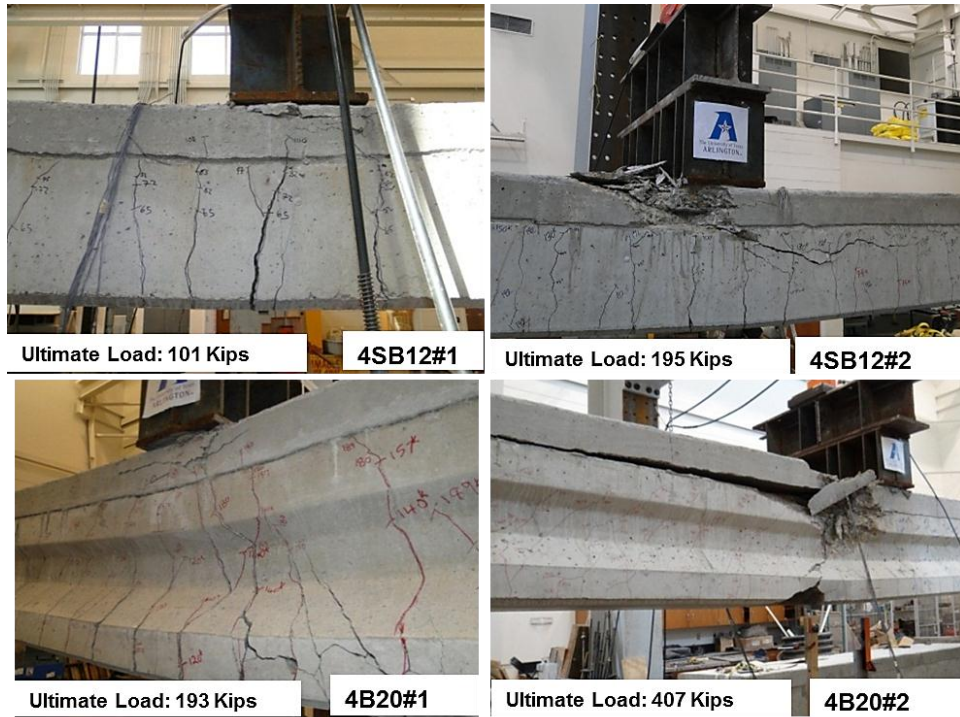
Figure 5-31 Full-scale beam specimens at failure

Table 5-3 Task 6 Full-scale Beam Test Results

Specimen	Horizontal Shear Reinforcement	Design load (kips)	Failure Load (kips)	Failure Mode	Strain ε_{su} on horizontal shear reinforcement at failure (µε)
4SB12#1	Yes	82	101	Flexure	100
4SB12#2 - modified	No reinforcement	160	195	Flexure	-
4B20 #1	Yes	160	193	Flexure	250
4B20#2 - modified	No reinforcement	318	407	Flexure / Horizontal Shear*	-

* Horizontal shear failure was a secondary failure after flexural failure had occurred.

5.4 Task 7 Results

5.4.1 4SB12#3 (conventional concrete slab beam)

The load was first applied at 5 to10 kips interval until the first flexural crack was observed at 55 kips, near the mid-span of the beam. With continued increase in applied load, the crack was observed to progress towards the top of the beam. More cracks began to form along the length of the beam and also at the bottom of the beam with gradual increase in crack width. The crack continued to progress towards the interface with every increment in load up to a load of 120 kips. The crack did not continue propagating towards the interface upon further increase in the load. However, an increase in the strain in the horizontal shear reinforcements was observed at 150 kips, and yielding of the horizontal shear reinforcements at the quarter span in the West-end of the beam was also observed. Slip was realized at a load of 156 kips.

At 170 kips and a mid-span displacement of 3.6-in., a slip of 0.015-in. was recorded at the East-end of the beam with an increase in the crack width at that end of the beam. With the development of shear cracks at the beam ends, the strain on the horizontal shear reinforcement continued to increase.

At a load of 175 kips, the strain on the horizontal shear reinforcement increased and yielding was observed on the horizontal shear reinforcement located at the beam ends as shown in the load-slip plot (Figure 5-32). The width of the flexural cracks increased to 1 mm. At a displacement of 5.24-in. and a load of 180 kips (Figure 5-33), the slip at the East-end increased to 0.12-in. with an increase in the crack width at the interface.
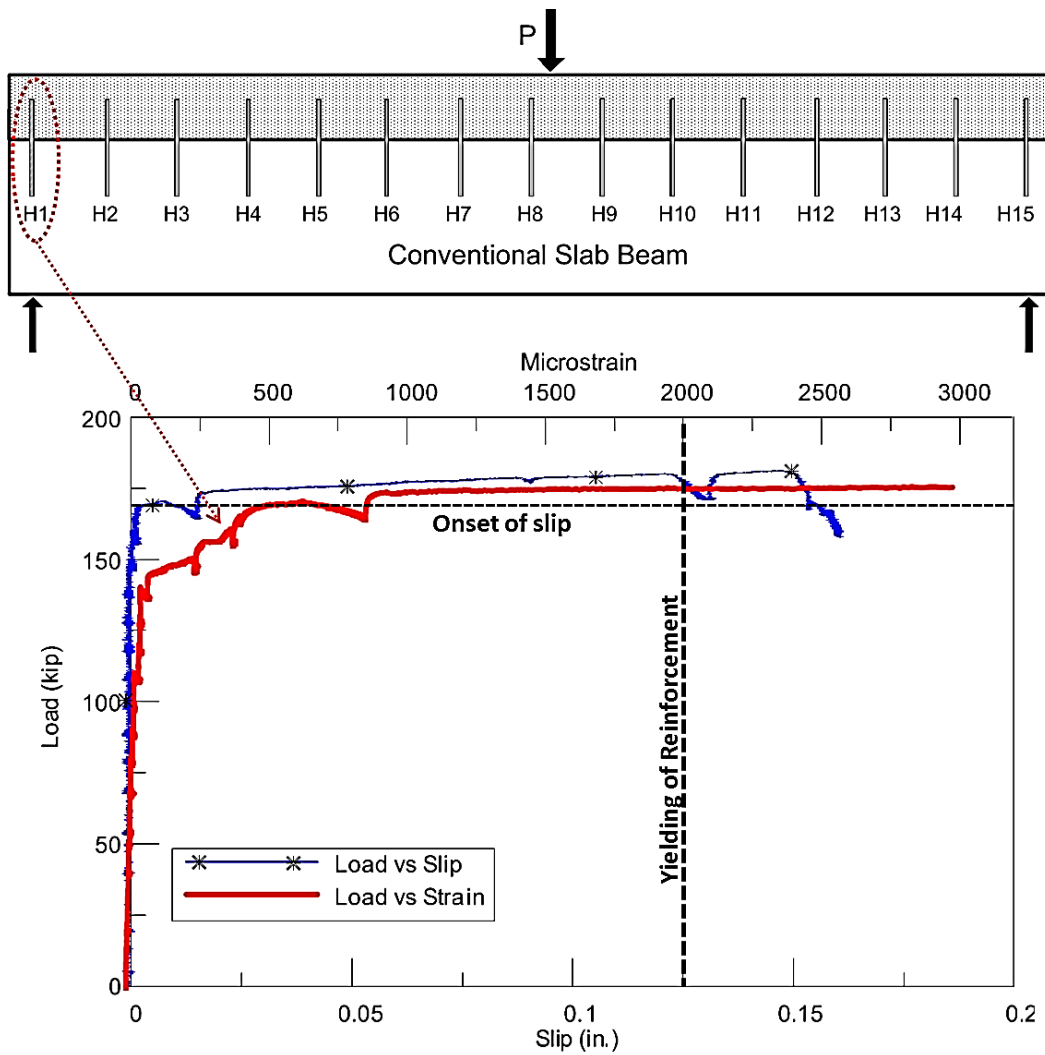
Figure 5-32 Load-slip and load-strain plots for conventional slab beam
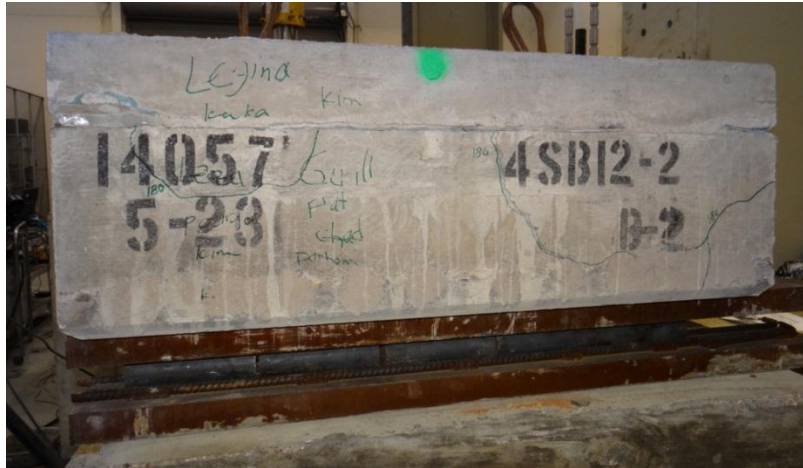
(a) Full view
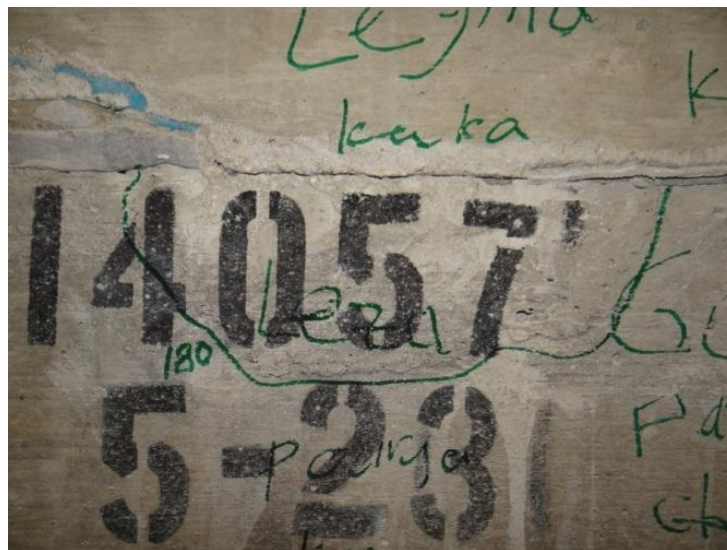
(b) Close view

Figure 5-33 Crack at the interface widens at 180 kips

Fracture of the concrete was also observed on the East-end of the beam. The beam failed in flexure at a load of 181 kips and a displacement of 6.65-in. Crushing of concrete occurred near the loading point and the flexural cracks significantly widened to more than 6 mm. A separation between the CIP slab and the precast beam was also observed with a slip of 0.15-in. being recorded (Figure 5-35).

Figure 5-34 Beam at failure

Figure 5-35 Separation of the interface at failure

From strain gauge information of the horizontal shear reinforcement, it was clear that almost all the horizontal shear reinforcement had yielded at this point as shown in Appendix G which shows the strain profile at different levels of slip.

5.4.2 4SB12#4 (SCC slab beam)

The beam was loaded at intervals of 10 kips with inspection after each interval to identify cracks. At a load of 50 kips, the first crack was observed on the beam. With increase in load to 80 kips, the cracks propagated upward and new flexural cracks formed along the beam. Cracks continued to progress upward as the load was increased with new cracks forming along the beam. At a load of 130 kips, the LVDTs started registering slip at the interface of 0.0024-in. Strains on the horizontal shear reinforcement began increasing gradually. The flexural cracks continued to propagate towards the loading point with new flexural cracks forming along the length of the beam

Slip gradually increased as the load was increased and at a load of 160 kips, a slip of 0.015-in. was recorded. Cracks at the interface became noticeably larger at both ends of the beam (Figure 5-36 and Figure 5-37).
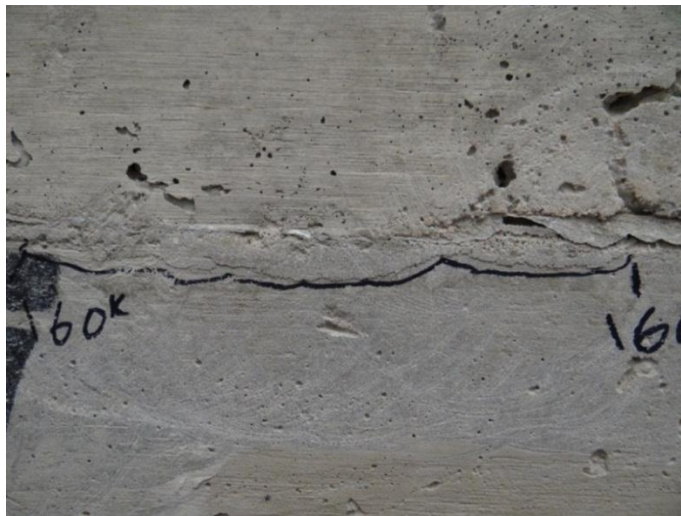
Figure 5-36 Crack on the East-end of beam

Figure 5-37 Visible interface cracks East-edge of beam

Cracks propagating from the interface towards the bottom of the beam started to appear at a load of 170 kips (Figure 5-38 through Figure 5-40). The crack positions were approximately at the location of horizontal shear reinforcement.

Figure 5-38 Vertical cracks close to beam ends (South-West side)
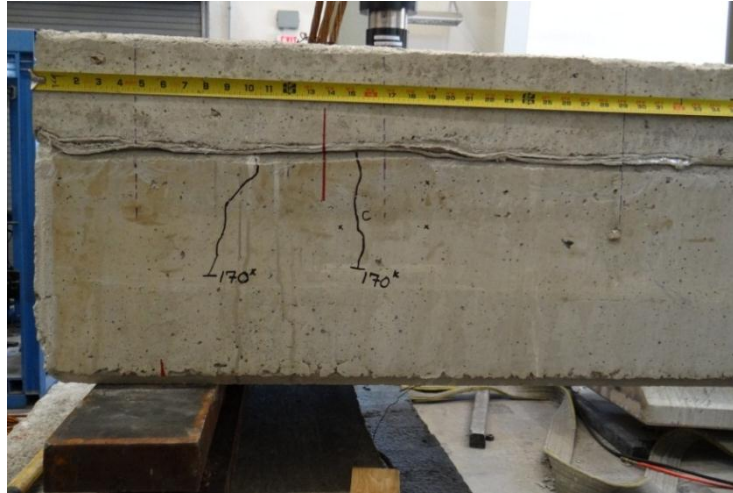
Figure 5-39 Vertical cracks close to beam ends (North-East side)
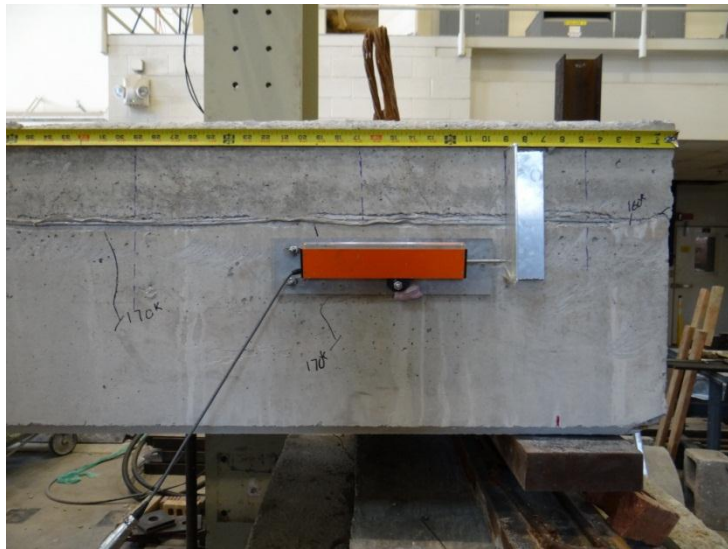
Figure 5-40 Vertical cracks close to beam ends (South-East side)

Horizontal shear reinforcement near the support yielded at a load of 173 kips and a slip of 0.04-in. (Figure 5-41). Cracks at the beam ends and the interface were also observed to widen with increase in load (Figure 5-42), as well as an increase in slip at a load of 180 kips as demonstrated by the red line in Figure 5-43.
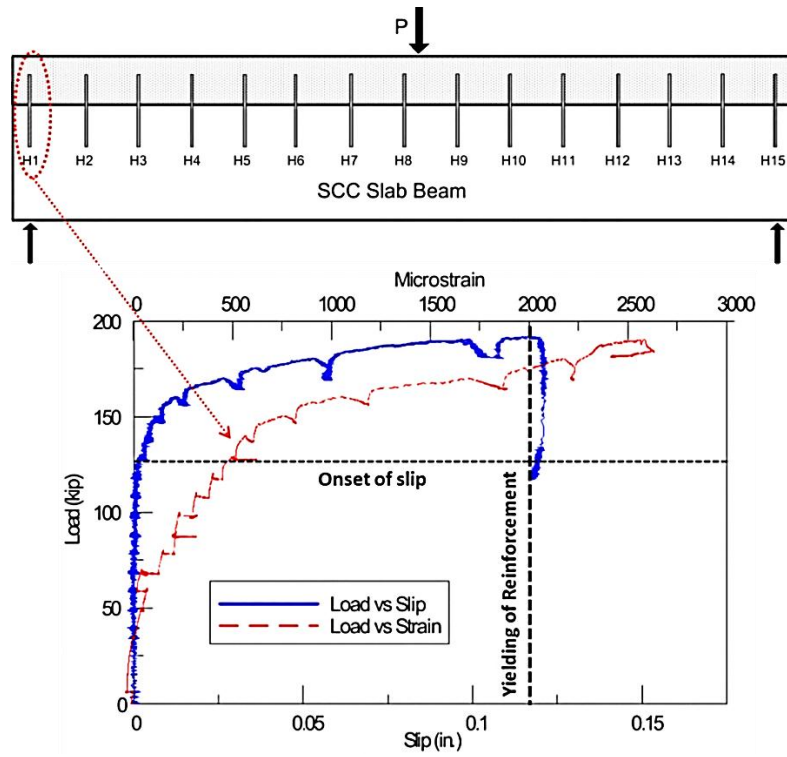
Figure 5-41 Load-slip and load-strain plots for SCC slab beam

Figure 5-42 Interface cracks at beam ends

Figure 5-43 Interface slip at 180 kips

Cracks started to form at the CIP slab at a loading of 190 kips. These cracks did not originate from flexural cracks on the precast beam. Interface cracks were now wider and more visible on both ends of the beam as shown in Figure 5-44. More vertical cracks continued to appear on the beam with a slip of 0.10-in.

Figure 5-44 Cracking at the interface (photo taken at the beam end)

The beam failed by flexure at a load of 191.7 kips with crushing of the concrete under the loading point. A slip of 0.12-in. was recorded. Crushing of concrete was however observed on both the CIP slab and the precast beam (Figure 5-45). The wide crack opening at the interface (Figure 5-46) and the concrete crushing at both the slab and the beam indicated that the composite action is partly lost.
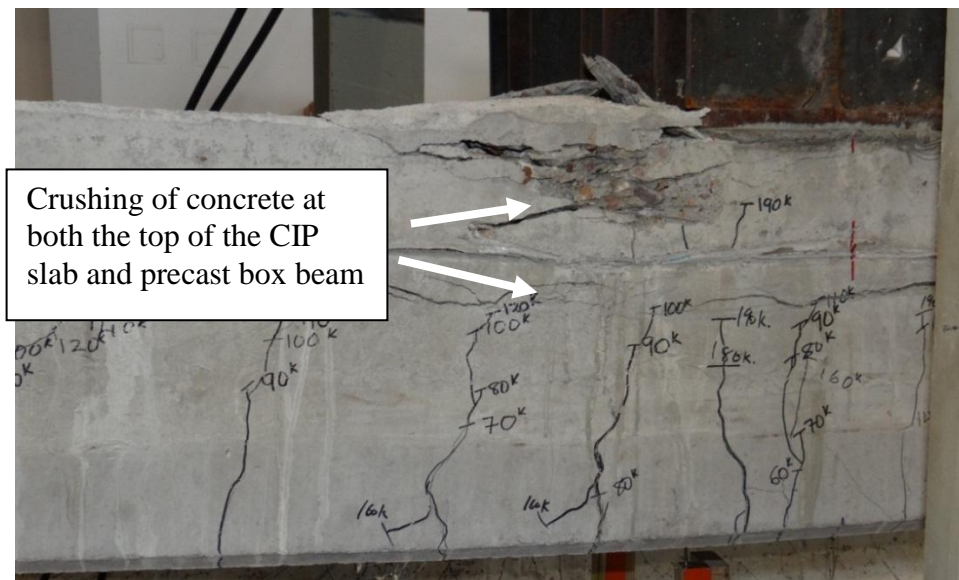
Figure 5-45 Crushing of concrete at failure

Figure 5-46 Separation between CIP slab and precast beam

5.4.3 4B20#3- (box beam without block-out)

As shown in Figure 5-47, the loading was applied at 7 ft. away from the end on which the CIP slab did not extend into the blockout.

(a) Top view

7 ft

Slab does not extend into blockout
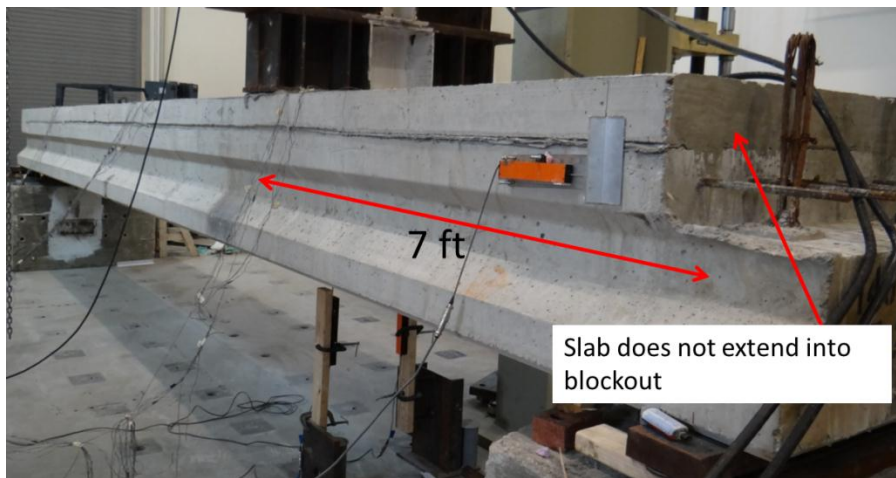
(b) South-side view

Figure 5-47 Test set-up (a) top view and (b) side elevation of test set-up

Load was applied at intervals of 10 kips until the first crack was observed at a load of 160 kips. With an increase in the applied load to 190 kips, more flexural cracks formed along the beam. Very little strain was recorded from the horizontal shear reinforcement at this point. Shear cracks began to form close to the support within the beam's web. At a load of 230kips, flexural cracks continued to propagate towards the top of the beam and new shear cracks formed near the support. At a load of 247 kips, a cracking noise was heard and the load dropped to 225 kips as evident from the load vs slip plot in Figure 5-58. Interface slip was recorded to be 0.024-in. at that instance. Strains in the horizontal shear reinforcement also began to increase. Cracks were also observed on the beam ends along the interface measuring 0.5 mm (Figure 5-48).

Figure 5-48 Cracks form at the interface

Cracks on the CIP slab began to appear at a load of 250 kips. These cracks were observed not to have originated from the flexural cracks on the precast beam. Interface

cracks were markedly wider with a slip of 0.08-in. being recorded. Fracture of concrete close to the interface on the beam end was also observed (Figure 5-49 to Figure 5-50).

Figure 5-49 Cracking at the interface on beam end

Figure 5-50 Fracture of concrete at beam end

Yielding of horizontal shear reinforcement close to the end of the beam occurred at a load of 263 kips with a slip of 0.09-in. The crack at the interface widened to 1.5 mm.

With an increase in load to 270 kips, the crack at the interface widened to 1.25 mm. More cracks formed at the CIP slab with increased number of yielded horizontal shear reinforcement. Cracking of concrete around the interface at the beam end also became more obvious (Figure 5-51 and Figure 5-52), which is likely due to the interface bars being pulled out.

Figure 5-51 Cracking of concrete at East-end

Figure 5-52 Cracking at the interface at beam end

Flexural failure occurred at 287 kips with a deflection of 5.4-in. (Figure 5-53). Crushing of concrete was observed on both the CIP slab and the precast beam. A slip of 0.60-in. was recorded at the end of the test. Severe concrete fracture was observed on the East-end of the beam near the interface as shown in Figure 5-54 and Figure 5-55. A large separation along the interface was also observed (Figure 5-56) as well as noticeable slip at the beam end (Figure 5-57).
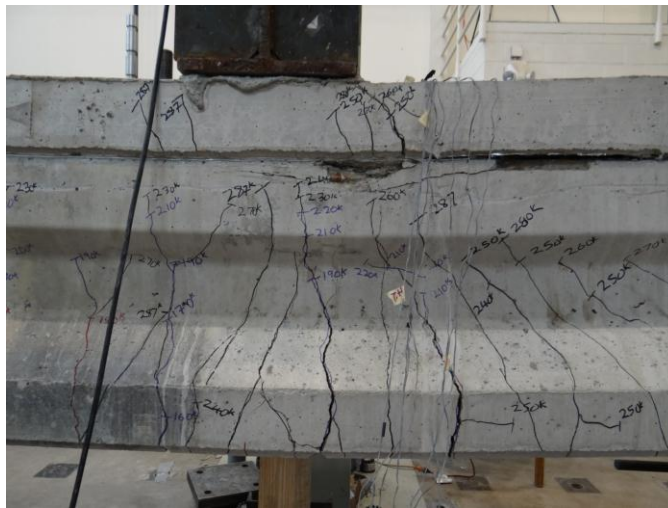
Figure 5-53 Crack propagation at failure

Figure 5-54 Fracture of concrete at East-end (close view)

Figure 5-55 Fracture of concrete at East-end

Figure 5-56 Separation between the CIP slab and precast beam

Figure 5-57 Interface slip at failure

Figure 5-58 shows the load vs. slip and strain plots for the box beam without the slab extending into the block-out.
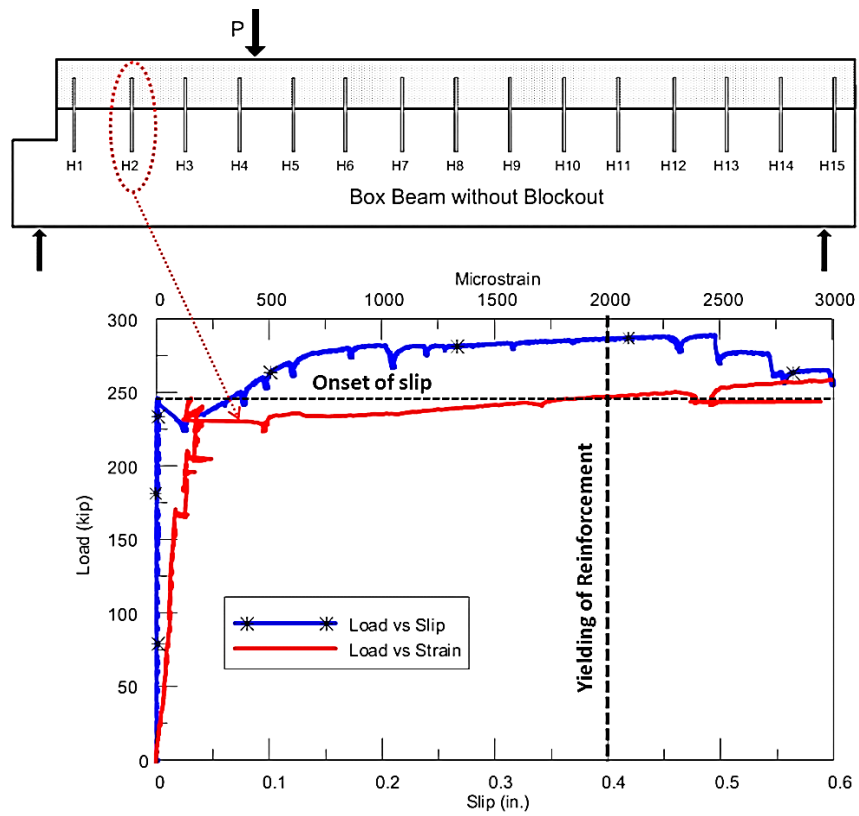
Figure 5-58 Load-slip and load-strain plot for box beam without block-out

It is important to note the majority of the shear strength before the onset of slip can be attributed to the cohesion and friction of the concrete. However, it can be observed that there is a slight load drop after the onset of slip in which a separation at the interface occurs that engages the horizontal shear reinforcement followed by an increase in strain up to yielding of the horizontal shear reinforcement as shown in the load-strain plot. This may suggest that the AASHTO (2014) horizontal shear equation does not accurately predict the true behavior of composite beams.

5.4.4 4B20#4- (box beam with block-out)

The box beam was then flipped and the beam loaded 7 ft. from the other side of the box beam with the slab extending into the blockout. The overall test set-up for specimen 4B20#4 can be seen in Figure 5-60.

Figure 5-59 Overall test set-up of specimen (top view)

Figure 5-60 Overall test set-up of specimen (south side)

The load was applied in constant intervals and the beam was periodically inspected for cracks until the first crack was observed at 190 kip. With increase in applied load, flexural cracks increased and were observed to progress further up towards the loading beam. Some shear cracks at the beam end were also observed (Figure 5-61). Cracks started to appear within the CIP slab at a load of 240 kips. At 250 kips, more cracks appeared at the CIP slab with a hairline crack forming at the interface between the CIP slab and the block-out area (Figure 5-62).
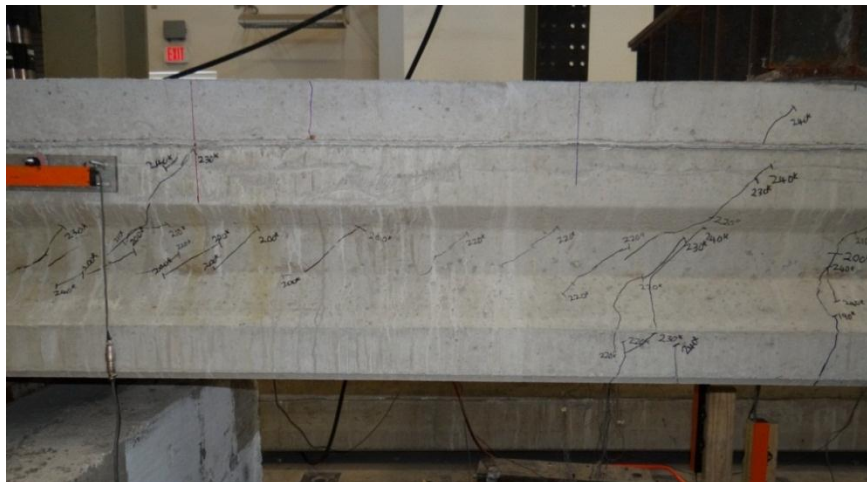
Figure 5-61 Shear cracks near the South-East support

Figure 5-62 Interface cracks at the blockout

Interface slip of 0.008-in. was recorded at a load of 250 kips with a widening of the interface crack being observed. There was however low strains recorded in the horizontal shear reinforcements. At a load of 320 kips, the interface crack widened with interface slip increasing to 0.028-in. Cracks at the CIP progressed to the top of the slab (Figure 5-63). At 380 kips additional cracks propagate into the CIP slab as shown in Figure 5-64.

Figure 5-63 Shear cracks and interface cracks near the southeast support
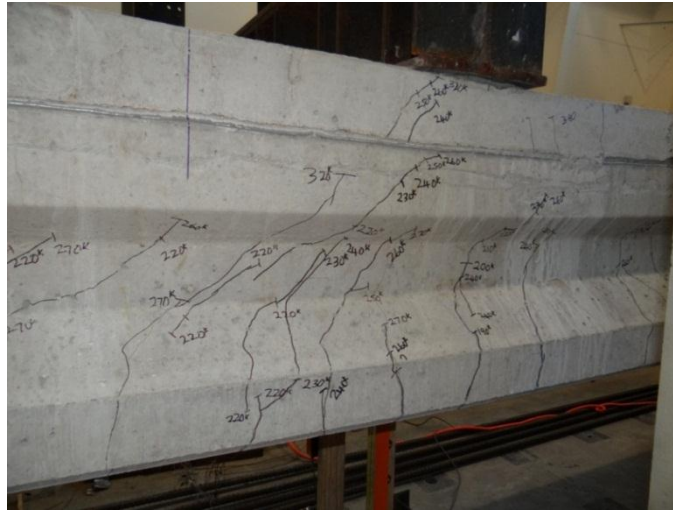
Figure 5-64 Crack propagation at 380 kips

The beam failed by flexure at a load of 388 kips due to crushing of the concrete at the CIP slab and precast beam underneath the loading point (Figure 5-65 and Figure 5-66). An interface slip of 0.25-in. was recorded at failure (Figure 5-67). Cracks at the interface of the CIP slab and blockout on the North and South side are shown in Figure 4-59.

Figure 5-65 Failure of specimen (top view)

Figure 5-66 Failure of specimen (side view)

Figure 5-67 Interface slip at failure

Figure 5-68 Cracks at the interface of the CIP slab and blockout

Figure 5-69 shows the load-slip and load-strain plots for the box beam with the slab extending into the blockout. It is important to note that the strain in the horizontal shear reinforcement does increase until close to the onset of slip, after which the strain continues to increase up to yielding. The strain in the horizontal shear reinforcement at the onset of slip is observed to be 500 µε which then rapidly increases to yielding (2000 µε) with increase in load after slip occurs. This observation is consistent with that observed on 4B20#3 (box beam without the blockout).
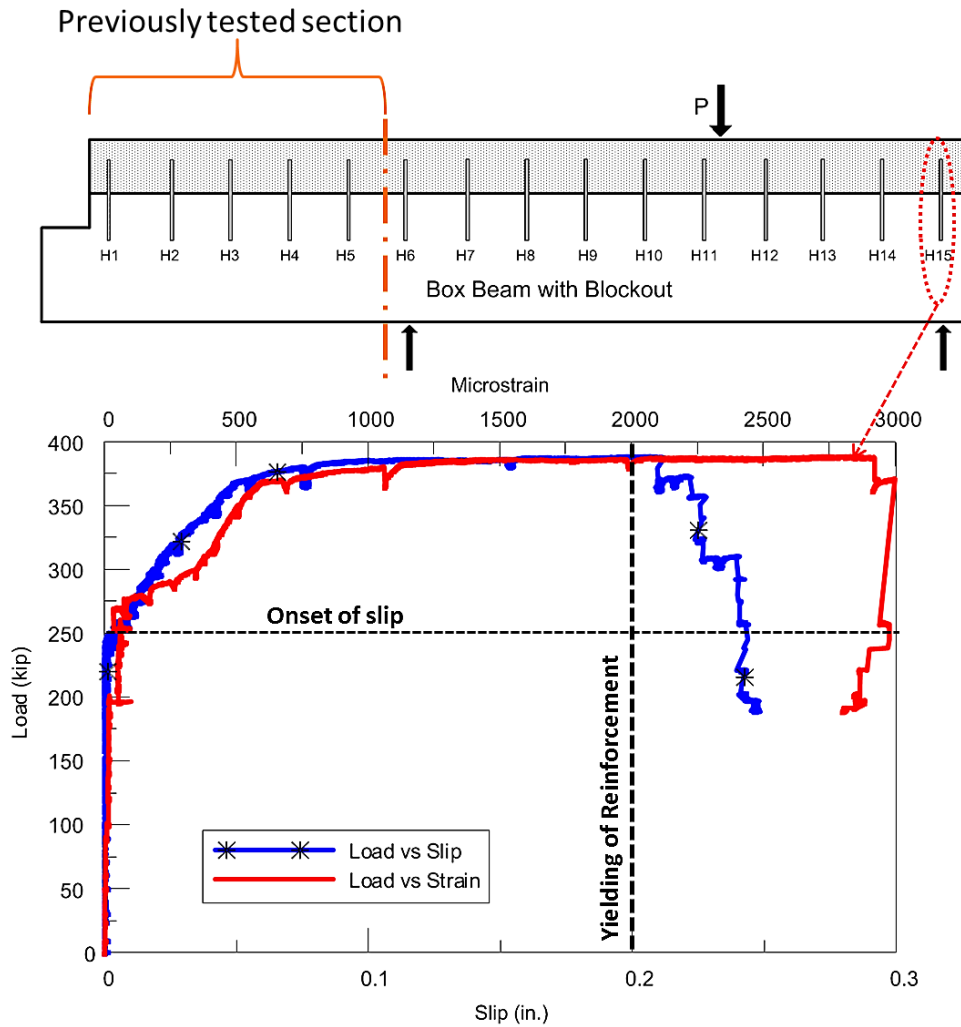
Figure 5-69 Load-slip and load-strain plot for box beam with blockout

Table 5-4 Task 7 Full-scale Beam Results

Specimen	Failure Load (kips)	Load at the onset of slip (kips)	Failure Mode	Strain ε_{su} on horizontal shear reinforcement at onset of slip (µε)
4SB12#3-conventional	181	156	Flexure*/Horizontal Shear	340
4SB12#4 -SCC	192	130	Flexure*/Horizontal Shear	560
4B20#3-no block-out	284	247	Flexure*/Horizontal Shear	200
4B20#4 –block-out	388	250	Flexure*/Horizontal Shear	500

5.5 Validation of results using Finite Element analysis

A finite element model was created to verify the distribution of the applied load along the full-scale specimens. The FE model was used to check the compressive stresses at the interface along the composite beam. LUSAS FE program was chosen because of its ease in modeling and analysis.

A simply supported T-beam was chosen as a model for the FE analysis. The beam consisted of a precast beam measuring 96×10×10-in. (length×width×height) and a CIP slab measuring 96×24×5-in. (length×width×height) as shown in Figure 5-70. A 3 dimensional (3D) analysis of the beam was conducted (Figure 5-71).

P

48"

CIP Slab

5"

15"

Precast Beam

Span Length= 96"

(a)

Bar A 6" spacing

Bar B 6" spacing

1.9"

24"

CIP

5"

Bar C No. 6 bars

Precast Beam

10"

10"

(b)
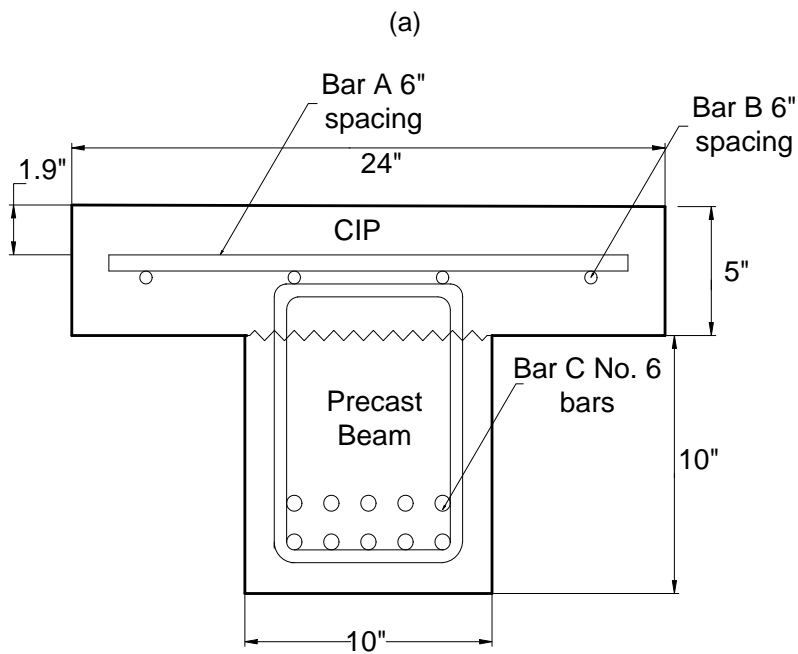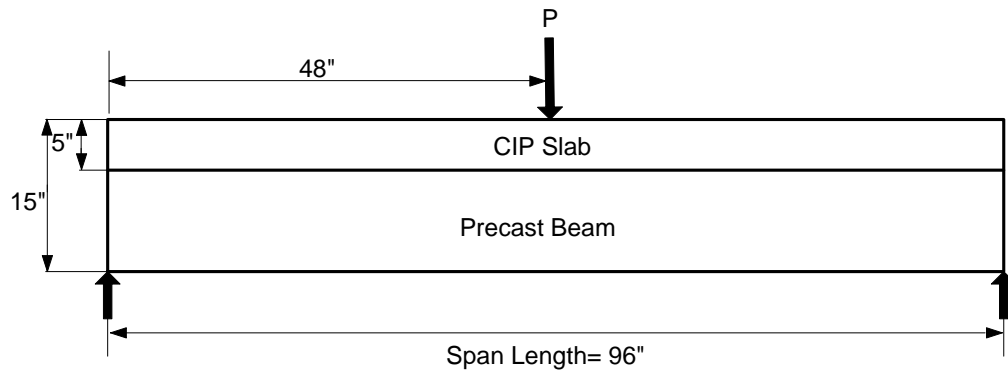
Figure 5-70 Geometry of the finite element model (a) elevation view and (b) section view

For simplicity, the reinforcements and prestressing strands were not incorporated into the model. The concrete to concrete interface was connected to one another assuming a perfect bond. The model was created in two sections to allow for the

formation of the interface. Thick shell elements were used to model the specimen. The beam and slab element were given a regular mesh (Figure 5-72).

Figure 5-71 T-beam 3D model
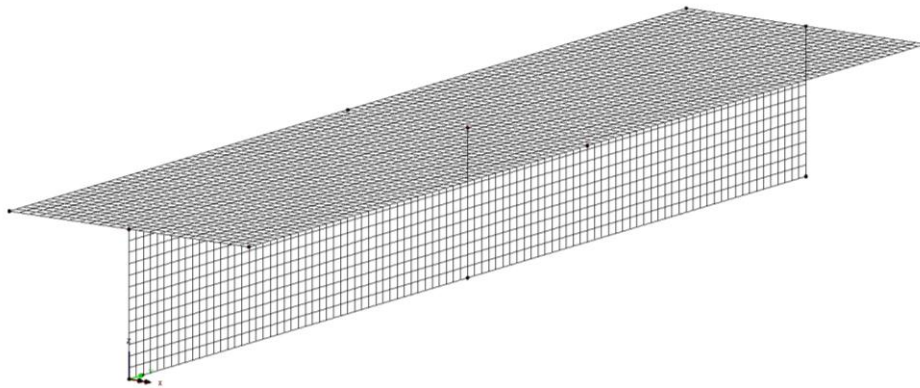
Figure 5-72 Mesh layout

The beam was modeled as simply supported with a pin connection on one end and a roller connection on the other. The supports acted through the centerline of the supported area. A point load was applied at a distance 48-in. from the support. The load acted through the entire width of the composite beam similar to the loading on the full-scale specimens (Figure 5-73).
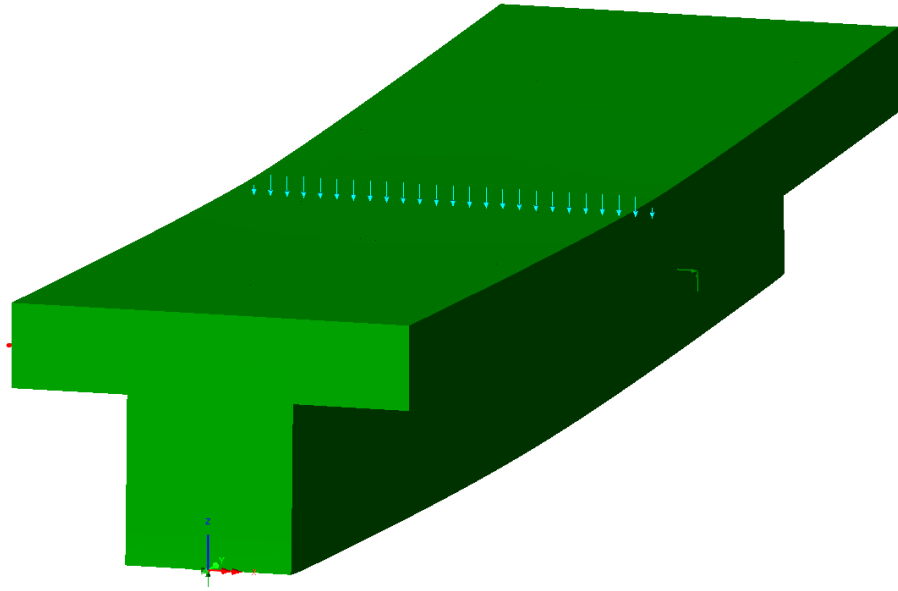
Figure 5-73 Model with load applied along the width of the specimen

5.5.1 FE analysis report and summary

The compression stresses along the entire beam were analyzed as shown in Figure 5-75. The interface stresses were also analyzed and the compressive stresses along the beam plot as shown in Figure 5-75. It is clear that the compressive stresses are highest at the loading point and gradually reduce (almost linearly) towards the support. This results support our hypothesis that the high compressive stresses at the loading point restraint the interface crack from opening at that point hence lower strains recorded in the horizontal shear reinforcements.
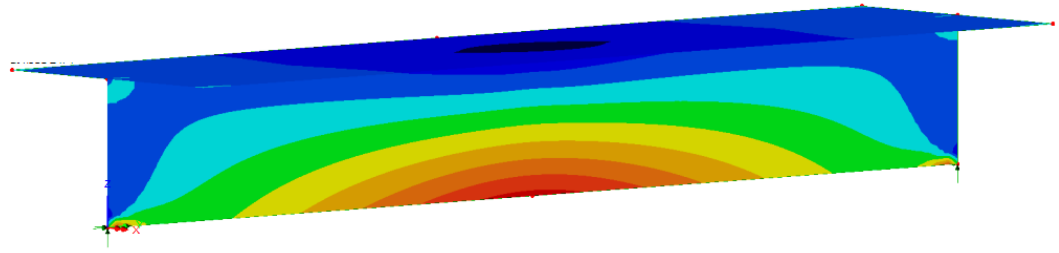
(a)
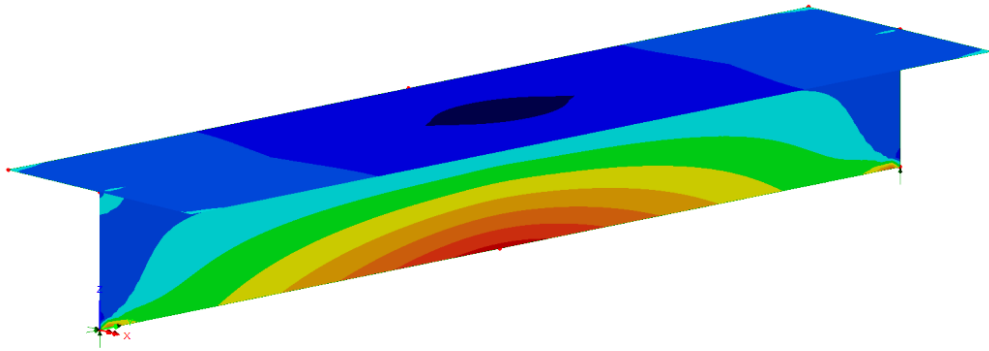
(b)

Figure 5-74 Contour of compressive stress along beam.
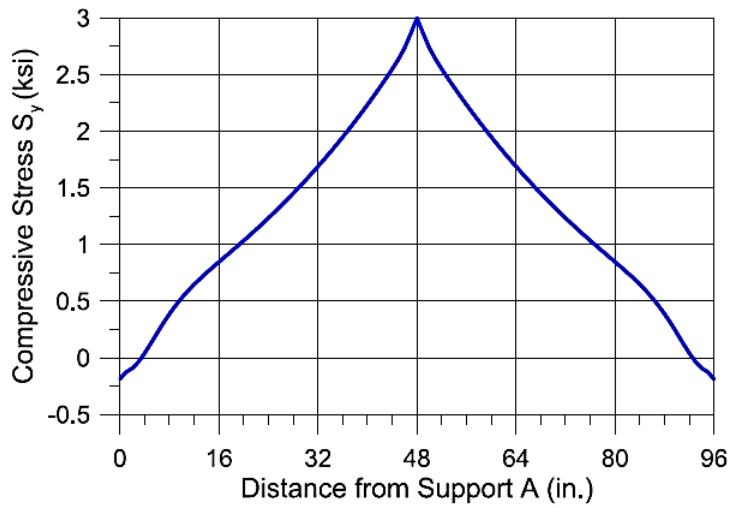
Figure 5-75 Compressive stress vs distance from support plot

Chapter 6

SUMMARY, CONCLUSIONS, AND RECOMMENDATIONS

6.1 Summary of Results

6.1.1 Behavior of component specimens

Comparing the results from Task 2 specimens with a wood float finish (Palacios, 2015) and Task 4 specimens, it is clear that there is an increase in the horizontal shear strength of the specimen when horizontal shear reinforcement is provided. For the 3.5-in. horizontal shear reinforcement, the mode of failure was brittle similar to what was observed in Task 2 (Palacios, 2015). This can be attributed to the pullout of the horizontal shear reinforcement at failure rather than yielding of bars. The enhanced strength shown in the push-off specimens can be attributed to the contribution from concrete that was engaged by the embedded bars.

Figure 6-1 Typical failure mode of push-off specimens with 2-in. embedment

This engaged concrete had to be fractured before slip could occur. It is also observed that there is no significant difference in shear strength when the horizontal shear reinforcement was placed longitudinal to the beam length and when placed transversely.

The same was observed for 6-in. width horizontal shear reinforcement. There was however an increase in the shear strength when a 6-in. horizontal shear reinforcement was used having a 4-in. embedded length. Unlike the 2-in. embedded length specimens where the load dropped by almost 80% of the peak load at failure and keeps declining after that, the shear strength of the specimens with 4-in. embedded length had less degradation and started to rise again as the bar picked up load and provided a clamping force that restrained the two parts from slipping against each other. From the strain gauge information (Figure 5-5) it can be seen that there was negligible clamping force across the interface for the 2-in. embedded bar because of the low strain recorded during and after cracking of the interface. On the other hand, the 4-in. embedded length specimens showed higher strains at failure as shown in Figure 5-5 and Figure 5-6 suggesting that the bars were providing ample clamping force thus preventing the slip and crack opening. It should be noted that sudden failure was also experienced in the 4-in. embedded length specimens. This may be attributed to the lack of confinement and concrete continuity available for smaller scale push-off specimens compared to full-scale beams.

The specimens having reinforcement with a 9-in. width showed overall a slightly higher shear strength compared to all other specimens. For a 2-in. embedded length the 9-in. width had an increase in shear strength of 28% and 24% compared to the 3.5-in. and 6-in. width reinforcement (Figure 5-8). Specimens having a 4-in. embedded length showed similar behavior as the 6-in. width reinforcement with a 4-in. embedded length in

that the bar became engaged after interface failure with increase in slip (see Table 5-1). Strain measurements also showed that the bars in all specimens with 4-in. embedded length had yielded at a slip of 0.1-in.

6.1.2 Behavior of full-scale specimens

Task 6 results revealed that horizontal shear failure will not occur for TxDOT box and slab beams with current design practice. Throughout the testing of box and slab beams with horizontal shear reinforcement, no significant strain was measured from the strain gauge data of the horizontal shear reinforcement because the beams always failed by flexure first. The shear strength from concrete alone was sufficient to resist the shear stress at ultimate flexural failure.

In Task 7, interface areas of all beams were purposely reduced by foam tape to decrease the horizontal resistance to force the beams to fail along interface before flexural failure. This was done to obtain the actual horizontal shear strength and to verify the data from the component tests. The reduced areas in the slab and box beams were reduced by 75% and 66% respectively. Slab beams tested in Task 7 revealed Slab beam made with self-compacting concrete (SCC) experienced slip at a lower load (130 kips) as compared to the slab beam having conventional concrete (156 kips) (Figure 6-2). The slip was noted to be equal on both ends of the beam for the SCC slab beam whereas the slip on the conventional concrete occurred on only the East half of the beam. At ultimate failure, the slip at a deflection of 6.8-in. was found to be higher in conventional concrete compared to SCC (Figure 6-3). Although the SCC slab beam experienced interface slip at a smaller load than the conventional concrete slab beam, it reached a slightly higher peak load compared to the conventional concrete. This shows that it still maintained some form of composite action. This is evident also from strain gauge information whereby the horizontal shear reinforcements yielded at a load of 190 kips compared to

the conventional concrete whereby most horizontal shear reinforcement yielded at a load of 160 kips.
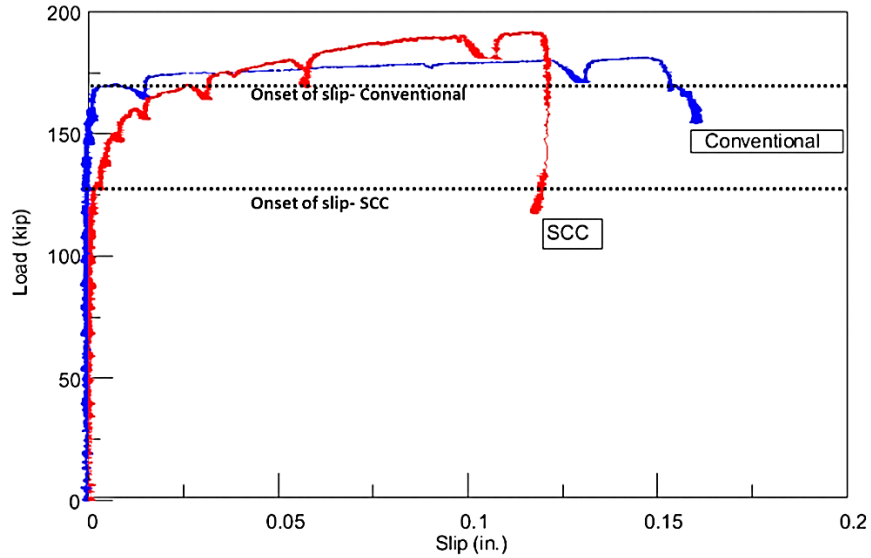
Figure 6-2 Slab beam load-slip comparison

Slip was observed to occur in both beams before the yielding in the horizontal shear reinforcement. It is noted from Figure 6-3 that in SCC beam the separation was much smaller than that in the beam with conventional concrete.
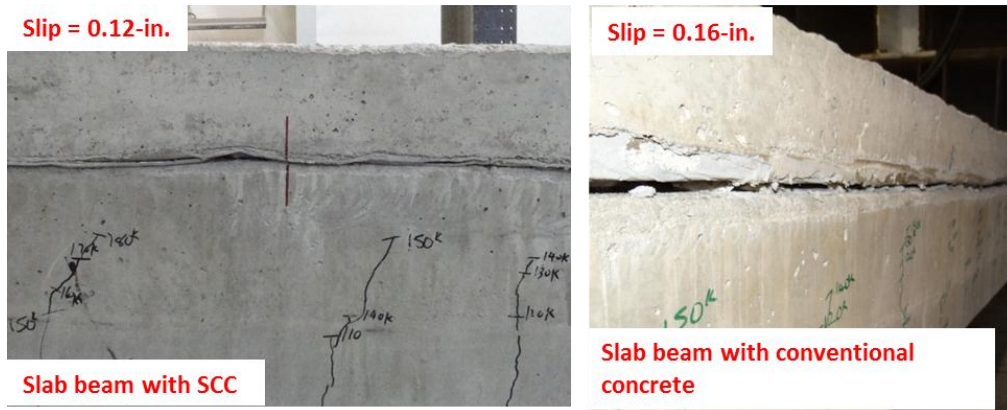
Figure 6-3 Slab beam slip at failure

This separation can be attributed to smaller asperities in SCC compared to conventional concrete. As aggregate/crack surface ride on each other during slip, smaller asperities will lead to less crack width at interface thus leading to SCC retaining more composite action and thus lower slip at failure and a 6% higher failure load.

The box beam as described above was loaded at 7 ft. from the support to increase the shear demand. Test results revealed cracking at the interface occurred at nearly the same load to the side with the slab extending into the blockout. Slip was however observed to be higher in the side where the slab did not extend to the blockout whereby the blockout provided resistance to slipping (Figure 6-4). Hence, the blockout on box beam provides significant amount of additional resistance to slip essentially acting as a shear key. Both tests resulted in flexural failure with crushing being observed on both the CIP slab and the precast beam.
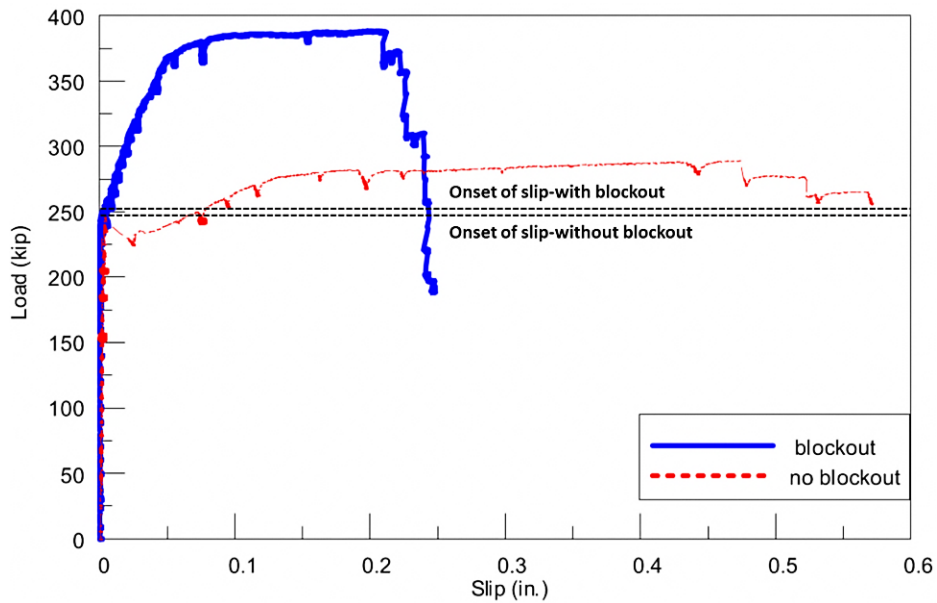
Figure 6-4 Box beam load-slip comparison

This is an indication that composite action had been partially lost. As was observed in the slab beams, the horizontal shear reinforcement did not yield before the onset of slip at the interface.
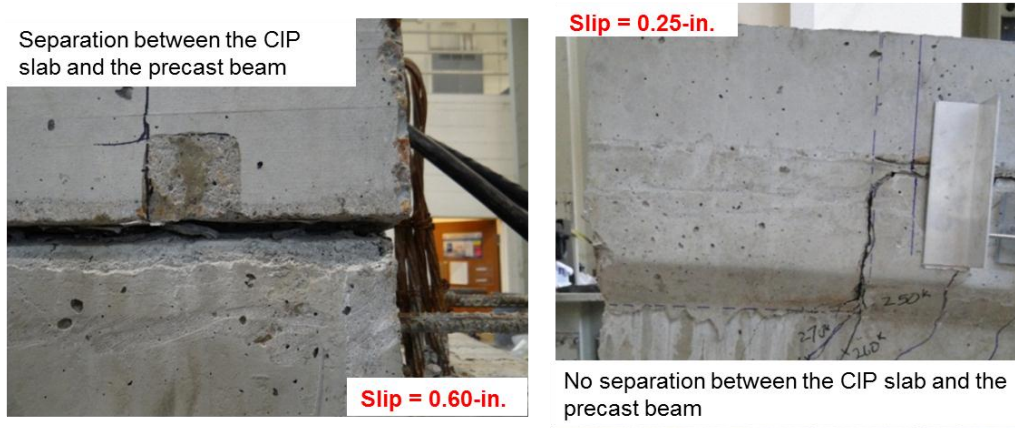
Figure 6-5 Box beam (a) without blockout and (b) with blockout slip at failure

6.1.3 Effect of high compression force due to loading

It was also noted that due to a high compression force at the loading point, there was increased confinement and resistance to slip due to increased friction. This is also evident on the beams at failure as no slip was observed at or near the loading point. Strain gauge profile plots support these findings as shown in Appendix G. The strain gauge profile shows that while the strains increase rapidly after slip on horizontal shear reinforcements away from the loading point (especially the ones at the ends), horizontal shear reinforcements at or near the loading point experience much lower strains from slip to failure of the beam. FE analysis also supports this finding as shown in Section 5.5 whereby the compressive stresses at the interface are seen to be high and decrease almost linearly towards the supports. This may also be the case in actual bridges. Bridge design usually considers distributed live load (HL-93 loading). The HL-93 design load consists of a combination of the design truck or design tandem, and design lane load
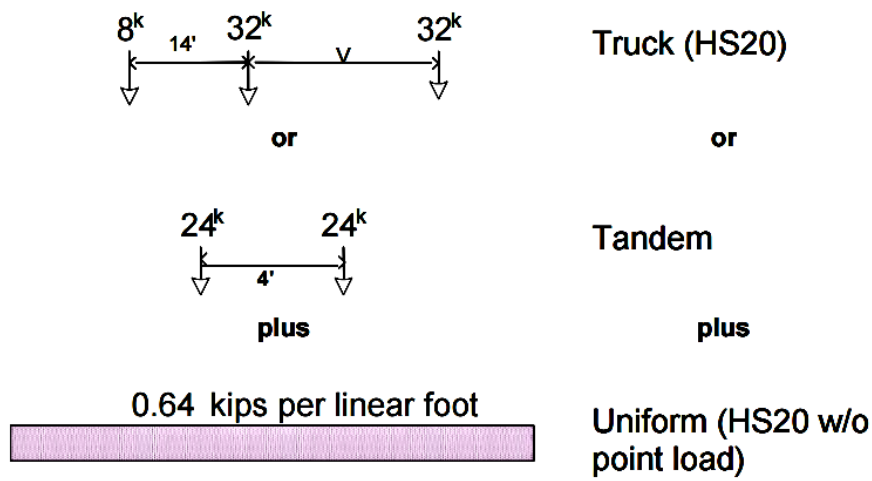
Figure 6-6 HL-93 loading

The compressive force from the live load on the bridge girder could provide additional friction resistance at the interface. AASHTO equation considers the deck weight and other superimposed load as contributing to the P_c factor but fail to consider that service loads are the dominant loads that lead to failure of a beam either in flexure, shear or horizontal shear.

The P_c (permanent net compressive force) force from the AASHTO equation could be modified to consider part of the live load which will lead to an increase in the friction force (μP_c) and consequently to an increase in the horizontal shear capacity.

6.2 Conclusions and Recommendations

1. TxDOT slab and box beams (with the 2-in. embedded length in the CIP deck) have sufficient horizontal shear strength up to flexural failure (even only with the surface roughness). This was evident in Task 6 whereby box and slab beams representing the strongest TxDOT box and slab beams failed by flexural failure even with the exclusion of horizontal shear reinforcements.

2. The use of SCC does reduce slightly the horizontal shear strength by 17% due to the reduction in cohesion and friction. However SCC has less separation at the interface thus maintaining a higher degree of composite action. Test results from this project indicate that using SCC can provide sufficient strength for the slab beams.

3. Blockout at the end of box beams provides high additional resistance to slip, which could be considered in the design. Task 7 results prove that the presence of the blockout reduces slip by more than 50%.

4. Although the push-off tests show that the interface reinforcement with 2-in. embedded length could not be fully developed, the full-scale tests (with reduced interface area) indicate that the actual boundary conditions in the composite beams could provide abundant confinement to develop the reinforcement. Also, the compressive force resulting from loading on the full-scale beams prevents bars from being pulled out.

5. At ultimate horizontal shear capacity the horizontal shear force is mainly resisted by the cohesion/aggregate interlock and friction from the concrete, with minor contribution from the reinforcement. The interface shear reinforcement became engaged only after slip/separation occurred at the interface (also indicated by Seible and Latham (1990), Hofbeck et al. (1969), and Kent et al. (2012)).

6. Current AASHTO equation overestimates the contribution of the interface shear reinforcement at ultimate horizontal shear capacity by assuming that the reinforcement has yielded when ultimate horizontal shear capacity is reached. According to full-scale beams tested (Task 7), the strength of horizontal shear reinforcement at horizontal shear failure was 30% of the expected contribution from the bars.

7. Although the horizontal shear strength is predominantly controlled by the concrete behavior and not the interface shear reinforcement, the minimum amount of reinforcement currently specified by AASHTO (24-in. spacing) is useful in restraining separation of the interface after slip occurs (if that happens).

8. Current TxDOT practice for box and slab beams can be simplified (for example increasing the spacing of the horizontal shear reinforcement from 12-in. to 24-in. and providing a wood finish rather than rake finish) to aid in fabrication process.

9. Based on the finding from this study, in order to reflect the actual behavior of horizontal resistance, the interface shear resistance contribution from the reinforcement can be reduced, while the force (μP_c) can be increased by considering not only the permanent load but partial live load.   The increase or decrease in the aforementioned components of horizontal shear resistance is under analytical and experimental investigation.

Appendix A

Review of Other Department of Transportation Practices

An investigation was conducted on other DOT practices as pertains to the construction of box and slab beams. Our main concern was on the details of the horizontal shear reinforcement (and the surface roughness implemented. Some of states do not have either box beams or slab beams and although others do use them; they do not have the plans on their website. The table below summarizes the findings on all the states.

STATE	BOX BEAM	SLAB BEAM
Alabama	No box beam	Has slab beam
Alaska	No box beam	No slab beam
Arizona	Have both box and slab beams. Do not have any standard drawings just follow AASHTO specifications	
Arkansas	No box beam	No slab beam
California	Has box beam (no response on horizontal shear reinforcement details)	Has slab beam
Colorado	Has box beam	Has slab beam
Connecticut	Has box beam	Has slab beam
Delaware	Has box beams	Has slab beams
Florida	No box beam	Has slab beam
Georgia	Has box beam	No slab beam
Hawaii		
*Idaho	Has box beam	Has slab beam

Illinois	Has box beams	No slab beams
Indiana	Has box beam (No information on beams on website)	No slab beam
Iowa	Do not typically use box beam or slab beams	
Kansas	No box beam	No slab beam
Kentucky	Has box beam	No slab beam
Louisiana	Box beams rarely used	No slab beam
Maine	Has box beam	Has slab beam
Maryland	No box beam	Has slab beam
Massachusetts	Has box beam	Has deck beam
Michigan	Has box beam	No slab beam
Minnesota	Has rectangular beam	No slab beam
Mississippi	No slab or box beams	
Missouri	Has box beam	Has slab beam
Montana	No box beam	No slab beam
Nebraska	No box beam	No slab beam
Nevada	No information on beams on website (No box beams)	
New Hampshire	Has box beam	Has slab beam
New Jersey	Has box beam	Has slab beam
New Mexico	Has box beam	No slab beam
New York	Has box beam	Has slab beam

North Carolina	Has box beam	Has slab beam
North Dakota	Has box beam	No slab beam
Ohio	Has box beam	Has slab beam
Oklahoma	No box beam	No slab beam
Oregon	Has box beam	Has slab beam
Pennsylvania	Has box beam	No slab beam
Rhode Island	Has box beam	Has slab beam
South Carolina	No box beam	Has slab beam
Tennessee	Has box beam	No slab beam
South Dakota	No box beam	No slab beam
Texas	Has slab beam	Has box beam
Utah	No box beam	No slab beam
Vermont	Plans not available on website (no response)	
Virginia	Use them infrequently so no statewide standard available	
Washington	No box beam	Has slab beam
West Virginia	Has box beam	No slab beam

Wisconsin	Has box beam	No slab beam
Wyoming	Has only one box beam	No slab beams

There are generally five surface finishes that can be applied on concrete.

- As-placed roughness: No attempt is made to smooth or roughened the surface after concrete is poured and vibrated.

- Float finish: After concrete is poured and vibrated, a rough wooden float is run through the surface to smoothen it.

- ¼" rake finish: A rake is run across the interface transverse to the beam length leaving a very rough textured finish.

- Rough broom finish: A stiff broom is run across the surface of the beam in the transverse direction.

- Sheepsfoot voids: This represents a mechanical surface finish consisting of 1-in. diameter, ½-in. deep impressions made at a spacing of 3½-in.

Only three kinds of finishes are currently being used; that is the broom, rake and float finish as will be seen below. It has also been noticed that there are six different shapes of horizontal shear reinforcement used. The following summary is based on the forms of horizontal shear resistance.

Alaska DOT

Does not typically use slab beams with CIP decks therefore they do not have any standard plans for this type of structure. When they have designed this type of bridge in the past, they extended the vertical shear reinforcing into the deck and verified that the

requirements of AASHTO LRFD article 5.8.4 are met. They however specify a roughened interface.

California DOT

California uses both box beam and slab although the plans that are available on their website are very vague. A float finish is specified in the plans.
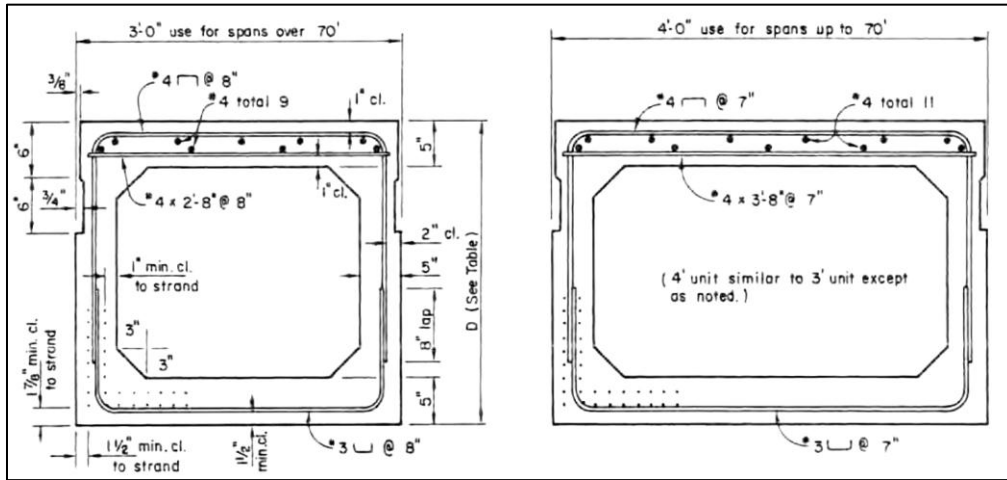
Typical box beam section (the layout of horizontal shear reinforcement is not
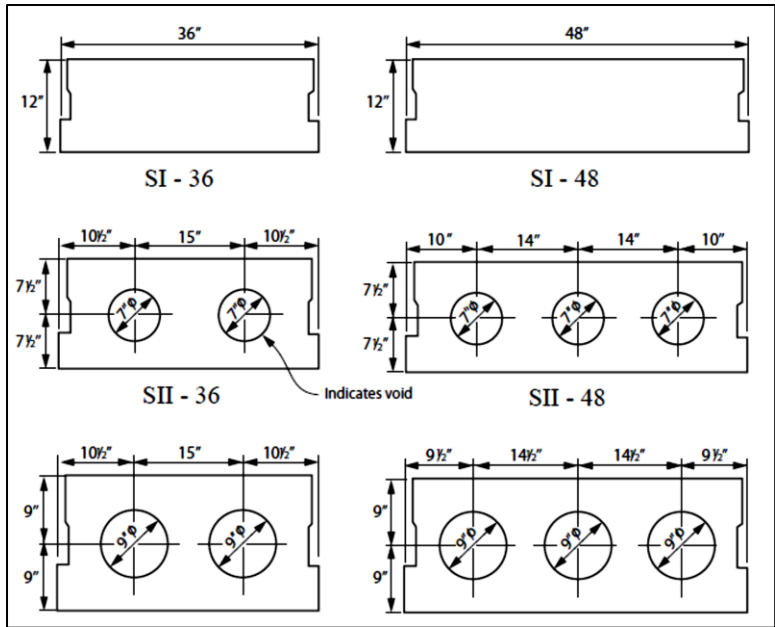
clear)

Typical slab beam sections

Colorado DOT

The Colorado department of transportation use both the slab and box beams in their bridges. Although not much information is given in their design drawings, it is clear that the embedded length of the horizontal shear reinforcement in slab beams is 2.5-in. With the surface roughened to an amplitude of ¼-in.. The box beam standard drawings specify that horizontal shear reinforcement should be field bent over the top mat of longitudinal slab steel. The width is however not clear.

TYPICAL SECTION

Typical slab beam section

Typical box beam section (the layout of horizontal shear reinforcement is not

clear)

Delaware DOT

They do not provide any standard drawings on their website. They however have both slab and box beams and they use the M-shaped bar (Type 1) as the horizontal shear reinforcement. A broom finish is specified for the top of the slab and box beams.

Georgia DOT
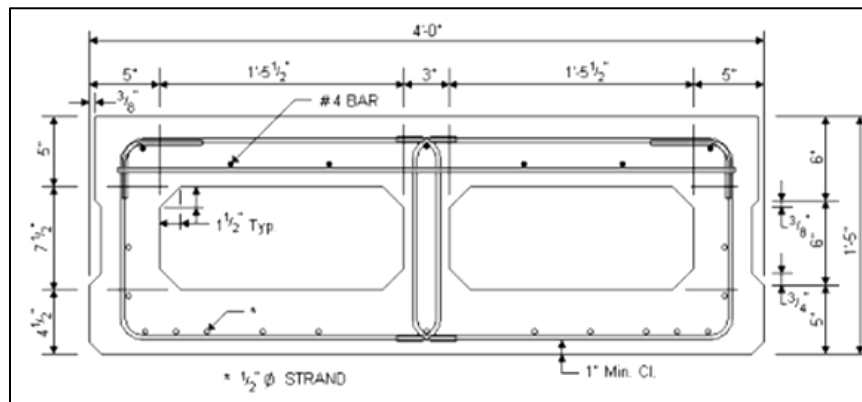
Typical box beam section

Indiana DOT

Uses box beams on their bridges. Plans could not clearly show if there is horizontal reinforcement. The plan below is from a bridge replacement project on Pruce road. The embedded length of the horizontal reinforcement is seen to be $2\frac{1}{8}$-in. The horizontal reinforcement seems not to cover the entire length of the beam. The plans specify that the top of the beams should be scored transversely at approximately 3-in. centers with a pointed tool.

Typical box beam section

Elevation

222
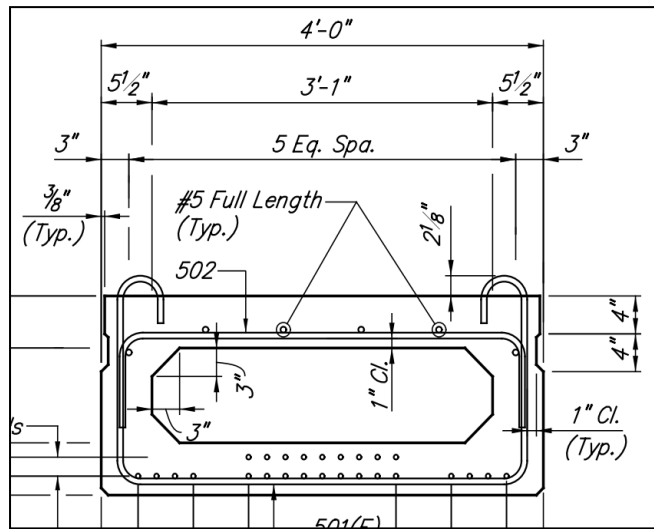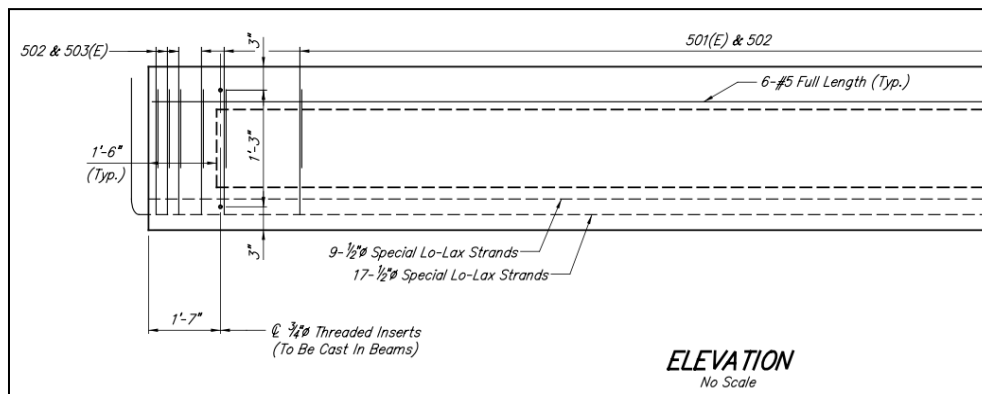
Idaho DOT

They do use slab beams and box beams on their bridges although no information is provided for the horizontal shear reinforcement. On further inquiry I was informed that the girder stirrups are designed to project into the concrete decks and the top surface of the girders have a float finish. No details and drawings are provided for the box beams.
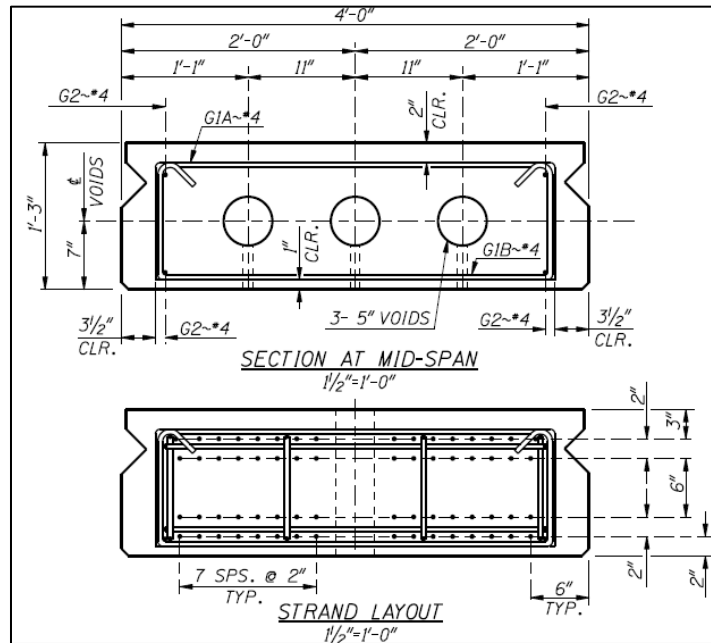
Slab beam section

Illinois DOT

They use precast prestressed box beams on their bridges. The 5-in. concrete wearing surface on deck beams is non-composite. It just serves as a plate to help reduce reflective shear key cracking and improve rideability hence there is no interface shear reinforcement provided.
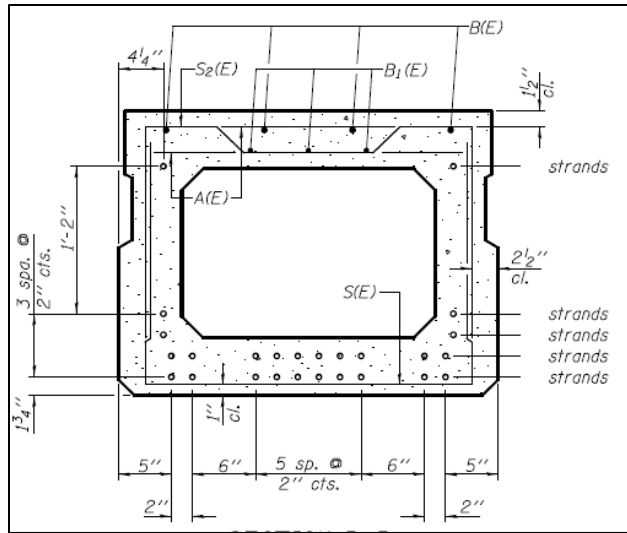
(a)
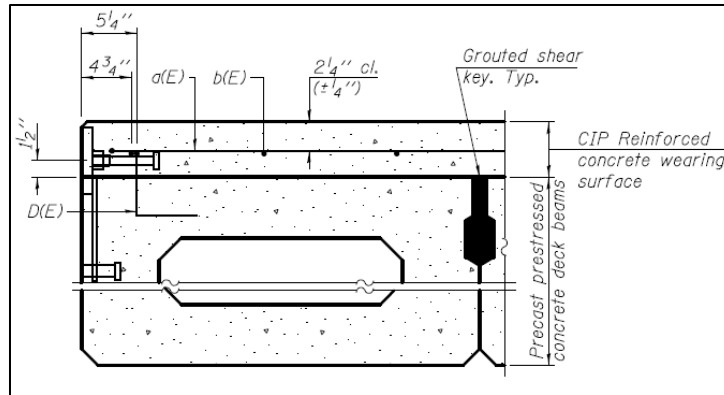
(b)

Box beam section

New Jersey DOT

The specifications specify that the surface will be finished according to the designers specifications thus not giving a specific surface roughness to be used. Both the the slab and box beam have type 1 horizontal shear reinforcement as shown below.
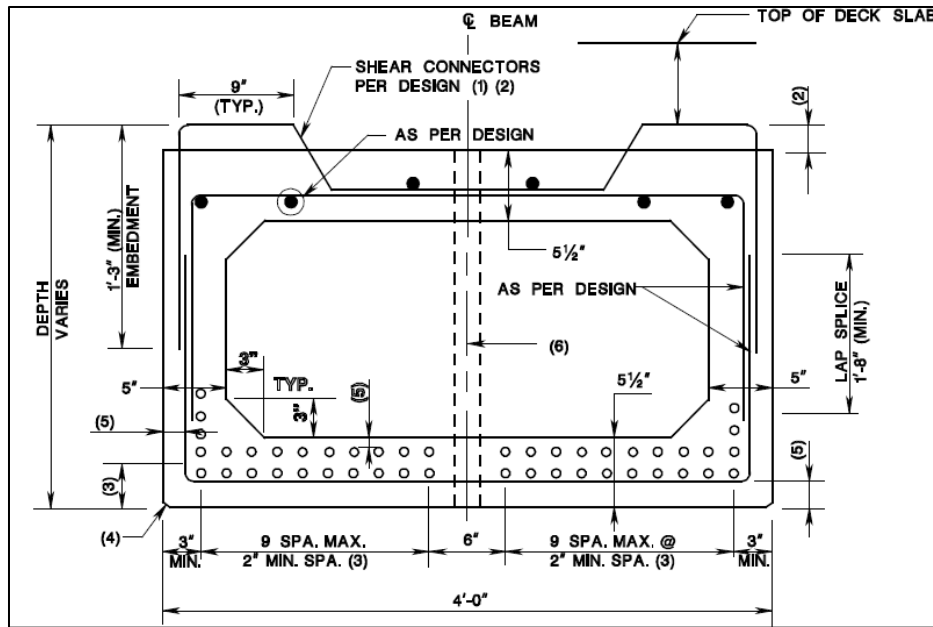
Box beam section

Kentucky DOT

Kentucky utilizes box beams in their bridges. The height of the horizontal shear reinforcement is seen to be about 2.5-in. whereas the width is unclear. A floated surface finish is specified.
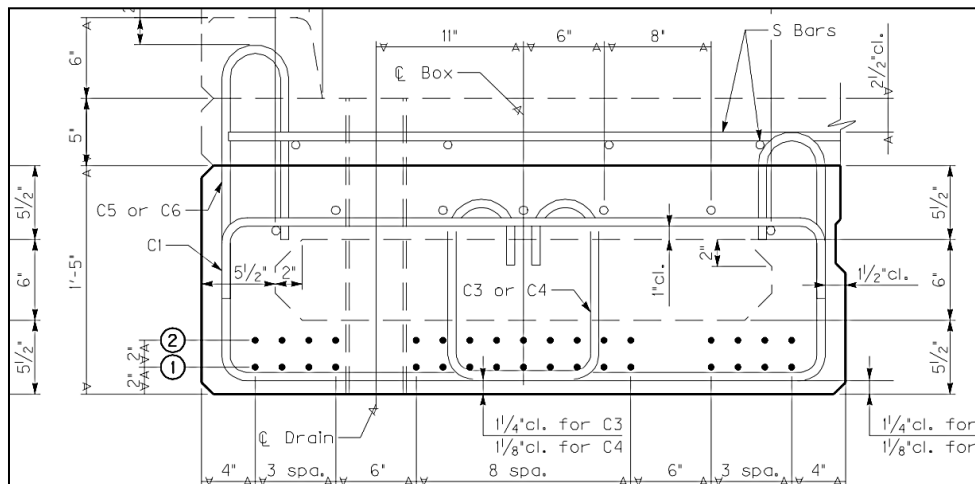
Typical box beam section
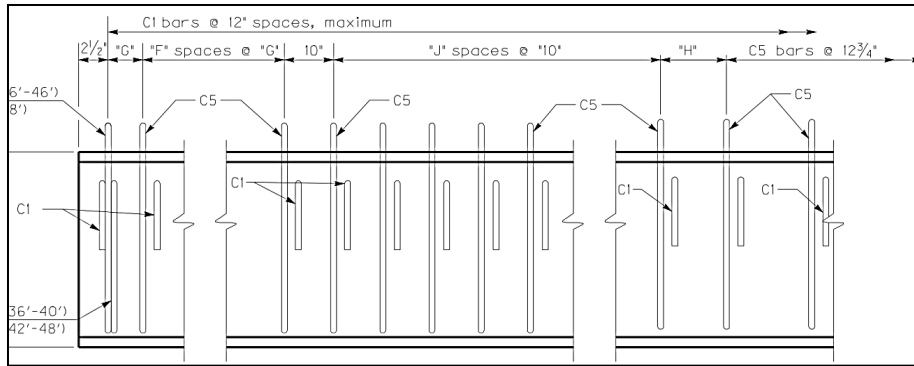
Elevation

Maine DOT

Details of Maine department of transportation box and slab beams are shown below. The embedded length of the horizontal shear reinforcement is shown to be 3-in.. Similar horizontal shear reinforcement is specified for the box beams.
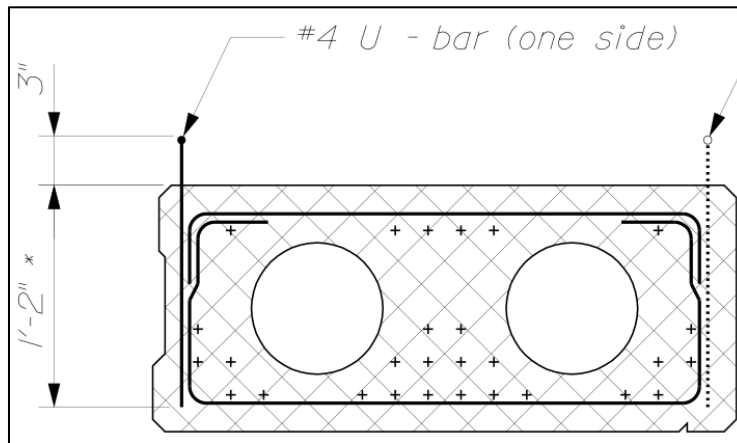
Typical slab beam section (Note that the direction of the horizontal shear reinforcement is perpendicular to the cross-section)

226
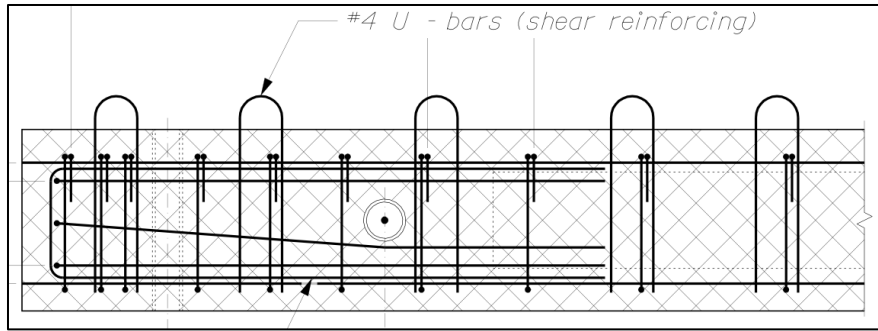
Elevation
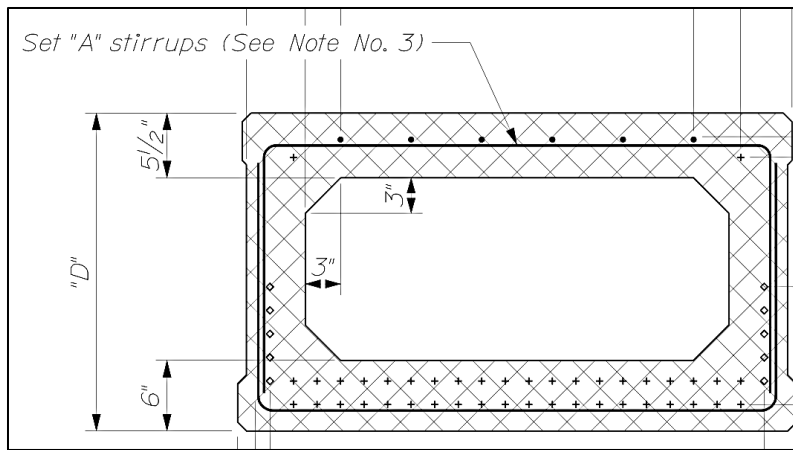
Typical Box beam section

Massachusetts DOT

Massachusetts utilizes both box and deck beams on their bridges. The deck beam is essentially similar to a slab beam as can be seen in the diagram below. The embedded length of the horizontal shear reinforcement is seen to be 2-in. whereas the width is not specified. A rake finish is specified (1/4-in.. amplitude) across the width.
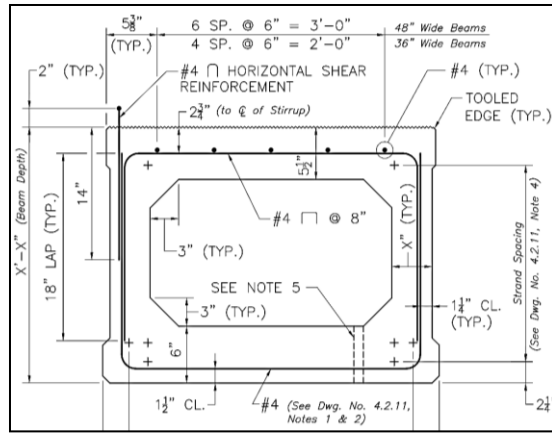
Typical box section (Note that the direction of the horizontal shear reinforcement

is perpendicular to the cross-section)
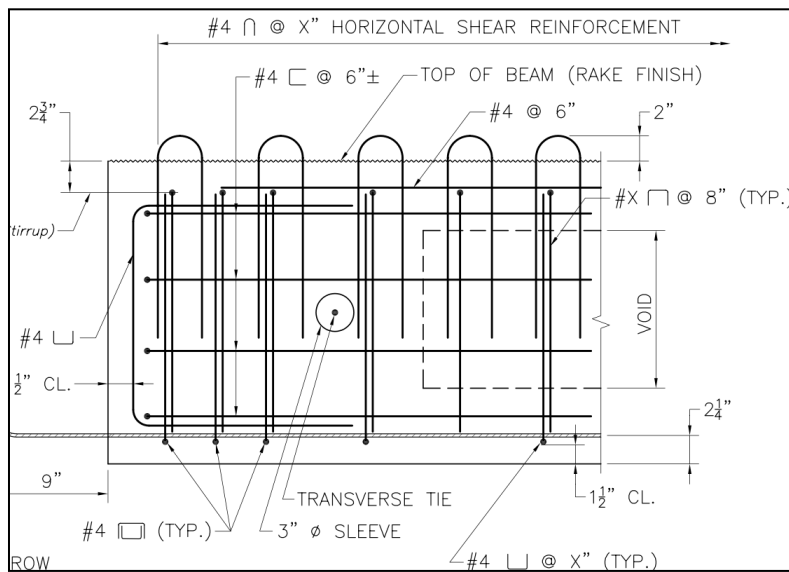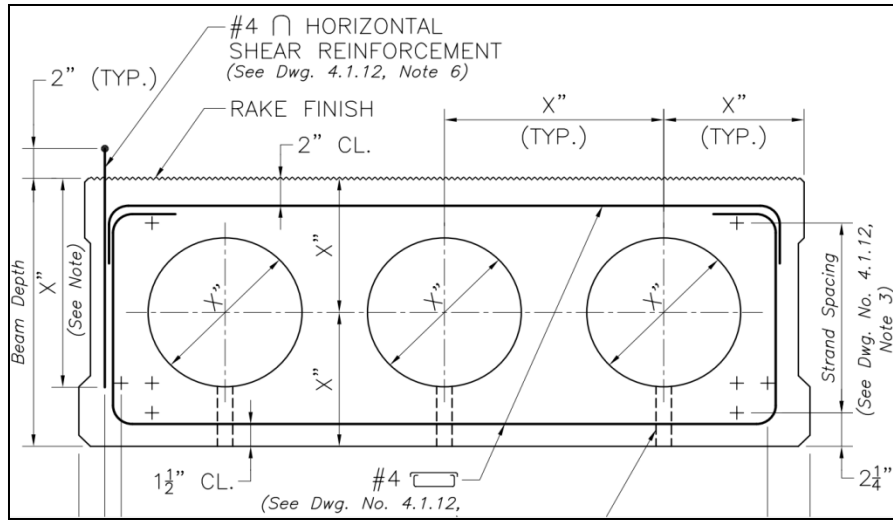
Elevation

Typical slab (deck) beam section (Note that the direction of the horizontal shear

reinforcement is perpendicular to the cross-section)
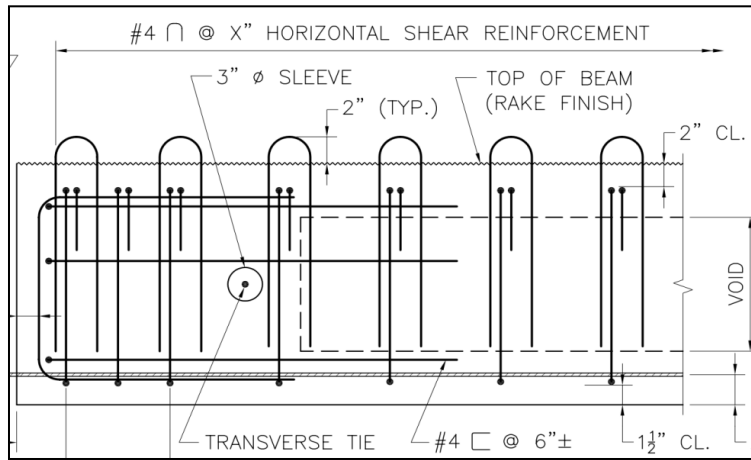
Slab (deck) beam elevation

Minnesota DOT

Minnesota utilizes rectangular beams as shown below. The embedded length is
seen to be 6-in.. The plans specify that the tops of beam should be rough floated and
broomed transversely for bond.
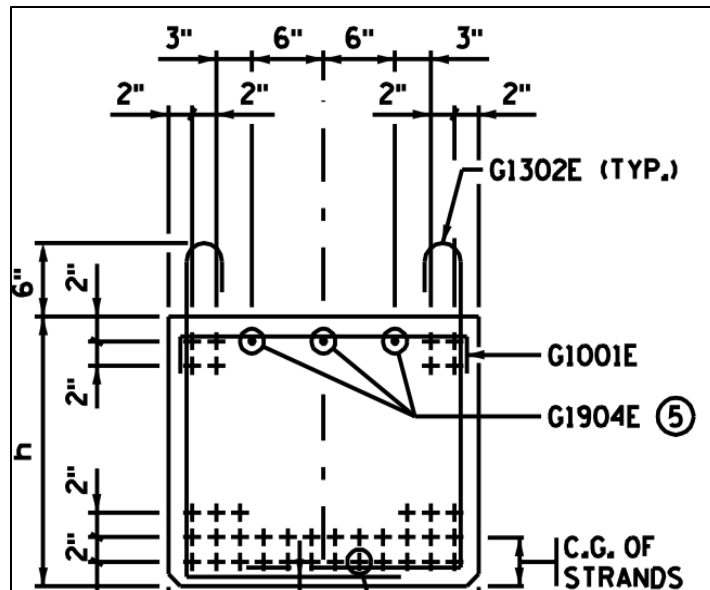
Typical rectangular beam section
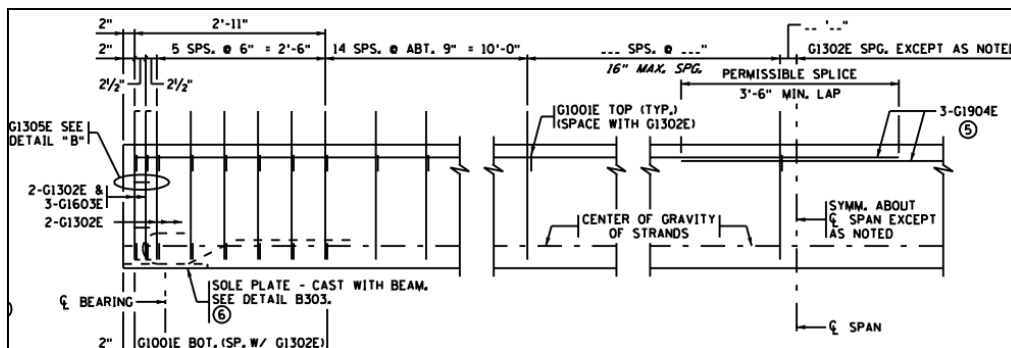
Elevation

Missouri DOT

Missouri does not have standard drawings for prestressed box and slab bridges. They however use prestressed box beams and voided slab beams (no solid slabs) and rely on experience and their inventory of bridges they have designed in the past. The diagrams below show some of the details that have been used by consultants and the department. Top surface of all beams shall receive a scored finish (depth of scoring ¼-in.) perpendicular to prestressing strands.
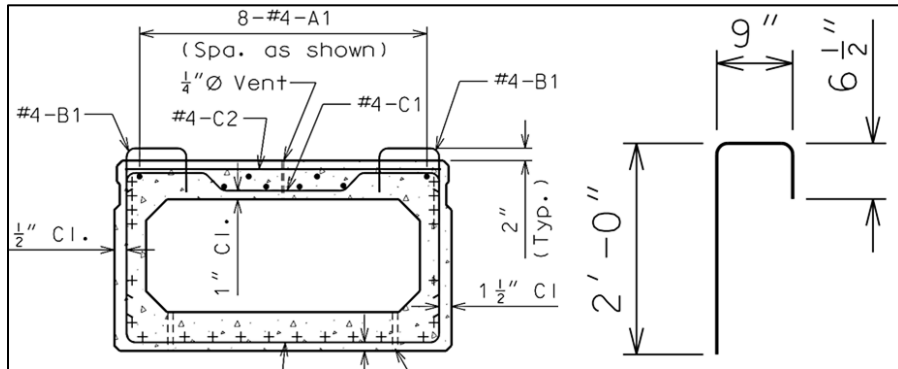
Typical box beam section
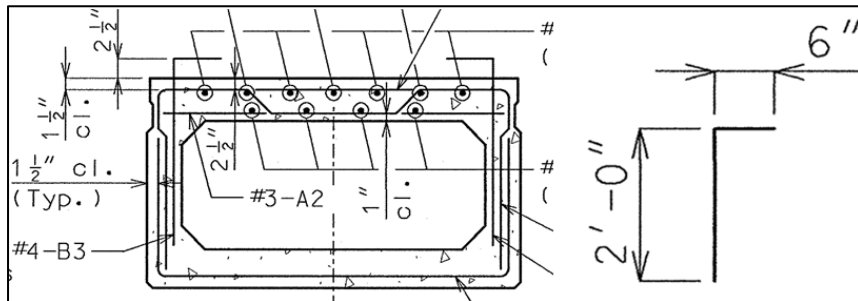
Typical box beam section
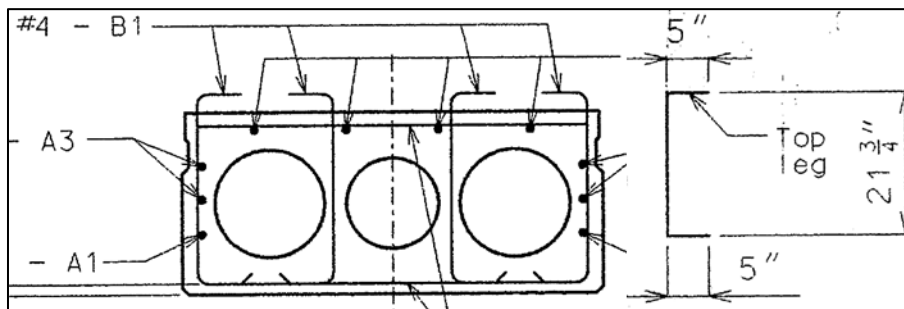
Typical slab beam section

Pennsylvania DOT

Uses box beams in their bridges. The embedded length of the horizontal shear reinforcement is seen to be 3-in. whereas the width is 4-in..

231
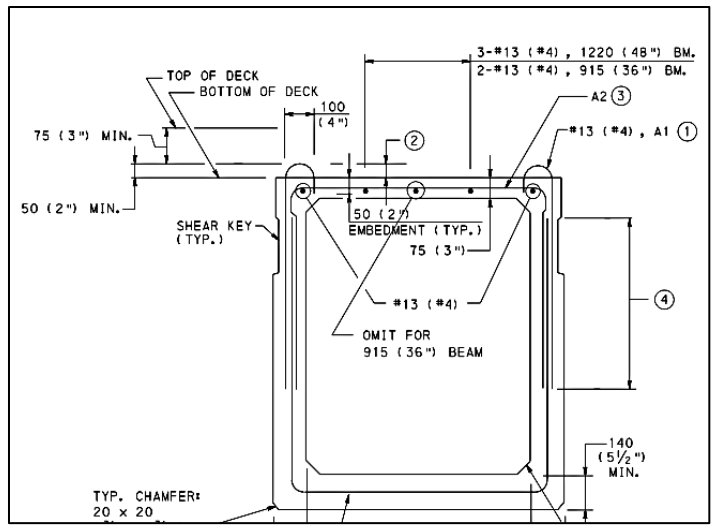
Typical box beam section

Rhode Island DOT

Has both slab and box beams. The embedded length is seen to be 2-in. for the horizontal shear reinforcement whereas no details are given on the width of the reinforcement. A raked surface finish is specified for butted box beam girders having a minimum of 5-in. composite deck overlay.
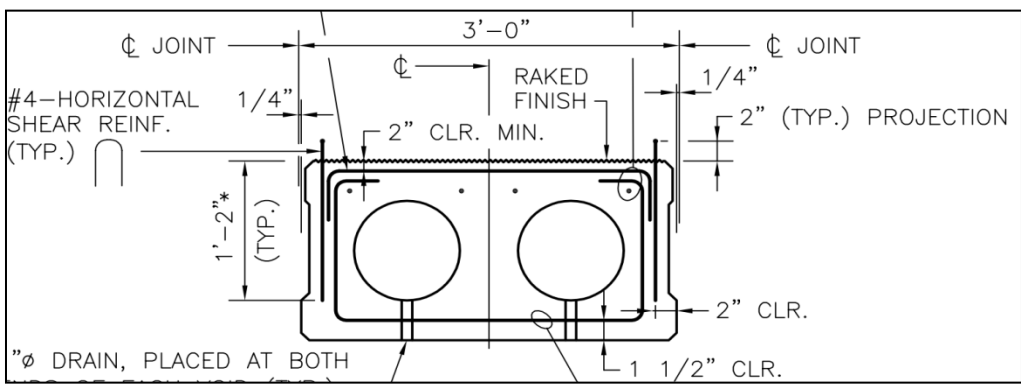
Typical slab section (Note that the direction of the horizontal shear reinforcement is

perpendicular to the cross-section)

Elevation

Typical box beam section (Note that the direction of the horizontal shear reinforcement is

perpendicular to the cross-section)

Elevation

233
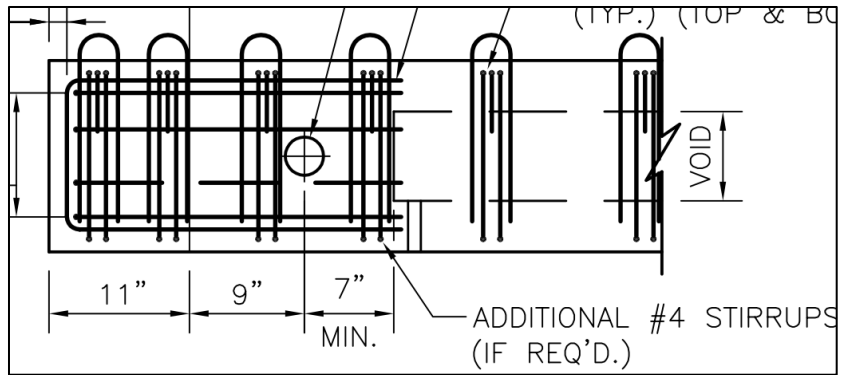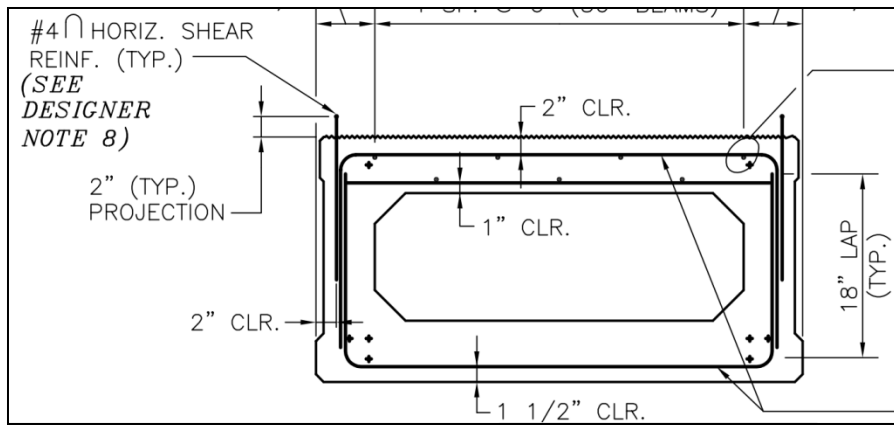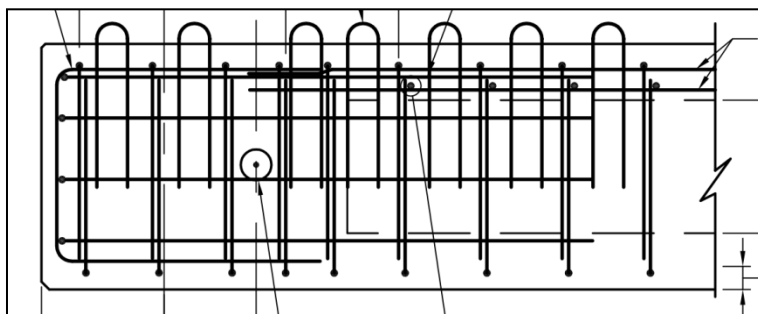
New York DOT

Utilizes both the box and slab beam on their bridges. The embedded length of the horizontal shear reinforcement is shown to be 2-in.. No information is provided on the width of the horizontal shear reinforcement. A transverse rough surface finish with an amplitude of ¼-in. is specified.
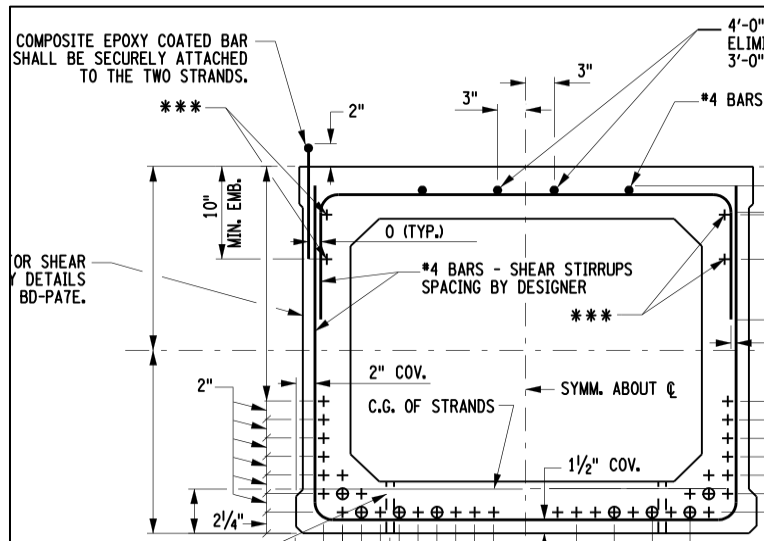
Typical box beam section (Note that the direction of the horizontal shear reinforcement is perpendicular to the cross-section)
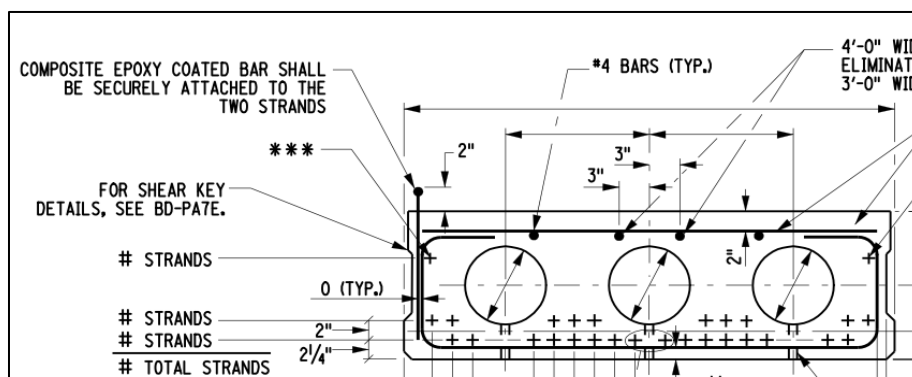
Typical slab section (Note that the direction of the horizontal shear reinforcement is perpendicular to the cross-section)

Connecticut DOT

Details on both the box beam and slab beam are shown below. A water proof membrane is used on top of the precast beams with a minimal of 3.5-in. bituminous overlay. However, 20 years later, they began to experience some pre-mature failures of those structure types due to the failure of the waterproof membrane. They have more recently started using cast-in-place slab but have not yet have standard details available yet. The plans specify a float finish on the top of the beams.
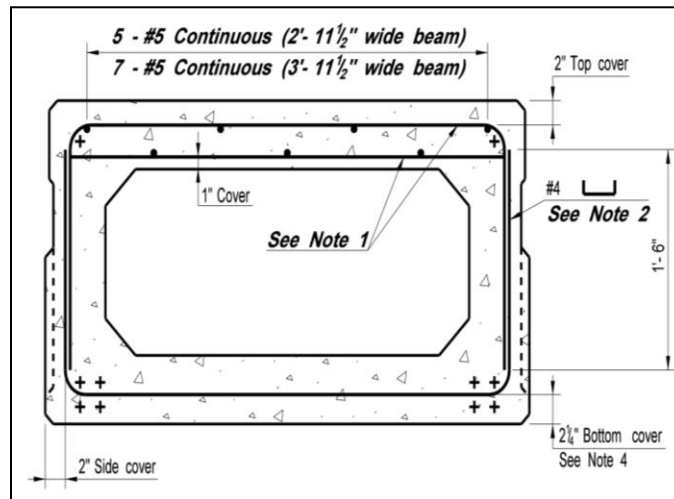
Typical mid-span box beam section (the layout of horizontal shear reinforcement is not clear)
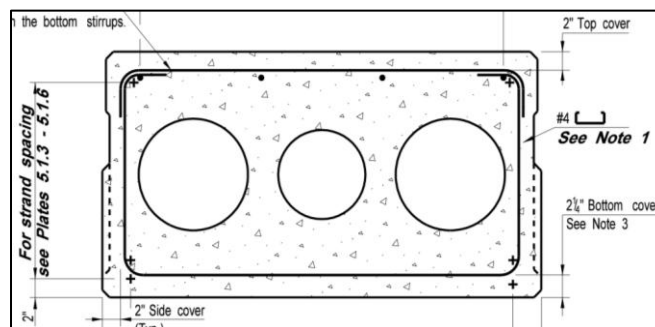
Typical mid-span slab beam section (the layout of horizontal shear reinforcement is not clear)

Oregon DOT

Uses both the slab and box beams on their bridges. Dowels are provided only at the ends of the beams to provide bearing as shown in the end elevation. An asphaltic concrete wearing surface is used hence the lack of horizontal shear reinforcement. A float finish is specified.
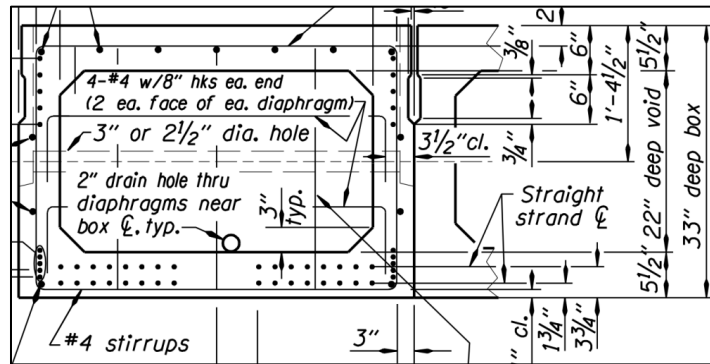
Typical box section
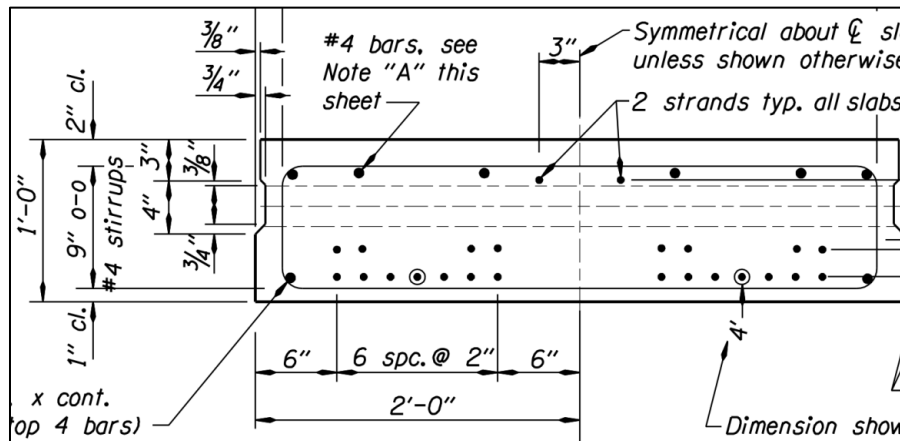
Typical slab section

Alabama DOT

The Alabama DOT has voided slab beams but no box beams. The details are as shown below whereby the width of the horizontal reinforcement is seen to be 4-in. whereas the embedded length is 2.5-in.
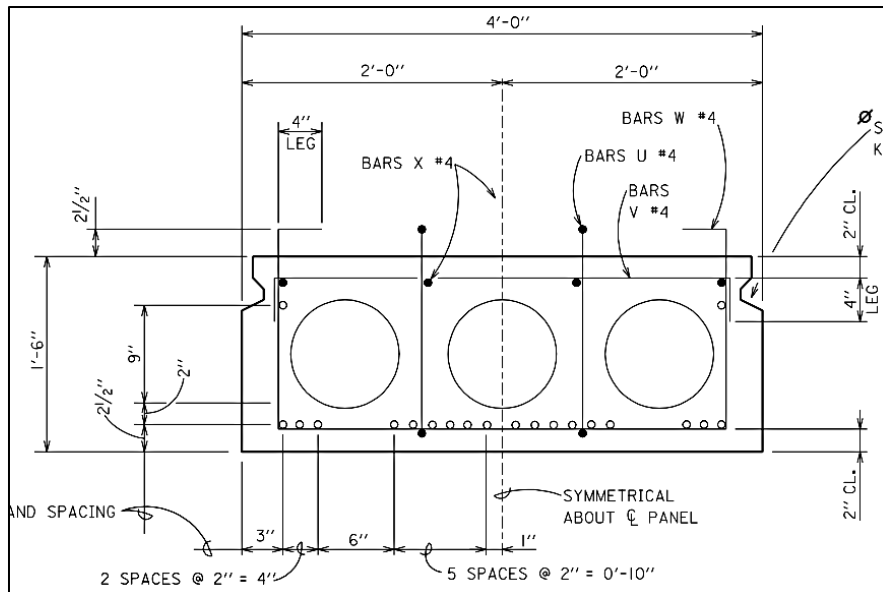
Typical slab beam section

Tennessee DOT

Although Tennessee use box beams, little information is given on their website. Below is the only plan available on box beams. It does not give much information on the horizontal shear reinforcement.
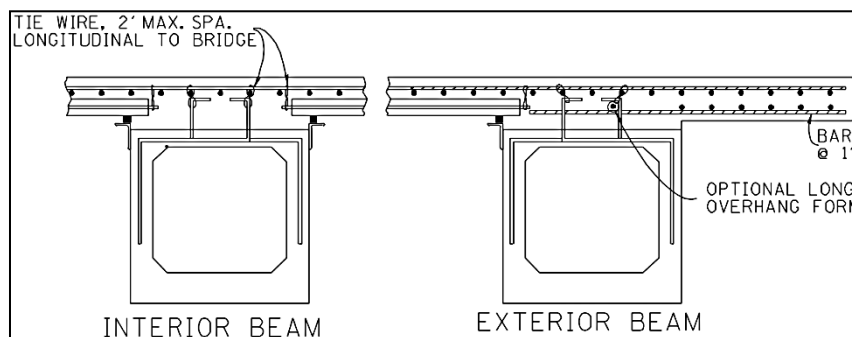
Typical prestressed box beam with bridge deck panels

Washington DOT

Has only the slab beam whose details are shown below. The width of the horizontal reinforcement is 9-in. while the embedded length is 2.5-in. The top surface of the beam is float finished.
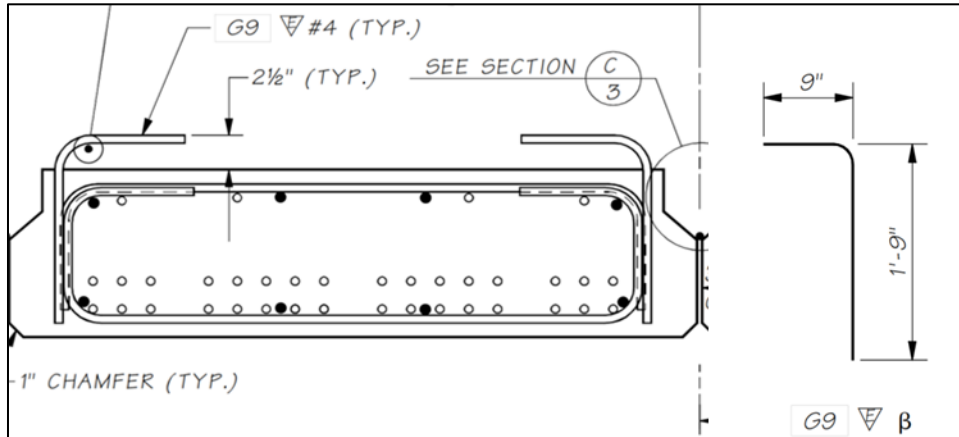
Typical Slab section
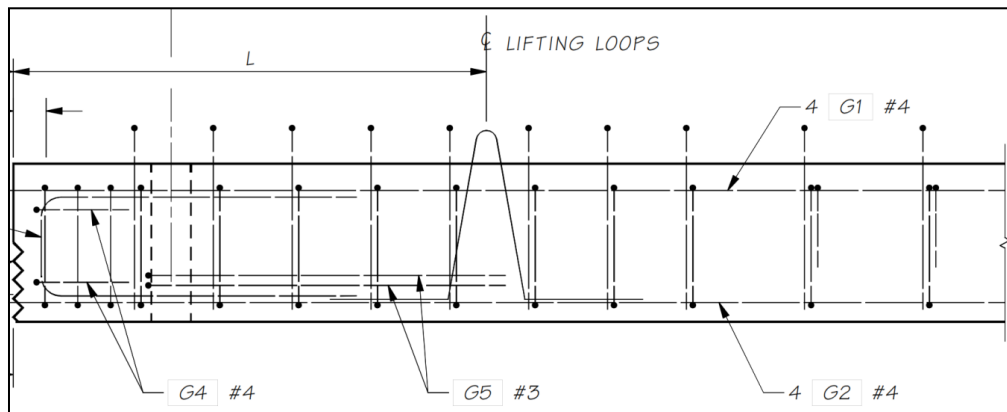
Elevation

Maryland DOT

Maryland typically uses slab beams on their bridges. The section below is an example of the slab beam detail from a bridge over Israel Creek. The embedded length is shown to be 2.125-in.
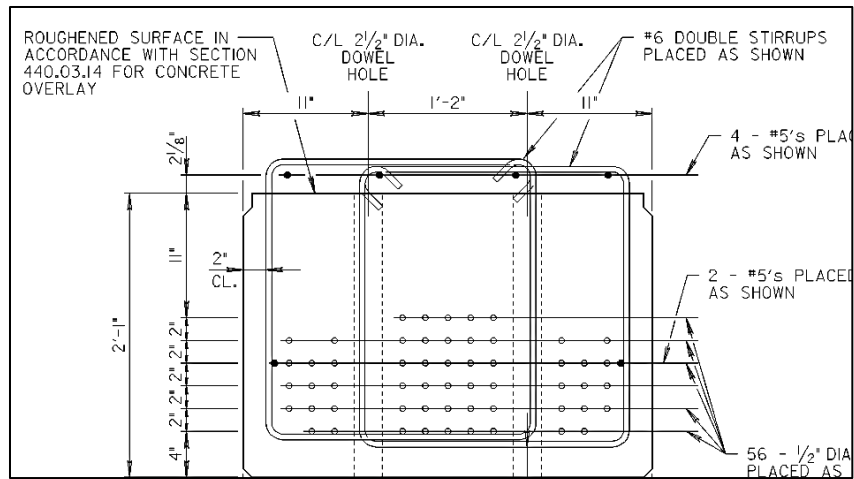
Typical slab section

Michigan DOT

Uses only slab beams whose section is shown below. The height of the horizontal shear reinforcement is shown to be 2.75-in. whereas the width of the reinforcement is 31-in.. The top of the beam is float finished.
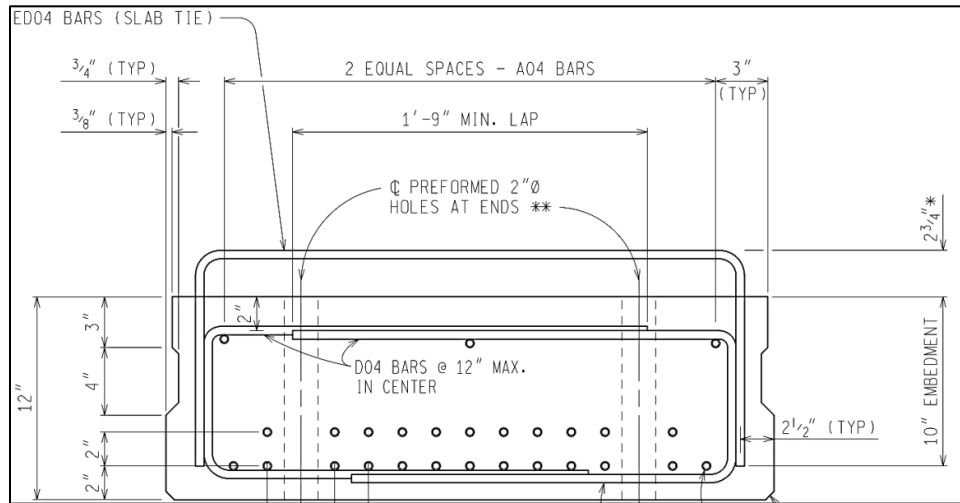
Typical box beam section

North Carolina DOT

Typically use both slab and box beams but employ an asphalt wearing/riding surface or thin lightly reinforced concrete overlay. As such, the beams are designed to perform as non-composite structural elements and hence do not require horizontal shear reinforcement.

Ohio DOT

Has both the slab and box beams. The specifications recommend roughening the surface to an amplitude of ¼-in..
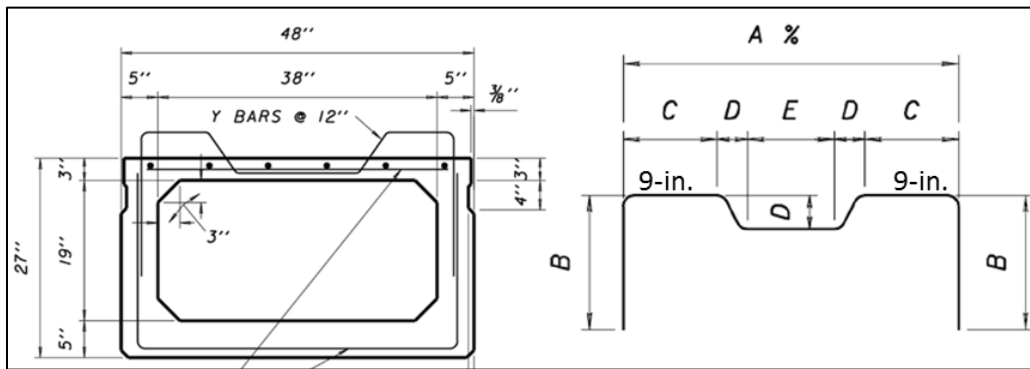
Typical box beam section

Florida DOT

Utilizes slab beams in their bridges with a horizontal shear reinforcement width of 12-in. and an embedded length of 2.5-in.
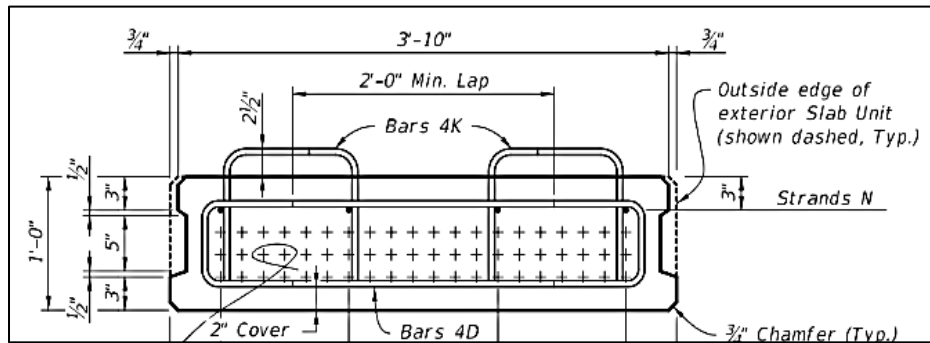
Typical slab beam section

North Dakota DOT

Utilizes box beams in their bridges. The diagram below shows a typical box beam section. The embedded length of the horizontal shear reinforcement is shown to be 3-in. whereas the width is 6-in. A wood float finish is specified.
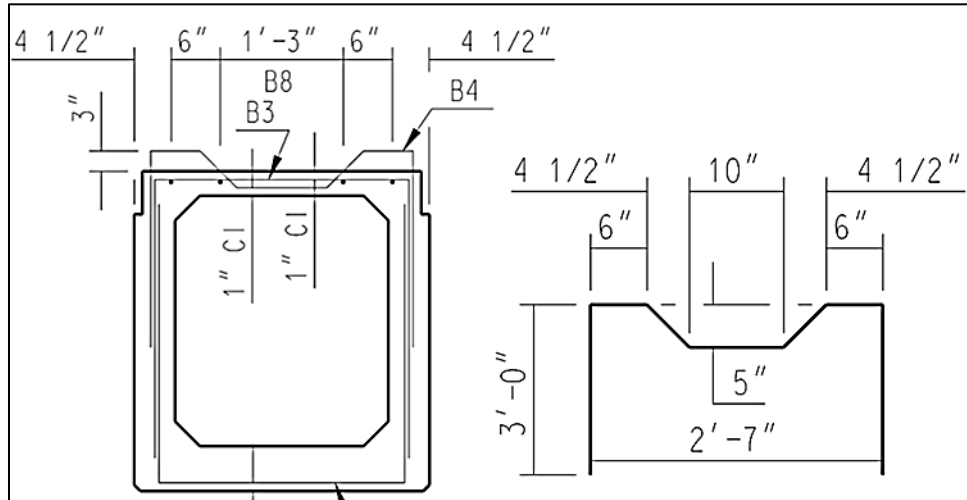
Typical box beam section

West Virginia DOT

Has box beams. The embedded length is seen to be 5-in. whereas the width is 7-in. The plans specify that the top surface should be roughened to an amplitude of ¼-in.
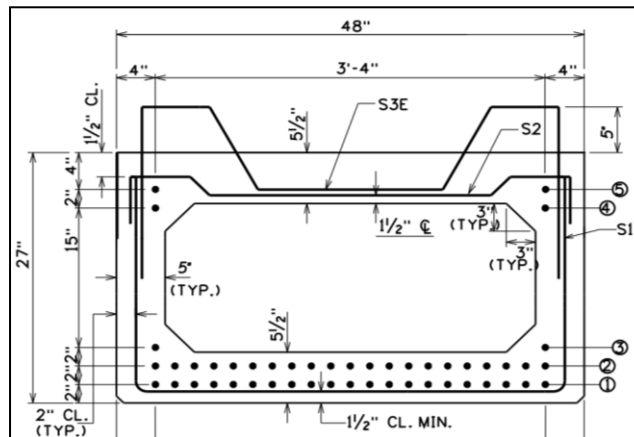
Typical box beam section
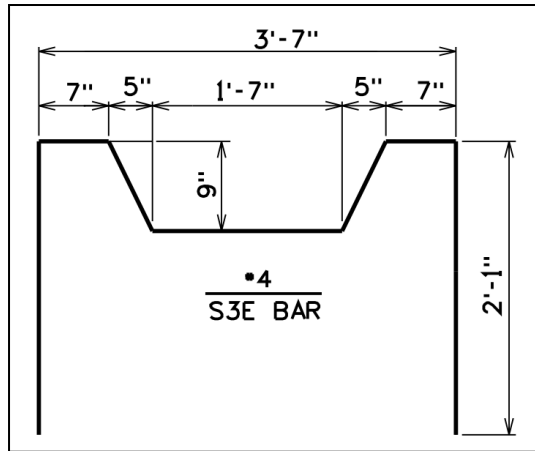
Horizontal shear reinforcement

Wisconsin DOT

Has both box and slab beams however, only box beam details are available on their website. From the plans it seems not horizontal shear reinforcement is used instead a bonding coat is used. The top of the beam should be finished by a rough float and broom transversely.
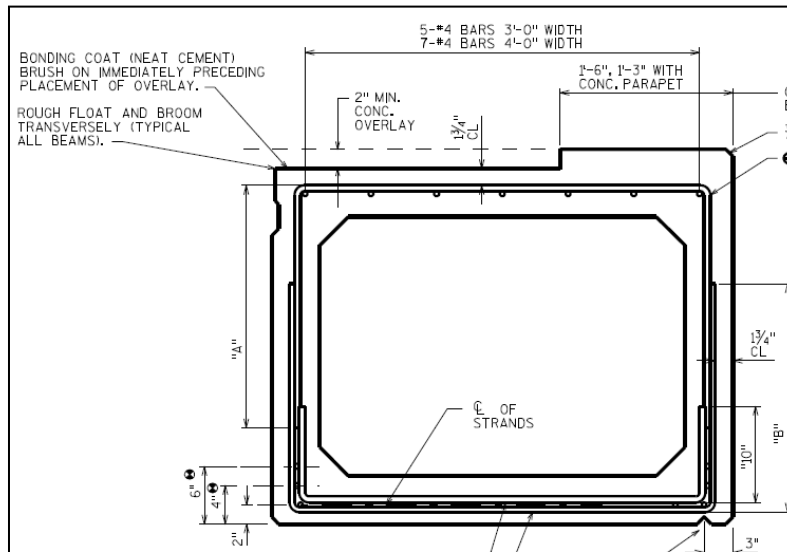
Typical box beam section
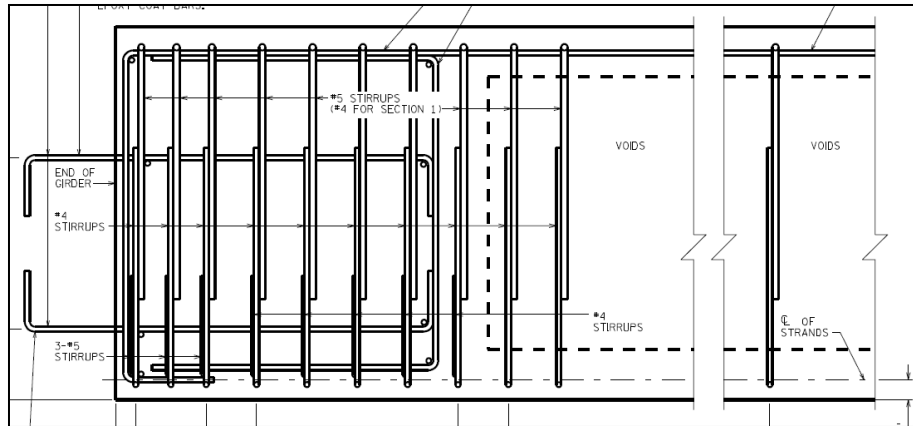
Elevation

SUMMARY

From the study conducted it has been observed that there are essentially six types of horizontal shear reinforcement as shown below.

Type 1

This type has been used by three of the states (West Virginia, North Dakota and Ohio) investigated although the width (w) and the embedded length (h) of the horizontal shear reinforcement varies.

TYPE 1
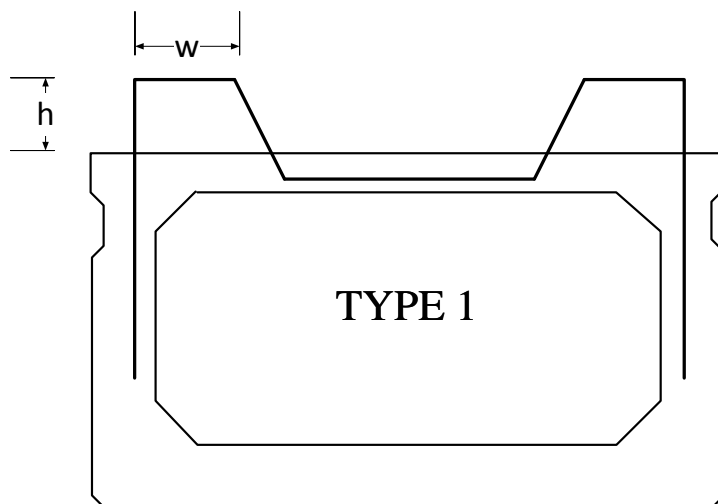
This is one of the least used horizontal reinforcement. It is used in two of the states (Michigan and Maryland) investigated. This kind of reinforcement almost runs the whole width of the beam.
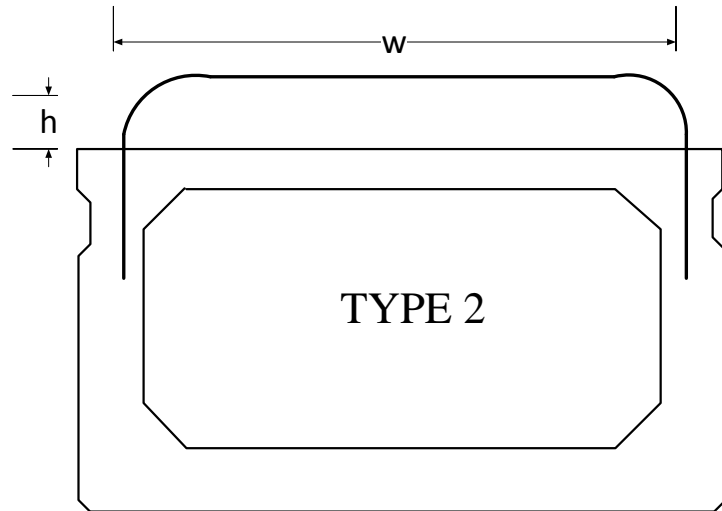
Type 3

This type of horizontal shear reinforcement is in use in Colorado and Missouri. A 90° curvature is utilized in this kind of reinforcement.
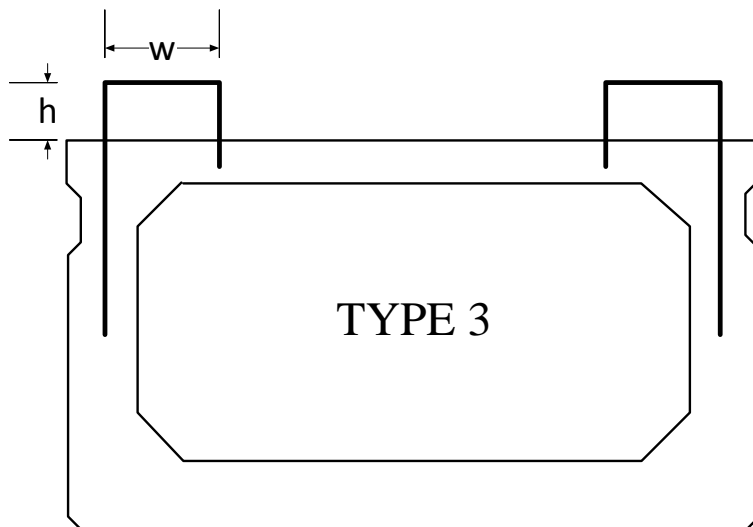
<u>Type 4</u>

Three states (Washington, Alabama and Missouri) use this type of reinforcement that utilizes a 90° curvature as seen.
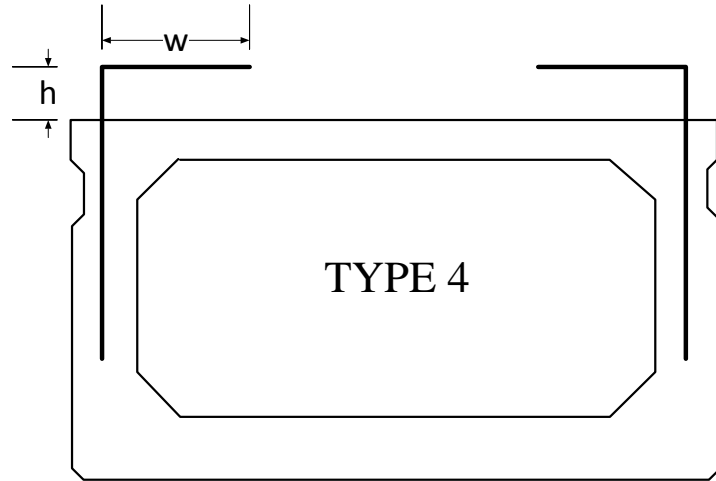
<u>Type 5</u>

This is the most popular horizontal shear reinforcement. Eight of the states investigated use this type of reinforcement. A 180° curvature is utilize in this kind of reinforcement.
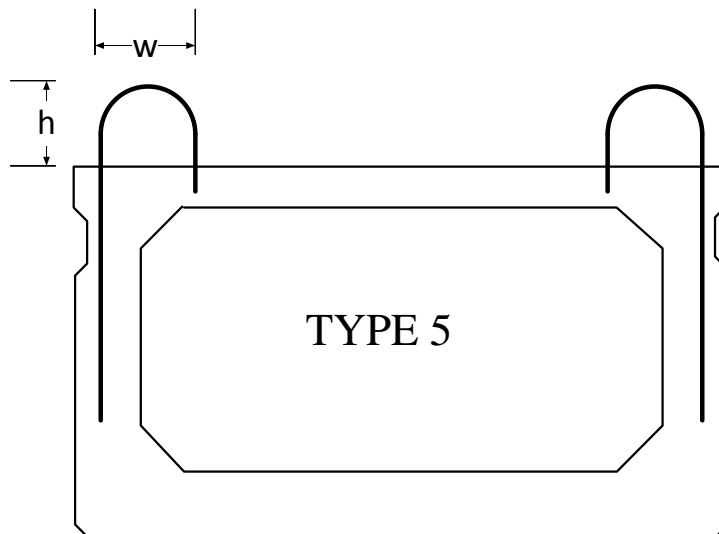
<u>Type 6</u>

This type of reinforcement is similar to Type 5 except the horizontal shear reinforcements are oriented perpendicular to the cross-section in Maine, Rhode Island and Massachusetts. It should be designed in accordance to AASHTO.

TYPE 6
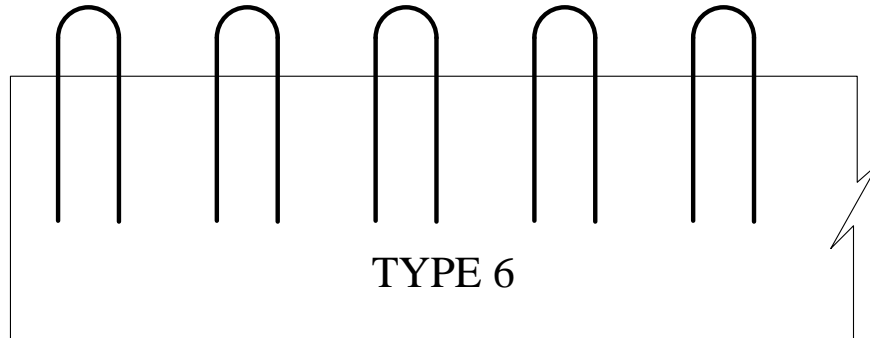
A wood float surface finish is also shown to be the most used type of finishing on the beams. The table below gives a summary of the findings.

State	Type of horizontal shear reinforcement	Width (in.)	Embedded length (in.)	Surface finish
Ohio	Type1	9	2	Wood float
North Dakota	Type 1	6	3	Wood float
West Virginia	Type 1	7	5	Wood float
Maryland	Type 2	-	2.125	-
Michigan	Type 2	31	2.75	Wood float
Colorado	Type 3	-	2.5	Wood float
Missouri	Type 3	9	2	-
Texas	Type 3	6	2	Wood float
Florida	Type 3	12	2.5	-
Missouri	Type 4	6	2.5	-
Alabama	Type 4	4	2.5	Rake finish
Washington	Type 4	9	2.5	Wood float

State	Type of horizontal shear reinforcement	Width (in.)	Embedded length (in.)	Surface finish
Indiana	Type 5	-	2 1/8	Scoring
Kentucky	Type 5	-	2.5	Wood float
Maine	Type 6	(perpendicular to cross-section)	3	Wood float
Massachusetts	Type 6	(perpendicular to cross-section)	2	Rake finish
Minnesota	Type 5	3	6	Broom finish
Pennsylvania	Type 5	4	3	Broom finish
Rhode Island	Type 6	-	2	Rake finish
Texas	Type 5	3.5	2	Wood float

Appendix B

Box and Slab Beam Standard Designs

Slab Beam Standard Design

DESIGNED BEAMS (STRAIGHT STRANDS) / OPTIONAL DESIGN

STRUCTURE	SPAN LENGTH (ft)	BEAM NO.	BEAM TYPE	NON-STD STRAND PATTERN	PRESTRESSING STRANDS TOTAL NO.	SIZE (in)	STRGTH fpu (ksi)	"e" ℄ (in)	"e" END (in)	TOT NO. DCB	DIST FROM BOTTOM (in)	NO. OF STRANDS TOTAL	DEBOND 1/2 ROW 1	3	6	9	12	15	RELEASE STRGTH f'ci (ksi)	MIN 28 DAY COMP STRGTH f'c (ksi)	DESIGN LOAD COMP STRESS (TOP) fct (ksi)	DESIGN LOAD TENSILE STRESS (BOTT) fcb (ksi)	REQUIRED NOMINAL ULTIMATE MOMENT CAPACITY (ft-kips)	LLDF Moment	LLDF Shear
24' Rdwy SB12 Beam	25	ALL	5SB12		10	1/2	270	3.50	3.50	0	2.50	10	0 0 0 0 0 0 0 0 0 0						4.000	5.000	0.916	-1.221	400	0.45	0.45
	30	ALL	5SB12		14	1/2	270	3.50	3.50	0	2.50	14	0 0 0 0 0 0 0 0 0 0						4.000	5.000	1.293	-1.688	532	0.45	0.45
	35	ALL	5SB12		20	1/2	270	3.50	3.50	6	2.50	20	6 6 0 0 0 0 0 0 0 0						4.000	5.000	1.722	-2.202	666	0.44	0.44
	40	ALL	5SB12		26	1/2	270	3.50	3.50	12	2.50	26	12 10 2 0 0 0 0 0 0 0						4.000	5.000	2.219	-2.798	821	0.44	0.44
24' Rdwy SB15 Beam	25	ALL	5SB15		8	1/2	270	5.00	5.00	0	2.50	8	0 0 0 0 0 0 0 0 0 0						4.000	5.000	0.727	-0.900	428	0.45	0.45
	30	ALL	5SB15		12	1/2	270	5.00	5.00	0	2.50	12	0 0 0 0 0 0 0 0 0 0						4.000	5.000	1.021	-1.246	556	0.45	0.45
	35	ALL	5SB15		14	1/2	270	5.00	5.00	0	2.50	14	0 0 0 0 0 0 0 0 0 0						4.000	5.000	1.362	-1.641	709	0.45	0.45
	40	ALL	5SB15		20	1/2	270	5.00	5.00	6	2.50	20	6 6 0 0 0 0 0 0 0 0						4.000	5.000	1.739	-2.070	865	0.44	0.44
	45	ALL	5SB15		26	1/2	270	5.00	5.00	12	2.50	26	12 8 4 0 0 0 0 0 0 0						4.000	5.000	2.186	-2.585	1062	0.44	0.44
	50	ALL	5SB15		36	1/2	270	4.56	4.20	16	2.50	28	16 10 2 4 0 0 0 0 0 0						4.000	5.000	2.686	-3.163	1284	0.44	0.44
28' Rdwy SB12 Beam	25	ALL	5SB12		10	1/2	270	3.50	3.50	0	2.50	10	0 0 0 0 0 0 0 0 0 0						4.000	5.000	0.905	-1.187	384	0.43	0.43
	30	ALL	5SB12		14	1/2	270	3.50	3.50	0	2.50	14	0 0 0 0 0 0 0 0 0 0						4.000	5.000	1.277	-1.642	510	0.43	0.43
	35	ALL	5SB12		18	1/2	270	3.50	3.50	4	2.50	18	4 4 0 0 0 0 0 0 0 0						4.000	5.000	1.709	-2.161	649	0.43	0.43
	40	ALL	5SB12		26	1/2	270	3.50	3.50	12	2.50	26	12 10 2 0 0 0 0 0 0 0						4.000	5.000	2.201	-2.745	800	0.43	0.43
28' Rdwy SB15 Beam	25	ALL	5SB15		8	1/2	270	5.00	5.00	0	2.50	8	0 0 0 0 0 0 0 0 0 0						4.000	5.000	0.717	-0.876	426	0.43	0.43
	30	ALL	5SB15		10	1/2	270	5.00	5.00	0	2.50	10	0 0 0 0 0 0 0 0 0 0						4.000	5.000	1.008	-1.214	534	0.43	0.43
	35	ALL	5SB15		14	1/2	270	5.00	5.00	0	2.50	14	0 0 0 0 0 0 0 0 0 0						4.000	5.000	1.344	-1.599	682	0.43	0.43
	40	ALL	5SB15		20	1/2	270	5.00	5.00	6	2.50	20	6 6 0 0 0 0 0 0 0 0						4.000	5.000	1.726	-2.033	843	0.43	0.43
	45	ALL	5SB15		26	1/2	270	5.00	5.00	12	2.50	26	12 8 4 0 0 0 0 0 0 0						4.000	5.000	2.156	-2.520	1021	0.42	0.42
	50	ALL	5SB15		34	1/2	270	4.65	4.33	16	2.50	28	16 10 4 2 0 0 0 0 0 0						4.000	5.000	2.649	-3.083	1235	0.42	0.42
30' Rdwy SB12 Beam	25	ALL	4SB12		8	1/2	270	3.50	3.50	0	2.50	8	0 0 0 0 0 0 0 0 0 0						4.000	5.000	0.906	-1.191	307	0.34	0.34
	30	ALL	4SB12		10	1/2	270	3.50	3.50	0	2.50	10	0 0 0 0 0 0 0 0 0 0						4.000	5.000	1.279	-1.648	408	0.34	0.34
	35	ALL	4SB12		16	1/2	270	3.50	3.50	4	2.50	16	4 4 0 0 0 0 0 0 0 0						4.000	5.000	1.712	-2.171	519	0.34	0.34
	40	ALL	4SB12		20	1/2	270	3.50	3.50	8	2.50	20	8 6 2 0 0 0 0 0 0 0						4.000	5.000	2.206	-2.760	641	0.34	0.34
30' Rdwy SB15 Beam	25	ALL	4SB15		6	1/2	270	5.00	5.00	0	2.50	6	0 0 0 0 0 0 0 0 0 0						4.000	5.000	0.725	-0.890	327	0.35	0.35
	30	ALL	4SB15		8	1/2	270	5.00	5.00	0	2.50	8	0 0 0 0 0 0 0 0 0 0						4.000	5.000	1.018	-1.233	435	0.35	0.35
	35	ALL	4SB15		12	1/2	270	5.00	5.00	2	2.50	12	2 2 0 0 0 0 0 0 0 0						4.000	5.000	1.347	-1.607	546	0.34	0.34
	40	ALL	4SB15		16	1/2	270	5.00	5.00	6	2.50	16	6 6 0 0 0 0 0 0 0 0						4.000	5.000	1.730	-2.044	675	0.34	0.34
	45	ALL	4SB15		22	1/2	270	5.00	5.00	12	2.50	22	12 8 2 0 0 0 0 0 0 0						4.000	5.000	2.174	-2.554	830	0.34	0.34
	50	ALL	4SB15		28	1/2	270	4.57	4.25	12	2.50	22	12 8 2 2 0 0 0 0 0 0						4.000	5.000	2.671	-3.125	1004	0.34	0.34

GENERAL NOTES:

Designed according to AASHTO LRFD Specifications.
All concrete shall be Class H. Provide Class H (HPC) if shown elsewhere in the plans. All reinforcing bars shall be Grade 60.

Beam designs are applicable for 5" concrete slabs without overlay and 0 through 30 degree skews.

When shown on this sheet, the Fabricator has the option of furnishing either the designed straight strand beam or an approved optional beam design. All optional design submittals shall be signed, sealed and dated by a registered Professional Engineer.

Prestress losses for the designed beams have been calculated for a relative humidity of 60 percent. Optional designs must likewise conform.

Strands for the designed beam shall be located as low as possible on the 2" grid system. Fill row "2.5" completely, then row "4.5".

Strands shall be placed within a row as follows:
1) Locate a strand in each "1" position.
2) Place strand pattern symmetrically about vertical centerline of slab beam.
3) Space strands as equally as possible across the entire width.

Strands in the position "1" shall not be debonded. Debonded strands shall be distributed equally about the vertical centerline. Debonded lengths shall decrease working inward, with debonding staggered in each row.

Debonded strands shall be encased in plastic tubing along entire debonded length, and ends of tubing shall be sealed with waterproof tape. Split plastic tubing may be used provided the seam of the tubing is sufficiently sealed with waterproof tape to prohibit grout infiltration. Wrapping of strands with tape to provide debonding will not be permitted.

Strands for the designed beam shall be low relaxation strands pretensioned to 75 percent of fpu each.

Full-length debonded strands are not permitted in strand positions 1 and 2. If debonding strands full-length, double wrap strands and internal vibrator diameter cannot exceed 1 1/4" each. Full-length debonding must comply with Item 426.4.F.4.

① Based on the following allowable stresses (ksi):
Compression = 0.65 f'ci
Tension = 0.24√f'ci
Optional designs must likewise conform.

② Portion of full HL93.

HL93 LOADING

Texas Department of Transportation
Bridge Division Standard

PRESTRESSED CONCRETE SLAB BEAM STD DESIGNS (TY SB12 OR SB15) 24', 28' & 30' ROADWAY

PSBSD

TxDOT 4SB12 SLAB BEAM   TxDOT 5SB12 SLAB BEAM   TxDOT 4SB15 SLAB BEAM   TxDOT 5SB15 SLAB BEAM

Box Beam Standard Design

STANDARD SBBS-B20-30	DESIGNED BEAMS (STRAIGHT STRANDS)																													OPTIONAL DESIGN				
				PRESTRESSING STRANDS						DEBONDED STRAND PATTERN PER ROW																CONCRETE							
	SPAN LENGTH	BEAM NO.	BEAM TYPE	NON-STD STRAND PATTERN	TOTAL NO.	SIZE	STRGTH f_{pu} (ksi)	"e" $\bar{c}$ (in)	"e" END (in)	TOT NO. DEB	DIST FROM BOTTOM (in)	NO. OF STRANDS		NUMBER OF STRANDS DEBONDED TO (ft from end)											RELEASE STRGTH ① f'_{ci} (ksi)	MINIMUM 28 DAY COMP STRGTH f'_c (ksi)	DESIGN LOAD COMP STRESS (TOP ⓒ) (SERVICE I) f_{ct} (ksi)	DESIGN LOAD TENSILE STRESS (BOT'L ⓒ) (SERVICE III) f_{cb} (ksi)	REQUIRED MINIMUM ULTIMATE MOMENT CAPACITY II (STRENGTH I) (ft-kips)	LIVE LOAD DISTRIBUTION FACTOR ②	
												TOTAL	DE-BONDED	3	6	9	12	15												Moment	Shear
30' Rdwy 5" Slab	30	1267	5B20		10	1/2	270	7.38	7.38	0	2.50	10	0	0	0	0	0	0	0	0	0	0	0	4.000	5.000	0.649	-0.819	687	0.440	0.790
	30	3-5	4B20		8	1/2	270	7.31	7.31	0	2.50	8	0	0	0	0	0	0	0	0	0	0	0	4.000	5.000	0.689	-0.854	550	0.370	0.570
	35	1267	5B20		10	1/2	270	7.38	7.38	0	2.50	10	0	0	0	0	0	0	0	0	0	0	0	4.000	5.000	0.856	-1.061	667	0.430	0.790
	35	3-5	4B20		8	1/2	270	7.31	7.31	0	2.50	8	0	0	0	0	0	0	0	0	0	0	0	4.000	5.000	0.907	-1.105	559	0.360	0.570
	40	1267	5B20		12	1/2	270	7.38	7.38	0	2.50	12	0	0	0	0	0	0	0	0	0	0	0	4.000	5.000	1.081	-1.316	797	0.410	0.800
	40	3-5	4B20		10	1/2	270	7.31	7.31	0	2.50	10	0	0	0	0	0	0	0	0	0	0	0	4.000	5.000	1.153	-1.382	680	0.350	0.580
	45	1267	5B20		14	1/2	270	7.38	7.38	0	2.50	14	0	0	0	0	0	0	0	0	0	0	0	4.000	5.000	1.348	-1.623	965	0.400	0.810
	45	3-5	4B20		12	1/2	270	7.31	7.31	0	2.50	12	0	0	0	0	0	0	0	0	0	0	0	4.000	5.000	1.435	-1.703	821	0.340	0.580
	50	1267	5B20		18	1/2	270	7.38	7.38	0	2.50	18	0	0	0	0	0	0	0	0	0	0	0	4.000	5.000	1.656	-1.984	1167	0.400	0.810
	50	3-5	4B20		16	1/2	270	7.31	7.31	0	2.50	16	0	0	0	0	0	0	0	0	0	0	0	4.000	5.000	1.749	-2.059	975	0.330	0.590
	55	1267	5B20		22	1/2	270	7.38	7.38	0	2.50	22	0	0	0	0	0	0	0	0	0	0	0	4.000	5.500	1.980	-2.352	1362	0.390	0.820
	55	3-5	4B20		20	1/2	270	7.31	7.31	0	2.50	20	0	0	0	0	0	0	0	0	0	0	0	4.000	5.500	2.089	-2.438	1136	0.320	0.600
	60	1267	5B20		28	1/2	270	7.38	7.38	6	2.50	28	6	6	0	0	0	0	0	0	0	0	0	4.000	6.000	2.328	-2.745	1565	0.380	0.830
	60	3-5	4B20		24	1/2	270	7.14	7.08	6	2.50	22	6	4	2	0	0	0	0	0	0	0	0	4.000	6.000	2.472	-2.871	1324	0.320	0.600
	65	1267	5B20		34	1/2	270	7.03	6.92	8	2.50	28	8	2	2	2	2	0	0	0	0	0	0	4.000	6.500	2.700	-3.160	1775	0.370	0.840
	65	3-5	4B20		30	1/2	270	6.64	6.40	8	2.50	22	8	2	2	2	2	0	0	0	0	0	0	4.250	6.750	2.864	-3.302	1498	0.310	0.610

GENERAL NOTES:
Designed according to AASHTO LRFD Specifications.
Use Class H concrete. Use Class H (HPC) if required elsewhere in plans. All reinforcing bars must be Grade 60.
When shown on this sheet, the Fabricator has the option of furnishing either the designed beam or an approved optional beam design. All optional design submittals and shop drawings must be signed, sealed and dated by a Professional Engineer registered in the State of Texas.
Prestress losses for the designed beams have been calculated for a relative humidity of 60 percent. Optional designs must likewise conform.
Locate strands for the designed beam as low as possible on the 2" grid system unless a Non-Standard Strand Pattern is indicated. Fill row "2.5", then row "4.5", then row "6.5", etc. Place strands within a row as follows:
   1) Locate a strand in each "1" position
   2) Place strand pattern symmetrically about vertical centerline of box
   3) Space strands as equally as possible across the entire width
Strands in the position "1" may not be debonded.
Distribute debonded strands equally about the vertical centerline. Decrease debonded lengths working inward, with debonding staggered in each row.
Encase debonded strands in plastic sheathing along entire debonded length, and seal ends of sheathing with waterproof tape. Split plastic sheathing may be used provided the seam of the sheathing is sufficiently sealed with waterproof tape to prohibit grout infiltration. Wrapping of strands with tape to provide debonding is not allowed.
Use low relaxation strands pretensioned to 75 percent of fpu.

① Based on the following allowable stresses (ksi):

Compression = 0.65 f'ci

Tension = 0.24√f'ci

Optional designs must likewise conform.

② Portion of full HL93.

③ Full-length debonded strands are only permitted in strand positions marked △. Double encase all full-length debonded strands. Internal vibrator diameter cannot exceed 1 ⅛" diameter for bottom flange concrete placement. Full-length debonding must comply with Item 426.4.F.4.
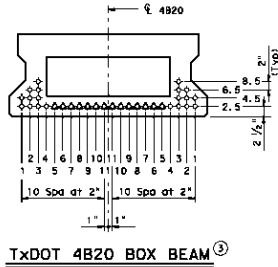
TxDOT 4B20 BOX BEAM ③
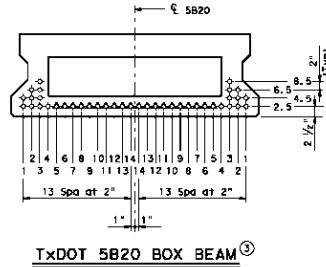
TxDOT 5B20 BOX BEAM ③

HL93 LOADING

Texas Department of Transportation
Bridge Division Standard

PRESTR CONC BOX BEAM
STANDARD DESIGNS
TYPE B20   30' RDWY
(WITH SLAB)

BBSDS-B20-30

FILE: bbstds39.dgn	DW: TxDOT	CK: TxDOT	DW: JTR	CW: TxDOT
©TxDOT December 2006	CONT	SECT	JOB	HIGHWAY
REVISIONS				
04-11: f'ci and LLDF.	DIST	COUNTY	SHEET NO.

Appendix C

Shop drawings Task 6 and Task 7

SLAB BEAM TYPE "4B20"
QUANTITY: 1

PLAN

SECTION

SECTION C
#3 BAR PLACED WITH MIDDLE STRAND

END MAT REINFORCING

STRAIGHT STRAND PATTERN

PART PLAN

ADDED BARS Z

STRAND

D1 BAR IN BETWEEN STRAND

REINFORCING STEEL SCHEDULE	
BARS	QTY./BM.
BAR A	65
BAR B	65
BAR C	71
BAR D	6
BAR M	18
BAR N	24
BAR U	70
BAR Z	58
BAR D1	2

FOAM SCHEDULE

WIDTH	HGHT	LNGTH	QTY.

CONCRETE SCHEDULE

LOCATION	# YDS.
BOTTOM	1.84
TOP	2.92
TOTAL	4.76

LO-LAX STRAND PATTERN

NUMBER OF STRANDS : 16 ~ 1/2"∅ 270k @ 31.0K EACH

NUMBER OF DEBONDED STRANDS : 0

CONCRETE RELEASE STRENGTH : 4,000 P.S.I.

CONCRETE 28-DAY STRENGTH : 5,000 P.S.I.

BEAM WEIGHT : 19,400 lbs.

PROJECT: UT ARLINGTON TEST BEAMS			DRAWN BY: HN
LOCATION: ARLINGTON, TX		**flexicore** CONCRETE SOLUTIONS SINCE 1953	CHECKED BY: GF
CONTRACTOR: REGINA WAWERU			DATE: 6/13/13
CONTROL NUMBER:	P.O. NUMBER: 2013C00912 —	P.O. BOX 450049 HOUSTON, TEXAS 77245 OFFICE: 888-359-4287 FAX: 281-437-8913 WEBSITE: www.flexicoreoftexas.com	FILE NAME: 4B20-1
PROJECT NUMBER:			JOB NUMBER: 13-082
ENGINEER:			PAGE: 1 of 2

4B20#1

252

PLAN

29'-9"

30'-0"

1'-4"

3'-11 3/4"

-11 7/8"

BARS D2
BOTH SIDES EQUAL
FROM CENTER LINE

2'-0"

SECTION

3'-7 3/4"

2'-5 3/4"

BAR D – 5 EQ. SP.
BAR D
BAR B
BAR A

2" CLR

BAR U
BAR C

3'-11 3/4"

END MAT REINFORCING

BAR M
BAR N

PART PLAN

BARS A & B
1'-2"   12 SPA. @ 4" – 4'-0"   8" MAX. SPA.
BARS U – 2¼"   2 ES ½"   12" MAX SPA.
BARS C – 2¼"   2 ES ½"   12 SPA. @ 4" – 4'-0"   6" MAX. SPA.

BAR U
BAR C
BAR A & B
BAR D

SECTION C
D2 BAR PLACEMENT

STRAND   D2 BAR
DO NOT TIE TO STRAND

1'-0" BLOCKOUT

BAR N – 2 1/4"
2 ES 8 1/4"
2 ES 8 1/4"

4~BAR N & 3~BAR M
4~BAR N & 3~BAR M
4~BAR N & 3~BAR M

BAR M

BAR N #4
BAR D2 #3
BAR D #3
BAR A & C #4
BAR U #5
BAR M #4

SLAB BEAM TYPE "4B20"
QUANTITY: 1

STRAIGHT STRAND PATTERN
• BONDED STRAND   ◦ DEBOND STRAND

REINFORCING STEEL SCHEDULE

BARS	QTY./BM.
BAR A	65
BAR B	65
BAR C	71
BAR D	6
BAR M	18
BAR N	24
BAR U	70
D2	15

FOAM SCHEDULE

WDTH	HGHT	LNGTH	QTY.
1'-6 3/4"	1 1/2"	27'-6"	1

CONCRETE SCHEDULE

LOCATION	# YDS.
BOTTOM	1.84
TOP	2.92
TOTAL	4.76

LO-LAX STRAND PATTERN

NUMBER OF STRANDS = 16 ~ 1/2"# 270k @ 31.0k EACH
NUMBER OF DEBONDED STRANDS : 0
CONCRETE RELEASE STRENGTH : 4,000 P.S.I.
CONCRETE 28-DAY STRENGTH : 5,000 P.S.I.
BEAM WEIGHT : 19,400 lbs.

4B20#2

PROJECT: **UT ARLINGTON TEST BEAMS**	DRAWN BY: HN
	CHECKED BY: GF
LOCATION: **ARLINGTON, TX**	DATE: 6/13/13
CONTRACTOR: **REGINA WAWERU**	FILE NAME: 4B20-2
CONTROL NUMBER:	P.O. NUMBER: 2013C00912	JOB NUMBER: 13-082
PROJECT NUMBER:		PAGE: 2 of 2
ENGINEER:		

flexicore
OF TEXAS
CONCRETE SOLUTIONS SINCE 1953

P.O. BOX 450049   HOUSTON, TEXAS 77245
OFFICE: 888-359-4287 FAX: 281-437-8913
WEBSITE: www.flexicoreoftexas.com

RESERVED FOR APPROVAL STAMP

⚠ LENGTHENED BAR D2

PLAN

30'-0"

3'-11 3/4"
1'-11 7/8"
3'-11 7/8"

2'-8" 2'-8"

▶C

▶C

D1 BARS

SECTION C

BAR D - 4 EQ. SP.

8"

2" CLR COV

1'-0"

1 1/2" CLR COV

BAR C (IN PAIRS)

3'-11 3/4"

END MAT REINFORCING

1'-4" 1'-3 3/4" 1'-4" BAR N

2'-0"

5 EQ. SPA. = 1'-8"

BAR M

BAR N

BAR M

BAR N

2 1/4"

BAR M

PART PLAN

BARS N

BARS C - 2 1/4"

MATCH BARS C AS SHOWN

5 EQ SPA = 1'-8"   3 EQ SPA = 1'-8"   9" MAX.

BAR H
BAR C
BAR N

BAR H - 4 3/4"   1'-0" MAX   BAR D

REINFORCING STEEL SCHEDULE

BARS	QTY./BM.
BAR C	98
BAR D	5
BAR D1	2
BAR H	62
BAR M	4
BAR N	24
BAR U	4

5'-0"   29'-9"

BAR D1 #3   BAR D #6

6"
1'-0"
BAR H #4

2'-9"
BAR C #4

2'-0"
BAR M #4   BAR U #5   BAR N #4

1'-10 1/2"

FOAM SCHEDULE

WDTH	HGHT	LNGTH	QTY.

CONCRETE SCHEDULE

LOCATION	# YDS.
BOTTOM	
TOP	
TOTAL	4.5

SLAB BEAM TYPE "4SB12"
QUANTITY: 1

BARS D1

1 2 3 4 5 6 7 8 9 10 11 11 10 9 8 7 6 5 4 3 2 1

3" 4 SP @ 2" 2 SP @ 5" 5" 2 SP @ 4 SP @ 3"
2" - 8" 4"-8"   2" 1D 2" 4"-8" 2"-8"

2 1/2"

14 -1/2"∅-270K
STRAND L-L 31.0K

LO-LAX STRAND PATTERN

NUMBER OF STRANDS : 14 ~ 1/2"∅ 270k @ 31.0K EACH
NUMBER OF DEBONDED STRANDS : 0
CONCRETE RELEASE STRENGTH : 4,000 P.S.I.
CONCRETE 28-DAY STRENGTH : 5,000 P.S.I.
BEAM WEIGHT : 18,200 lbs.

4SB120#1

PROJECT: UT ARLINGTON TEST BEAMS

LOCATION: ARLINGTON, TX

CONTRACTOR: REGINA WAWERU

CONTROL NUMBER:
PROJECT NUMBER:
ENGINEER:

P.O. NUMBER: 2013C00912 –

flexicore
OF TEXAS
CONCRETE SOLUTIONS SINCE 1953

P.O. BOX 450049   HOUSTON, TEXAS 77245
OFFICE: 888-350-4267 FAX: 281-437-8913
WEBSITE: www.flexicoreoftexas.com

DRAWN BY: HN
CHECKED BY: GF
DATE: 6/21/13
FILE NAME: 4SB12-2BAR
JOB NUMBER: 13-082
PAGE: 1 of 2

RESERVED FOR APPROVAL STAMP

PLAN

30'-0"
27'-4"
1'-4"
1'-11 7/8"
3'-11 3/4"
1'-11 7/8"
5'-0"
10'-0"
10'-0"
5'-0"
BAR D2 — 3 SPA. @ 3" = 9"
BAR F
▶A
▶A

SECTION

3'-7 3/4"
2'-5 3/4"
2"
5"
5"
2"
BAR D — 5 EQ. SP.
BAR A
BAR Z
BAR B
BAR U
BAR C
3'-11 3/4"
5 1/2"
2"
9 1/2"

END MAT REINFORCING

BAR M
BAR N
1'-0" BLOCKOUT
BAR N — 2 1/4"
2 ES 6 1/4"
4—BAR N & 3—BAR M
4—BAR N & 3—BAR M
4—BAR N & 3—BAR M
1 1/2"
BAR M

PART PLAN

BARS Z
1'-2"
24" MAX SPA.
BARS A & B
1'-2"
12 SPA. @ 4" = 4'-0"
6" MAX. SPA.
BARS U — 2 1/4"
2 ES 3 1/2"
12" MAX SPA.
BARS C — 2 1/4"
2 ES 3 1/2"
12 SPA. @ 4" = 4'-0"
6" MAX. SPA.
BAR U
BAR C
BAR A & B
BAR D

BAR N #4
5 1/2"
5 1/2"
10 1/4"
4 1/2"

29'-9"
BAR D2 #5

29'-9"
BAR D #5

BAR B #4
3'-4"

BAR F #4
1'-0"

BAR Z #4

4 3/8"
2 1/2"
1'-1 1/2"
BAR U #4

3'-0"
BAR A & C #4

2'-11"
BAR M #4

SLAB BEAM TYPE "4B20"
QUANTITY: 1

STRAIGHT STRAND PATTERN
● BONDED STRAND ○ DEBOND STRAND

SECTION A—A
D2 BAR PLACEMENT
BAR D2 — 3 SPA. @ 3" = 9"
STRAND
BAR F

REINFORCING STEEL SCHEDULE	
BARS	QTY./BM.
BAR A	81
BAR B	81
BAR C	86
BAR D	6
BAR M	18
BAR N	24
BAR U	70
BAR Z	30
BAR F	3
BAR D2	4

FOAM SCHEDULE			
WIDTH	HGHT	LNGTH	QTY.
2'-4 3/4"	9 1/2"	10'	3

CONCRETE SCHEDULE	
LOCATION	# YDS.
BOTTOM	1.85
TOP	2.95
TOTAL	4.80

LO-LAX STRAND PATTERN
NUMBER OF STRANDS : 16 ~ 1/2"∅ 270k @ 31.0K EACH
NUMBER OF DEBONDED STRANDS : 0
CONCRETE RELEASE STRENGTH : 4,000 P.S.I.
CONCRETE 28-DAY STRENGTH : 5,000 P.S.I.
BEAM WEIGHT : 19,440 lbs.

PROJECT: UT ARLINGTON TEST BOX BEAM 4B20-1
LOCATION: ARLINGTON, TEXAS
CONTRACTOR: REGINA WAWERU
CONTROL NUMBER:
PROJECT NUMBER:
ENGINEER:
P.O. NUMBER: 2014C0072B

4SB12#2, #3 and #4

flexicore
OF TEXAS
CONCRETE SOLUTIONS SINCE 1953
P.O. BOX 450049   HOUSTON, TEXAS 77245
OFFICE: 888-350-4287 FAX: 281-437-8913
WEBSITE: www.flexicoreoftexas.com

DRAWN BY: MAF
CHECKED BY: JDZ
DATE: 4/29/14
FILE NAME: 4B20-1
JOB NUMBER: 14-057
PAGE: 3 of 3

RESERVED FOR APPROVAL STAMP

Appendix D

PGSuper Analysis

Slab beam analysis 4SB12

Girder Details

TxDOT Girder Schedule	
Span	**1**
Girder	**E**
Girder Type	Slab 4SB12
Prestressing Strands	**Total**
NO. ($N_h + N_s$)	12
Size	0.500 in Dia.
Strength	Grade 270 Low Relaxation
Eccentricity @ CL	3.500 in
Eccentricity @ End	3.500 in
Prestressing Strands	**Debonded**
NO. (# of Debonded Strands)	0
Concrete	
Release Strength f'_{ci}	4.000 KSI
Minimum 28 day compressive strength f'_c	5.000 KSI
Optional Design	
Design Load Compressive Stress (Top CL)	1.313 KSI
Design Load Tensile Stress (Bottom CL)	-1.678 KSI
Required minimum ultimate moment capacity	416.04 kip-ft
Live Load Distribution Factor for Moment (Strength and Service Limit States)	0.34139
Live Load Distribution Factor for Shear (Strength and Service Limit States)	0.34139
Live Load Distribution Factor for Moment (Fatigue Limit States)	0.28449

Strand Layout

Moment Capacity

Location from Left Support (ft)	M_u (kip-ft)	ϕM_n (kip-ft)	ϕM_n Min (kip-ft)	Status	
				ϕM_n Min $\leq \phi M_n$ ($\phi M_n / \phi M_n$ Min)	$M_u \leq \phi M_n$ ($\phi M_n / M_u$)
(0.0L$_s$) 0.000	0.00	72.13	0.00	Pass (∞)	Pass (∞)
(FoS) 0.542	32.67	155.24	43.45	Pass (3.57)	Pass (4.75)
0.750	44.80	186.69	59.59	Pass (3.13)	Pass (4.17)
1.399	81.17	281.12	107.95	Pass (2.60)	Pass (3.46)
1.500	86.64	295.07	115.24	Pass (2.56)	Pass (3.41)
(CS) 1.682	96.35	318.98	128.15	Pass (2.49)	Pass (3.31)
(1.5H, PSXFR) 2.042	115.13	366.48	153.12	Pass (2.39)	Pass (3.18)
2.542	140.09	389.19	186.33	Pass (2.09)	Pass (2.78)
2.899	157.16	405.21	209.02	Pass (1.94)	Pass (2.58)
(0.1L$_s$) 2.908	157.60	405.63	209.61	Pass (1.94)	Pass (2.57)
5.542	266.05	519.20	353.84	Pass (1.47)	Pass (1.95)
(0.2L$_s$) 5.817	275.80	520.61	366.82	Pass (1.42)	Pass (1.89)
8.542	354.84	520.70	408.27	Pass (1.28)	Pass (1.47)
(0.3L$_s$) 8.725	359.01	520.71	407.49	Pass (1.28)	Pass (1.45)
11.542	404.84	520.77	398.60	Pass (1.31)	Pass (1.29)
(0.4L$_s$) 11.633	405.76	520.77	398.41	Pass (1.31)	Pass (1.28)
(0.5L$_s$) 14.542	416.04	520.79	395.38	Pass (1.32)	Pass (1.25)
(0.6L$_s$) 17.450	405.76	520.77	398.41	Pass (1.31)	Pass (1.28)
17.542	404.84	520.77	398.60	Pass (1.31)	Pass (1.29)
(0.7L$_s$) 20.358	359.01	520.71	407.49	Pass (1.28)	Pass (1.45)
20.542	354.84	520.70	408.27	Pass (1.28)	Pass (1.47)
(0.8L$_s$) 23.267	275.80	520.61	366.82	Pass (1.42)	Pass (1.89)
23.542	266.05	519.20	353.84	Pass (1.47)	Pass (1.95)

Location from Left Support (ft)	M_u (kip-ft)	ϕM_n (kip-ft)	ϕM_n Min (kip-ft)	ϕM_n Min $\leq \phi M_n$ ($\phi M_n/\phi M_n$ Min)	$M_u \leq \phi M_n$ ($\phi M_n/M_u$)
				Pass (1.94)	Pass (2.57)
26.184	157.16	405.21	209.02	Pass (1.94)	Pass (2.58)
26.542	140.09	389.19	186.33	Pass (2.09)	Pass (2.78)
(1.5H, PSXFR) 27.042	115.13	366.48	153.12	Pass (2.39)	Pass (3.18)
(CS) 27.402	96.34	318.95	128.13	Pass (2.49)	Pass (3.31)
(H) 27.542	88.89	300.58	118.22	Pass (2.54)	Pass (3.38)
27.583	86.64	295.07	115.24	Pass (2.56)	Pass (3.41)
27.684	81.17	281.12	107.95	Pass (2.60)	Pass (3.46)
28.333	44.80	186.69	59.59	Pass (3.13)	Pass (4.17)
(FoS) 28.542	32.67	155.24	43.45	Pass (3.57)	Pass (4.75)
(1.0L$_s$) 29.083	0.00	72.13	0.00	Pass (∞)	Pass (∞)

Shear

Location from Left Support (ft)	Stirrups Required	Stirrups Provided	$|V_u|$ (kip)	ϕV_n (kip)	Status ($\phi V_n/V_u$)
(CS) 1.682	No	Yes	55.99	300.84	Pass (5.37)
(1.5H, PSXFR) 2.042	No	Yes	54.80	301.71	Pass (5.51)
2.542	No	Yes	53.16	299.33	Pass (5.63)
2.899	No	Yes	51.98	267.81	Pass (5.15)
(0.1L$_s$) 2.908	No	Yes	51.95	267.75	Pass (5.15)
5.542	No	Yes	43.84	253.75	Pass (5.79)
(0.2L$_s$) 5.817	No	Yes	43.05	253.26	Pass (5.88)
8.542	No	Yes	35.28	248.41	Pass (7.04)
(0.3L$_s$) 8.725	No	Yes	34.76	248.17	Pass (7.14)
11.542	No	Yes	26.84	191.87	Pass (7.15)
(0.4L$_s$) 11.633	No	Yes	26.59	190.95	Pass (7.18)

Shear-Continued

Location from Left Support (ft)	Stirrups Required	Stirrups Provided	$|V_u|$ (kip)	ϕV_n (kip)	Status ($\phi V_n/V_u$)
($0.5L_s$) 14.542	No	Yes	18.52	188.83	Pass (10+)
($0.6L_s$) 17.450	No	Yes	26.59	190.95	Pass (7.18)
17.542	No	Yes	26.84	191.87	Pass (7.15)
($0.7L_s$) 20.358	No	Yes	34.76	248.17	Pass (7.14)
20.542	No	Yes	35.28	248.41	Pass (7.04)
($0.8L_s$) 23.267	No	Yes	43.05	253.26	Pass (5.88)
23.542	No	Yes	43.84	253.75	Pass (5.79)
($0.9L_s$) 26.175	No	Yes	51.95	267.75	Pass (5.15)
26.184	No	Yes	51.98	267.81	Pass (5.15)
26.542	No	Yes	53.16	299.33	Pass (5.63)
(1.5H, PSXFR) 27.042	No	Yes	54.80	301.71	Pass (5.51)
(CS) 27.402	No	Yes	55.99	300.84	Pass (5.37)

Horizontal Interface Shears/Length for Strength I Limit State [5.8.4]

Location from Left Support (ft)	5.8.4.2			5.8.4.4			5.8.4.1		
	s (in)	s_{max} (in)	Status	a_{vf} (in^2/ft)	$a_{vf\ min}$ (in^2/ft)	Status	$|v_{ui}|$ (kip/ft)	ϕv_{ni} (kip/ft)	Status ($\phi v_{ni}/|v_{ui}|$)
(CS) 1.682	12	24	Pass	0.8	0	Pass	49.24	187.78	Pass (3.81)
(1.5H, PSXFR) 2.042	12	24	Pass	0.8	0	Pass	48.19	187.78	Pass (3.9)
2.542	12	24	Pass	0.8	0	Pass	46.74	187.78	Pass (4.02)
2.899	12	24	Pass	0.8	0	Pass	45.71	187.78	Pass (4.11)
($0.1L_s$) 2.908	12	24	Pass	0.8	0	Pass	45.68	187.78	Pass (4.11)
5.542	12	24	Pass	0.8	0	Pass	38.55	187.78	Pass (4.87)

Location from Left Support (ft)	5.8.4.2			5.8.4.4			5.8.4.1		
	(in)	(in)		a_{vf} (in^2/ft)	$a_{vf\ min}$ (in^2/ft)	Status	$\|v_{ui}\|$ (kip/ft)	ϕv_{ni} (kip/ft)	Status ($\phi v_{ni}/\|v_{ui}\|$)
(0.2L$_s$) 5.817	12	24	Pass	0.8	0	Pass	37.85	187.78	Pass (4.96)
8.542	12	24	Pass	0.8	0	Pass	31.02	187.78	Pass (6.05)
(0.3L$_s$) 8.725	12	24	Pass	0.8	0	Pass	30.57	187.78	Pass (6.14)
11.542	12	24	Pass	0.8	0	Pass	23.60	187.78	Pass (7.96)
(0.4L$_s$) 11.633	12	24	Pass	0.8	0	Pass	23.38	187.78	Pass (8.03)
(0.5L$_s$) 14.542	12	24	Pass	0.8	0	Pass	16.29	187.78	Pass (10+)
(0.6L$_s$) 17.450	12	24	Pass	0.8	0	Pass	23.38	187.78	Pass (8.03)
17.542	12	24	Pass	0.8	0	Pass	23.60	187.78	Pass (7.96)
(0.7L$_s$) 20.358	12	24	Pass	0.8	0	Pass	30.57	187.78	Pass (6.14)
20.542	12	24	Pass	0.8	0	Pass	31.02	187.78	Pass (6.05)
(0.8L$_s$) 23.267	12	24	Pass	0.8	0	Pass	37.85	187.78	Pass (4.96)
23.542	12	24	Pass	0.8	0	Pass	38.55	187.78	Pass (4.87)
(0.9L$_s$) 26.175	12	24	Pass	0.8	0	Pass	45.68	187.78	Pass (4.11)
26.184	12	24	Pass	0.8	0	Pass	45.71	187.78	Pass (4.11)
26.542	12	24	Pass	0.8	0	Pass	46.74	187.78	Pass (4.02)
(1.5H, PSXFR) 27.042	12	24	Pass	0.8	0	Pass	48.19	187.78	Pass (3.9)
(CS) 27.402	12	24	Pass	0.8	0	Pass	49.24	187.78	Pass (3.81)

4B20#1

TxDOT Girder Schedule	
Span	**1**
Girder	**A**
Girder Type	Box 4B20
Prestressing Strands	**Total**
NO. ($N_h + N_s$)	16
Size	0.500 in Dia.
Strength	Grade 270 Low Relaxation
Eccentricity @ CL	7.305 in
Eccentricity @ End	7.305 in
Prestressing Strands	**Debonded**
NO. (# of Debonded Strands)	0
Concrete	
Release Strength f'_{ci}	4.000 KSI
Minimum 28 day compressive strength f'_c	5.000 KSI
Optional Design	
Design Load Compressive Stress (Top CL)	0.696 KSI
Design Load Tensile Stress (Bottom CL)	-0.863 KSI
Required minimum ultimate moment capacity	602.26 kip-ft
Live Load Distribution Factor for Moment (Strength and Service Limit States)	0.36427
Live Load Distribution Factor for Shear (Strength and Service Limit States)	0.61951
Live Load Distribution Factor for Moment (Fatigue Limit States)	0.30356

Strand Layout

Moment Capacity

Location from Left Support (ft)	M_u (kip-ft)	ϕM_n (kip-ft)	ϕM_n Min (kip-ft)	Status	
				ϕM_n Min $\leq \phi M_n$ ($\phi M_n/\phi M_n$ Min)	$M_u \leq \phi M_n$ ($\phi M_n/M_u$)
(0.0L$_s$) 0.000	0.00	749.03	0.00	Pass (∞)	Pass (∞)
(FoS) 0.542	35.51	781.86	47.23	Pass (10+)	Pass (10+)
1.208	76.85	821.85	102.21	Pass (8.04)	Pass (10+)
1.250	79.35	824.33	105.54	Pass (7.81)	Pass (10+)
(H) 2.208	134.37	880.98	178.71	Pass (4.93)	Pass (6.56)
(CS) 2.289	138.77	885.70	184.56	Pass (4.80)	Pass (6.38)
2.500	150.11	898.04	199.65	Pass (4.50)	Pass (5.98)
2.542	152.32	900.47	202.59	Pass (4.44)	Pass (5.91)
(0.1L$_s$) 2.908	171.37	921.79	227.92	Pass (4.04)	Pass (5.38)
(1.5H) 3.042	178.11	929.52	236.88	Pass (3.92)	Pass (5.22)
4.712	255.20	1024.90	339.42	Pass (3.02)	Pass (4.02)
5.542	289.37	1071.37	384.86	Pass (2.78)	Pass (3.70)
(0.2L$_s$) 5.817	299.98	1086.65	398.98	Pass (2.72)	Pass (3.62)
8.542	386.01	1093.04	513.40	Pass (2.13)	Pass (2.83)
(0.3L$_s$) 8.725	390.55	1093.04	519.43	Pass (2.10)	Pass (2.80)
11.542	440.50	1093.10	585.86	Pass (1.87)	Pass (2.48)
(0.4L$_s$) 11.633	441.50	1093.10	587.19	Pass (1.86)	Pass (2.48)
(0.5L$_s$) 14.542	452.83	1093.12	602.26	Pass (1.82)	Pass (2.41)
(0.6L$_s$) 17.450	441.50	1093.10	587.19	Pass (1.86)	Pass (2.48)
17.542	440.50	1093.10	585.86	Pass (1.87)	Pass (2.48)
(0.7L$_s$) 20.358	390.55	1093.04	519.43	Pass (2.10)	Pass (2.80)
20.542	386.01	1093.04	513.40	Pass (2.13)	Pass (2.83)
(0.8L$_s$) 23.267	299.98	1086.65	398.98	Pass (2.72)	Pass (3.62)

Location from Left Support (ft)	M_u (kip-ft)	ϕM_n (kip-ft)	ϕM_n Min (kip-ft)	ϕM_n Min $\leq \phi M_n$ ($\phi M_n/\phi M_n$ Min)	$M_u \leq \phi M_n$ ($\phi M_n/M_u$)
				Pass (2.78)	Pass (3.70)
24.371	255.20	1024.90	339.42	Pass (3.02)	Pass (4.02)
(1.5H) 26.042	178.11	929.52	236.88	Pass (3.92)	Pass (5.22)
($0.9L_s$) 26.175	171.37	921.79	227.92	Pass (4.04)	Pass (5.38)
26.542	152.32	900.47	202.59	Pass (4.44)	Pass (5.91)
26.583	150.11	898.04	199.65	Pass (4.50)	Pass (5.98)
(CS) 26.794	138.77	885.70	184.56	Pass (4.80)	Pass (6.38)
(H) 26.875	134.37	880.98	178.71	Pass (4.93)	Pass (6.56)
27.833	79.35	824.33	105.54	Pass (7.81)	Pass (10+)
27.875	76.85	821.85	102.21	Pass (8.04)	Pass (10+)
(FoS) 28.542	35.51	781.86	47.23	Pass (10+)	Pass (10+)
($1.0L_s$) 29.083	0.00	749.03	0.00	Pass (∞)	Pass (∞)

Shear

Location from Left Support (ft)	Stirrups Required	Stirrups Provided	$|V_u|$ (kip)	ϕV_n (kip)	Status ($\phi V_n/V_u$)
(CS) 2.289	Yes	Yes	88.04	235.88	Pass (2.68)
2.542	Yes	Yes	86.74	235.56	Pass (2.72)
($0.1L_s$) 2.908	Yes	Yes	84.84	235.09	Pass (2.77)
(1.5H) 3.042	Yes	Yes	84.16	234.91	Pass (2.79)
4.712	Yes	Yes	75.92	208.35	Pass (2.74)
5.542	Yes	Yes	72.26	206.97	Pass (2.86)
($0.2L_s$) 5.817	Yes	Yes	71.05	206.52	Pass (2.91)
8.542	Yes	Yes	59.16	204.74	Pass (3.46)
($0.3L_s$) 8.725	Yes	Yes	58.37	204.66	Pass (3.51)

Location from Left Support (ft)	Stirrups Required	Stirrups Provided	$\|V_u\|$ (kip)	ϕV_n (kip)	Status ($\phi V_n/V_u$)
11.542	Yes	Yes	46.28	203.90	Pass (4.41)
(0.4L$_s$) 11.633	Yes	Yes	45.89	203.89	Pass (4.44)
(0.5L$_s$) 14.542	No	Yes	33.61	204.14	Pass (6.07)
(0.6L$_s$) 17.450	Yes	Yes	45.89	203.89	Pass (4.44)
17.542	Yes	Yes	46.28	203.90	Pass (4.41)
(0.7L$_s$) 20.358	Yes	Yes	58.37	204.66	Pass (3.51)
20.542	Yes	Yes	59.16	204.74	Pass (3.46)
(0.8L$_s$) 23.267	Yes	Yes	71.05	206.52	Pass (2.91)
23.542	Yes	Yes	72.26	206.97	Pass (2.86)
24.371	Yes	Yes	75.92	208.35	Pass (2.74)
(1.5H) 26.042	Yes	Yes	84.16	234.91	Pass (2.79)
(0.9L$_s$) 26.175	Yes	Yes	84.84	235.09	Pass (2.77)
26.542	Yes	Yes	86.74	235.56	Pass (2.72)
(CS) 26.794	Yes	Yes	88.04	235.88	Pass (2.68)

Horizontal Interface Shears/Length for Strength I Limit State [5.8.4]

Location from Left Support (ft)	5.8.4.2			5.8.4.4			5.8.4.1		
	s (in)	s_{max} (in)	Status	a_{vf} (in^2/ft)	$a_{vf\,min}$ (in^2/ft)	Status	$|v_{ui}|$ (kip/ft)	ϕv_{ni} (kip/ft)	Status ($\phi v_{ni}/|v_{ui}|$)
(CS) 2.289	12	24	Pass	0.8	0	Pass	40.12	175.58	Pass (4.38)
2.542	12	24	Pass	0.8	0	Pass	39.53	175.58	Pass (4.44)
(0.1L$_s$) 2.908	12	24	Pass	0.8	0	Pass	38.66	175.58	Pass (4.54)
(1.5H) 3.042	12	24	Pass	0.8	0	Pass	38.35	175.58	Pass (4.58)
4.712	12	24	Pass	0.8	0	Pass	34.60	175.58	Pass (5.08)
5.542	12	24	Pass	0.8	0	Pass	32.93	175.58	Pass (5.33)
(0.2L$_s$) 5.817	12	24	Pass	0.8	0	Pass	32.38	175.58	Pass (5.42)
8.542	12	24	Pass	0.8	0	Pass	26.96	175.58	Pass (6.51)
(0.3L$_s$) 8.725	12	24	Pass	0.8	0	Pass	26.60	175.58	Pass (6.6)
11.542	12	24	Pass	0.8	0	Pass	21.09	175.58	Pass (8.33)
(0.4L$_s$) 11.633	12	24	Pass	0.8	0	Pass	20.91	175.58	Pass (8.4)
(0.5L$_s$) 14.542	12	24	Pass	0.8	0	Pass	15.32	175.58	Pass (10+)
(0.6L$_s$) 17.450	12	24	Pass	0.8	0	Pass	20.91	175.58	Pass (8.4)
17.542	12	24	Pass	0.8	0	Pass	21.09	175.58	Pass (8.33)
(0.7L$_s$) 20.358	12	24	Pass	0.8	0	Pass	26.60	175.58	Pass (6.6)
20.542	12	24	Pass	0.8	0	Pass	26.96	175.58	Pass (6.51)
(0.8L$_s$) 23.267	12	24	Pass	0.8	0	Pass	32.38	175.58	Pass (5.42)
23.542	12	24	Pass	0.8	0	Pass	32.93	175.58	Pass (5.33)
24.371	12	24	Pass	0.8	0	Pass	34.60	175.58	Pass (5.08)
(1.5H) 26.042	12	24	Pass	0.8	0	Pass	38.35	175.58	Pass (4.58)
(0.9L$_s$) 26.175	12	24	Pass	0.8	0	Pass	38.66	175.58	Pass (4.54)
26.542	12	24	Pass	0.8	0	Pass	39.53	175.58	Pass (4.44)
(CS) 26.794	12	24	Pass	0.8	0	Pass	40.12	175.58	Pass (4.38)

4B20#3 and #4

TxDOT Girder Schedule	
Span	**1**
Girder	**A**
Girder Type	Box 4B20
Prestressing Strands	**Total**
NO. ($N_h + N_s$)	16
Size	0.500 in Dia.
Strength	Grade 270 Low Relaxation
Eccentricity @ CL	7.305 in
Eccentricity @ End	7.305 in
Prestressing Strands	**Debonded**
NO. (# of Debonded Strands)	0
Concrete	
Release Strength f'_{ci}	4.000 KSI
Minimum 28 day compressive strength f'_c	5.000 KSI
Optional Design	
Design Load Compressive Stress (Top CL)	0.947 KSI
Design Load Tensile Stress (Bottom CL)	-1.266 KSI
Required minimum ultimate moment capacity	889.02 kip-ft
Live Load Distribution Factor for Moment (Strength and Service Limit States)	0.36427
Live Load Distribution Factor for Shear (Strength and Service Limit States)	0.61951
Live Load Distribution Factor for Moment (Fatigue Limit States)	0.30356

Strand Layout

267

Moment Capacity

Location from Left Support (ft)	M_u (kip-ft)	ϕM_n (kip-ft)	ϕM_n Min (kip-ft)	Status	
				ϕM_n Min $\leq \phi M_n$ ($\phi M_n / \phi M_n$ Min)	$M_u \leq \phi M_n$ ($\phi M_n / M_u$)
(0.0L_s) 0.000	0.00	139.28	0.00	Pass	Pass
(FoS) 0.542	82.49	300.42	109.72	Pass (2.74)	Pass (3.64)
1.208	183.48	493.71	244.03	Pass (2.02)	Pass (2.69)
1.250	189.77	505.45	252.39	Pass (2.00)	Pass (2.66)
(PSXFR) 2.042	308.86	721.61	410.78	Pass (1.76)	Pass (2.34)
(H) 2.208	333.82	738.36	443.98	Pass (1.66)	Pass (2.21)
(CS) 2.308	348.67	748.29	463.73	Pass (1.61)	Pass (2.15)
2.500	377.41	767.47	501.96	Pass (1.53)	Pass (2.03)
2.542	383.63	771.61	510.23	Pass (1.51)	Pass (2.01)
(0.1L_s) 2.908	438.25	807.81	582.87	Pass (1.39)	Pass (1.84)
(1.5H) 3.042	458.06	820.88	609.22	Pass (1.35)	Pass (1.79)
5.542	825.13	1057.49	898.66	Pass (1.18)	Pass (1.28)
(0.2L_s) 5.817	864.99	1082.61	898.08	Pass (1.21)	Pass (1.25)
7.000	1035.32	1092.98	895.79	Pass (1.22)	Pass (1.06)
7.045	1033.89	1092.99	895.71	Pass (1.22)	Pass (1.06)
8.542	984.59	1093.04	893.31	Pass (1.22)	Pass (1.11)
8.712	978.80	1093.04	893.07	Pass (1.22)	Pass (1.12)
(0.3L_s) 8.725	978.34	1093.04	893.05	Pass (1.22)	Pass (1.12)
11.542	876.60	1093.10	890.09	Pass (1.23)	Pass (1.25)
(0.4L_s) 11.633	873.10	1093.10	890.03	Pass (1.23)	Pass (1.25)
11.712	870.11	1093.11	889.98	Pass (1.23)	Pass (1.26)
(0.5L_s) 14.542	756.36	1093.12	889.02	Pass (1.23)	Pass (1.45)
17.372	631.71	1093.11	840.17	Pass (1.30)	Pass (1.73)

Location from Left Support (ft)	M_u (kip-ft)	ϕM_n (kip-ft)	ϕM_n Min (kip-ft)	ϕM_n Min $\leq \phi M_n$ ($\phi M_n/\phi M_n$ Min)	$M_u \leq \phi M_n$ ($\phi M_n/M_u$)
				Pass (1.31)	Pass (1.74)
17.542	623.88	1093.10	829.75	Pass (1.32)	Pass (1.75)
(0.7L$_s$) 20.358	488.34	1093.04	649.49	Pass (1.68)	Pass (2.24)
20.372	487.67	1093.04	648.61	Pass (1.69)	Pass (2.24)
20.542	479.15	1093.04	637.26	Pass (1.72)	Pass (2.28)
22.038	402.36	1092.99	535.14	Pass (2.04)	Pass (2.72)
(0.8L$_s$) 23.267	337.07	1082.61	448.30	Pass (2.41)	Pass (3.21)
23.542	322.17	1057.49	428.49	Pass (2.47)	Pass (3.28)
(1.5H) 26.042	182.00	820.88	242.07	Pass (3.39)	Pass (4.51)
(0.9L$_s$) 26.175	174.29	807.81	231.80	Pass (3.48)	Pass (4.63)
26.542	152.95	771.61	203.42	Pass (3.79)	Pass (5.04)
26.583	150.51	767.47	200.18	Pass (3.83)	Pass (5.10)
(CS) 26.776	139.23	748.29	185.18	Pass (4.04)	Pass (5.37)
(H) 26.875	133.39	738.36	177.41	Pass (4.16)	Pass (5.54)
(PSXFR) 27.042	123.56	721.61	164.33	Pass (4.39)	Pass (5.84)
27.833	76.32	505.45	101.51	Pass (4.98)	Pass (6.62)
27.875	73.81	493.71	98.17	Pass (5.03)	Pass (6.69)
(FoS) 28.542	33.33	300.42	44.33	Pass (6.78)	Pass (9.01)
(1.0L$_s$) 29.083	0.00	139.28	0.00	Pass	Pass

Shear

Location from Left Support (ft)	Stirrups Required	Stirrups Provided	$|V_u|$ (kip)	ϕV_n (kip)	Status ($\phi V_n/V_u$)
(CS) 2.308	Yes	Yes	149.53	238.41	Pass (1.59)
2.542	Yes	Yes	149.21	238.04	Pass (1.60)
(0.1L$_s$) 2.908	Yes	Yes	148.71	237.41	Pass (1.60)
(1.5H) 3.042	Yes	Yes	148.53	237.18	Pass (1.60)
5.542	Yes	Yes	145.13	231.84	Pass (1.60)
(0.2L$_s$) 5.817	Yes	Yes	144.75	220.75	Pass (1.53)
7.000	Yes	Yes	143.14	182.91	Pass (1.28)
7.045	Yes	Yes	34.95	176.08	Pass (5.04)
8.542	Yes	Yes	36.38	187.18	Pass (5.14)
8.712	Yes	Yes	36.54	135.15	Pass (3.70)
(0.3L$_s$) 8.725	Yes	Yes	36.56	135.24	Pass (3.70)
11.542	Yes	Yes	39.25	158.29	Pass (4.03)
(0.4L$_s$) 11.633	Yes	Yes	39.34	159.26	Pass (4.05)
11.712	Yes	Yes	39.41	120.11	Pass (3.05)
(0.5L$_s$) 14.542	Yes	Yes	42.12	151.94	Pass (3.61)
17.372	Yes	Yes	45.97	154.43	Pass (3.36)
(0.6L$_s$) 17.450	Yes	Yes	46.08	199.26	Pass (4.32)
17.542	Yes	Yes	46.20	199.35	Pass (4.31)
(0.7L$_s$) 20.358	Yes	Yes	50.03	202.52	Pass (4.05)
20.372	Yes	Yes	50.05	202.53	Pass (4.05)
20.542	Yes	Yes	50.28	230.94	Pass (4.59)
22.038	Yes	Yes	52.32	230.95	Pass (4.41)
(0.8L$_s$) 23.267	Yes	Yes	53.99	231.21	Pass (4.28)
23.542	Yes	Yes	54.37	231.84	Pass (4.26)

Location from Left Support (ft)	Stirrups Required	Stirrups Provided	$|V_u|$ (kip)	ϕV_n (kip)	Status ($\phi V_n/V_u$)
(1.5H) 26.042	Yes	Yes	57.77	237.18	Pass (4.11)
(0.9L$_s$) 26.175	Yes	Yes	57.95	237.41	Pass (4.10)
26.542	Yes	Yes	58.45	238.04	Pass (4.07)
(CS) 26.776	Yes	Yes	58.77	238.41	Pass (4.06)

Horizontal Interface Shears/Length for Strength I Limit State [5.8.4]

Location from Left Support (ft)	5.8.4.2			5.8.4.4			5.8.4.1		
	s (in)	s$_{max}$ (in)	Status	a$_{vf}$ (in²/ft)	a$_{vf\,min}$ (in²/ft)	Status	$|v_{ui}|$ (kip/ft)	ϕv_{ni} (kip/ft)	Status ($\phi v_{ni}/|v_{ui}|$)
(CS) 2.308	24	24	Pass	0.4	0	Pass	68.14	153.98	Pass (2.26)
2.542	24	24	Pass	0.4	0	Pass	68.00	153.98	Pass (2.26)
(0.1L$_s$) 2.908	24	24	Pass	0.4	0	Pass	67.77	153.98	Pass (2.27)
(1.5H) 3.042	24	24	Pass	0.4	0	Pass	67.69	153.98	Pass (2.27)
5.542	24	24	Pass	0.4	0	Pass	66.14	153.98	Pass (2.33)
(0.2L$_s$) 5.817	24	24	Pass	0.4	0	Pass	65.97	153.98	Pass (2.33)
7	24	24	Pass	0.4	0	Pass	65.23	153.98	Pass (2.36)
7.045	24	24	Pass	0.4	0	Pass	15.93	153.98	Pass (9.67)
8.542	24	24	Pass	0.4	0	Pass	16.58	153.98	Pass (9.29)
8.712	24	24	Pass	0.4	0	Pass	16.65	153.98	Pass (9.25)
(0.3L$_s$) 8.725	24	24	Pass	0.4	0	Pass	16.66	153.98	Pass (9.24)
11.542	24	24	Pass	0.4	0	Pass	17.89	153.98	Pass (8.61)
(0.4L$_s$) 11.633	24	24	Pass	0.4	0	Pass	17.93	153.98	Pass (8.59)
11.712	24	24	Pass	0.4	0	Pass	17.96	153.98	Pass (8.57)
(0.5L$_s$) 14.542	24	24	Pass	0.4	0	Pass	19.20	153.98	Pass (8.02)
17.372	24	24	Pass	0.4	0	Pass	20.95	153.98	Pass (7.35)
(0.6L$_s$) 17.450	24	24	Pass	0.4	0	Pass	21.00	153.98	Pass (7.33)

Location from Left Support (ft)	5.8.4.2			5.8.4.4			5.8.4.1		
	s (in)	s_{max} (in)	Status	a_{vf} (in^2/ft)	$a_{vf\ min}$ (in^2/ft)	Status	$\lvert v_{ui}\rvert$ (kip/ft)	ϕv_{ni} (kip/ft)	Status ($\phi v_{ni}/\lvert v_{ui}\rvert$)
17.542	24	24	Pass	0.4	0	Pass	21.06	153.98	Pass (7.31)
(0.7L$_s$) 20.358	24	24	Pass	0.4	0	Pass	22.80	153.98	Pass (6.75)
20.372	24	24	Pass	0.4	0	Pass	22.81	153.98	Pass (6.75)
20.542	24	24	Pass	0.4	0	Pass	22.92	153.98	Pass (6.72)
22.038	24	24	Pass	0.4	0	Pass	23.84	153.98	Pass (6.46)
(0.8L$_s$) 23.267	24	24	Pass	0.4	0	Pass	24.61	153.98	Pass (6.26)
23.542	24	24	Pass	0.4	0	Pass	24.78	153.98	Pass (6.22)
(1.5H) 26.042	24	24	Pass	0.4	0	Pass	26.33	153.98	Pass (5.85)
(0.9L$_s$) 26.175	24	24	Pass	0.4	0	Pass	26.41	153.98	Pass (5.83)
26.542	24	24	Pass	0.4	0	Pass	26.64	153.98	Pass (5.78)
(CS) 26.776	24	24	Pass	0.4	0	Pass	26.78	153.98	Pass (5.75)

Appendix E

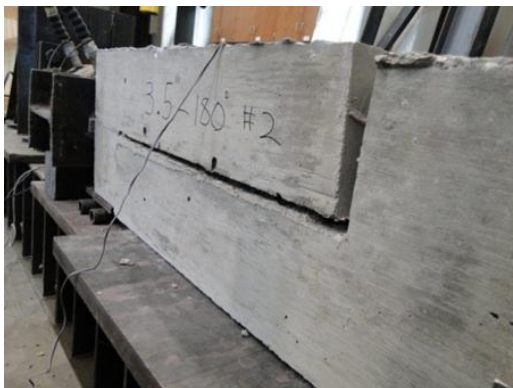Task 4-Push-off Test

Specimen 3.5"-180° #1

Precast failure plane
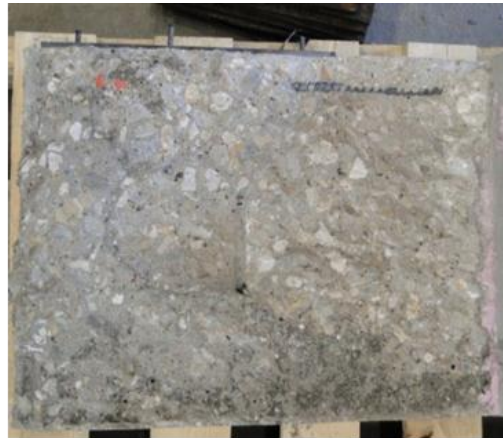
CIP slab failure plane

Specimen 3.5"-180° #2

Precast failure plane

CIP slab failure plane

Specimen 3.5"-180° #3

Precast failure plane

CIP slab failure plane
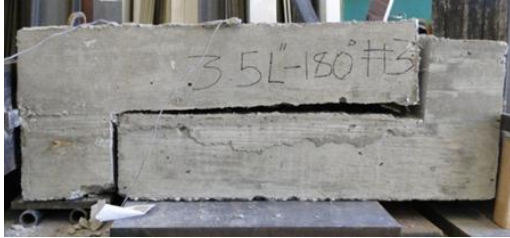
Specimen 3.5"L-180° #1

Precast failure plane

CIP slab failure plane

Specimen 3.5"L-180° #2

Specimen 3.5"L-180° #3

Precast failure plane   CIP slab failure plane

Specimen 6"-90° #1

Precast failure plane

CIP slab failure plane

Specimen 6"-90° #2

Precast failure plane

CIP slab failure plane
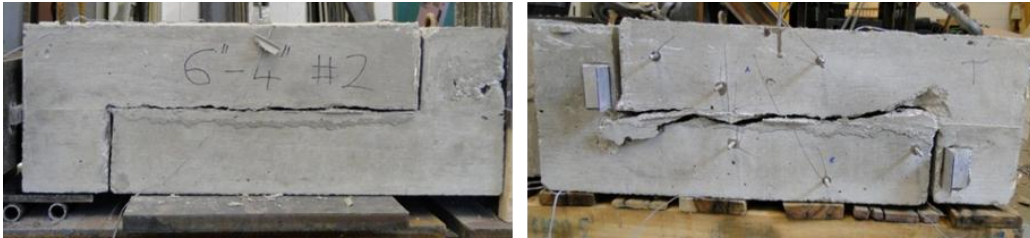
Specimen 6"-90° #3

Precast failure plane

CIP slab failure plane

Specimen 6"-4"-90° #1

Specimen 6"-4"-90° #2

Specimen 6"-4"-90° #3

Specimen 9"-90° #1

Precast failure plane

CIP slab failure plane

Specimen 9"-90° #2

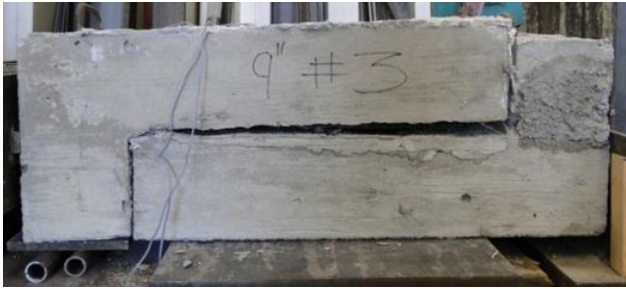Precast failure plane

CIP slab failure plane

Specimen 9"-90° #3

Precast failure plane   CIP slab failure plane

Specimen 9"-4"-90° #1

Specimen 9"-4"-90° #2

Specimen 9"-4"-90° #3

Appendix F

Task 5-Pullout Test

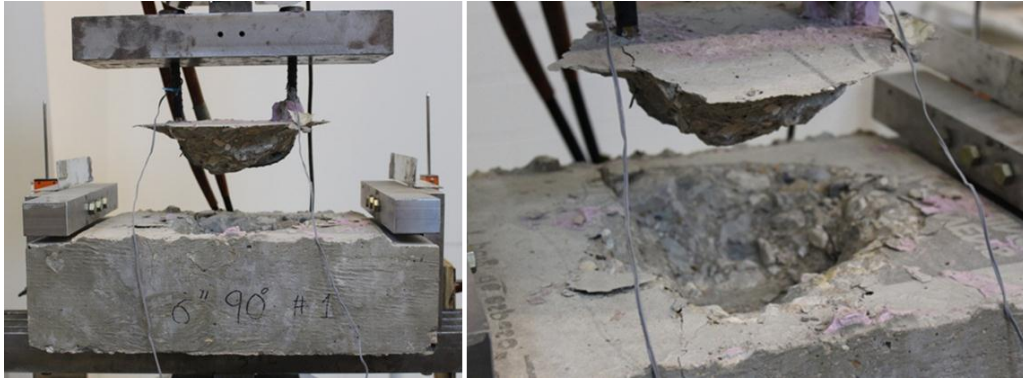## 3.5-in. 180° bend
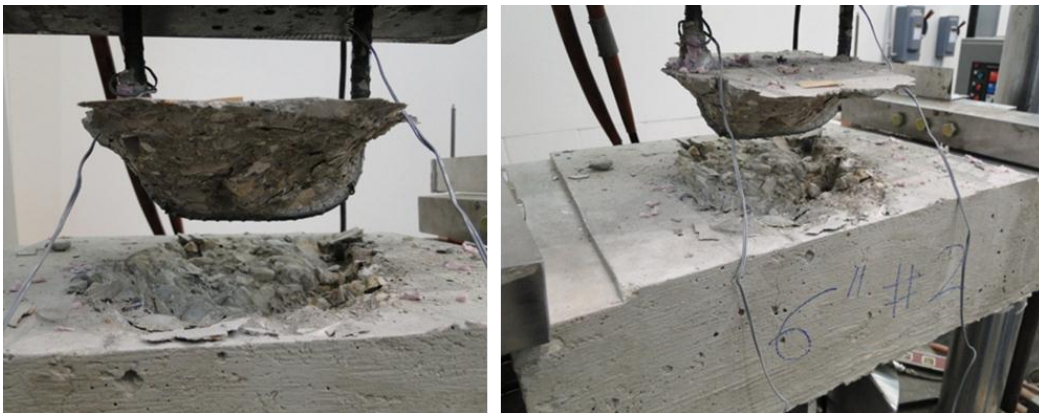
1

#2

#3
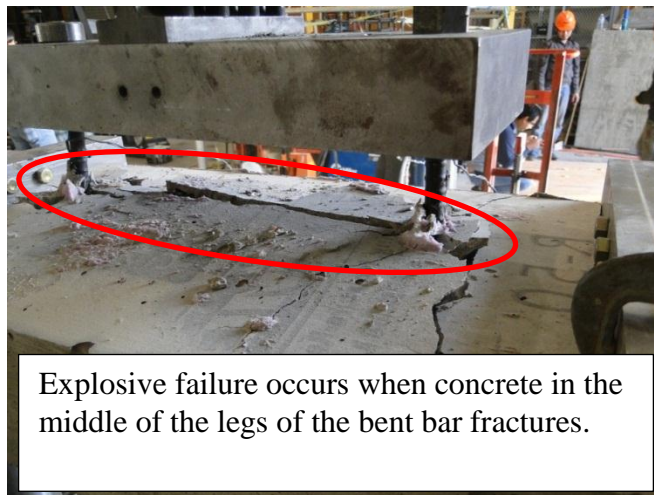
3.5-in. 90° bend

#1

#2

#3

#1

#2

#3

6" Lap 90° bend

#1

#2

9" 90° bend

#1

#2

#3

9" Lap 90° bend

#1

#2

#3

12" 90° bend

Explosive failure occurs when concrete in the
middle of the legs of the bent bar fractures.

#1

Bar deformation during pull-out.

#2
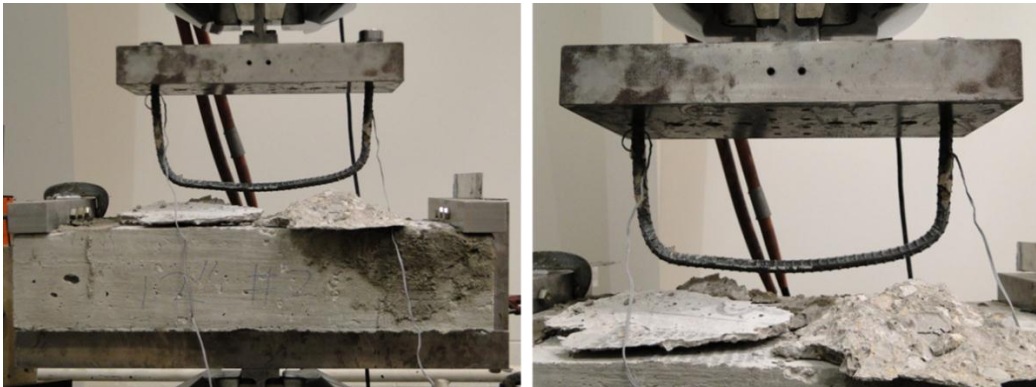
#3

12" Lap 90° bend

#1

#2

#3

Appendix G

Task 7-Strain Profile

Previously tested section

P

Box Beam with Blockout

H1 H2 H3 H4 H5 H6 H7 H8 H9 H10 H11 H12 H13 H14 H15
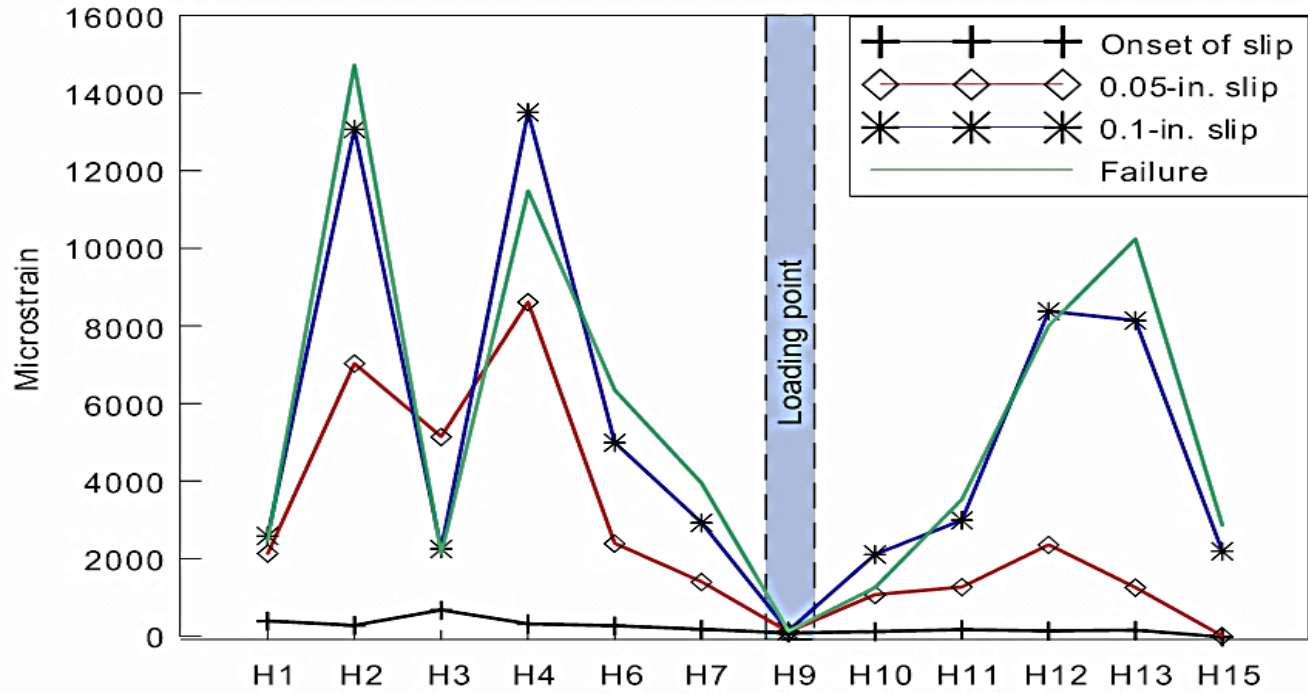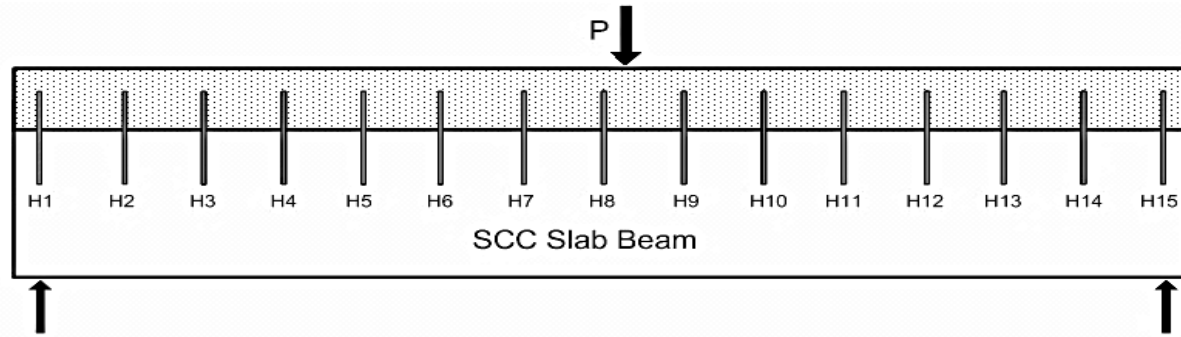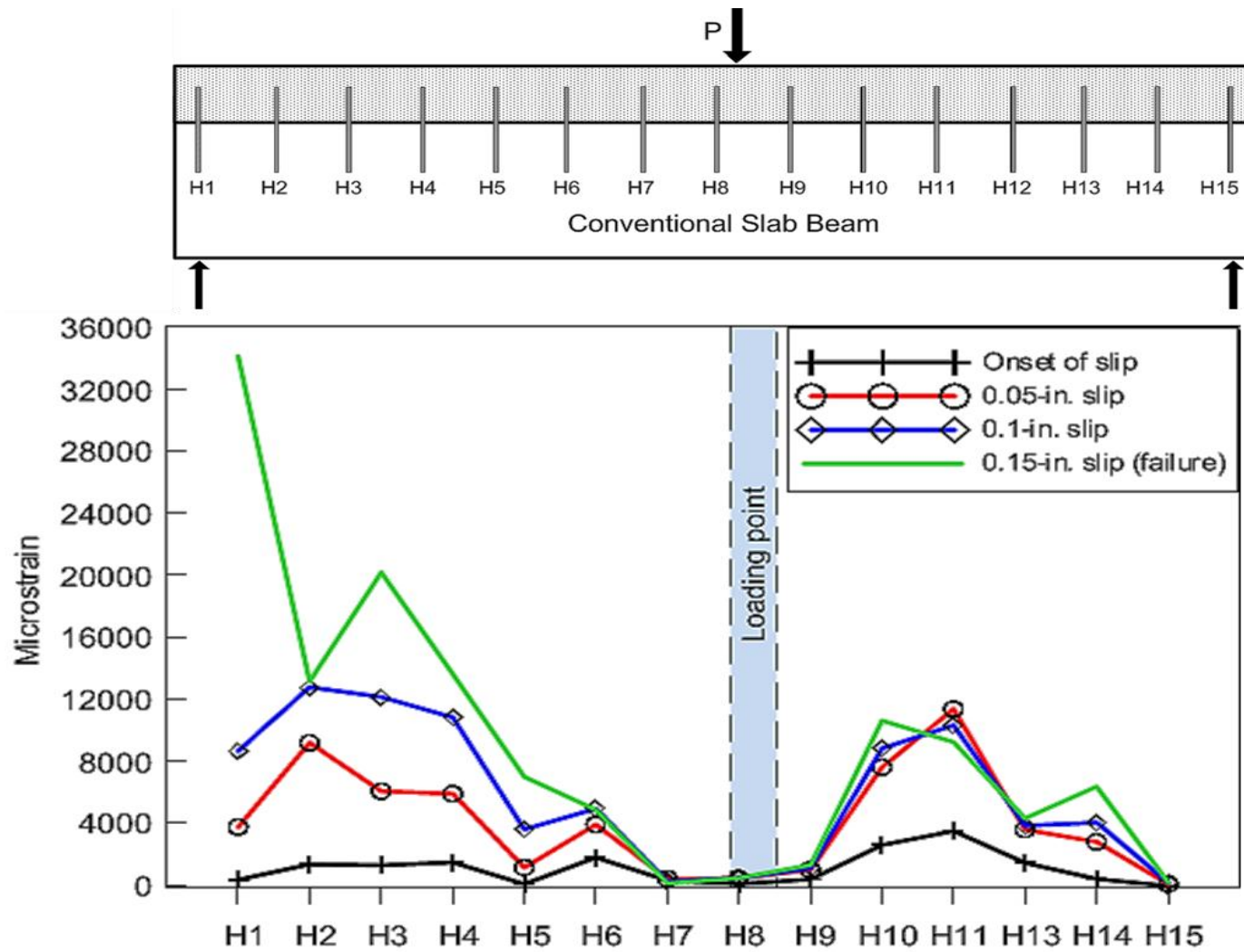
References

1) AASHTO, "LRFD Bridge Design Specifications," 6th edition, American Association of State Highway and Transportation Officials (AASHTO), Washington, D.C., 2012.

2) AASHTO Highway Subcommittee on Bridges and Structures-2013 Survey, from http://bridges.transportation.org/Pages/Bridge%20Surveys.aspx

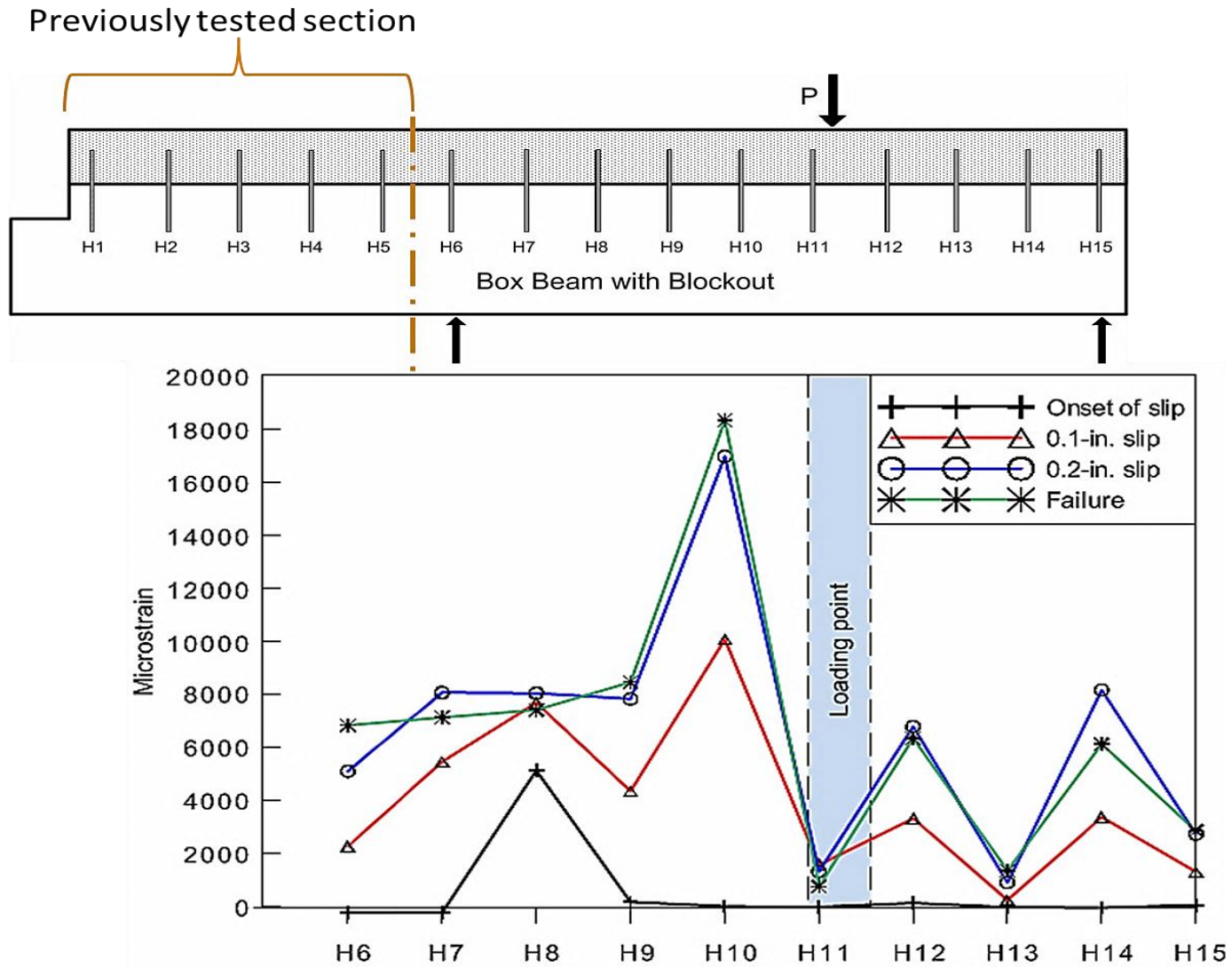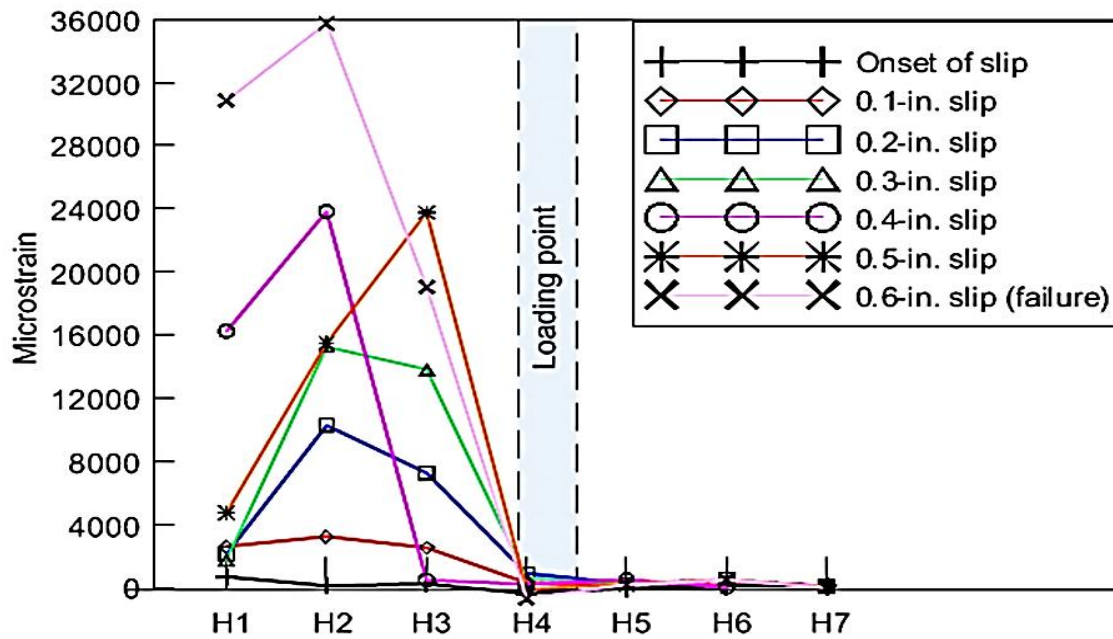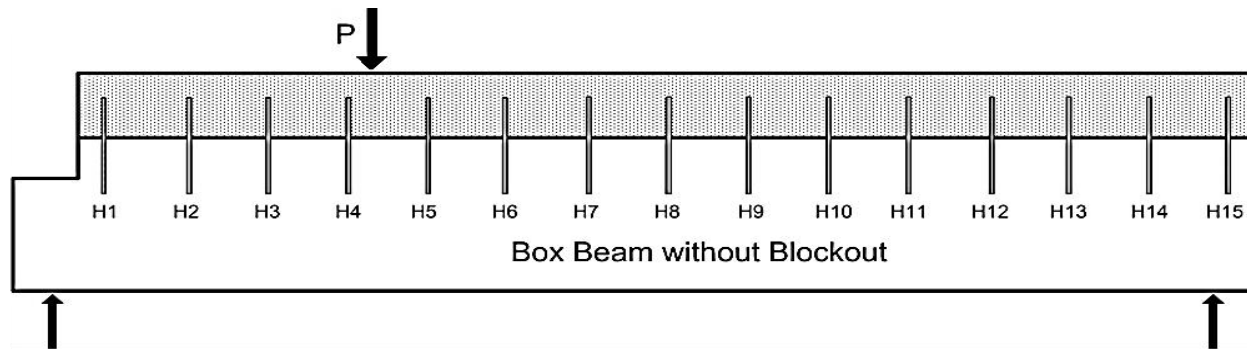3) ACI Committee 318, "Building Codes Requirements for Structural Concrete (ACI 318-14)," American Concrete Institute, Farmington Hills, MI., 2014.

4) Ali, M. A., and White, R. N., "Enhanced Contact Model for Shear Friction of Normal and High-Strength Concrete," ACI Structural Journal, 96(3): 348-360, 1999.

5) Anderson, A.R., "Composite Designs in Precast and Cast-in place Concrete," Progressive Architecture, 41(9): 172-179, 1960.

6) ASTM C39/C39M, "Standard Test Method for Compressive Strength of Cylindrical Concrete Specimens," Annual Book of ASTM Standards, ASTM International, Vol. 04. 02, West Conshohocken, PA, 2014.

7) ASTM A615/A615M, "Standard Specification for Deformed and Plain Carbon-Steel Bars for Concrete Reinforcement," Annual Book of ASTM Standards, ASTM International, Vol. 01. 04, West Conshohocken, PA, 2014.

8) ASTM A416/A416M, "Standard Specification for Steel Strand, Uncoated Seven-Wire for Prestressed Concrete," Annual Book of ASTM Standards, ASTM International, Vol. 01. 04, West Conshohocken, PA, 2014.

9) Badoux, J. C., and Hulsbos, C. L., "Horizontal Shear Connection in Composite Concrete Beams under Repeated Loads," ACI Journal, 64(12): 811-819, 1967.

10) Bass, R. A., Carrasquillo, R. L., and Jirsa, J. O., "Shear Transfer across New and Existing Concrete Interfaces," ACI Structural Journal, 86(4): 383-393, 1989.

11) Birkeland, P., and Birkeland, H., "Connections in Precast Concrete Construction," ACI Journal, 63(3): 345-368, 1966.

12) Birkeland, H. W., Class Notes for Course, "Precast and Prestressed Concrete," University of British Columbia, 1968.

13) Chung, H. W. and Chung, T. Y., "Prestressed Concrete Composite Beams Under Repeated Loading," ACI Journal, 1976.

14) Evans, R. H., and Chung, H. W., "Horizontal Shear Failure of Prestressed Composite T-Beams with Cast-in-Situ Lightweight Concrete Deck," Concrete, pp. 124 – 126, 1969.

15) Frenay, J. W., "Shear Transfer Across a Single Crack in Reinforced Concrete Under Sustained Loading," Part 1, Experiments, Stevin Report, 5-85-5, 1985.

16) Gohnert, M., "Horizontal Shear Transfer Across a Roughened Surface," Cement & Concrete Composites, V. 25, No. 3, pp 379 – 385, 2003.

17) Hofbeck, J. A., Ibrahim, I. O., and Mattock, A. H., "Shear Transfer in Reinforced Concrete," ACI Journal, 66(13): 119-128, 1969.

18) Hanson, N. W., "Precast-Prestressed Concrete Bridges: (2) Horizontal Shear Connections," PCA Journal, 2(2): 38-58, 1960.

19) Hsu, T. T. C., Mau, S. T., and Chen, B., "Theory of Shear Transfer Strength of Reinforced Concrete." ACI Journal, 84(2), 149-160, 1987.

20) Hsu, T. T. C., "Horizontal Shear Tests of PSI Prestressed Composite Beams," Report to Prestressed Systems Inc., 1976.

21) Hwang, S. J., Yu, H. W., and Lee, H. J., "Theory of Interface Shear Capacity of Reinforced Concrete," Journal of Structural Engineering, 126(6): 700-707, 2000.

22) ICRI Technical Guideline No. 03732 "Specifying Concrete Surface Preparation for Sealers, Coatings, and Polymer Overlays," 2012.

23) Kaar, P.H., Kriz, L.B., and Hognestad, E., "Precast-prestressed concrete bridges, Pilot Tests of Continuous Girders." J. PCA Research and Development Laboratories, 2(2), 21-37, 1960.

24) Kahn, L. F., and Mitchell, A. D., "Shear Friction Tests with High-Strength Concrete," ACI Structural Journal, 99(1): 98-103, 2002.

25) Kamel M. R., "Innovative Precast Concrete Bridge Systems," Dissertation, University of Nebraska, Lincoln, Nebraska, 1996.

26) Kent, A. H., Gabriel, Z., Bahram, S., "Toward an Improved Understanding of Shear-Friction Behavior," ACI Journal, 109(6): 835-844, 2012.

27) Kono, S., and Tanaka, H., "Interface Shear Transfer for High Strength Concrete and High Strength Shear Friction Reinforcement," ASCE Journal, 2003.

28) Kovach, J. D., and Naito, C., "Horizontal Shear Capacity of Composite Concrete Beams without Interface Ties," ATLSS report 08-05, ATLSS Center, Lehigh University, Bethlehem, Pa, 2008.

29) Kriz, L. B., and Raths, C. H., "Connections in Precast Concrete Structures- Strength of Corbels," PCI Journal 10(1): 16–6, 1965.

30) Loov, R.E., "Design of Precast Connections," Paper presented at a seminar organized by Compa International Ltd., Singapore, 1978.

31) Loov, R. E., and Patnaik, A. K., "Horizontal Shear Strength of Composite Concrete Beams with a Rough Interface," PCI Journal, 39(1): 48-69, 1994.

32) Marques, J. L. G., and Jirsa, J. O., "A Study of Hooked Bar Anchorages in Beam-Column Joints," ACI Journal, 72(5): 198-209, 1975.

33) Mast R. F., "Auxiliary Reinforcement in concrete Connections, "Journal of the Structural Division, ASCE, 94(6)6: 1485-1504, 1968.

34) Mattock, A.H., Johal, L., and Chow, H.C., "Shear Transfer in Reinforced Concrete with Moment or Tension Acting Across the Shear Plane," PCI Journal, 20(4): 76-93, 1975.

35) Mattock, A. H., "Shear Transfer in Concrete Having Reinforcement at an Angle to the Shear Plane," ACI, Special Publication, 42: 17-42, 1974.

36) Mattock, A. H., "Cyclic Shear Transfer and Type of Interface," ASCE Structural Journal, 107(10): 1945-1964, 1981.

37) Mattock, A. H., Hofbeck, J. A., and Ibrahim, I. O., "Shear Transfer in Reinforced Concrete," ACI Journal, American Concrete Institute, 66(2): 119-128, 1969.

38) Mattock, A. H., Discussion of the paper, "Modified Shear-Friction Theory for Bracket Design," by B. R. Hermansen and J. Cowan, ACI Journal, 71(8): 421-423, 1974.

39) Mattock, A. H., and Hawkins, N. M., "Research on Shear Transfer in Reinforced Concrete," PCI Journal, 17(2): 55-75, 1972.

40) Mattock, A. H., Li, W. K., and Wang, T. C., "Shear Transfer in Lightweight Reinforced Concrete," PCI Journal, 21(1): 20-39, 1976.

41) Mattock, A. H., "Anchorage of Stirrups in a Thin Cast-in-Place Topping," PCI Journal, 32(6): 70-85, 1987.

42) Mattock, A. H., "Shear Friction and High-Strength Concrete," ACI Structural Journal, 98(1): 50-59, 2001.

43) Menkulasi, F., "Horizontal Shear Connectors for Precast Prestressed Bridge Deck Panels," Virginia Tech, Blacksburg, 2002.

44) Menkulasi, F. and Roberts-Wollmann, C. L., "Horizontal Shear Connections for Full-Width, Full-Depth Precast Concrete Bridge Deck Panels on Prestressed I-Girders," Virginia Tech, Blacksburg, 2003.

45) Mitchell, A. D., and Kahn, L. F., "Shear Friction Behavior of High-Strength Concrete", Georgia Department of Transportation Project No. 2005, , School of Civil and Environmental Engineering, Georgia Institute of Technology, Atlanta, Georgia, 2001.

46) Mones, R. M., and Brena, S. F., "Hollow-Core Slabs with Cast-in-Place Concrete Toppings: A Study of Interfacial Shear Strength", PCI Journal, 58(3), 124-141, 2013.

47) Naaman, A. E., "Prestress Concrete Analysis and Design: Fundamentals," Third Edition. Techno Press 3000, Ann Arbor MI, 2012.

48) NCHRP Report 584, "Full-Depth Precast Concrete Bridge Deck Panel System." Transportation Research Board, Washington, D.C, 2008.

49) Palacios, G., "Performance of Full-Scale Ultra-High Performance Fiber-Reinforced Concrete Column Subjected to Extreme Earthquake type Loading and Effect of Surface Preparation on the Cohesion and Friction Factors of the AASHTO Interface Shear Equation," Master's Thesis, University of Texas at Arlington, Arlington, Texas, 2015.

50) Park R., and Paulay T., "Reinforced Concrete Structures," John Wiley and Sons, 1975.

51) Patnaik, A. K., "Behavior of Composite Concrete Beams with Smooth Interface." Journal of Structural Engineering 127(4): 359-366, 2001.

52) Paulay T., Park R., and Phillips M. H., "Horizontal Construction Joints in Cast in Place Reinforced Concrete," Shear in Reinforced Concrete, ACI Special Publications 42, Vol. 2: 599-616, Detroit, 1974.

53) PCI Design Handbook, Precast and Prestressed Concrete, Seventh Edition, Precast/Prestressed Institute, Chicago, IL, 1992.

54) PGSuper Bridge Design Software, version 2.8.2, 2014.

55) Pruijssers, A. F., and Lung, G., "Shear Transfer Across a Crack in Concrete Subjected to Repeated Loading—Experimental Results," Part 1, Stevin Report, 1985.

56) Rehm, G., "Criteria for Evaluation of Reinforcement Bars with High Quality Composite, Reinforced Concrete, Reports from Research and Practice", Commemorative frilly, Wilhelm Ernst & Sohn, Berlin, pp. 79-96, 1969.

57) Revesz, S., "Behavior of Composite T-Beams with Prestressed and Un-prestressed Reinforcement," ACI Journal, V. 24, No. 6, (Proceedings V.49), pp. 585 – 592, 1953.

58) Saemann, J. C., and Washa, G. W., "Horizontal Shear Connections between Precast Beams and CIP Slabs," ACI Journal, 61(11): 1383-1409, 1964.

59) Seible, F., and Latham, C. T., "Horizontal Load Transfer in Structural Concrete Bridge Deck Overlays," Journal of Structural Engineering, ASCE, V. 116, No. 10, pp. 2691 – 2710, 1990.

60) Shaikh, A. F., "Proposed Revisions to Shear-Friction Provisions." PCI Journal, 23(2), 12 -21, 1978.

61) Shim C., Lee P., Chang S., "Design of Shear Connection in Composite Steel and Concrete Bridges with Precast Decks," Journal of Constructional Steel Research, 57: 203-219, 2001.

62) Shim C., Lee P., Yoon T., "Static Behavior of Large Stud Shear Connectors," Journal of Engineering Structures, 26: 1853-1860, 2004.

63) Shim, C. S., Kim, J. H., Chang, S. P., and Chung, C. H., "The Behavior of Shear Connections in a Composite Beam with a Full-Depth Precast Slab," Proceedings of the Institute of Civil Engineers, Structures and Buildings, Vol. 140:101-110, 2000.

64) Sholz D. P., "Performance Criteria Recommendations for Mortars used in Full-depth Precast Concrete Bridge Deck Panels Systems," Master's Thesis, Virginia Polytechnic Institute and State University, Blacksburg, Virginia, 2004.

65) Tan, K. H., Guan, L. W., Lu, X., and Lim, T. Y., "Horizontal Shear Strength of Indirectly Loaded Composite Concrete Beams," ACI Structural Journal, 96(4): 533 – 539, 1999.

66) Tassios, T. P., and Vintzeleou, E. N., "Concrete to Concrete Friction," Journal of Structural Engineering, 113 (4): 832-849, 1987.

67) Texas Department of Transportation, Standard Specifications for Construction and Maintenance of Highways, Streets, and Bridges, June 1, 2004.

68) Texas Department of Transportation, "Material Producer List, 2015. Retrieved from http://www.txdot.gov/inside-txdot/division/construction/producer-list.html

69) Trejo, D. and Kim, Y.H., "Development of Precast Bridge Deck Overhang System," Research Report 0-6100-3, FHWA/TX-10/0-6100-R3, 2011.

70) Walraven, J., Frenay, J., and Pruijssers, A., "Influence of Concrete Strength and Load History on the Shear Friction Capacity of Concrete Members," PCI Journal, 32(1): 66-84, 1987.

Biographical Information

Regina Waweru was born in Nairobi, Kenya on April 24, 1983. She joined Moi University in 2003 to pursue a Bachelor of Technology degree in Civil and Structural Engineering. During her undergraduate studies, she was employed by Howard Humphreys (EA) Consulting Firm as an intern in 2007. She then defended her fifth year project ("Investigation of the influence of Super-plasticisers on the flowability and Strength of Self-Compacting Concrete (SCC) using Locally Available Materials") in 2008 and was awarded the "Best Concrete Project Award" by Bamburi Cement Company. She went on to graduate the same year with First Class Honors.

From 2008 to 2009, she was hired as a research assistant at Moi University. She worked with the lead Professor on "Mix design for Self Compacting Concrete: Pilot Tests with Crushed Stone as Coarse Aggregates" and presented the same on the 2nd International Conference on Civil Engineering and Sustainable Development held in Mombasa Kenya.

In August of 2009, she joined Graduate School at the University of Texas at Arlington for her Master's and consequently PhD. She has been working on a number or research projects related to steel fiber-reinforced concrete and prestressed concrete. Her long-term goals are to gain experience in design (especially bridge design) and become a registered engineer. She is a member of a number of professional organizations such as the American Concrete Institute (ACI), American Society of Civil Engineers (ASCE), Precast/Prestressed Concrete Institute (PCI) among others.